The Microbial Ecology of Anaerobic Digestion:

- characterising novel biogas configurations through molecular and statistical methods

Thesis submitted to the National University of Ireland, Cork, for the degree of Doctor of Philosophy, May 2018

Volume 1 of 1

Jamie A. FitzGerald
School of Microbiology
104517431

Prof. Alan D. W. Dobson
Prof. Jerry D. Murphy
Supervisors

Prof. Gerald F. FitzGerald
Head of School of Microbiology

ucc

Coláiste na hOllscoile Corcaigh, Éire
University College Cork, Ireland

Table of Contents

Title

Declaration of Authorship

I, Jamie A. FitzGerald, assert that this thesis and the works presented in it are fully my own, and have not been submitted for other qualifications at University College Cork, or elsewhere.

Signed,

_____

Jamie A. FitzGerald

This one is for

the mothers

and the teachers

An incomplete list of acknowledgements

I could not have attempted this without the tireless love and support of Michelle, Mary, George, Olwyn, Maurice, Clio, Rowan, Jade, Conleth, the Kielys, the O' Learys and the Orjelas (in descending order of those who were forced to hear about it the most). Thank you to Mr Peter O' Rourke, for his kind ear and sound guidance. There is also a wide and motley crew of dear friends who have, in various and significant ways, steered me through the last few years: Alan, Ciarán, Claire, Eoghan, Jonathan, Sinéad, Shane, Steed, Tom and many others: thank you all.

My gratitude to my colleagues, who by turns encouraged and guided me: Erik Borchert, Eduardo Leao de Almeida, Beatrice Gil-Pulido, Wada Maureen Ihua, Stephen Jackson, Lekha Menon Margassery, and Lynn Naughton. Thanks also to the excellent staff at UCC and the School of Microbiology: in particular Ms Mary Cotter, Mr Paddy O' Reilly, Mr John O' Callaghan, Mr Maurice O' Donoghue, Ms Carmel Shortiss, Mr Dan Walsh, and Mr James Woods.

A third round of thanks to the residents of the Environmental Research Institute at UCC, who I had the pleasure to work with closely while learning the aromatic language of anaerobic digestion. Notably, thanks to Eoin Ahern, Eoin Allen, Amita Guneratnam, Christianne Herrmann, Markus Voelklein and David Wall for the great company. A very special thanks to Mr Paul Bolger, Ms Helen McMahon and Prof. Jerry Murphy for making the ERI the wonderful place to work that it is.

Thanks also to Science Foundation Ireland (SFI) and the Marine Renewable Energy Ireland (MaREI) institute, who have funded this work alongside the works of countless others.

However, none of this work would be possible without the consideration, support, and guidance of Prof. Alan Dobson, Prof. Jerry Murphy, and Dr. Stephen Jackson, whose reserves of patience and good advice are, apparently, inexhaustible: my sincere thanks for all that you have done.

Abstract

The microbiological generation of methane from organic substrates is a process with incredible flexibility, which has allowed continual innovations in its application as a source of renewable energy. Ireland's renewable energy sector is gradually expanding, and although biogas is as-yet a minor component, it currently presents an opportunity to capitalise on prevalent feedstocks and existing gaps in the country's energy infrastructure. In order for anaerobic digestion to succeed in this context, several criteria need to be optimised, particularly improving process stability and yields in order to make the technology competitive and deliver on the promise of biogas. Despite the efforts to harness anaerobic digestion as a sustainable energy technology, it remains a microbial phenomenon which is incompletely characterised and difficult to scale to industrial requirements. Indeed, many applications of anaerobic digestion for biogas require microbial communities to endure sustained stresses (high organic loading rates, high concentrations of inhibitive breakdown products, high temperatures) which can further destabilise the process and make certain configurations appear unfeasible.

An alternative application of anaerobic digestion focuses on a subset of the biogas community (the methanogenic archaea) to convert supplies of CO_2 and H_2 to biomethane at efficiencies approaching natural gas production (i.e. near-pure methane). This technology is highly attractive as it could allow conversion of both exogenous/industrially-produced H_2 and CO_2 to biomethane, as well as upgrading the methane content of 'raw' biogas. However, addition of hydrogen to anaerobic communities can paradoxically prevent biogas formation, by disrupting the finely-balanced thermodynamics of fermentation. It has been suggested that to avoid the inhibition caused by adding hydrogen to the microbial community *in situ*, methanogens could be cultured and fed CO_2 and H_2 in a specialised *ex situ* reactor, independent of feedstock hydrolysis and fermentation. Although hydrogenotrophic methanogens are autotrophs and can fix CO_2 to cellular material, it has not been clear what sort of

microbial communities are encouraged by upgrading setups, nor is it clear how the supply of H_2 disrupts the biogas community.

This thesis explores the microbial ecology underlying several anaerobic digestion configurations relevant to renewable energy production in both Irish and international contexts. Microbial community structures were considered in relation to feedstock composition and biogas output, and shifts in the abundance of functional microbial populations were related to changes in reactor environment and biomethane output, thereby identifying factors which appear to inhibit or support biogas production in these novel setups.

Chapters 2 and 3 consider anaerobic digestion of feedstocks which represent promising biogas resources in Ireland and beyond (seaweed/dairy slurry and grass silage/dairy slurry respectively), but can be recalcitrant or problematic for digestion due to their compositions. In both chapters, next-generation sequencing of 16S microbial community profiles clearly indicates disruption between the metabolism of end-fermentation products and subsequent methanogenesis when operated at relatively high loading rates of substrate (2-3kgVS$m^{-3}d^{-1}$). In the case of seaweed/dairy slurry digestion (chapter 2), large quantities of seaweed release excess ammonia, correlating with collapse of the methanogen populations (acetoclastic *Methanosarcina*) necessary to metabolise accumulating acetate, ultimately leading to reactor failure. In the case of grass silage/dairy slurry digestion, high organic loading of grass silage appears to inhibit or exhaust fermenting bacteria (*Clostridia*), as shown through a supplementation regime which restores process function and increases abundance of fermenting bacteria. Surprisingly, this treatment does not encourage archaeal populations (*Methanobacterium*), and may even reduce their abundance. In both chapters, conditions which inhibit biogas production lead to microbial communities which are distinct from those seen when inhibition was resolved.

Chapters 4 and 5 explore biogas upgrading communities, charting how these communities relate to variables in the upgrading process. Chapter 4 characterises the microbial community in a minimal example of *ex situ* biogas upgrading at two thermophilic temperatures (55°C, 65°C), demonstrating the persistence and stability of methanogen populations (in particular, the family *Methanobacteriaceae*) alongside a surprisingly complex bacterial community. Chapter 5 expands on this finding, comparing the upgrading communities between *in situ* and *ex situ* operation during increasing flow rates of H_2, showing that the presence (*in situ*) or absence (*ex situ*) of feedstock delineates these communities. This in turn governs community response to rates of H_2 supply, with *in situ* communities showing a far greater susceptibility to inhibition, population flux, and displacement of methanogens (*Methanothermobacter*). In comparison, *ex situ* upgrading communities saw little change at much higher H_2 flow rates, and instead encouraged larger populations of closely related methanogens (*Methanobacterium*). These large *ex situ* hydrogenotrophic populations were significantly associated with smaller, 'satellite' populations of hydrogen-producing bacteria, indicating a thermophilic upgrading community centred on biogas metabolism.

Chapter 1

Introduction – the microbial ecology of anaerobic digestion

1.1 ANAEROBIC DIGESTION AS AN ECOLOGICAL PROCESS

Despite the ongoing interest and continued investment in anaerobic digestion (AD)-based technologies for both energy and waste treatment applications, it is not a 'new' technology - nor is it strictly a technology at all. Anaerobiosis was the original condition under which life arose on Earth, and is thought to have been the unchallenged paradigm until around 2.1-2.4 billion years ago. Life is assumed to have initially revolved around fermentation, where energy is captured directly from the breaking of molecular bonds, and later anaerobic respiration, where energy is harvested through transmission of electrons between different energetic states. Current opinions on the origins of life suggest a proximity to hydrothermal vents, where elements such as iron, sulphur, nitrogen, manganese, and nitrogen would have been relatively available (Martin, 2011; Herschy *et al.*, 2014). This could have provided end-points for depositing low-potential electrons, i.e. many of these elements could act as terminal electron acceptors, facilitating respiration (Martin, 2011). Due to their strong affinity for electrons, these terminal electron acceptors provide large energetic yields, allowing more exergonic metabolism. The value of such elements in metabolic function is apparent in their ubiquitous roles in enzymes and co-factors for respiration (and beyond), as well as their requirement in micro- or trace-nutrients. This may have lead to the sequestration of these elements within cell machinery, as seen in the metal-ligand sites of many essential enzymes and cofactors, such as translocating and transferase factors (Ni, Co), ligases (Mn), respiratory globins (Fe) and hydrogenases (Fe, Ni, S) to name a few.

The scarcity of alternative terminal electron acceptors must also have played a role in the evolution of carbon as a terminal electron acceptor, despite its lower electron affinity; in particular, a distinct archaeal clade (the methanoarchaea, or methanogens) generate energy and fix cellular carbon using a modified version of the Wood-Ljungdal pathway (reductive acetyl-CoA pathway), priming CO_2 through

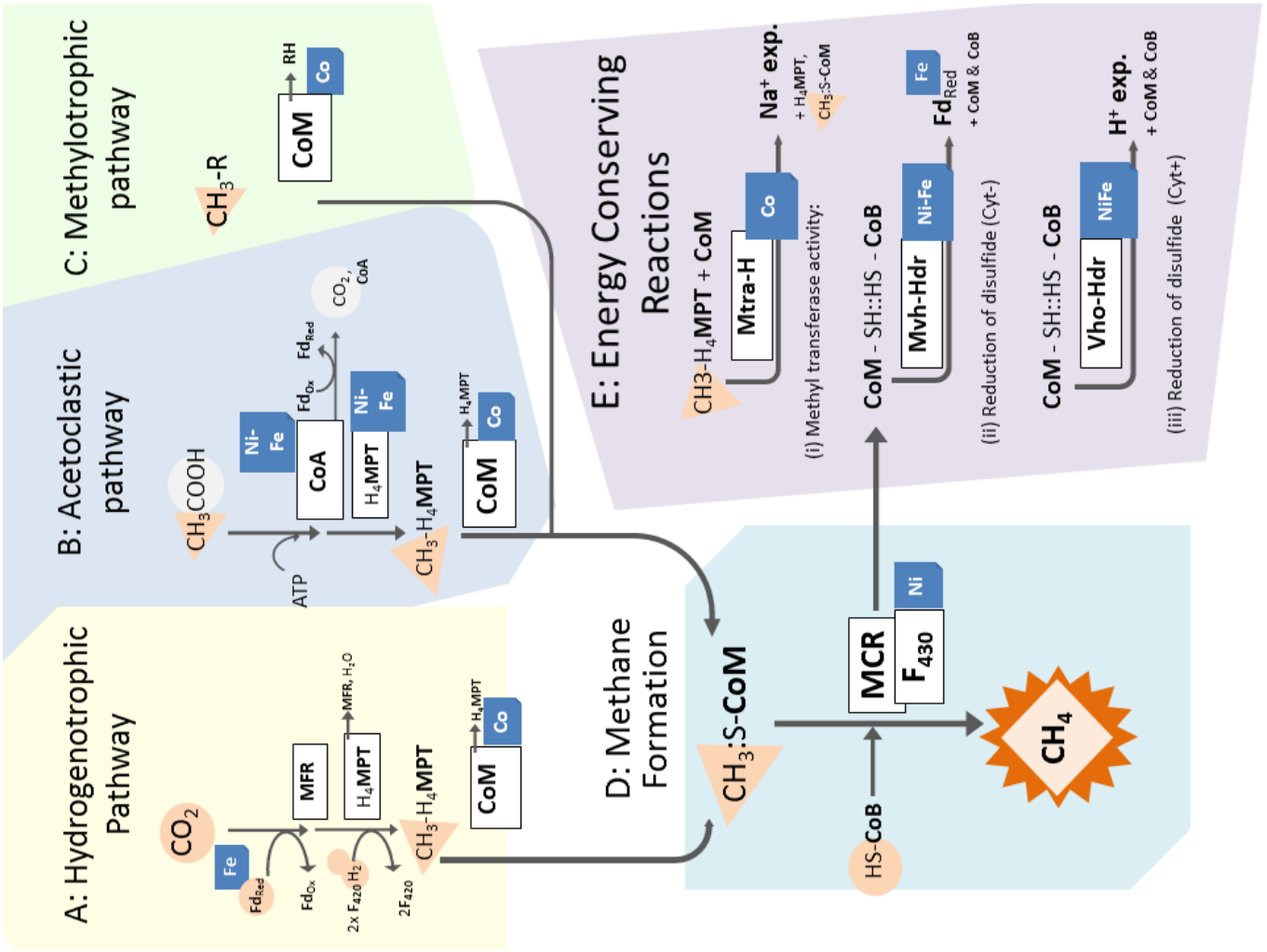

Figure 1: Major methanogenic reactions. *Methanogens use one of three pathways (A, B, C) to provide methyl groups to the final step of methane formation (D): the process includes a number of reactions which contribute to the cell's chemiosmotic potential (exporting H+, Na+) or reduce ferredoxin for later use (D) .The path of the methanised carbon and hydrogen atoms are highlighted in orange. Trace elements involved (cobalt: Co; iron: Fe; nickel: Ni) are also marked for reference. Enzymes and cofactors are in bold to better distinguish from functional groups (CH_3, H, S, R).*

Abbreviations*: CoA: Acetyl-Coenzyme A; CoB: coenzyme B; CoM: Coenzyme M; Cyt+: cytochrome containing methanogens (i.e. Methanosarcinales); Cyt-: methanogens without cytochromes (i.e. non-Methanosarcinales orders);Fd: ferredoxin (reduced/oxidised); F430: MCR cofactor F430; MCR: Methyl Co-enzyme M Reductase; MFR: methanofuran; H_4Mpt: Tetra-hydromethanopterin; Mtra-H: methyl-H_4MPT Co-M methyltransferase; Mvh-Hdr: NiFe-hydrogenase hetero-disulfide reductase (membrane bound); Vho-Hdr: NiFe-hydrogenase hetero-disulfide*

the stepwise addition of low-potential electrons to form a methyl group (CH_3) (Liu and Whitman, 2008). Rather than synthesise this methyl group *de novo*, many methanogens can also capture the methyl groups from e.g. methanol, trichlorofluoromethane, or methylamines (Liu and Whitman, 2008; Whitman *et al.*, 2014) using cobalt-containing corrinoid proteins, while a third, important, and thus-far monophyletic clade (the *Methanosarcinales*) are capable of splitting acetate (CH_3COOH) into methyl and carboxyl groups, the former of which is converted to methane. In all three cases, the methyl group is ultimately transported by Coenzyme-M (M:Co-M) to a nickel-ligand site formed between factor 430 (F430) and methyl-Co-M reductase (MCR), where the methyl group is reduced to methane (coordinated by F430's nickel-ligand site (Ermler *et al.*, 1997)) and released to diffuse out of the digestate, while Co-M is oxidised to form a disulphide complex with Coenzyme B (Co-M-S::S-Co-B). The actual production of energy in methanogenesis comes through restoring Co-M for the transport of further methyl groups (Figure 1 D. ii, iii), and through transfer of the methyl group from tetrahydromethanopterin (THMP) to Co-M via THMP:Co-M methyl transferase (Figure 1 D. i) which incorporates a primary sodium pump activity (Gottschalk and Thauer, 2001). Both activities provide an ion gradient from which the cell can generate ATP. In the *Methanosarcinales* order, additional energy is harvested by the membrane-bound Co-M-S::S-Co-B disulphide reductase, which renews the coenzymes while also exporting protons, adding further to the cell's ion gradient. Other methanogen clades are thought to use the same exergonic disulphide uncoupling to instead reduce ferrodoxin, an iron-rich electron transporter (Thauer *et al.*, 2008). The synthesis of ATP and methane are therefore decoupled: however it is thought that methanogens can produce 1 ATP molecule per 2 to 4 ions pumped into the cell (Schink, 1997; Thauer *et al.*, 2008). This low return reflects the tight energetic budget under which methanogens exist, and may help to explain their slow growth rate, with doubling times of between 7 hours and >1 day (Thauer *et al.*, 2008; Whitman *et al.*, 2014)**.** Although this may enable other bacterial genera employing different respiratory strategies (S, N, Fe etc.) to

outcompete them, methanogens thrive in a variety of different ecosystems globally as seen by their importance in the global carbon cycle with ~2% of total carbon fixed by plants per year (70 gigatons) (Thauer, 1998) being converted to methane. It is also worth noting that although they are not the only organisms capable of forming methane (so-called 'mini-methane' bacteria; Rimbault *et al.*, 1988), they are to date the only significant biological source of methane, and so are fundamental in the context of biomethane production as an alternative source of energy or fuel.

1.2 ANAEROBIC DIGESTION AS A TECHNOLOGY

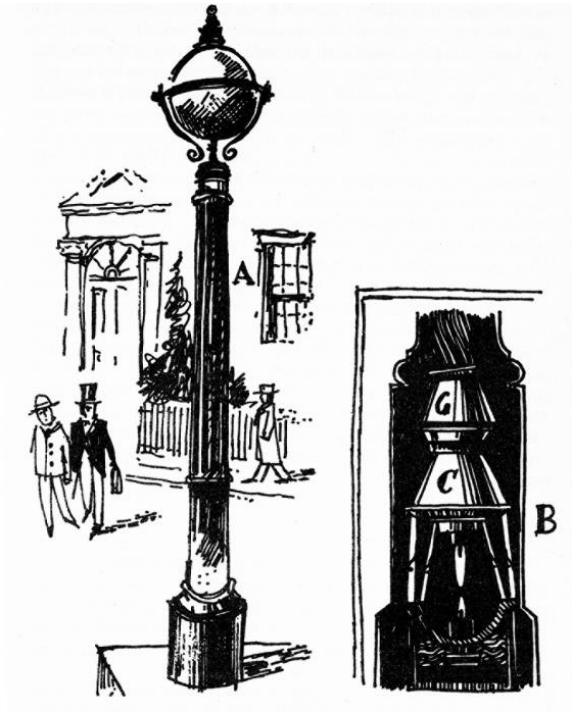

***Figure 2**: Biogas has long been considered a source of renewable and inexpensive fuel, if only it can be properly harnessed and distributed. Above, a contracted proposal by the Irish polymath and inventor, Myles na Gopaleen, c. 1940.*

Interest in the use of AD and bigoas as a fuel is not a new development. Apocryphal use of biogas is reported as far back as 9th century B.C.E. in Assyria, where it was supposedly used to heat bathwater. Between the 18th and early 20th centuries many scientists were involved in determining the composition and origins of biogas, notably Volta, Davies, Dalton and Buswel (Abbasi *et al.*, 2012).

Several European cities have used biomethane from sewers to light gas-burning street lamps (Abbasi *et al.*, 2012). However, intense research into biogas production during the late 20th and 21st century has transformed the field of anaerobic digestion from a pragmatic and curious method of waste disposal to one

which provides 2.429 GW of energy globally in 2017 (McCabe and Schmidt, 2018) (total renewable production 2015: 1,856 GW; total energy production 2015: 280,835,000 GW (McCabe and Schmidt, 2018; Sawin *et al.,* 2017). While still relatively small, this quantity is growing rapidly: biogas production grew by 11% between 2000 and 2014 worldwide, with strong implications for regional socio-economic development (McCabe and Schmidt, 2018), while also providing novel solutions to larger concerns in energy supply. The value of AD as an energy solution can be seen in the framework set out by the European Union's Renewable Energy Directive (RED; European Parliament and European Council, 2009). RED specifies that 20% of the Union's energy demands must be renewable by 2020, including RED-derived renewable targets in transport of 10%, placing an emphasis on biofuel. RED also determined energy from biogas provides one of the greatest reductions in greenhouse gas emissions (European Parliament and European Council, 2009). To avoid any potential negative effects associated with the cultivation and harvesting of feedstocks such as sugar, oil, or starch-rich crops for traditional biofuel production, these 'first generation biofuels' have been capped at 7% of overall renewable contribution (European Parliament and European Council, 2015). Instead, RED specifies that 'advanced' biofuels (second generation: ligno-cellulosics, food waste, municipal solid waste; third generation: seaweeds, macro and micro algae) should contribute at least 3% of energy by 2020. As such, biogas produced through AD can provide an attractive route to convert advanced biofuels to bioenergy, in a medium which can be distributed easily using existing natural gas infrastructure. Optimising AD systems for these modern substrates is therefore an active area of research.

The ideal biomethane feedstock for AD should contain a high ratio of carbon to nitrogen or sulphur (e.g. low-complexity carbohydrates), decay at a stable rate, not have high levels of sodium (<8g/L, Chen *et al.*, 2008), and contain a diverse mix of micronutrients (Fe, Co, Ni, Se etc.) so as to reduce the need for supplementation (Drosg, 2013). With amenable substrates, it should be possible to sustain

AD at very high organic loading rates (OLR), allowing large quantities of biogas to be produced in a relatively short period of time. However, OLR also governs the Hydraulic and Solid Retention Times (HRT, SRT) of the reactor. Excessively high rates of operation may result in 'wash-out', where active biomass or micronutrients are lost due to excessive reactor turnover, leading to reactor inhibition. Inhibited or sub-optimal AD can also arise from the accumulation of fermentation products due to overfeeding or instability, causing decreases in pH (accumulations of butyrate, propionate, acetate) or increased toxicity in the reactor (H_2S, NH_3). Feedstock substrate is typically managed to provide a stable, balanced diet for the microbial populations involved (Drosg, 2013). In practice, variability in feedstock and reactor setup requires advanced planning be employed, with the desired parameters being reached gradually (i.e. over days or weeks) to allow adaptation and establishment of the underlying microbial community structures. Once established, sustaining the acclimatised community is crucial for long term production of biogas and process success, and can be aided through process monitoring.

A second role for AD in energy production is closely related to the growth of renewable energy sources, both biological and otherwise. Energy demand is a reasonably predictable factor in both the short and long term, with traditional energy generators (e.g. coal, nuclear, hydro-electrical) increasing or decreasing output to accommodate daily patterns of national/international energy usage. In contrast, supply of energy from renewable sources often depends on factors dictated by climate (e.g. weather in wind and wave turbines) rather than demand, or can be out of phase with demand (e.g. tidal volumes in tidal generators). In these situations, energy production in excess of requirements commonly leads to this power being curtailed and lost as so-called 'overspill'. To maximise the efficiency of renewables, methods of storing this asynchronously-produced energy are required which allow return of energy to the grid as needed, or transfer to a different point of consumption (e.g. in transport or heating). Such a technology is *ex situ* biomethanation (Figure 3 C), where a methanating

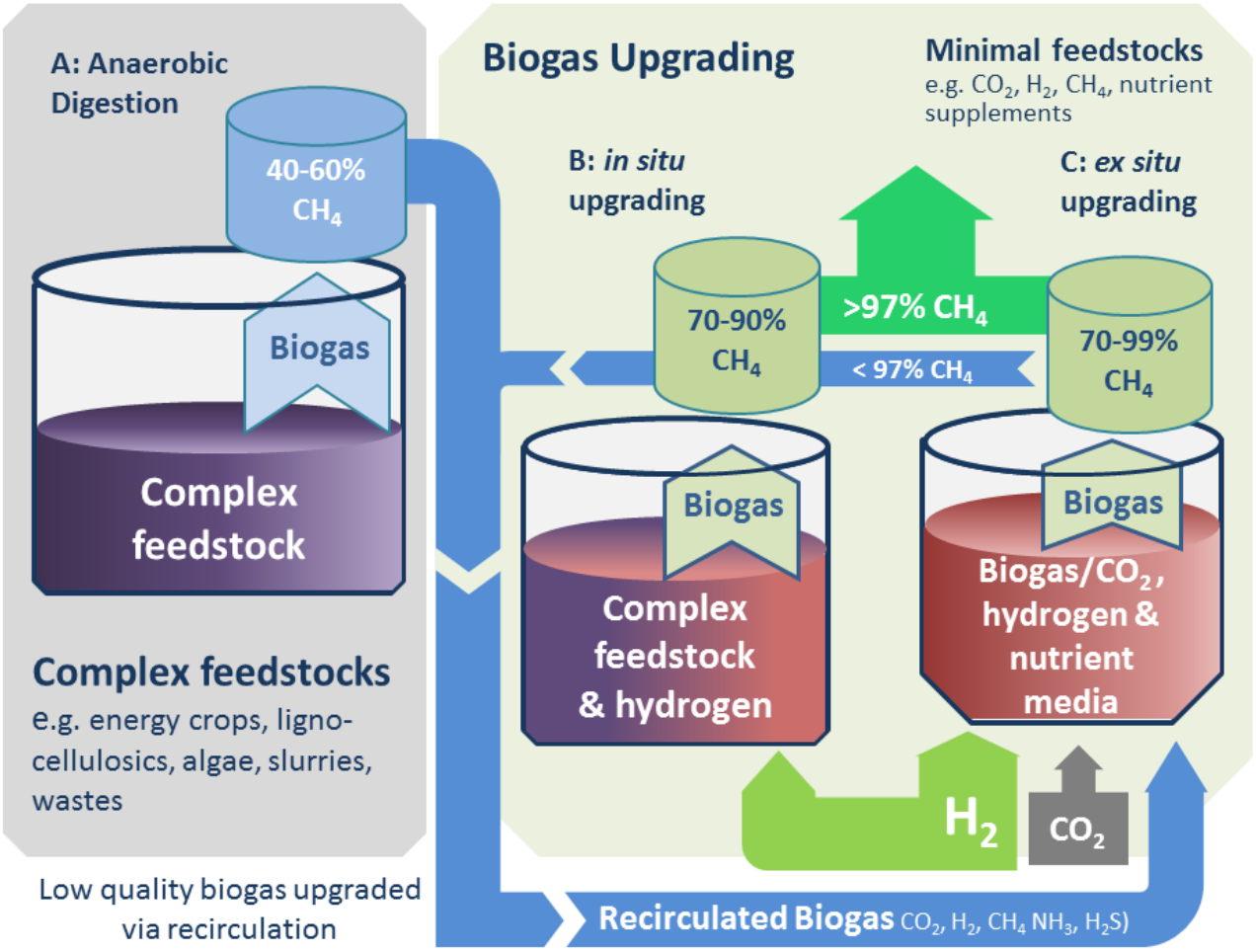

Figure 3: Overview of anaerobic digestion (A),* in situ *upgrading (B), and* ex situ *upgrading (C) configurations, similar to the setups covered in this thesis. *Biogas produced in A is of low CH4 content (typically 40-60%) and must be refined before being transferred to energy infrastructure. Biogas from in situ upgrading (B) has a theoretically higher methane content than A due to the increased supply of H_2, promoting conversion of CO_2 to CH_4. Ex situ upgrading (C) is not given feedstock, so must rely on methanation of the biogas or CO_2 provided in order to fix carbon and create energy, ideally reaching very high biomethanation levels.*

community is fostered outside the anaerobic digestion vessel, i.e. an anaerobic community is supplied biogas substrates (usually CO_2 and H_2) in the absence of fermentable materials in order to produce biomethane directly without the degradative steps required in AD. The benefit of this technology is twofold: it firstly converts excess or 'overspill' energy into hydrogen production through hydrolysis, allowing curtailed power to be easily stored and redistributed as biomethane; and secondly it allows a biological route for purifying biomethane to a standard comparable with natural gas (Sun *et al.*, 2015), reducing the cost of biogas purification.

1.3 ANAEROBIC DIGESTION AS A BIOLOGICAL PROCESS

Use of AD as a waste-remediation and biofuel technology has led to its delineation into four sequential stages which result in the conversion of feedstock to carbon dioxide and methane (see Figure 4):

1. *hydrolysis of feedstock material*
2. *primary fermentation of oligomers and monomers*
3. *secondary fermentation leading to acidogenesis and acetogenesis*
4. *conversion of acetate, CO_2 and methyl groups to methane.*

The central trend running through the four stages of AD is the stepwise degradation of organic materials to simpler products by bacteria, and the eventual sequestration and removal of these materials by the methanogenic archaea resulting in the formation of biomethane as a by-product.

1.3.1 Stage 1: Hydrolysis:

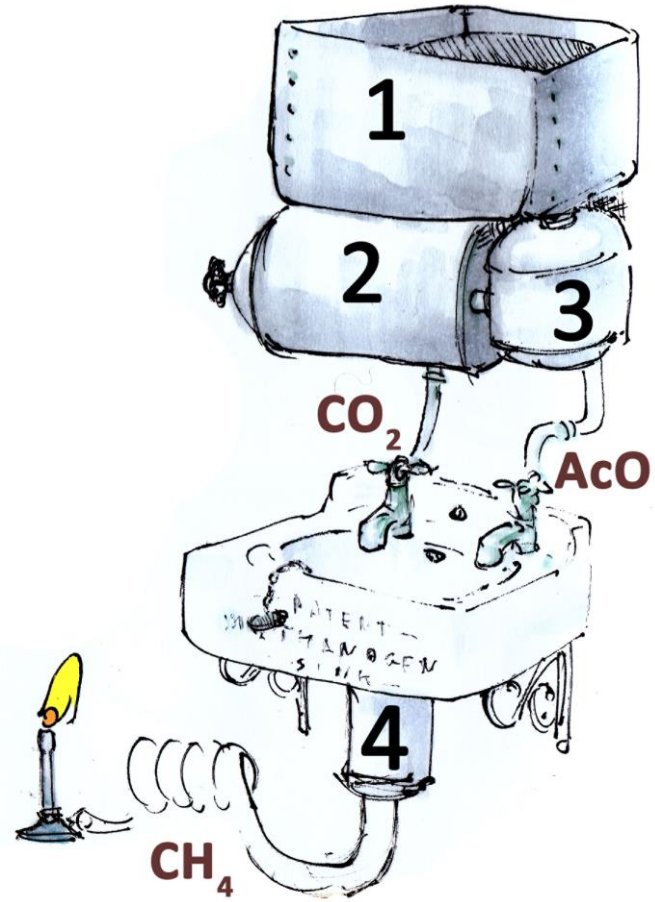

***Figure 4**: Although the digestion process is dynamic, feedstock 'flows down' through the connected communities, becoming progressively catabolised (stages 1, 2) until it pools as various end-fermentation products (stage 3): in the final stage (4), methanogens provide an 'electron sink' which drains the community of low oxidation/reduction potential materials – the product is biogas (CH_4).*

Hydrolysis is perhaps the widest ranging stage of AD, covering both the physical disintegration of the biomass as well as the disruption of molecular bonds via the splitting of water, allowing fragmentation of macromolecules and increasing the effective surface area. Digestion of 'energy rich' organic substrates often refers to materials where the amount of preparatory hydroylsis required is minimal. For example, the AD of oils or organic leachate from municipal solid waste requires little hydrolysis as substrates for fermentation are readily accessible. In contrast, although recalcitrant materials such as ligno-cellulosics (grasses, timbers, agricultural wastes) or algal biomass (brown and green seaweeds, cultivated microalgae) are rich in saccharides and other fermentables, significant effort must be undertaken to make these materials bioavailable. As the first step in AD, effective hydrolysis is crucial and if inhibited can quickly become rate limiting. To improve rates of

digestion, feedstock can be hydrolysed as a pre-treatment, such as with steam or acid hydrolysis**,** or even through simple maceration (Carrere *et al.*, 2016). However, by far the most important effectors of hydrolysis in AD are the incredibly diverse range of hydrolytic bacteria and fungi, which secrete an extensive range of enzymes (hydrolases, proteases, amylases, cellulases, lignases etc.) and enzyme complexes (e.g. proteosomes, cellulosomes) in order to degrade macromolecules and polymers. The enormous diversity among bacterial hydrolysers reflects the range (and ready availability) of substrates which are subject to hydrolysis, and although hydrolysis is not restricted to a particular clade, certain phyla (*Firmicutes, Bacteroidetes, Proteobacteria*) are prolific degraders (Hanreich *et al.*, 2013; Yutin and Galperin, 2013; Jiménez *et al.*, 2014; Güllert *et al.*, 2016). At time of writing, the Kyoto Encyclopedia of Genes and Genomes (KEGG: Kanehisa *et al.*, 2014**)** contains over 336,000 hydrolase enzymes, and is likely to represent an as-yet incomplete catalogue.

1.3.2 Stage 2: Primary Fermentation

Primary fermentation is the second stage of AD. In the absence of electron acceptors used for respiration (Fe, S, N, O), materials released through hydrolysis into the anaerobic environment (oligomer nucleotides, amino acids, saccharides) provide abundant substrates for fermenting bacteria. However, the lack of high-potential electron acceptors leads to meagre yields from an energy perspective for many fermentative reactions, especially when energy must be consumed to renew reducing equivalents (NADH+, FADH) or activate substrates through phosphorylation (as in glucose-6 phosphate). By way of comparison, the aerobic catabolism of a glucose molecule yields a net return of ~30 molecules of ATP, while anaerobic catabolism provides a net yield of just two ATP molecules. Perhaps more significantly, acetate (a central product of anaerobiosis) can be metabolised aerobically through the citric acid cycle to provide 16 ATP equivalents per molecule, while syntrophic

acetate oxidation (SAO) affords a much poorer return of c. -30kJ/mol (i.e., ~1/2 ATP molecule) per molecule of acetate oxidised, *shared between two syntrophic partners* (oxidiser and methanogen) (Thauer *et al.*, 1977; Schink, 1997). In fermentation, energy is produced through the catabolism of hydrolysis products, providing energy to the cell through substrate-level production of ATP, generation of proton or sodium gradients, and the cycling of reducing equivalents (NADH). Fermentation of sugars releases CO_2 and H_2, and produces a range of organic acids (succinate, lactate, butyrate, propionate, acetate), alcohols and solvents (butanediol, butanol, ethanol, acetone), while fermentation of nucleotides and amino acids produce similar organic by-products in addition to releasing ammonia and sulphur. The lack of high-potential electron acceptors leads to generation of by-products that retain some energy content. As a result many products are re-absorbed by the community and further oxidised/reduced. This allows for a stepwise but thorough degradation of the substrate, eventually producing simple molecules with relatively little energy content (formate, acetate, propionate, ethanol). Given the large quantities of biomass in question, the overlap between hydrolytic and fermenting activities, and relatively small size of methanogenic populations, fermenters likely comprise the most abundant metabolic group in the reactor, and typically represent the majority of bacterial populations present in successful AD (Hanreich *et al.*, 2013; Jiménez *et al.*, 2014; Güllert *et al.*, 2016).

1.3.3 Stage 3: Secondary Fermentation

CO_2 is continuously produced at all stages of anaerobic digestion through the oxidation of organic material. Although a large portion of this escapes the digestate to contribute to biogas, a significant portion of the CO_2 will dissolve into the digestate (influenced by temperature and pH). In solution, this forms bicarbonate and improves the buffering capacity of the reactor, as well as providing a carbon

source for microbes including methanongens. Acetate is a major product of the fermenting microbial community; not just in AD, but in anaerobic environments globally. Estimations of acetate production have suggested 10^{12} kg of acetate are produced annually worldwide in sediments, together with a further 10^{12}kg of acetate within the cellulolytic hindguts of termites alone (Drake *et al.*, 2008). Although the overall worldwide turnover of acetate must be greater than this, measuring actual total turnover may not be tractable (Drake *et al.*, 2008). Suffice to say that along with CO_2, acetate represents the major product of carbon fermentation. That acetate is not entirely oxidised to CO_2 reflects a lack of energetic motivation to do so during anaerobiosis where in the absence of terminal electron acceptors (e.g. sulfates, nitrates), bacteria must engage in syntrophy with a hydrogen consumer in order to further oxidise acetate, and even then the yield remains low as detailed above. Accumulation of acetate can inhibit AD reactors**,** through physiological inhibition due to decreased pH (Delbes *et al.*, 2000; FitzGerald *et al.*, 2015), or due to inhibited equilibria, where further feedstock catabolism and acetogenesis becomes unfavourable due to the high concentration of the acetate product already present (Fukuzaki *et al.*, 1990; Stams and Plugge, 2009). Conversely, acetate is thought to be the major substrate worldwide for methanogenesis (Drake *et al.*, 2013), and so represents a major resource for biogas production. In reality, the majority of this acetoclastic methanogenesis occurs in areas that are impractical for biogas due to accessibility (ocean-floor sediments), scale (within vegetative matter, animal gut tracts etc.) or rate (beneath permafrosts). In AD systems for biogas production, acetate can be exploited when digesting substrates that decompose rapidly to produce large volumes of volatile fatty acids (VFA) (i.e. 'high-energy' substrates), ultimately leading to large quantities of acetate which can support acetoclastic methanogens.

1.3.4 Stage 4: Methanogenesis

The archaea responsible for methane formation form a deeply-rooted mono-phyletic clade, with several shared features despite a variety of niche adaptations. All are obligate anaerobes, are obliged to form methane to produce energy, and all nest in the archaeal phylum *Euryarchaeota* near the halobacteria. In spite of their monophyletic lineage, they clearly diverge into at least six separate orders (*Methanobacetriales, Methanosarcinales, Methanococcales, Methanomicrobiales*, *Methanopyrales* and *Thermoplasmatales*) sharing less than 82% 16S similarity (Liu and Whitman, 2008), with additional members likely to be awaiting discovery. *Methanopyrales* is the most deeply rooting order (Nölling *et al.*, 1996; Yu *et al.*, 2017), containing a single hyperthermophilic taxon, repeatedly isolated from high-temperature ecosystems such as hot springs, geothermal fields and 'black smoker' ocean vents). *Methanobacteriales* also contains a number of notable thermophiles, while other orders are largely mesophilic or even psychrophilic. These phylogenetic orders can be consistently partitioned along metabolic and physiological grounds: as well as representing the most recent branch, *Methanosarcinales* is to date the only methanogen order containing cytochromes for energy conservation(Thauer *et al.*, 2008) and is also the only clade capable of independently utilising acetate (the 'acetoclastic' methanogens). The ability to metabolise acetate makes this order (in particular, the genus *Methanosarcina*) particularly useful in AD, as acetate accumulation can arise from heterogeneity in the feedstock or process instability elsewhere, rapidly causing further inhibition or failure. All other methanogens are considered 'hydrogenotrophic', and use CO_2, or in some cases can fix methyl groups from molecules like methanol or methylamines ('methylotrophic'), for energy metabolism (Whitman *et al.*, 2014). *Methanosphaera stadtmaniae* and *Methanomassiliicoccus lumiyensis* are novel exceptions, in that they cannot fix CO_2 and must rely on reduction of methanol (*M. stadtmaniae, M. luminyensis*) and trimethylamines (*M. luminyensis*). Interestingly, they represent

two of only three methanogen genera isolated so far from the human colon (Liu and Whitman, 2008; Dridi *et al.*, 2012; Vanderhaeghen *et al.*, 2015).

Methanogenesis is the focal point for the applied process of AD; however within the anaerobic environment it is the 'lowest common denominator' of an energy balance in conditions starved of alternative electron acceptors. The success of methanogens derives from their ability to use carbon as a terminal electron acceptor in a secure niche and in a manner that is energetically sustainable: unlike acetogenesis which can become self-limiting, the escape of methane from the digestate ensures the end product does not accumulate and inhibit further methanogenesis. As a result, methanogenesis can proceed, enabling digestion of acetate (acetoclasty) and creating the extremely low concentrations of hydrogen (10-100Pa) required to enable fermentation (Fukuzaki *et al.*, 1990; Schink, 1997; Stams and Plugge, 2009). Through removal of these highly oxidised (CO_2, CH_3COOH) and reduced (H_2) materials from the reactor environment, methanogens function as an organic 'sink' for low-potential electrons (Figure 2). As such, the true service provided by methanogens from a microbial ecology standpoint is not their formation of methane as a by-product, but rather their crucial role as facilitators of anaerobiosis in numerous ecological systems.

1.4 ANAEROBIC DIGESTION AS A FIELD OF ACTIVE RESEARCH

Despite delineation into the semi-canonical 'four stages', the processes of AD (hydrolysis, fermentation, acidogenesis, methanogenesis) occur dynamically and in parallel. The heterogeneity of solid substrates allows formation of micro-environments where concentrations of products or reactants may vary locally from other areas within the wider reactor. It can be imagined that such micro-environments afford different niches than would be found in an even distribution of planktonic cells, with metabolism focused on the immediate conditions to which the microbial populations

present are being exposed. In reality, the microbial groups described above are not partitioned into four distinct phases, but instead organise in communities which are best-suited to their metabolic capabilities. For example, hydrolysers are known to aggregate on the outside of cellulose fibrils (Artzi *et al.*, 2017), while microbes which use interspecies transfer of formate, hydrogen or electrons localise in close proximity, upon or near the substrate at hand (Stams and Plugge, 2009). Strict anaerobes for their part are known to localise to the anoxic interior of particles, while the outside may be colonised by more tolerant facultative anaerobes, allowing microbes to cooperate across various environmental niches (Liu and Whitman, 2008; Drake *et al.*, 2013).

These interactions, when combined with the phylogenetic and metabolic diversity of anaerobic communities, provide a huge scope for variety which is accentuated by variations in process setup and operation. To better understand the interactions central to anaerobic digestion, a number of molecular biology techniques are often used to give either compositional information on the populations present, functional information on the metabolic activity of the microbes present, or a combination of the two. Molecular methods usually begin with polymerase chain reaction (PCR), allowing specified nucleic acid sequences (usually genomic DNA) to be selectively amplified from sample material for further characterisation. These amplified sequences (amplicons) can be used in various ways, as discussed below in order of increasing complexity.

Before such a study commences, the most appropriate target nucleic acid sequences for the situation at hand are decided. The sequences provide a ‘marker’, and should be conserved enough to have a known incidence (number of copies) within all clades of interest, while also incorporating enough sequence variety to allow populations to be distinguished. Ideally, divergence in marker sequences should also consistently reflect phylogenetic distance, providing a measure of relation for

community members. By far the most popular sequences used in microbial ecology are those from the 16S ribosomal subunit gene, which is homologous across known prokaryotes (Klindworth *et al*., 2012). Although use of the 16S subunit sequences has some limitations (Eloe-Fadrosh *et al*., 2016; Pinto and Raskin, 2012; Větrovský and Bladrian, 2013; Wilkins *et al*., 2015), their utility and popularity have revolutionised microbial ecology, greatly expanding our knowledge of the microbial kingdom and its interactions with other organisms (Moissl *et al*., 2008; Huttenhower *et al*., 2012; McKenny *et al*, 2015; Hammer *et al.*, 2017; Thompson *et al*., 2017).

Preliminary community investigations can be carried out using simple presence/absence tests via PCR to indicate whether a clade or metabolic function is present, irrespective of activity or abundance. This can be a useful diagnostic if a population is tightly linked to a given metabolic activity or ecological role (e.g. assaying for the methane-forming gene *mcrA* methanogens in the gastro-intestinal tract; assaying for genes related to direct interspecies electron transfer (DIET); assaying for nitrogenases in the rhizosphere), allowing presence to be earmarked or ruled out. Once amplified from a sampled environment, the next step is often to determine whether the marker sequence represent a homogenous population, or a community of sequences. The success of this step is strongly affected by the chosen marker sequence, as differentiation of community components requires observable and consistent differences in the amplicons produced. A number of techniques have been developed to differentiate amplicons based on sequence composition: two methods which do not require sequence information are restriction fragment-length polymorphism (RFLP), and denaturing gradient gel electrophoresis (DGGE). Both allow sequence diversity to be visualised in a reproducible manner, differentiating variants based on the pattern of restriction enzyme recognition sites in the sequence (RFLP) or variation in the self-annealing strengths of different amplicon sequences (DGGE). In either technique, a signature banding pattern is produced through

electrophoresis which allows community structure to be compared between timepoints, locations, or treatments.

Increasingly, the emphasis has shifted to identifying populations in order to draw conclusions about the functional role and importance of different community members. Investigations through DGGE and/or RFLP are greatly improved when visualised amplicons can be assigned a solid identity, for later reference and comparability between studies. Use of 'dideoxy', 'chain-termination', 'Sanger', 'classic', or 'first generation' sequencing has been an indispensable tool in determining sequence composition, allowing reference databases of function and taxonomy to be established. In microbial ecology, classical sequencing is often carried out through construction of a marker gene (e.g. 16S) clone library, where DNA is ligated into a plasmid vector, to be amplified within a host prior to 'classical' sequencing. Each sequence ligated into a vector represents a single observation of the marker sequence from the environment being studied, allowing low-throughput identification of sequences isolated through other techniques (e.g. major electrophoresis bands from RFLP or DGGE), of sampling amplicon populations produced through PCR, or of size-sorted, purified environmental DNA.

When relatively short sequences (<1000bp) are required to distinguish between amplicons (as in microbial ecology), sequence lengths generated through clone libraries are often adequate (ABI 3730 platform: 400-900bp read length). However, throughput of cloning (the volume of sampled sequences) is low, which restricts total sampling. Sequencing depth (number of times a specific base position is determined) can also be as low as 1, rendering small phylogenetic differences (e.g. single nucleotide polymorphisms) indistinguishable from sequencing artefacts.

Building on classical approaches and a need for more affordable technologies, new types of sequencing become available early this century, providing sequence outputs of millions (e.g. 20Mb, 454 Genome Sequencer, 2005; 500Mb, PacBio RS II, 2014), billions (e.g. 15Gb, Illumina MiSeq, 2011),

and more recently trillions (1.8Tb, Illumina HiSeq X Platform) of base-pairs (van Dijk *et al.*, 2014). Depending on the application, this increased volume provides increases in the sequence length (up to 20kb/read in PacBio) or increases the number of sequence reads generated up to 25 million reads/run in Illumina) (van Dijk *et al.*, 2014). The latter approach is particularly powerful when determining microbial community composition, where the large volume of short sequences allows more extensive sampling of the ecosystem in question. These 'deep' studies provide two major advantages over earlier outlooks on microbial ecology: firstly, they provide a window into the prevalence of low-abundance marker sequences, allowing us to catalogue rare community members. Secondly, larger libraries allow sequencing errors to be better modelled and corrected (Callahan *et al.*, 2016), giving more accurate reconstructions of the actual community sequence composition (see Chapter, 5 Section 1.2). Correcting for sequencing artefacts in this way allows a greater comparability between samples, but also between independent studies which would otherwise be partitioned by variation in the sequencing process. Perhaps the most significant improvement provided by second generation sequencing is the breadth of sampling now possible: instead of investigating a single location or comparing observations from two events, tens or hundreds of samples can be compared within a single study (Huttenhower *et al.*, 2012; McKenny *et al.*, 2015; Thompson *et al.*, 2017; Hammer *et al.*, 2017). This increase in scope allows more complex comparisons to be made, and more robust statistical conclusions to be drawn about how microbial communities differ between conditions.

Several draw-backs remain in community profiling through marker sequences. As mentioned previously, the marker sequence used has a fundamental bearing on the image of community composition that will be produced. This is especially relevant when applying second-generation sequencing to marker sequences like 16S, where compromises in read length versus throughput (e.g. ABI 3730DA: 400-900bp x96 capillaries; 454 GS FLX: 400-500bp x 1 million reads; Illumina MiSeq

Paired-End: 350bp x 25 million reads) reduce the phylogenetic information available, therefore reducing the capacity to distinguish between sequences from different sources.

Another limitation in community sequencing is the gap that must be bridged between a sequence's taxonomic identity and the metabolic activities observed in that ecosystem. Given the enormous variety of microbial life, the meagre portion that have been physiologically characterised, and the possible variation in gene content and expression, determining the actual metabolic activities of a community based solely on taxonomy is not possible. In some cases, activities can be directly assigned to functional populations with well defined roles: methanogenic archaea are a good example of such a group, as methanogenesis is limited to this clade. Although such connections are informative, cataloguing all possible metabolisms from a community marker study in this way quickly becomes impractical, especially when only a fraction of the thousands of encountered taxa have been thoroughly characterised. An attractive alternative for population marker studies is the use of inferential metabolomics through programs such as PICRUSt (Langille *et al.*, 2013). These programs calculate the phylogeny between observed taxa and annotated genomes, allowing a phylogenetic distance-based estimate of metabolic capabilities within the dataset. The inferred metabolic datasets produced can provide great insight into how microbes and their environment interact (see Chapter 2, Section 3.6.2 for further examples).

Many methods have been developed to directly relate microbial metabolism and ecology. Although not used in this work, such methods give invaluable information on actual metabolic activity, directly determining ecological functions. Relatively simple tests can be carried out by assaying a metabolic activity, such as measuring rates of substrate conversion (e.g. formate uptake in a sulphur-reducing model; Urschel *et al.*, 2016) or product formation (e.g. phosphatase-linked release of p-nitrophenyl; Tabatabai *et al.*, 1969) under defined conditions. Improved insight into metabolic pathways can be

given through the use of isotope labelling, where substrates are doped with known quantities of tracable isotopes (e.g. C^{13} or C^{14} instead of C^{12}, or N^{15} instead of N^{14}) in place of the more common isotopes. When the cell is interrupted and its contents analysed (through radiography in the case of radio-isotope labelling, or nuclear magnetic resonance in the case of stable isotope labelling), the progress of these isotopes through the cell can be used to determine the metabolic pathways in operation (e.g. competitive inhibition of autotrophy by use of formate as an energy and carbon source; Urschel *et al.*, 2016). Similar to microbial community analysis, high-throughput sequencing has also revolutionised metabolomics, with sequencing of complemented messenger RNA allowing actual gene expression to be determined, highlighting important metabolic activities ("RNA-seq"). Alternatively, messenger RNA can be extracted from the ribosomes, providing a focused image of translation activity in the cell (Ribo-seq). When applied to metagenomic RNA extracts, these techniques give an image of gene expression across an ecosystem and can be related to changes in function or process.

Many studies have used these technologies to explore the relationships between community components and the operation of biogas reactors; Sundberg *et al.* (2013) compared community composition between 21 reactors, and showed through multivariate analysis that different substrates (e.g. waste from food, municipal, or slaughterhouse sources) and operation temperatures (mesophilic, thermophilic) encourage specific AD communities; Goux *et al.* (2015) used 16S Illumina sequencing to show the influence of reactor parameters on community composition in monodigestion, through induced inhibition and recovery of biogas function via reactor over-feeding; using 16S Illumina sequencing again, Goux *et al.* (2016) also characterised the biogas community dynamics during acclimatisation and establishment of a mesophilic reactor, highlighting the influence of process variables on community structure; Cai *et al.* (2017) demonstrated the efficacy of

supplementing micronutrients to accelerate VFA consumption and methane production, with implications for diversity and biogas output. While biogas processes can be informed and even directed by observations in microbial ecology (Carballa *et al.*, 2015), AD communities have also become a model system to further develop aspects of microbial and molecular ecology: Wilkins *et al.* (2015) combined pyrosequencing of archaeal 16S ribosomal subunit variants and methanogen reductase mcrA subunit variants to characterise methanogen populations in sludge/waste-water digesters, indicating a greater diversity in methane metabolism (mcrA) than indicated by archaeal community composition (16S); in a two-step AD setup digesting lingo-cellulosics, Lebuhn *et al.* (2014) showed 16S pyrosequencing and metagenomic sequencing of AD communities produced community profiles which were in agreement, with 16S sequencing allowing improved taxonomic resolution; Fischer *et al.* (2016) used biogas communities as a test-bed for developing and evaluating bacteria- and archaeal-specific primers, while Leng *et al.* (2018) approach the thermodynamic limits of microbial life through consideration of metabolisms central to anaerobic digestion.

Research in microbiology and biogas continue to provide insights, due in part both to the metabolic and phylogenetic diversity of anaerobic microbes, and the variety of AD configurations being trialled. However, a third factor in advancing the microbial ecology of AD is the rapid progress in primer design, next generation sequencing (NGS) technologies, and development of improved bioinformatic pipelines with which to analyse sequence data. These factors allow our understanding of the microbial populations present in AD systems to continue expanding, revealing 'new' microbial community features and interactions. Although the function or mechanism of these features are not always clear, further study can provide clues as to their potential roles within AD. As a result, microbial ecology's perspective on biogas continues to change.

Biogas production through anaerobic digestion is not a recent discovery, but rather a process that is continuously re-imagined by engineers and microbiologists to address current requirements in renewable energy and sustainability. The work presented in this thesis characterises the microbial ecology underlying a number of biogas setups designed for the current Irish energy landscape, and addresses how these industrial-process microcosms can be best managed to maximise both sustainable output and operation. Communities digesting macro-algae (*Ulva lactuca*), dairy slurries, grass silage (*Lolium perenne*), and synthetic gas/media mixes were characterised using both 'classic' and 'next generation' techniques. The influences of abiotic factors (i.e. reactor parameters) on community structure were assessed, with particular attention focusing on biogas output and the organic: inorganic carbon ratio (a.k.a. 'FOS:TAC'; Nordmann, 1977), which acted as a proxy for 'good' community function during reactor operation. In each study setup, the goal was to identify the major functional microbial populations associated with biogas productivity and identify how shifts in operational parameters related to changes in community structure; in particular changes which are statistically significant and biologically meaningful. Based on these patterns of community and environmental conditions, the roles of key populations and metabolic activities were extrapolated, and bottlenecks in the biogas process were identified which should provide avenues for further research.

2. References

1. Abbasi, T., Tauseef, S.M., and Abbasi, S.A. (2012) A Brief History of Anaerobic Digestion and "Biogas." In, *Biogas Energy*, SpringerBriefs in Environmental Science. Springer, New York, NY, pp. 11–23.

2. Artzi, L., Bayer, E.A., and Moraïs, S. (2017) Cellulosomes: bacterial nanomachines for dismantling plant polysaccharides. *Nat. Rev. Microbiol.* **15**: 83–95.

3. Cai, Y., Hua, B., Gao, L., Hu, Y., Yuan, X., Cui, Z., et al. (2017) Effects of adding trace elements on rice straw anaerobic mono-digestion: Focus on changes in microbial communities using high-throughput sequencing. *Bioresour. Technol.* **239**: 454–463.

4. Callahan, B.J., McMurdie, P.J., Rosen, M.J., Han, A.W., Johnson, A.J.A., and Holmes, S.P. (2016) DADA2: High-resolution sample inference from Illumina amplicon data. *Nat Meth* **13**: 581–583.

5. Carballa, M., Regueiro, L., and Lema, J.M. (2015) Microbial management of anaerobic digestion: exploiting the microbiome-functionality nexus. *Curr. Opin. Biotechnol.* **33**: 103–111.

6. Carrere, H., Antonopoulou, G., Affes, R., Passos, F., Battimelli, A., Lyberatos, G., and Ferrer, I. (2016) Review of feedstock pretreatment strategies for improved anaerobic digestion: From lab-scale research to full-scale application. *Bioresour. Technol.* **199**: 386–397.

7. Chen, Y., Cheng, J.J., and Creamer, K.S. (2008) Inhibition of anaerobic digestion process: A review. *Bioresour. Technol.* **99**: 4044–4064.

8. Delbes, C., Moletta, R., and Godon, J.-J. (2000) Monitoring of activity dynamics of an anaerobic digester bacterial community using 16S rRNA polymerase chain reaction–single-strand conformation polymorphism analysis. *Environ. Microbiol.* **2**: 506–515.

9. van Dijk, E.L., Auger, H., Jaszczyszyn, Y., and Thermes, C. (2014) Ten years of next-generation sequencing technology. *Trends in Genetics* **30**: 418–426.

10. Drake H., Gößner A., and Daniel S. (2008) Old Acetogens, New Light. *Ann. N. Y. Acad. Sci.* **1125**: 100–128.

11. Drake, H.L., Küsel, K., and Matthies, C. (2013) Acetogenic Prokaryotes. In, Rosenberg,E., DeLong,E.F., Lory,S., Stackebrandt,E., and Thompson,F. (eds), *The Prokaryotes*. Springer Berlin Heidelberg, Berlin, Heidelberg, pp. 3–60.

12. Dridi, B., Fardeau, M.-L., Ollivier, B., Raoult, D., and Drancourt, M. (2012) Methanomassiliicoccus luminyensis gen. nov., sp. nov., a methanogenic archaeon isolated from human faeces. *Int. J. Syst. Evol. Microbiol.* **62**: 1902–1907.

13. Drosg, B. (2013) Process monitoring in biogas plants. *IEA Bioenergy.*

14. Eloe-Fadrosh, E.A., Ivanova, N.N., Woyke, T., and Kyrpides, N.C. (2016) Metagenomics uncovers gaps in amplicon-based detection of microbial diversity. *Nature Microbiology* **1**: 15032.

15. Ermler, U., Grabarse, W., Shima, S., Goubeaud, M., and Thauer, R.K. (1997) Crystal Structure of Methyl-Coenzyme M Reductase: The Key Enzyme of Biological Methane Formation. *Science* **278**: 1457–1462.

16. European Parliament and European Council (2015) Directive (EU) 2015/1513: Amending Directive 98/70/EC relating to the quality of petrol and diesel fuels and amending Directive 2009/28/EC on the promotion of the use of energy from renewable sources.

17. European Parliament and European Council (2009) Directive 2009/28/EC: on the promotion of the use of energy from renewable sources and amending and subsequently repealing Directives 2001/77/EC and 2003/30.

18. Fischer, M.A., Güllert, S., Neulinger, S.C., Streit, W.R., and Schmitz, R.A. (2016) Evaluation of 16S rRNA Gene Primer Pairs for Monitoring Microbial Community Structures Showed High Reproducibility within and Low Comparability between Datasets Generated with Multiple Archaeal and Bacterial Primer Pairs. *Front. Microbiol.* **7**:.

19. FitzGerald, J.A., Allen, E., Wall, D.M., Jackson, S.A., Murphy, J.D., and Dobson, A.D.W. (2015) Methanosarcina Play an Important Role in Anaerobic Co-Digestion of the Seaweed Ulva lactuca: Taxonomy and Predicted Metabolism of Functional Microbial Communities. *PLoS ONE* **10**: e0142603.

20. Fukuzaki, S., Nishio, N., Shobayashi, M., and Nagai, S. (1990) Inhibition of the Fermentation of Propionate to Methane by Hydrogen, Acetate, and Propionate. *Appl. Environ. Microbiol.* **56**: 719–723.

21. Gottschalk, G. and Thauer, R.K. (2001) The Na+-translocating methyltransferase complex from methanogenic archaea. *Biochim. Biophys. Acta BBA - Bioenerg.* **1505**: 28–36.

22. Goux, X., Calusinska, M., Fossépré, M., Benizri, E., and Delfosse, P. (2016) Start-up phase of an anaerobic full-scale farm reactor - Appearance of mesophilic anaerobic conditions and establishment of the methanogenic microbial community. *Bioresour. Technol.* **212**: 217–226.

23. Goux, X., Calusinska, M., Lemaigre, S., Marynowska, M., Klocke, M., Udelhoven, T., et al. (2015) Microbial community dynamics in replicate anaerobic digesters exposed sequentially to increasing organic loading rate, acidosis, and process recovery. *Biotechnol. Biofuels* **8**: 122.

24. Güllert, S., Fischer, M.A., Turaev, D., Noebauer, B., Ilmberger, N., Wemheuer, B., et al. (2016) Deep metagenome and metatranscriptome analyses of microbial communities affiliated with an industrial biogas fermenter, a cow rumen, and elephant feces reveal major differences in carbohydrate hydrolysis strategies. *Biotechnol. Biofuels* **9**: 121.

25. Hammer, T.J., Janzen, D.H., Hallwachs, W., Jaffe, S.P., and Fierer, N. (2017) Caterpillars lack a resident gut microbiome. *Proc Natl Acad Sci U S A* **114**: 9641–9646.

26. Hanreich, A., Schimpf, U., Zakrzewski, M., Schlüter, A., Benndorf, D., Heyer, R., et al. (2013) Metagenome and metaproteome analyses of microbial communities in mesophilic biogas-producing anaerobic batch fermentations indicate concerted plant carbohydrate degradation. *Syst. Appl. Microbiol.* **36**: 330–338.

27. Herschy, B., Whicher, A., Camprubi, E., Watson, C., Dartnell, L., Ward, J., et al. (2014) An Origin-of-Life Reactor to Simulate Alkaline Hydrothermal Vents. *J. Mol. Evol.* **79**: 213–227.

28. Huttenhower, C., Gevers, D., Knight, R., Abubucker, S., et al. (2012) Structure, function and diversity of the healthy human microbiome. *Nature* **486**: 207–214.

29. Jiménez, D.J., Dini-Andreote, F., and van Elsas, J.D. (2014) Metataxonomic profiling and prediction of functional behaviour of wheat straw degrading microbial consortia. *Biotechnol. Biofuels* **7**: 92.

30. Kanehisa, M., Goto, S., Sato, Y., Kawashima, M., Furumichi, M., and Tanabe, M. (2014) Data, information, knowledge and principle: back to metabolism in KEGG. *Nucleic Acids Res.* **42**: D199–D205.

31. Klindworth, A., Pruesse, E., Schweer, T., Peplies, J., Quast, C., Horn, M., and Glöckner, F.O. (2012) Evaluation of general 16S ribosomal RNA gene PCR primers for classical and next-generation sequencing-based diversity studies. *Nucl. Acids Res.* gks808.

32. Langille, M.G.I., Zaneveld, J., Caporaso, J.G., McDonald, D., Knights, D., Reyes, J.A., et al. (2013) Predictive functional profiling of microbial communities using 16S rRNA marker gene sequences. *Nat Biotech* **31**: 814–821.

33. Lebuhn, M., Hanreich, A., Klocke, M., Schlüter, A., Bauer, C., and Pérez, C.M. (2014) Towards molecular biomarkers for biogas production from lignocellulose-rich substrates. *Anaerobe* **29**: 10–21.

34. Leng, L., Yang, P., Singh, S., Zhuang, H., Xu, L., Chen, W.-H., et al. (2018) A review on the bioenergetics of anaerobic microbial metabolism close to the thermodynamic limits and its implications for digestion applications. *Bioresour. Technol.* **247**: 1095–1106.

35. Liu, Y. and Whitman, W.B. (2008) Metabolic, Phylogenetic, and Ecological Diversity of the Methanogenic Archaea. *Ann. N. Y. Acad. Sci.* **1125**: 171–189.

36. Martin William F. (2011) Hydrogen, metals, bifurcating electrons, and proton gradients: The early evolution of biological energy conservation. *FEBS Lett.* **586**: 485–493.

37. McCabe, B.K. and Schmidt, T. (2018) Integrated biogas systems. *IEA Bioenergy*: Task 37: 5

38. McKenney, E.A., Rodrigo, A., and Yoder, A.D. (2015) Patterns of Gut Bacterial Colonization in Three Primate Species. *PLoS One* **10**: (5) e0124618.

39. Moissl, C., Bruckner, J.C., and Venkateswaran, K. (2008) Archaeal diversity analysis of spacecraft assembly clean rooms. *The ISME journal* **2**: 115.

40. Nölling, J., Elfner, A., Palmer, J.R., Steigerwald, V.J., Pihl, T.D., Lake, J.A., and Reeve, J.N. (1996) Phylogeny of Methanopyrus kandleri based on methyl coenzyme M reductase operons. *Int. J. Syst. Bacteriol.* **46**: 1170–1173.

41. Nordmann, W. (1977) Die Überwachung der Schlammfaulung. KA-Informationen für das Betriebspersonal, Beilage zur Korrespondenz Abwasser.

42. O'Brien, F. (1999) The best of Myles. *Dalkey Archive Press*, Dublin, Ireland.

43. Pinto, A.J. and Raskin, L. (2012) PCR Biases Distort Bacterial and Archaeal Community Structure in Pyrosequencing Datasets. *PLOS ONE* **7**: e43093.

44. Rimbault, A., Niel, P., Virelizier, H., Darbord, J.C., and Leluan, G. (1988) l-Methionine, a Precursor of Trace Methane in Some Proteolytic Clostridia. *Appl. Environ. Microbiol.* **54**: 1581–1586.

45. Sawin, J.L., Sverrisson, F., Seyboth, K., Adib, R., Murdock, H.E., Lins, C., et al. (2017) Renewables 2017 Global Status Report. *Int. Nuclear Information Sys **48**:27.*

46. Schink, B. (1997) Energetics of syntrophic cooperation in methanogenic degradation. *Microbiol. Mol. Biol. Rev.* **61**: 262–280.

47. Stams, A.J.M. and Plugge, C.M. (2009) Electron transfer in syntrophic communities of anaerobic bacteria and archaea. *Nat. Rev. Microbiol.* **7**: 568–577.

48. Sun, Q., Li, H., Yan, J., Liu, L., Yu, Z., and Yu, X. (2015) Selection of appropriate biogas upgrading technology-a review of biogas cleaning, upgrading and utilisation. *Renew. Sustain. Energy Rev.* **51**: 521–532.

49. Sundberg, C., Al-Soud, W.A., Larsson, M., Alm, E., Yekta, S.S., Svensson, B.H., et al. (2013) 454 pyrosequencing analyses of bacterial and archaeal richness in 21 full-scale biogas digesters. *FEMS Microbiol. Ecol.* **85**: 612–626.

50. Tabatabai, M.A. and Bremner, J.M. (1969) Use of p-nitrophenyl phosphate for assay of soil phosphatase activity. *Soil Biology and Biochemistry* **1**: 301–307.

51. Thauer, R.K. (1998) Biochemistry of methanogenesis: a tribute to Marjory Stephenson:1998 Marjory Stephenson Prize Lecture. *Microbiology* **144**: 2377–2406.

52. Thauer, R.K., Jungermann, K., and Decker, K. (1977) Energy conservation in chemotrophic anaerobic bacteria. *Bacteriol. Rev.* **41**: 100–180.

53. Thauer, R.K., Kaster, A.-K., Seedorf, H., Buckel, W., and Hedderich, R. (2008) Methanogenic archaea: ecologically relevant differences in energy conservation. *Nat. Rev. Microbiol.* **6**: 579–591.

54. Thompson, L.R., Sanders, J.G., McDonald, D., Amir, A., Ladau, J., Locey, K.J., et al. (2017) A communal catalogue reveals Earth's multiscale microbial diversity. *Nature* **551**:7681.

55. Urschel, M.R., Hamilton, T.L., Roden, E.E., and Boyd, E.S. (2016) Substrate preference, uptake kinetics and bioenergetics in a facultatively autotrophic, thermoacidophilic crenarchaeote. *FEMS Microbiol Ecol* **92**:5:fiw069.

56. Vanderhaeghen, S., Lacroix, C., and Schwab, C. (2015) Methanogen communities in stools of humans of different age and health status and co-occurrence with bacteria. *FEMS Microbiol. Lett.* **362**: fnv092.

57. Whitman, W.B., Bowen, T.L., and Boone, D.R. (2014) The Methanogenic Bacteria. In, Rosenberg,E., DeLong,E.F., Lory,S., Stackebrandt,E., and Thompson,F. (eds), *The Prokaryotes*. Springer Berlin Heidelberg, Berlin, Heidelberg, pp. 123–163.

58. Wilkins, D., Lu, X.-Y., Shen, Z., Chen, J., and Lee, P.K.H. (2015) Pyrosequencing of mcrA and Archaeal 16S rRNA Genes Reveals Diversity and Substrate Preferences of Methanogen Communities in Anaerobic Digesters. *Appl. Environ. Microbiol.* **81**: 604–613.

59. Větrovský, T. and Baldrian, P. (2013) The Variability of the 16S rRNA Gene in Bacterial Genomes and Its Consequences for Bacterial Community Analyses. *PLoS ONE* **8**: e57923.

60. Yu, Z., Ma, Y., Zhong, W., Qiu, J., and Li, J. (2017) Comparative Genomics of Methanopyrus sp. SNP6 and KOL6 Revealing Genomic Regions of Plasticity Implicated in Extremely Thermophilic Profiles. *Front. Microbiol.* **8**: 1278.

61. Yutin, N. and Galperin, M.Y. (2013) A genomic update on clostridial phylogeny: Gram-negative spore formers and other misplaced clostridia: Genomics update. *Environ. Microbiol.* **15**: 2631–2641.

Chapter 2

Methanosarcina play an important role in Anaerobic Co-Digestion of the Seaweed *Ulva lactuca* : Taxonomy and Predicted Metabolism of Functional Microbial Communities.

Jamie A. FitzGerald[1,2,4], Eoin Allen[1,3,4], David M. Wall[1,3,4], Stephen A. Jackson[1,2], Jerry D. Murphy[1,3,4], Alan D.W. Dobson[1,2]

[1] *Environmental Research Institute, University College Cork, Lee Road, Cork, Ireland*

[2] *School of Microbiology, University College Cork, Cork, Ireland*

[3] *School of Engineering, University College Cork, Cork, Ireland*

[4] *Marine Renewable Energy Ireland (MaREI) Centre, Ireland .*

This chapter has been previously published under the same title in the journal *PLoS ONE*, **10**: e0142603 and is available at http://dx.doi.org/10.1371/journal.pone.0142603.

ABSTRACT

Macro-algae represent an ideal resource of third generation biofuels, but their use necessitates a refinement of commonly used anaerobic digestion processes. In a previous study, contrasting mixes of dairy slurry and the macro-alga *Ulva lactuca* were anaerobically digested in mesophilic continuously stirred tank reactors for 40 weeks. Higher proportions of *U. lactuca* in the feedstock led to inhibited digestion and rapid accumulation of volatile fatty acids, requiring a reduced organic loading rate. In this study, 16S pyrosequencing was employed to characterise the microbial communities of both the weakest (R1) and strongest (R6) performing reactors from the previous work as they developed over a 39 and 27-week period respectively. Comparing the reactor communities revealed clear differences in taxonomy, predicted metabolic orientation and mechanisms of inhibition, while constrained canonical analysis (CCA) showed ammonia and biogas yield to be the strongest factors differentiating the two reactor communities. Significant biomarker taxa and predicted metabolic activities were identified for viable and failing anaerobic digestion of *U. lactuca*. Acetoclastic methanogens were inhibited early in R1 operation, followed by a gradual decline of hydrogenotrophic methanogens. Near-total loss of methanogens led to an accumulation of acetic acid that reduced performance of R1, while a slow decline in biogas yield in R6 could be attributed to inhibition of acetogenic rather than methanogenic activity. The improved performance of R6 is likely to have been as a result of the large *Methanosarcina* population, which enabled rapid removal of acetic acid, providing favourable conditions for substrate degradation.

1. Introduction

While primarily a waste-treatment strategy, Anaerobic Digestion (AD) is increasingly being implemented as a viable renewable-energy technology, capable of converting diverse organic substrates into biofuels. In this respect, there is renewed interest in the use of seaweeds (macro-algae) as a substrate for biofuel production (Dave *et al.*, 2013; Vanegas and Bartlett, 2013), though some technical problems associated with their use still need to be resolved (Rodriguez *et al.*, 2015).

In contrast to plants, seaweeds possess lower quantities of recalcitrant structural polymers (e.g. lignin, cellulose, hemi-cellulose), contain large reserves of accessible carbohydrates, and produce biomass via a rapid life cycle. However, they also possess unique compounds. *U. lactuca* can yield high levels of protein, sulphur and nitrogen; seaweeds typically also contain excess marine salts (Percival, 1979; Briand and Morand, 1997; Wong and Cheung, 2000; Morand and Merceron, 2005; Allen *et al.*, 2013). To improve biogas yields, pre-treatments, co-digestion, and alternative reactor configurations have been investigated for seaweeds (Rodriguez *et al.*, 2015). Efficient management of AD via process parameters can also improve biogas yields, as well as helping to avoid toxic shock (e.g. rapid changes in pH, ammonia etc.), accumulation of intermediates (e.g. volatile fatty acids), or over/under-feeding of the reactor (i.e. maintaining an appropriate organic loading rate). However, these parameters provide only indirect information on biological processes within the reactor, and often must be re-evaluated at each new application, restricting informative comparisons and potentially obscuring underlying processes.

Recent reports have highlighted the need for microbial indicators of optimal AD performance as a prerequisite to allow “microbial-based management” of the process (Koch *et al.*, 2014; Carballa *et al.*, 2015). Thorough characterisation and a greater understanding of microbial populations and processes “driving” AD can better inform the design and operation of biogas reactors treating macro-algae and

other novel feedstocks. Identifying these 'indicators' has been greatly aided by the use of molecular sequencing technologies, allowing metagenomic-based analyses of microbial community structures in various AD systems. These approaches have successfully been employed to monitor the development of AD communities over time (St-Pierre and Wright, 2013; Solli *et al.*, 2014), identify core motifs in AD community structure (Sundberg *et al.*, 2013), and determine dominant methanogenic pathways which can be correlated to biogas yield (Wilkins *et al.*, 2015). Previous metagenomic studies on the use of algae as a biogas substrate have identified increases in the archaeal methanogenic order *Methanosarcinales* under addition of the macro-alga *Saccharina latissima* (Pope *et al.*, 2013), the importance of *Methanosarcinales* in supporting diverse metabolic pathways in AD of the micro-alga *Scenedesmus obliquus* (Wirth *et al.*, 2015), and the importance of retaining methanogenic *Archaea* in AD of the macro-alga *Laminaria hyperborea* (Hinks *et al.*, 2013).

In a previous study, Allen and co-workers approached difficulties in digesting the macro-alga *Ulva lactuca* (sea-lettuce) through co-digestion with the proven and abundant substrate, dairy slurry. Six *U. lactuca*-slurry feedstock ratios were trialled over a nine-month period, with five of the reactors (R1 through R5) encountering total or partial inhibition through overloading of volatile fatty acids (VFAs), which was dependant on the quantity of *U. lactuca* supplied (Allen *et al.*, 2014). A sixth reactor (R6) saw no immediate inhibition, but instead demonstrated a slow decline in biogas yield, which could not be explained through process variables (Allen *et al.*, 2014). Here, we present a microbial analysis of these trials, investigating how AD of *U. lactuca* shaped archaeal and bacterial populations in the best (R6) and worst (R1) performing reactors, with a particular focus on methanogenic processes. A taxonomic time-series was constructed which illustrates how microbial community structure and activity diverged between R1 and R6, suggesting two explanations for loss of methanogenic activity and a mechanism for *Methanosarcina* improving reactor stability.

Constrained canonical analysis (CCA) revealed the most significant effects of *U. lactuca* on microbial community structure and on predicted metabolic activity. To our knowledge, this is the first application of 'next-generation' 16S community sequencing to monitor microbial community structures involved in anaerobic digestion of green seaweeds (*Chlorophyta*).

2. Materials and Methods

2.1 Biogas reactor configuration.

A total of six, 5L one-step continuously stirred-tank reactors (CSTRs) were operated in parallel digesting mixes of *Ulva lactuca* and dairy slurry for a period up to 42 weeks at a constant temperature of 37°C. Three reactors treated dried *U. lactuca* in co-digestion mixes of 25, 50 and 75% with dairy slurry. A further 3 reactors co-digested fresh *U. lactuca* with slurry in the same ratios. Regular feeding and removal of substrate allowed a constant 4 L working volume, with an initial organic loading rate (OLR) of 2 kg VS m^3 d^{-1}. The wet weight of this substrate was also used to determine a hydraulic retention time (HRT) of 49 days. Of the 6 reactors, 3 failed to obtain steady state biogas production, 2 achieved steady state production profiles but incurred high levels of VFA-based inhibition, while the final reactor achieved satisfactory yields. Inhibition was characterised by variable levels of VFA and biogas yield, and an inability to maintain high rates of substrate input. Previous work (Allen *et al.*, 2013) assessing the optimal bio-methane potentials (BMP) for *U. lactuca*/slurry feedstocks allowed evaluation of reactor output.

Reactor 1 (R1: digesting 75% dried *U. lactuca*, 25% dairy slurry) provided the longest running example of *U. lactuca*-inhibited digestion, while Reactor 6 (R6: digesting 25% fresh *U. lactuca*, 75% dairy slurry) was the best performing reactor, with stable VFA concentrations and favourable yields at an OLR of 2.5 kg VS m^3 d^{-1}. R1 and R6 were subsequently chosen as best and worst case examples of *U. lactuca* co-digestion. Reactor R1 was operated for a total of 40 weeks. Initially an OLR of 2 kg VS m^3 d^{-1} and a HRT of 49 days was used for R1, however failure to reach the designated yields after the first HRT and the increase in VFA concentration resulted in the OLR being reduced to 1 kg VS m^3 $d^{-1}$and a HRT of 63 days, with subsequent steady-state biogas production being achieved. R6 was also operated for 40 weeks. An OLR of 2 kg VS m^3 d^{-1} and a HRT of 49 days was successfully maintained in R6 for a period of

3 HRTs, with OLR then being increased to 2.5 kg VS m^3 d^{-1}, decreasing the HRT to 42 days. Steady state biogas production was achieved throughout this period. A gradual decline was observed in the final HRT for R6 without a corresponding increase in VFA or ammonia concentrations accounting for this reduction (Allen *et al.*, 2014). The decision to increase OLR was determined by two factors: the relationship between VFA concentrations and reactor performance, and the biomethane conversion efficiency (B_{eff}). The effect of VFAs was determined using the Nordmann method (Nordmann, 1977) commonly known as the FOS:TAC ratio, measuring volatile organic acids and total inorganic carbonate. Operational ranges set out by this method dictate whether the reactor is being over, under or fed satisfactorily. The biomethane conversion efficiency (B_{eff}) is the specific methane yield (SMY) of that reactor in continuous digestion divided by the biochemical methane potential (BMP) yield obtained from a 30 day batch test on that exact substrate. Values closer to or higher than 1 are desirable, reflecting optimum conversion of feedstock to biogas. A comprehensive detailing of the laboratory methods used to analyse all the environmental parameters within R1 and R6 has been previously described (Allen *et al.*, 2014)

.

2.2 Sampling and Molecular Methods

Reactor sludges were sampled on a weekly basis, and frozen at -80°C until further analysis. For R1, weeks 1, 5, 13, 20, 30 and 39 were selected as representative time-points, spanning five retention times. For R6, weeks 1, 5, 13, 21 and 27 were selected as time-points, spanning four retention times. Sludge from these 11 time-points was processed with the PowerSoil DNA extraction kit (MoBio, CA, USA) with the following protocol modifications: 1) initial 'wet-spin' (30 seconds at 10,000 g) to remove an excess liquid fraction prior to cell lysis; 2) 3x cycles of 10 minute bead-beating followed by 5 minutes chilling at -20°C; 3) 2x washes of elution buffer. For each time-point, triplicate sludge-samples

were taken from each reactor. From each of these, three separate DNA extractions were performed, and then combined in equimolar quantities to ensure representative sampling. Extractions were quantified spectrophotometerically (ND-1000, Thermo-Fisher, DE, USA) and viewed on 1% agarose gel with ethidium bromide (1µg/ml).

16S gene sequences were amplified from the DNA extracts using 11 pyrosequencing PCR primers with the following motifs: adapter sequence (Roche-454 Lib-A and Lib-B chemistry); key sequence (TCAG); Roche-454 pyrosequencing MIDs 1-10 and 12 inclusive; and 16S universal primers S-*-Univ-0789-a-S-18 (5' TAG ATA CCC SSG TAG TCC 3') and S-*-Univ-1053-a-A-16 (5' CTG ACG RCR GCC ATG C 3')(Baker *et al.*, 2003). A program of initial denaturation at 94°C for 5 minutes, followed by 26 cycles of 30 seconds denaturing at 95°C, 30 seconds annealing at 53°C, and 45 seconds of extension at 72°C, with a final extension step of 72°C held for 6 minutes was followed. Products in the expected size range were extracted using a gel extraction kit (QIAGEN, Manchester, UK), which required subsequent use of a PCR purification kit (QIAGEN, Manchester, UK). Each DNA extract was amplified in triplicate, then pooled in equimolar quantities to produce 11 community samples, which were then pyrosequenced by MACROGEN (Seoul, Republic of Korea).

2.3 Bioinformatic Analysis

Denoising was performed in Acacia (Bragg *et al.*, 2012) before import into the Quantitative Insights Into Microbial Ecology software pipeline (Caporaso, *et al.*, 2010b) for de-multiplexing, chimera removal, aligning, taxonomic assignment and exploratory analyses. Sequences were split into sample libraries; Chimera filtering was carried out using USEARCH v6.1 (Edgar, 2010); Alignments and taxonomic assignments were carried out with reference to the Silva 111 Database release (Quast *et*

al., 2013) at 97% similarity using PyNast (Caporaso *et al.*, 2010a) and the RDP Classifier 2.2 (Wang *et al.*, 2007); Tree building was carried out using FastTree (Price *et al.*, 2010). Beta diversity was calculated using UniFrac (Lozupone and Knight, 2005) and 3D PCoA plots generated by Emperor (Vázquez-Baeza *et al.*, 2013).

Sequence data was combined with reactor process data from (Allen *et al.*, 2014) within the *R* statistics program (R Core Team, 2013). *R* packages *vegan* (Oksanen *et al.*, 2014) and *phyloseq* (McMurdie and Holmes, 2013) were used to subset population abundances by sample and/or reactor environment, and to perform statistical analysis.

Greengenes release 13.5 (DeSantis *et al.*, 2006) was used to perform closed-reference OTU picking in QIIME prior to generating metabolic predictions from the Kyoto Encyclopedia of Genes and Genomes (KEGG; release 73.1, Kanehisa *et al.*, 2014) with the Phylogenetic Investigation of Communities by Reconstruction of Unobserved States (PICRUSt, Langille *et al.*, 2013) package. Significant differences between the two reactors were calculated using the LDA Effect Size (LEfSe) resource (Segata *et al.*, 2011). To reduce spurious inferences on metabolic activity, a more conservative LDA threshold of 3 was used.

Sequence data was deposited in the MG-RAST database under project number 14106, and is publicly available at the URL http://metagenomics.anl.gov/linkin.cgi?project=14106.

It should be noted that although primers used in this study (Baker *et al.*, 2003) continue to see use in similar investigations (Mhuantong *et al.*, 2015; Santana *et al.*, 2015; Zhang *et al.*, 2015), primers are continuously refined to increase coverage as observed microbial diversity expands. Similarly, methodologies that minimise bias (Green *et al.*, 2015), and reference databases with improved taxonomic and metabolic representation continue to be developed (e.g. Silva, KEGG). As such, the

characterisation of communities in this study is necessarily incomplete and likely to contain errors at lower limits of taxonomic resolution – metabolic characterisation in particular is still in its infancy, with prediction best employed as an exploratory or complementary analysis. Improved, robust characterisations of AD community members are anticipated from future studies, employing updated biological data and methodologies.

3. Results and Discussion

3.1 Study Setting

A previous study trialled continuous anaerobic digestion of varying ratios of *Ulva lactuca* and dairy slurry, demonstrating severely inhibited biogas production at higher *U. lactuca* loading levels (Allen *et al.*, 2014). To determine potential causes of this inhibition, the microbial community profiles of two reactors digesting contrasting ratios of *U. lactuca* and dairy slurry were characterised and compared, with the overall aim of identifying significant 'biomarker' species or metabolic activities which differentiated successful and inhibited digestion of *U. lactuca*. Detailed accounts of reactor setup and performance have been provided by Allen *et al.* (2014).

3.2 Process results of biogas reactors, R1 and R6

Previous characterisations (Allen *et al.*, 2013) of feedstocks predicted ideal biomethane yields of 210 and 183 L per kilogram of volatile solids ($kgVS^{-1}$) for R1 and R6 respectively. R1 started at an OLR of 2 $kgVSm^{-3}d^{-1}$, changing to 1 $kgVSm^{-3}d^{-1}$ at Week 6 and 1.5 $kgVSm^{-3}d^{-1}$ at Week 33 in response to high VFA levels. R6 started at an OLR of 2 $kgVSm^{-3}d^{-1}$, elevating to 2.5 $kgVSm^{-3}d^{-1}$ at Week 22. A comparative summary of the reactors is provided in Table 1.

At steady-state operation, the specific methane yield (SMY) per $kgVS^{-1}$ was similar between the two reactors: R1 and R6 on average produced 177 and 174 L CH_4 L $kgVS^{-1}$, respectively (Allen *et al.*, 2014). Despite these similar volumes, the R1 feedstock had a higher potential biomethane output (as above; R1: 210 L versus R6: 183 L $kgVS^{-1}$; Allen *et al.*, 2013): R1 therefore exhibited lower efficiencies (B_{eff} = 0.4, 0.69, 0.84) compared to R6 (B_{eff} = 0.95, 0.93). However, the biggest difference between reactor performances was rate of substrate conversion.' At OLRs 1 and 1.5 $kgVSm^{-3}d^{-1}$, R1 produced

biomethane at efficiencies of 0.84 and 0.69; at OLRs of 2 and 2.5 kgVS$m^{-3}d^{-1}$, R6 was converting more substrate and at consistently higher efficiencies of 0.93-0.95.

Setup	**CSTR R1**			**CSTR R6**	
% *U. lactuca*	75 (dried)			25 (dried)	
TS (%)	29.61			10.55	
VS (%)	18.42			7.22	
BMP (CH_4 kg VS^{-1})	210 ± 6.3			183 ± 7.8	
Temperature (^oC)	37			37	
Parameters	**HRT 1**	**HRT 2**	**HRT3**	**HRT 1**	**HRT 2**
OLR (kg VS m^3 d^{-1})	2	1	1.5	2	2.5
Methane content (%)	33	47	47	51	52
SMY (CH_4 kg VS^{-1})	83.31	176.77	145.21	178.11	170.46
B_{eff}	0.4	0.84	0.69	0.95	0.93
VFA (mg l^{-1})	4954	4135	4355	1955	1720
FOS:TAC	0.56	0.34	0.43	0.39	0.3
TAN (mg l^{-1})	3443	5250	5300	2168	3000

Table 1: Highlights of results of semi continuous digestion trials. *Abbreviations:* ***B_{eff}****: Biomethane conversion efficiency;* ***BMP****: Biomethane Potential;* ***CSTR****: Continuously-Stirred Tank Reactor;* ***FOS:TAC****: Buffering capability of solution;* ***HRT****: Hydraulic Retention Time;* ***OLR****: Organic Loading Rate;* ***SMY****: Specific Methane Yield;* ***TS****: Total Solids;* ***VFA****: Volatile Fatty Acids;* ***VS****: Volatile Solids*

3.3 Process Inhibitors

3.3.1 Volatile Fatty Acids

VFA accumulation can occur as a product of instability (McCarty and McKinney, 1961b), can be transitional (Griffin *et al.*, 1998; Wijekoon *et al.*, 2011; Williams *et al.*, 2013) and can even have little

to no effect on biogas production (Pullammanappallil *et al.*, 2001). Initial accumulation of iso-valeric and acetic acids was seen in both reactors: the relative difference between build-ups (initially three-fold higher in R1; higher thereafter) suggests this was due to hydrolysis and fermentation of the most accessible fractions of *U. lactuca*.

3.3.2 NH3

The recommended ratio of carbon to nitrogen (C:N ratio) for anaerobic digestion is between 20:1 and 30:1. C:N ratios for *U. lactuca* range between 7:1 (Allen *et al.*, 2014) and 14.5:1 (Briand and Morand, 1997). C:N ratios for feedstocks in this study were 10.2:1 for R1 and 17.1:1 for R6, with higher values reflecting addition of slurry (C:N ratio often >20:1 (Seppälä *et al.*, 2013)). Proteins contribute nearly all of the nitrogen in *U. lactuca* (Wong and Cheung, 2000), entering solution as free ammonia (NH_3) or the ammonium ion (NH_4^+). Elevated pH, temperature, and headspace partial pressure increase concentration of the uncharged NH_3 state. At sufficiently high concentrations NH_3 diffusion across cell membranes can inhibit the biogas process by causing loss of cellular potassium, de-potentiating the cell membrane, and accumulating in the cytoplasm (Sprott *et al.*, 1984). Ammonia inhibition is well documented in methanogens (Sprott *et al.*, 1984; Sprott, 1986; Calli *et al.*, 2005; Fotidis *et al.*, 2013), affecting other taxa to a greater or lesser extent. Pure cultures of methanogens remain viable at TAN levels up to 10,000 mg/L but have been documented to decline at a range of TAN levels between 1,700 to 6,000 mg/L when a part of a reactor community. Differential responses between hydrogenotrophic and acetoclastic methanogens are documented but contradictory (see reviews by Chen *et al.*, 2008 and Yenigün and Demirel, 2013).

3.3.3 Mineral salts

An inhibitory role for salts has long been recognised in anaerobic digestion (McCarty and McKinney, 1961a). Cations (e.g. Na^+, Ca^{2+}, Mg^{2+}, K^+) affect biogas production in a charge-dependent manner, possibly by inhibiting a Na^+ export channel necessary for the final methanogenic reaction (Gottschalk and Thauer, 2001). However, complex and proportionate mixes of cations can offset the inhibitory effects of one another (McCarty and McKinney, 1961a; Feijoo *et al.*, 1995), as well as ameliorating inhibition of the biogas process due to ammonia (Sprott, 1986) and VFA inhibition (Rinzema *et al.*, 1994). Pre-trial characterisations showed slurry to have low (< 2,000 mg/L) total mineral content, while fresh *U. lactuca* provided 5,220, 5,310 and 9,950 mg/L of Mg^{2+}, Na^+ and Ca^{2+} respectively. Monitored levels of Cl^- infer that salt-loading was significantly higher in R1, with a two-fold difference between R1 and R6 at close of trial (~10,300 and ~5,400 mg/L respectively). Reported inhibitory levels of Na^+ and Ca^{2+} vary, with lower estimates of inhibition registering from 5,000 mg/L upwards (Chen *et al.*, 2008). Community acclimatisation and/or later inhibitory onset are likely, due to gradual accumulation and the variety of salts.

3.3.4 Hydraulic Retention Time

Hydraulic retention time (HRT) is a process measurement of how long liquids remain inside the reactor, based on the continuous displacement of digestate by the addition of fresh feedstock. In this trial, HRT was calculated relative to the wet-weight of digestate, with both R1 and R6 starting with HRTs of 49 days. However, as OLRs diverged to suit operation, there was a corresponding increase in retention time in R1 from 49 to 63 days at OLR 1 kgVS/m3/d (i.e. ‘slower’ feeding), and a decrease in retention time in R6 from 49 to 42 days at OLR 2.5 kgVS/m3/d (i.e. ‘faster’ feeding). HRT can influence

microbial community composition at shorter HRT (higher OLR) where there is a risk of displacing substrate or microbes before they can be significantly incorporated into the reactor environment: they are simply 'washed out' (Drosg, 2013). This issue can arise if operation depends on slow growing populations for stability e.g. some acetoclastic methanogens have long particularly long doubling times (*Methanothrix pelagica*: doubling time of 300 hours; Mori *et al.*, 2012). "Wash out" can also displace and dilute materials included in the original inoculum but not abundant within the feedstock, restricting their availability. Conversely, extending HRT (lower OLR) allows more time for substrate decomposition and proliferation of populations, but extremely long retention times can lead to underfeeding of the reactor and sub-optimal outputs.

In this study, there is no obvious indication that HRT inhibited reactor function in either R1 or R6. Although the longest HRT observed (lowest OLR of 1kgVS$m^{-3}d^{-1}$, weeks 8-34) allowed R1 to metabolise accumulated VFAs, R1 did not appear underfed as indicated by the availability of VFAs (particularly acetate) and improvement in SMY. As such, increasing HRT (decreasing OLR) is an effective way of improving substrate degradation, but comes at the cost of a lower throughput. The shortest HRT of 42 days (R6: weeks 23-40) should allow for proliferation of key AD taxa, as vindicated by the high abundance of methanogens in R6 Week 27 at this reduced HRT. A slight decline in methanogen relative abundance in R6 Weeks 20 & 27 is discussed in Section 3.5.2.

3.4 Community Composition

3.4.1 Sequencing Results and Diversity Measures

Pyrosequencing generated 270,111 raw sequences, which following denoising in Acacia and processing in QIIME resulted in 89,251 sequence reads (average length: 244bp) being produced, with

an average of 8,114 reads per trial time-point. To ensure representative samples from both reactors, diversity metrics were calculated to estimate sensitivity to species diversity (Chao1 index) and species abundances (Simpson's Index). Rarefaction curves of these indices indicate that the most abundant species were thoroughly characterised in this study (see Appendix A, Supplementary Figure 2.1). However, rarefaction curves also indicate that a large number of low-abundance *Archaea, Bacteria* and unidentified taxa remain undetected due to insufficient depth of sequencing. Finally, both diversity indices (Chao1, Simpson's) decreased in later samples, suggesting the maturation of trophic systems in both reactors, where 'surplus' diversity is marginalised beyond the sequencing threshold**.**

3.4.2 Community Makeup

The QIIME pipeline identified 2,824 Operational Taxonomic Units (OTUs) in the 89,251 sequence reads. Singleton and doubleton OTUs (abundances < 3 reads) were discarded to reduce statistical noise, leaving 1,320 OTUs (82,914 sequence reads). Of the 1,320 OTUs, 1,057 were present in R1 and 955 in R6. Taxonomic alignments provided by Silva (release 111) identified 2 phyla, at least 4 classes, 5 orders, 7 families and 8 genera of *Archaea* (20 OTUs, 9,010 sequences), and at least 34 phyla/candidate phyla, 44 classes, 86 orders, 124 families and 190 unique genera of *Bacteria* (1,206 OTUs, 73,185 sequence reads). Lower taxonomic classifications could not be assigned to 16% of *Bacteria* families and 53% of *Bacteria* genera. A final 94 OTUs remained unidentified and were not assigned t*o Bacteri*a o*r Archaea*. Unassigned taxa comprised 1% of sequence reads (72 OTUs) from R1, and <1% of reads (42 OTUs) from R6. A complete description of community abundances is provided as supplementary data in Appendix D.

3.4.3 Archaeal Communities

Methanosarcina was the most abundant genus in this study (7 OTUs, 9.7% of all sequence reads), the majority of which originated from R6 (9.5% of all sequence reads). Large *Methanosarcina* populations are known to effectively buffer against fluctuations in substrate availability, preventing accumulation or shock loading of acetic acid (Conklin *et al.*, 2006; Hori *et al.*, 2006). *Methanosarcina* has a documented tolerance for acetic acid up to 15,000 mg/L, and a higher tolerance for changes in pH and salt (see review in (De Vrieze *et al.*, 2012)) than hydrogenotrophic counterparts. *Methanothrix,* an obligate acetoclast (Huser *et al.*, 1982), was scarce or absent in this study, likely out-competed by the higher growth rate of *Methanosarcina* at non-limiting acetate concentrations (Griffin *et al.*, 1998; Conklin *et al.*, 2006; Oren, 2014), or inhibited by salt (Chen *et al.*, 2008) or ammonia (Sprott, 1986; Calli *et al.*, 2005; Chen *et al.*, 2008; Yenigün and Demirel, 2013).

Hydrogenotrophic methanogens (*Methanoculleus*, *Methanobrevibacter*, *Methanobacterium*, *Methanocorpusculum, Methanospirillum* and *Methanosphaera* in this study) are commonly found in anoxic sediments (Romesser *et al.*, 1979), as gut flora (Ohkuma *et al.*, 1999; Whitford *et al.*, 2001; Dridi *et al.*, 2012), and in AD reactors where they sometimes dominate (Schlüter *et al.*, 2008; Sundberg *et al.*, 2013). However, most archaeal OTUs were observed at consistently low frequencies (<0.5% of total sequence reads respectively), often disappearing below the threshold of sequencing coverage.

3.4.4 Bacterial Communities

Bacterial components of these reactors are typical of biogas communities, while some key and accessory species are associated with marine or salt environments. The most abundant phylum was *Firmicutes* (565 OTUs, 36% of all sequence reads), containing many groups known to hydrolyse polymers (e.g. cellulose, lignin, polysaccharides, proteins: *Lachnospiraceae, Peptostreptococcaceae,*

Ruminococcaceae), ferment carbohydrates (e.g. saccharides, amino acids, organic molecules: OPB54*, Gelria, Christensenellaceae*), and produce organic acids as metabolic endpoints (i.e.: acidogens: *Sedimentibacter Tissierella, Syntrophomondaceae*). *Firmicutes* are major components of anaerobic environments such as digesters (Schlüter *et al.*, 2008; Kröber *et al.*, 2009; Sundberg *et al.*, 2013) and alimentary tracts (Claesson *et al.*, 2009; Nyonyo *et al.*, 2014), and in this study accounted for over a third of sequences in both reactors: in short, they are highly diverse, widely distributed, and understood as essential components of anaerobic digestion.

The second-most abundant phylum, *Bacteroidetes* (126 OTUs, 16% of all sequence reads), is also frequently detected in anaerobic reactors, with important roles as fermenters and acidogens. In particular, species from the family *Porphyromonadaceae* (9% of all reads) are known to be involved in the degradation of proteins and amino acids, eschewing saccharides (genera *Petrimonas*, (Grabowski *et al.*, 2005) and *Proteiniphilum* (Chen and Dong, 2005)).

Phylum *Proteobacteria* (203 OTUs, 13% of sequence reads) comprises the most diverse known taxonomic group of the *Bacteria* to date. The sub-ordinate classes *Alpha*- and *Gamma-Proteobacteria* contributed 3% and 7% of reads in this study respectively, with remaining proteobacterial classes totaling 3%. *Proteobacteria* are typical residents of anaerobic digesters (13,69,75), known to incorporate nitrogen and/or sulphur as electron acceptors in the metabolism of varied carbohydrates (e.g.: *Nitrosimonas*, *Nitrobacter*). However, some species observed here are unexpected inclusions, with described preferences for aerobic metabolism (in some cases obligate: *Rhodobacteraceae*, *Granulosiococcaceae*, *Nannocystineae;*) and a high propensity for saline and marine environments (water: *Rhizobacteraceae*; sediments: *Desulfomicrobium*; seaweeds and plants: *Alteromonadaceae*, *Nannocystinaceae*, *Granulosiococcaceae*). As such, their presence in this study likely reflects

persistent contributions from the *U. lactuca* feedstock alongside species typical of a biogas digester habitat.

Phylum *Spirochaetes* (47 OTUs and 6% of sequence reads in this study) are diverse, highly motile, frequently anaerobic bacteria, but metabolic information on this phylum in anaerobic digesters is somewhat limited despite being frequently encountered in low or medium abundances. They have been characterised both as acetogens (76,77) and acetoclasts assisting methanogenic activity (as Syntrophic Acetate-Oxidising Bacteria) (Lee *et al.*, 2013).

Phylum *Synergistetes* comprised 6% of all sequence reads and 34 OTUs. *Synergistetes* are typically seen at lower abundances in a wide variety of environments (Jumas-Bilak and Marchandin, 2014), in syntrophic associations with hydrogenotrophic species (e.g. methanogens). A possible role in these reactors is likely to be oxidising amino acids as a substrate in the presence of methanogens (Baena *et al.*, 1998, 2000).

Most phyla were present at much lower levels (< 2% of reads): Phylum *Chloroflexi* contains fermentative, acido- and acetogenic, obligate and facultative anaerobes seen in anaerobic digesters and hot springs respectively, and requires removal of hydrogen which suggests syntrophic roles (Yamada *et al.*, 2006). Phylum *Tenericutes* is represented by *Acholeplasma* spp.- poorly characterised sugar fermenters (Martini *et al.*, 2014); Species from Phylum *Actinobacteria* contain many heterotrophic fermenters including lipidophiles, and obligate marine-associated species (Tauch and Sandbote, 2014); Phylum *Acidobacteria* species are uncharacterised but similar to sequences recovered from petrochemical-contaminated aquifers (isolate BPC102, NCBI accession AF154083.1); Taxa from Phylum *Armatimonadetes* are expected to be chemo-heterotrophs, and are suggested to associate with degradation of photosynthetic biomass (Lee *et al.*, 2014).

Although the eleven phyla outlined above describe over 94% of all sequence reads, the remaining *Bacteria* (only 6% of reads, 135 OTUs) correspond to at least a further 26 phyla/candidate phyla, again reflecting the huge diversity in anaerobic reactor communities.

3.5 Relating Community Makeup and Process Variables

A comparison of relative abundances for major Archaea and Bacteria (A), changes in levels of biogas inhibitors TAN and VFA (B), and biogas indicators B_{eff} and FOS:TAC (C) is given in Fig 1 for all time-points sampled in this study. Environmental process and community abundance data used in this study are provided via Appendix D.

3.5.1 Changes in R1 Community Makeup

Week 1 conditions were initially favourable for R1 at an OLR of 2 kg VS m^3 d^{-1}, albeit with slightly elevated TAN and VFA levels (~2,000mg/L respectively). Community abundances were relatively balanced between hydrolysers, fermenters and acido-/acetogens (*Clostridiales, Bacteroidales, Desulfovibrionales, Synergistales*), with environmental inclusions (*Rhizobiales, Rhodobacterales, Myxococcales*) characteristic of slurry, *U. lactuca*, or marine sources. Until Week 5, *Methanosarcina* abundances held at half (~1%) of all R1 archaeal sequence reads (~2%), suggesting conditions for acetoclasts were initially favourable. Canonical cellulose and protein degraders proliferated (*Ruminococcaceae, Lachnospiraceae, Proteiniphilum*). As TAN approached 3,500 mg/L, early accumulation of acetic and iso-valeric acid shifted to a sudden peak in iso-valeric acid (3,500mg/L) and depletion of acetic acid after Week 5. To reduce VFA content, OLR was reduced to 1 kg VS m^3 d^{-1} in Week 7, while Cl^- levels exceeded 5,000mg/L.

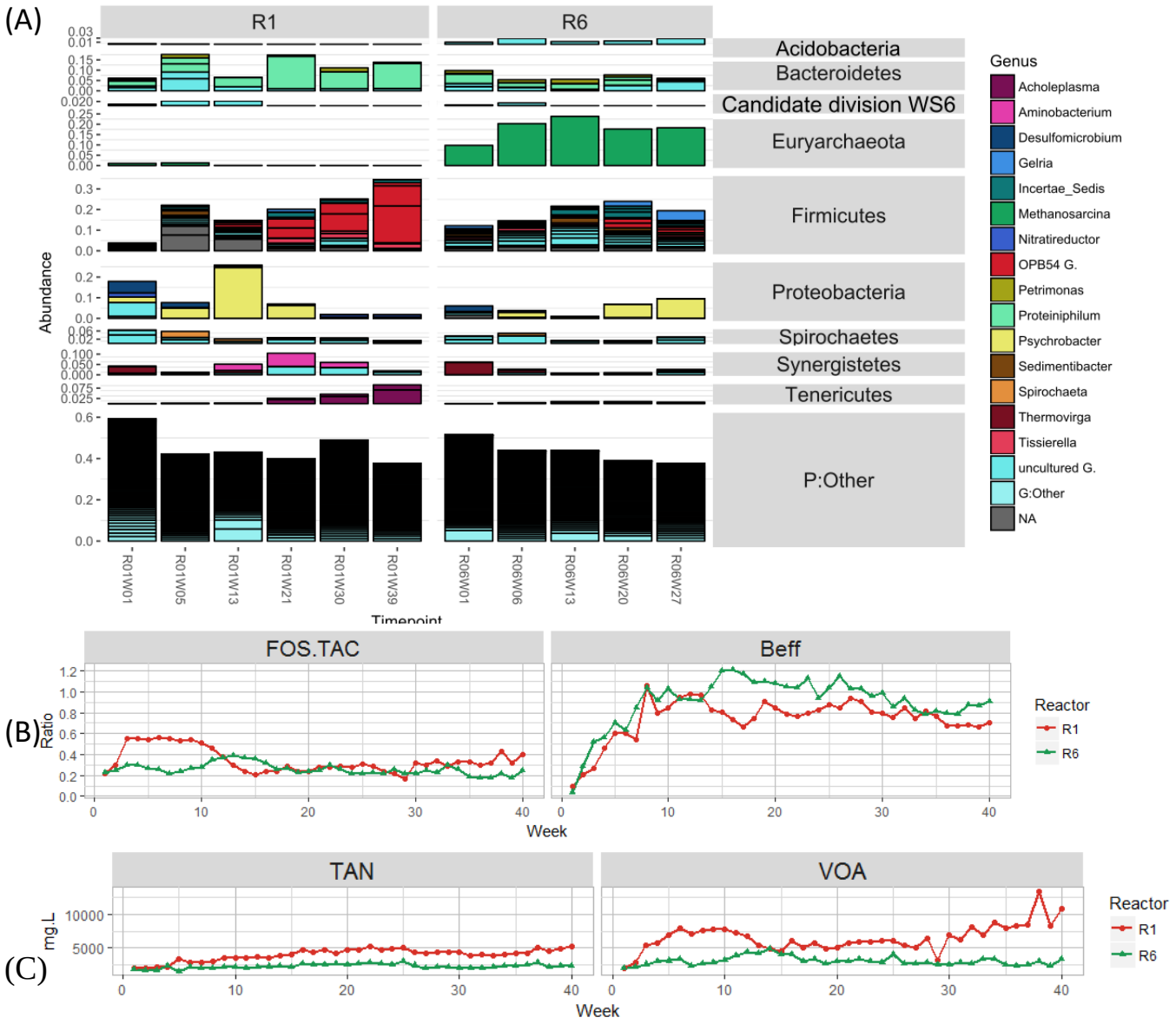

Figure 1: Interaction between community structure (at Order-level taxonomy) and major process variables. *(A) Differences in reactor operation induce different community structures: R1, which struggled under heavy U. lactuca loading, developed larger fermen ting populations and a lack of methanogens; R6, digesting less U. lactuca, retained large Methanosarcina populations even at higher OLRs. Comparing taxa abundances against levels of principal process inhibitors TAN and VOA (B), and indicators FOS:TAC and* B_{eff} *(C) illustrates the connection between community composition and biogas performance. Taxa which did not exceed 1% of reads in at least two timepoints are coalesced to 'Other' for convenience of viewing. Abbreviations: Total ammoniacal nitrogen (TAN), volatile organic acids (VOA), buffering ratio (FOS:TAC) and biomethane conversion efficiency (Beff, or* B_{eff}*).*

Week 13 sequence reads showed a sharp rise in abundance of the *Pseudomonadales* genus *Psychrobacter* to 25%, alongside catabolism of accumulated iso-valeric acid to propionic and acetic acid. Associated with cold marine environments, *Psychrobacter* is likely to reduce amino and organic acids to acetic acid (Teixiera and Merquior, 2014), suggesting an important role in continuous digestion of *U. lactuca* and slurry. However, *Methanosarcina* abundances were negligible (<0.1% of sequence reads) and not detected at end of trial, despite stable reactor conditions (FOS:TAC 0.21 – 0.31 until Week 26), a lack of inhibitory VFAs (<4,000 mg/L (De Vrieze *et al.*, 2012), and favourable levels of acetic acid for that genus (1100 – 1300 mg/L (De Vrieze *et al.*, 2012); evidenced by similar concentrations in R6, Week 13). Hydrogenotrophic *Methanobrevibacter* and *Methanoculleus* were then the dominant Archaea in R1, at <1% of sequence reads.

Metabolism of accumulated propionic acid by Week 21 coincided with receding *Psychrobacter* abundance and expansion of hydrolysing and fermenting populations emphasising protein/amino acid metabolism and acetogenesis (OPB54*, Ruminococcaceae, Peptostreptococcaceae, Proteiniphilum, Aminobacterium*). TAN continued to increase (~4,700mg/L) alongside steady levels of acetic acid (~1,000 mg/L) as the main VFA. Hydrogenotrophic methanogens persisted at low levels (<1% sequence reads).

After peaking at Week 23 (~5,000mg/L) TAN stabilised by Week 30 (~4,000mg/L), while acetic and propionic acid re-accumulated (~2,300 mg/L and ~500 mg/L respectively). Despite receding TAN, hydrogenotrophic methanogens declined further, with small shifts in bacterial populations from likely peptide (*Aminobacterium, Proteiniphilum, Psychrobacter, Peptostreptococcaceae*) to polysaccharide metabolisers (*Acholeplasmataceae, Ruminococcus*, OPB54).

Increasing OLR to 1.5 kg VS m^3 d^{-1} at Week 34 exacerbated accumulation of TAN (+5,000mg/L), Cl^- (~6,800mg/L), and VFAs (chiefly acetic and propionic acid: ~3,200 and ~700mg/L respectively; FOS:TAC >0.4; declining biogas output). By Week 39, OPB54 (36% of sequence reads), *Proteiniphilum* (13%) and *Acholeplasmataceae* (9%) represented the most relatively abundant populations while Archaea contributed only 0.3% of sequence reads.

3.5.2 Changes in R6 Community Makeup

Initial levels of VFA and TAN in R6 were similar to R1, with accumulation of acetic and iso-valeric acid at lower levels, and large hydrolysing, fermenting and aceto-/acidogenic populations (*Clostridiales*: 32% of sequence reads, *Bacteroidales*: 10%, *Synergistales*: 8%). Notably, *Methanosarcina* was considerably more abundant at Week 1 (10% of sequence reads, as compared to 1% in R1). This may reflect a rapid acclimatisation to substrate (uncharacteristic of methanogens), or contribution from the three-fold higher slurry portion. R6 Archaea were also more diverse, including *Methanspirillum*, *Methanocorpusculum*, *Methanomasciliicoccus*.

Week 6 saw TAN rise above 2,000mg/L, with iso-valeric acid quickly metabolised to acetic acid. *Methanosarcina* relative abundance doubled to 22% of sequence reads, while *Clostridiales* and *Synergistales* taxa showed some decline in relative abundance.

Cl^- levels passed 5,000mg/L at Week 10. Week 13 represented the high point in biogas production, acetic acid availability, and *Methanosarcina* abundance (24% of sequence reads), alongside diverse bacterial populations with low, evenly-distributed abundances. The largest populations were acetogenic gut-associated saccharide fermenters (*Christensenellaceae*, *Rikenellaceae*: 4-6%), cellulose (*Ruminococcaceae*, *Lachnospiraceae*: 4-5%) and peptide (*Peptostreptococceae*, *Proteiniphilum,*

Sedimentibacter: ~3%) degraders. Crucially, subsequent rises in propionic (700mg/L) and iso-caproic acids (600mg/l) were rapidly catabolised to acetic acid.

With TAN rising (~2,500mg/L) and a decrease in B_{eff} at Week 20, initially abundant bacterial taxa (*Peptostreptococcaceae, Lachnospiraceae, Christensenellaceae, Rikensellaceae*) were replaced by functionally similar populations (*Ruminococcaceae, Proteiniphilum, Psychrobacter,* OPB54) while *Methanosarcina* relative abundance decreased (18%) in conjunction with limiting acetic acid, similar to perturbation in the R1 community. An otherwise stable methanogen population (1.4%) suggests biogas obstruction prior to methanogenesis; sudden elevation of valeric acid (~500mg/L) implicates disrupted acetogenesis. Cl^- levels peaked at Week 21 (~6,800mg/L), but decreased thereafter (~6,000mg/L).

TAN peaked at 3,000mg/L in Week 25 before stabilising to ~2,000mg/L by Week 27, despite an increased loading rate of 2.5 kg VS m^3 d^{-1}. Abundances shifted towards larger, mono-typic populations of fermenters and acidogens, displacing degraders of cellulose and proteins, possibly in response to increased substrate availability. Relatively ideal reactor conditions (FOS:TAC 0.22-0.24; free ammonia and chloride below inhibitory levels; VFA concentrations below inhibitory levels despite an increased OLR (Chen *et al.*, 2008; De Vrieze *et al.*, 2012)) and stable levels of *Methanosarcina,* combined with accumulated higher VFAs despite limiting acetic acid again suggest some inhibition of acetogenesis rather than methanogenesis is responsible for the decreasing yield seen in later R6 time-points.

3.6 Statistical Resolution and Constrained Analysis

3.6.1 Taxonomic Characteristics

To improve characterisation of the different microbe communities digesting slurry/*U. lactuca* mixes, the LDA (Linear Discriminant Analysis) Effect Size package (LEfSe, Segata *et al.*, 2011) was used to detect taxa characteristic of digestion at high (R6) or low rates (R1), acting as potential 'biomarkers' for either setup (Figure 2). A complete LDA output for taxonomy is provided as supplementary data in Appendix D.

Taxa characteristic of R1 show a strong affinity for marine environments and/or halotolerance. Additionally, most were originally isolated from marine sources; three from *Ulva* species or other seaweeds (*Maritalea, Arenibacter, Alteromonadaceae*). Several are aerobes or facultative aerobes (*Nitratireductor, Altermonadaceae*) and many show degrees of fermentative and/or acidogenic activity. The most significantly associated taxa (LDA effect ≥4**,** α ≤0.05) are from the *Actinobacteria* (*Micrococcales*), *Alpha-Proteobacteria* (*Devosia, Nitratireductor, Rhizobium and Rhodobacteraceae sp.*), *Beta-Proteobacteria* (*Hydrogenophaga* and *Limnohabitans*), *Bacteroidetes* (*Proteiniphilum*) and *Firmicutes* (*Alkaliphilus*, *Bacillales, Lutispora, Syntrophomonadaceae, Tepidanaerobacterales, Tissierella*) phyla. As well as known fermenters, acidogens (*Proteiniphilum, Firmicutes*) and syntrophs (*Firmicutes*), these taxa suggest diverse saccharide use, and use of alternate electron acceptors (nitrogen, sulphur) detrimental to biogas production (*Alpha*- and *Betaproteobacteria*).

Indicators of the R6 environment were more closely linked to anaerobic digestion, but retained some associations with marine and saline habitats. The most significantly associated taxa (LDA effect ≥ 4, α ≤0.05) are more commonly anaerobic and documented as hydrolysers (*Alkaliflexus, Caldilineae, Lachnospiraceae, Proteiniphilum, Ruminococcaceae*), fermenters (*Caldilineae, Desulfomicrobia*) and

acetogens (*Alkaliflexus, BPC102, Caldilinea, Christensenellaceae, Syntrophomonas, etc.*), as well as including three Archaea: the acetoclastic *Methanosarcina* and hydrogenotrophic *Methanobacterium* and *Methanobrevibacterium*. Most methanogens were not significant indicators, as abundances were similar between reactors.

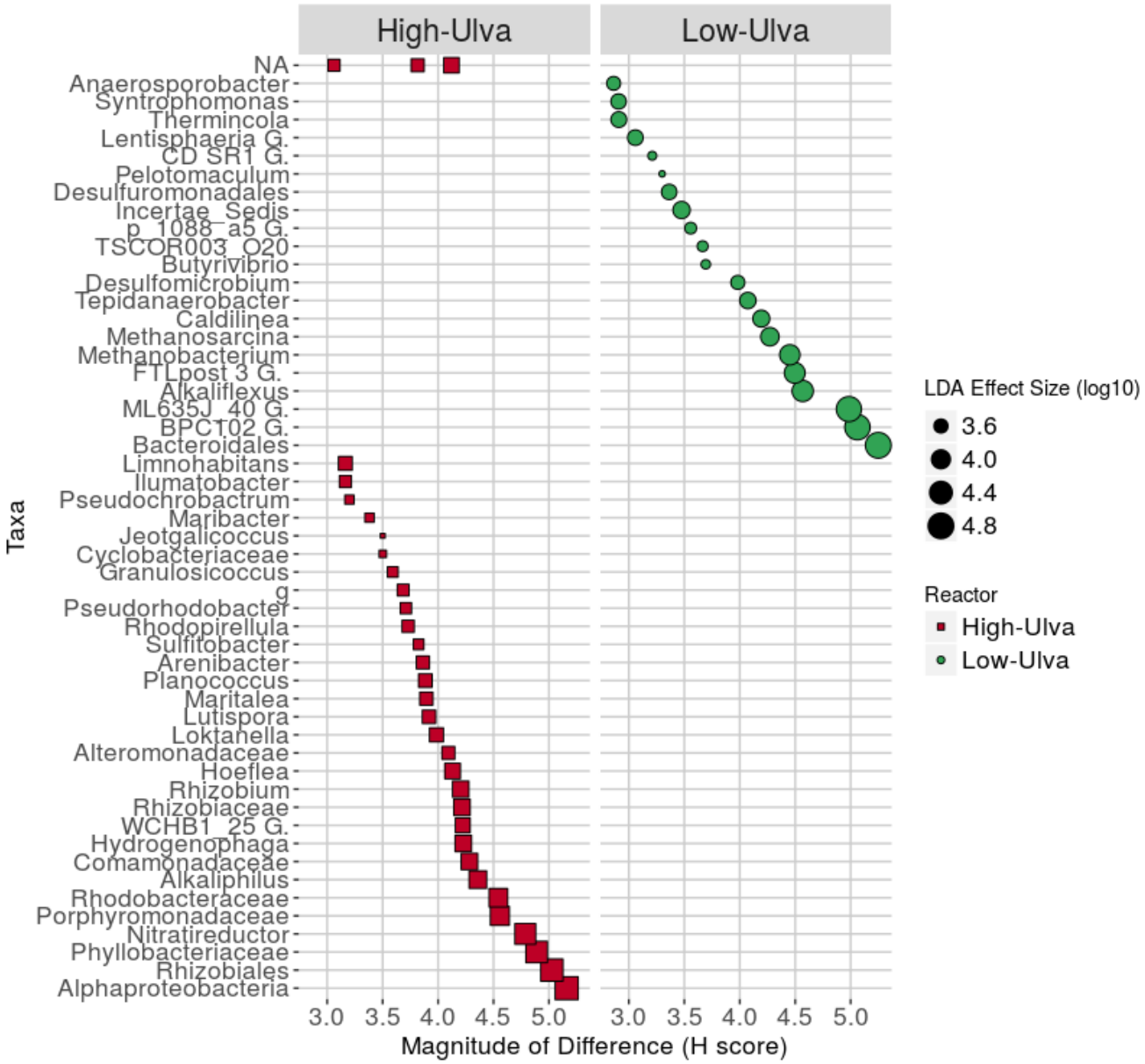

Figure 2: *Significant associations between taxa and reactor feedstock, ordered by increasing strength of association (H score). Size of point indicates reliability of association (linear discriminant analysis (LDA) score, log10 scale). Abbreviations: G., g: genus.*

3.6.2 Predicted Metabolic Characteristics

Attributing reactor performance to specific microbial populations is problematic, partially due to resource-intensive technologies necessary to profile metabolic activity, which may be unsuited to industrially scaled applications (e.g. mRNA/cDNA libraries, metabolic isotope analysis). A novel compromise afforded by metagenomics is to cross-reference taxonomic information (e.g. 16S sequence data) with a database of known metabolic capabilities, and compute inferred metabolic profiles which may help explain activities in a microbial community. Characterisation of functionality through inferred metabolism has been demonstrated in medical, ecological and biofuel contexts: identifying microbial metabolisms likely to improve dietary dysfunction (Chumpitazi *et al.*, 2015); demonstrating differential microbial activities in healthy and compromised habitats (Loudon *et al.*, 2014); and predicting and confirming enriched cellulolytic activity in microbial lignocellulose degradation (Jiménez *et al.*, 2014). By highlighting the metabolic capabilities of an inoculum or sludge, the same approach applied to AD has the potential to provide a more informed characterisation of biogas conditions, helping to "de-mystify" the roles of microbial populations.

Using the PICRUSt package (Langille *et al.*, 2013), taxonomic abundances for R1 and R6 were used to infer metabolic processes for the two communities. Predicted features characterising either reactor were then identified using LEfSe, with complete metabolic PICRUSt and LDA outputs provided as supplementary data in Appendix D.

Diverse carbohydrate metabolism is likely to characterise R1, with the highest LDA effect scores (4.1 – 3.9, α=0.006) for central carbohydrate metabolism and saccharide transport. Although carbohydrates are fundamental to all metabolism, the variety of metabolic pathways represented in these categories suggests that the R1 community utilises a more opportunistic and varied range of carbon sources, with significantly elevated predictions for the Entner-Doudoroff Pathway, Pentose Phosphate

Pathway and Citrate Cycle (LDA effects: 3.18 – 3.42, $\alpha<0.05$). Predicted markers for R1 also include transport of putrescine and spermidine, key components (Karatan and Michael, 2013) in the formation and regulation of biofilms (LDA effect: 3.47 – 3.71, $\alpha= 0.006 – 0.011$); and Type VI secretion systems which are likely to be used in competition for resources (LDA effect: 3.7, $\alpha=0.034$).

Metabolism of methane is a strong recurring prediction for R6 (LDA effect: 3.53 – 3.98, $p=0.006$) with the emphasis on methanogenesis via methanol and acetate (LDA effect: 3.64 and 3.58 respectively, $\alpha = 0.006$). However, the strongest predicted characteristics of R6 metabolism are transport of cobalt (LDA effect: 4, $\alpha=0.006$) and nickel (LDA effect: 4.2, $\alpha=0.006$). Cobalt is required for methylotrophic methanogenesis (Gottschalk and Thauer, 2001), while nickel is central to the final step of all methanogenic pathways (Pelmenschikov *et al.*, 2002; Thauer *et al.*, 2010). There is good evidence in the literature indicating that methane production increases substantially when nickel and cobalt are added (Murray and van den Berg, 1981; Gonzalez-Gil *et al.*, 1999; Zandvoort *et al.*, 2006). Increased archaeal ribosome metabolism (LDA effect: 3.64, $\alpha=0.006$) and reduction of quinones in energy metabolism (LDA effect: 3.52, $\alpha<0.02$) are also predicted to differentiate metabolism in R6 from R1.

3.7 Constrained Correlation Analysis

Constrained Correlation Analysis (CCA) measured the relationships between community structure and time-points, and metabolism and time-points, in the context of specified ('constraining') process variables. Several process variables were inter-correlated, describing the same source of variation in the dataset. In particular, levels of TAN, alkalinity and total dissolve solids (TDS) were strongly inter-correlated ($R=0.80 – 0.95$), as were B_{eff}, biogas output and specific methane yield (SMY) ($R= 0.81 – 0.97$); and chloride, total salinity, chemical oxygen demand (COD), volatile solids (VS) and duration of

trial (R=0.81 – 0.97). As such, three governing aspects described the reactor communities: inhibitor accumulation, biogas activity, and trial duration.

3.7.1 CCA of Community Abundances

CCA showed that levels of ammonia (specifically total ammoniacal nitrogen, TAN), chloride and raw biogas output had the strongest correlations with community make-up, with the most significant and non-redundant effects on taxonomic abundances (R=0.50, significant after 999 permutations, VIF< 8). Together, these 3 parameters described 49.8% of variation in community abundance and allowed the major interactions defining these communities to be visualised via bi-plot (Figure 3) showing clear segregation between the two reactors. Although initial community and process similarities cause both Week1 samples to cluster, R1 and R6 time-points diverged along X and Y axes respectively, with clustering of later time-points showing established communities. Despite low OLR in R1, accumulation of TAN exceeded 5,000 mg/L in later time-points, and was the most strongly correlated inhibitor of biogas process (X axis). R6 time-points show negligible interaction with ammonia levels or overloading along the X axis, indicating the R6 community was not inhibited by TAN levels up to 3,000 mg/L. Instead, R6 correlates strongly with increasing biogas output, seen as distribution along the Y axis. Note that Week 13 of R1 correlated with biogas production (movement on Y axis) before R1 reached higher ammonia levels. Rising chloride concentrations correlate with both reactor setups, relating trial duration and a gradual accumulation of dissolved content. A stronger association with R1 is explained through a higher *U. lactuca* loading, with no clear inhibitory effects.

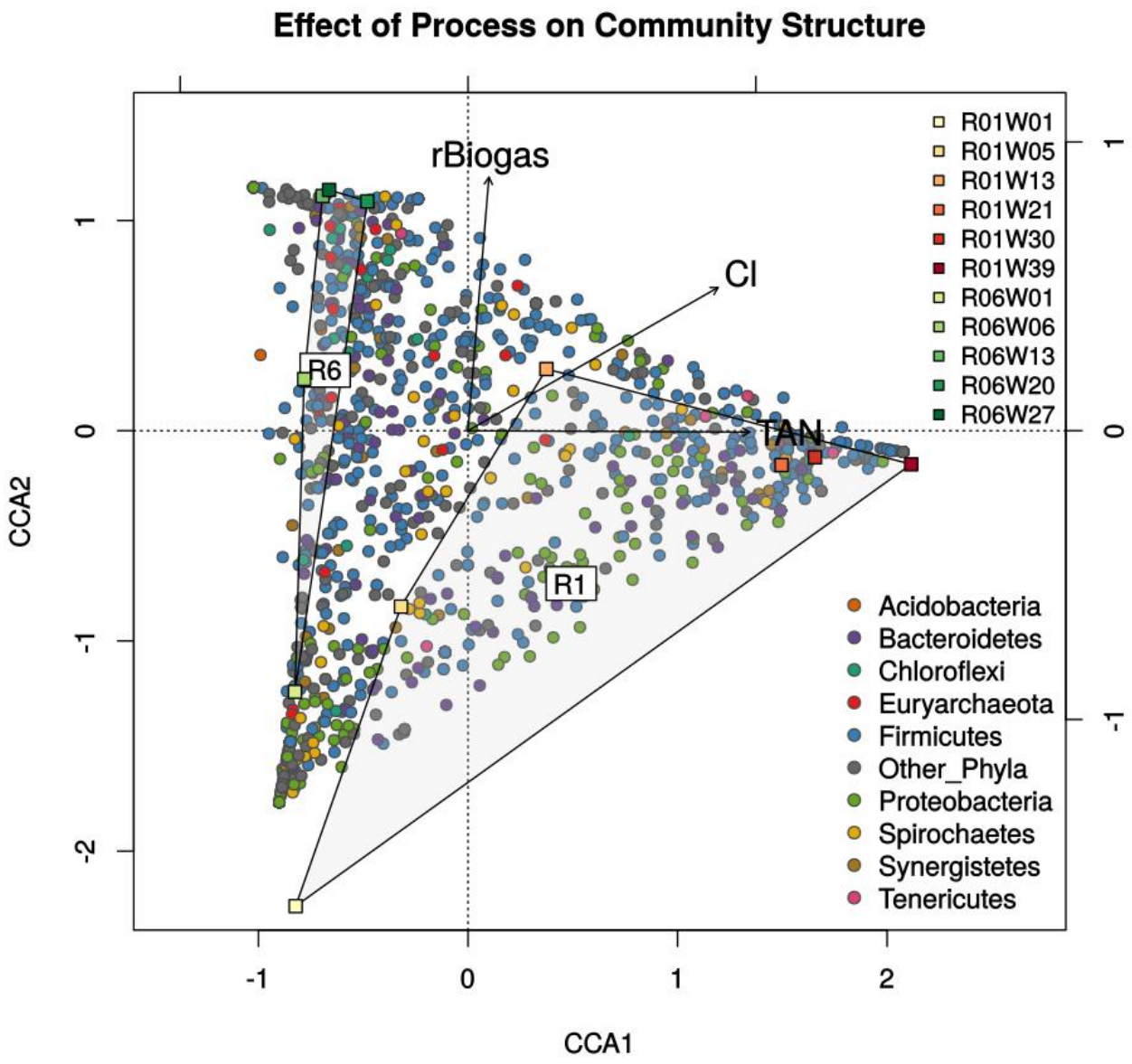

Figure 3: Levels of ammonia (TAN) and biogas best differentiate microbial communities between the two reactors. *Microbial community structures diverged over time despite initial similarities (lower left quadrant), with R1 communities showing a stronger correlation with levels of ammonia across the X axis and R6 communities showing a stronger correlation with increasing biogas along the Y axis. The perpendicular relationship between biogas and ammonia (total ammoniacal nitrogen, 'TAN') suggests the two parameters act on community structure independently. Chloride ('Cl') levels show a weaker interaction with community structure, likely reflecting the accumulation of material and maturation of the reactor as the trial progresses.*

Correlations with OLR, reactor alkalinity (Alk) and total ammoniacal nitrogen (TAN) were up to 1.5 times stronger for *Archaea*, while pH, salinity, COD, VS% and Cl correlated to *Bacteria* more strongly (1.5 – 2 times). Curiously, the bacterial community was more than twice as correlated to B_{eff} as the archaeal community (R: 0.21 v 0.12), reflecting the specialised bacterial community involved in methanogenesis and relatively consistent methanogen components. A negative correlation between biogas output and biodiversity indices (R>-0.6) could potentially be explained through 'niche exclusion', where taxa unsuited to anaerobic digestion are out-competed by “better-equipped” taxa, causing a decrease in diversity. Excluded taxa are known to persist at low abundances and form important reservoirs of metabolic capability, invoked during shifts in reactor conditions (Murray and van den Berg, 1981; Gonzalez-Gil *et al.*, 1999; Zandvoort *et al.*, 2006).

3.7.2 CCA of Predicted Metabolic Activities

CCA using predicted metabolic abundances showed strongest non-redundant correlations with TAN and B_{eff} (R=0.50, VIF=1, significant after 999 permutations). Ordination under these constraints (Fig 4) showed differences in energy metabolism along the X axis, with methanogenesis predictions related to R6 segregating from predicted alternative anaerobic metabolic pathways (Entner-Doudoroff, ethylmalonyl, and pentose-phosphate pathways) and carbon uptake pathways (multi-saccharide transport system) related to R1. Samples differentiated along the Y axis as reactors matured, with earlier metabolic diversity (e.g. sulphate reduction and transport, methane oxidation) absent in later samples as overall diversity decreased. Methanogenesis (acetate and methanol metabolism) and archaeal translation and transcription clearly associated with R6, while negatively correlating with TAN levels. Predictions for nickel and cobalt transport also associate with R6 time-points.

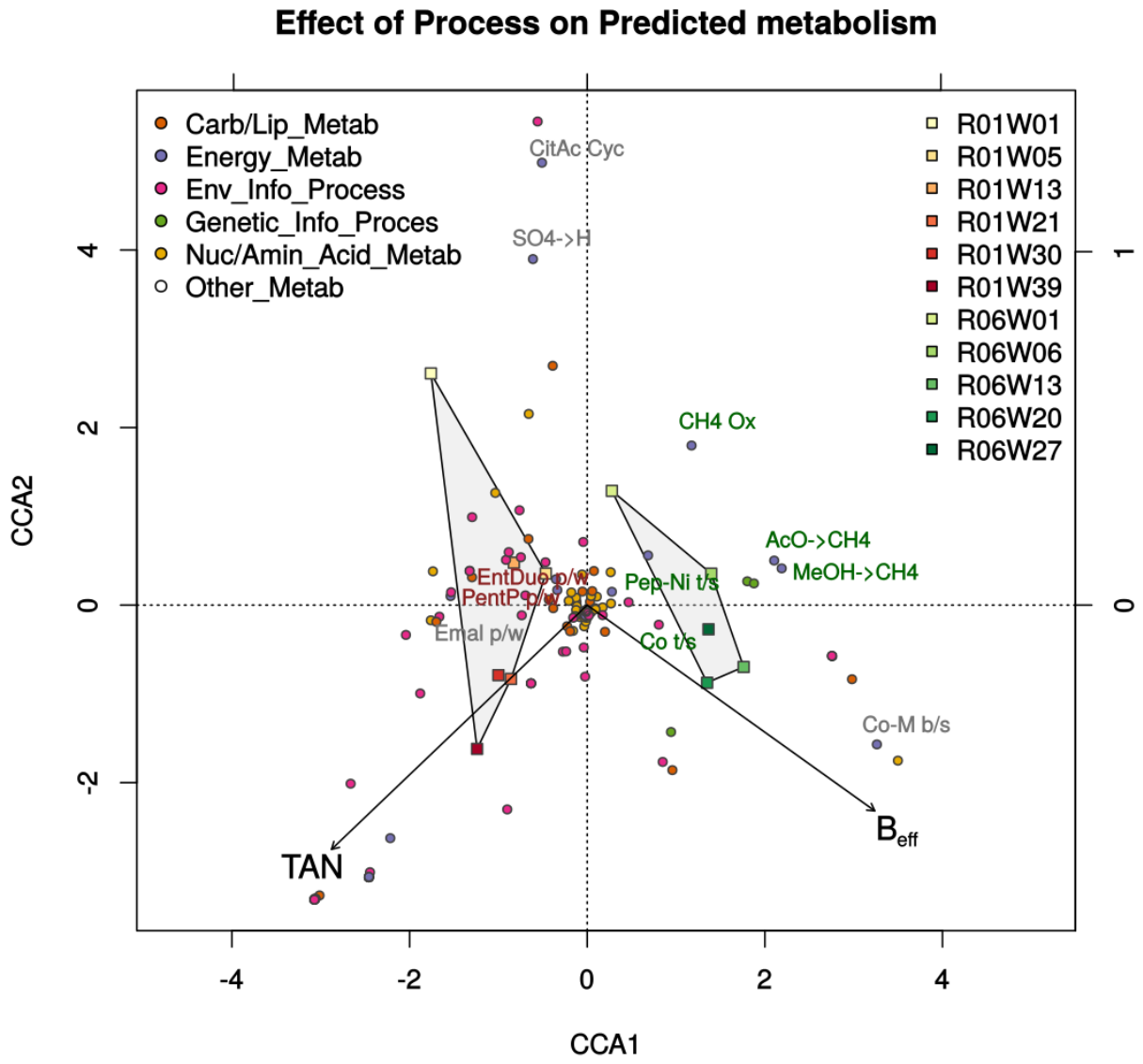

Figure 4. Ammonia levels (TAN) and biomethane conversion efficiency (B_{eff}) best differentiate predicted metabolisms between R1 and R6. *Carbon metabolisms segregate along the X axis, reflecting divergent environments under the contrasting reactor setups. R1 samples ordinate more closely with diverse carbon metabolism (Entner-Doudoroff: EntDu p/w; Pentose-Phosphate: PentP p/w; ethymalonyl: Emal p/w), while R6 samples ordinate strongly with methanogenic activities (Methanogenesis: AcO, MeOH → CH4; Co-Enzyme M biosynthesis: Co-M b/s)) and the uptake of trace elements (Cobalt: Co t/s; Nickel: Pep-Ni t/s). More diverse activities (Citric Acid Cycle: CitAc Cyc; sulphate reduction: SO4->H; methane oxidation: CH4 Ox) ordinate closer to earlier samples, suggesting metabolic activities detrimental to biogas production were excluded as reactor communities developed. Activities in green represent strongest predicted biomarkers for R6, activities in red represent strongest predicted biomarkers for R1.*

4. Conclusions

Anaerobic digestion of *U. lactuca* appears to indirectly inhibit acetogenic and methanogenic processes, with ammonia showing the strongest causative correlation. At high *U. lactuca* volumes, decreasing OLR was not sufficient to recover the acetoclastic methanogens required to remove acetic acid and prevent overloading, nor to retain hydrogenotrophic methanogens. At lower *U. lactuca* volumes, the inhibition of acetogenesis caused *Methanosarcina* populations yields to shrink, affecting overall biogas yield. *U. lactuca* loading significantly affected community composition within reactors, with higher volumes characterised by diverse, facultatively anaerobic, and marine and halotolerant taxa, a lack of methanogens, and a predicted reliance on alternative carbon metabolism.

5. References

1. Dave A, Huang Y, Rezvani S, McIlveen-Wright D, Novaes M, Hewitt N. Techno-economic assessment of biofuel development by anaerobic digestion of European marine cold-water seaweeds. Bioresour Technol. 2013 May;135:120–7.

2. Vanegas CH, Bartlett J. Green energy from marine algae: biogas production and composition from the anaerobic digestion of Irish seaweed species. Environ Technol. 2013 Aug 1;34(15):2277–83.

3. Rodriguez C, Alaswad A, Mooney J, Prescott T, Olabi AG. Pre-treatment techniques used for anaerobic digestion of algae. Fuel processing technology. 2015 Oct 1(138):765-79.

4. Allen E, Browne J, Hynes S, Murphy JD. The potential of algae blooms to produce renewable gaseous fuel. Waste Manag. 2013 Nov; 33(11):2425–33.

5. Briand X, Morand P. Anaerobic digestion of Ulva sp. 1. Relationship between Ulva composition and methanisation. J Appl Phycol. 1997 Dec; 9(6):511–24.

6. Morand P, Merceron M. Macroalgal Population and Sustainability. J Coast Res. 2005 Sep 1;1009–20.

7. Percival E. The polysaccharides of green, red and brown seaweeds: Their basic structure, biosynthesis and function. Br Phycol J. 1979 Jun; 14(2):103–17.

8. Wong KH, Cheung PC. Nutritional evaluation of some subtropical red and green seaweeds: Part I—proximate composition, amino acid profiles and some physico-chemical properties. Food Chem. 2000; 71(4):475–82.

9. Koch C, Müller S, Harms H, Harnisch F. Microbiomes in bioenergy production: From analysis to management. Curr Opin Biotechnol. 2014 Jun;27:65–72.

10. Carballa M, Regueiro L, Lema JM. Microbial management of anaerobic digestion: exploiting the microbiome-functionality nexus. Curr Opin Biotechnol. 2015 Jun;33:103–11.

11. Solli L, Håvelsrud OE, Horn SJ, Rike AG. A metagenomic study of the microbial communities in four parallel biogas reactors. Biotechnol Biofuels. 2014 Oct 14;7(1):146.

12. St-Pierre B, Wright A-DG. Comparative metagenomic analysis of bacterial populations in three full-scale mesophilic anaerobic manure digesters. Appl Microbiol Biotechnol. 2014 Mar;98(6):2709–17

13. Sundberg C, Soud WA Al-, Larsson M, Alm E, Yekta SS, Svensson BH, et al. 454 pyrosequencing analyses of bacterial and archaeal richness in 21 full-scale biogas digesters. FEMS Microbiol Ecol. 2013 Sep;85(3):612–26.

14. Wilkins D, Lu X-Y, Shen Z, Chen J, Lee PKH. Pyrosequencing of mcrA and Archaeal 16S rRNA Genes Reveals Diversity and Substrate Preferences of Methanogen Communities in Anaerobic Digesters. Appl Environ Microbiol. 2015 Jan 15;81(2):604–13.

15. Pope PB, Vivekanand V, Eijsink VGH, Horn SJ. Microbial community structure in a biogas digester utilizing the marine energy crop Saccharina latissima. 3 Biotech. 2013 Oct;3(5):407–14.

16. Wirth R, Lakatos G, Maróti G, Bagi Z, Minárovics J, Nagy K, et al. Exploitation of algal-bacterial associations in a two-stage biohydrogen and biogas generation process. Biotechnol Biofuels. 2015;8(1):59.

17. Hinks J, Edwards S, Sallis PJ, Caldwell GS. The steady state anaerobic digestion of Laminaria hyperborea – Effect of hydraulic residence on biogas production and bacterial community composition. Bioresour Technol. 2013 Sep;143:221–30.

18. Allen E, Wall DM, Herrmann C, Murphy JD. Investigation of the optimal percentage of green seaweed that may be co-digested with dairy slurry to produce gaseous biofuel. Bioresour Technol. 2014 Oct;170:436–44.

19. Nordmann W. Die Überwachung der Schlammfaulung. KA-Informationen für das Betriebspersonal, Beilage zur Korrespondenz Abwasser. 1977;3/77. German.

20. Baker GC, Smith JJ, Cowan DA. Review and re-analysis of domain-specific 16S primers. J Microbiol Methods. 2003 Dec;55(3):541–55.

21. Bragg L, Stone G, Imelfort M, Hugenholtz P, Tyson GW. Fast, accurate error-correction of amplicon pyrosequences using Acacia. Nat Meth. 2012 May;9(5):425–6.

22. Caporaso JG, Kuczynski J, Stombaugh J, Bittinger K, Bushman FD, Costello EK, et al. QIIME allows analysis of high-throughput community sequencing data. Nat Methods. 2010;7(5):335–6.

23. Edgar RC. Search and clustering orders of magnitude faster than BLAST. Bioinformatics. 2010 Oct 1;26(19):2460–1.

24. Quast C, Pruesse E, Yilmaz P, Gerken J, Schweer T, Yarza P, et al. The SILVA ribosomal RNA gene database project: improved data processing and web-based tools. Nucleic Acids Res. 2013 Jan 1;41(D1):D590–6.

25. Caporaso JG, Bittinger K, Bushman FD, DeSantis TZ, Andersen GL, Knight R. PyNAST: a flexible tool for aligning sequences to a template alignment. Bioinformatics. 2010;26(2):266–7.

26. Wang Q, Garrity GM, Tiedje JM, Cole JR. Naive Bayesian classifier for rapid assignment of rRNA sequences into the new bacterial taxonomy. Appl Environ Microbiol. 2007;73(16):5261–7.

27. Price MN, Dehal PS, Arkin AP. FastTree 2–approximately maximum-likelihood trees for large alignments. PloS One. 2010;5(3):e9490.

28. Lozupone C, Knight R. UniFrac: a new phylogenetic method for comparing microbial communities. Appl Environ Microbiol. 2005;71(12):8228–35.

29. Vázquez-Baeza Y, Pirrung M, Gonzalez A, Knight R. EMPeror: a tool for visualizing high-throughput microbial community data. Structure. 2013;585:20.

30. R Core Team. R: A Language and Environment for Statistical Computing (Internet). Vienna, Austria: R Foundation for Statistical Computing; 2013. Available from: http://www.R-project.org/

31. Oksanen J, Blanchet FG, Kindt R, Legendre P, Minchin PR, O'Hara RB, et al. vegan: Community Ecology Package (Internet). 2014. Available from: http://R-Forge.R-project.org/projects/vegan/

32. McMurdie PJ, Holmes S. phyloseq: An R Package for Reproducible Interactive Analysis and Graphics of Microbiome Census Data. Watson M, editor. PLoS ONE. 2013 Apr 22;8(4):e61217.

33. DeSantis TZ, Hugenholtz P, Larsen N, Rojas M, Brodie EL, Keller K, et al. Greengenes, a chimera-checked 16S rRNA gene database and workbench compatible with ARB. Appl Environ Microbiol. 2006;72(7):5069–72.

34. Kanehisa M, Goto S, Sato Y, Kawashima M, Furumichi M, Tanabe M. Data, information, knowledge and principle: back to metabolism in KEGG. Nucleic Acids Res. 2014 Jan 1;42(D1):D199–205.

35. Predictive functional profiling of microbial communities using 16S rRNA marker gene sequences. Langille, M. G.I.*; Zaneveld, J.*; Caporaso, J. G.; McDonald, D.; Knights, D.; a Reyes, J.; Clemente, J. C.; Burkepile, D. E.; Vega Thurber, R. L.; Knight, R.; Beiko, R. G.; and Huttenhower, C. *Nature Biotechnology*, 31(9), 814.

36. Segata N, IzardJ, Waldron L, Gevers D, Miropolsky L, Garrett WS, et al. Metagenomic biomarker discovery and explanation. Genome Biol. 2011;12(6):R60.

37. Giardine B, Riemer C, Hardison RC, Burhans R, Elnitski L, Shah P, et al. Galaxy: A platform for interactive large-scale genome analysis. Genome Res. 2005 Oct 1;15(10):1451–5.

38. Blankenberg D, Kuster GV, Coraor N, Ananda G, Lazarus R, Mangan M, et al. Galaxy: A Web-Based Genome Analysis Tool for Experimentalists. In: Current Protocols in Molecular Biology (Internet). John Wiley & Sons, Inc.; 2001 (cited 2015 Aug 6)

39. Goecks J, Nekrutenko A, Taylor J. Galaxy: a comprehensive approach for supporting accessible, reproducible, and transparent computational research in the life sciences. Genome Biol. 2010;11(8):R86.

40. Santana RH, Catão ECP, Lopes FAC, Constantino R, Barreto CC, Krüger RH. The Gut Microbiota of Workers of the Litter-Feeding Termite *Syntermes wheeleri* (*Termitidae*: *Syntermitinae*): Archaeal, Bacterial, and Fungal Communities. Microb Ecol. 2015 Aug;70(2):545–56.

41. Zhang J, Zhang Y, Quan X, Chen S. Enhancement of anaerobic acidogenesis by integrating an electrochemical system into an acidogenic reactor: Effect of hydraulic retention times (HRT) and role of bacteria and acidophilic methanogenic Archaea. Bioresour Technol. 2015 Mar;179:43–9.

42. Mhuantong W, Wongwilaiwalin S, Laothanachareon T, Eurwilaichitr L, Tangphatsornruang S, Boonchayaanant B, et al. Survey of Microbial Diversity in Flood Areas during Thailand 2011 Flood Crisis Using High-Throughput Tagged Amplicon Pyrosequencing. PLoS ONE. 2015 May 28;10(5):e0128043.

43. Green SJ, Vekatramanan R, Naqib A. Deconstructing the Polymerase Chain Reaction: Understanding and Correcting Bias Associated with Primer Degeneracies and Primer-Template Mismatches. PLoS ONE (Internet). 2015 May 21 (cited 2015 Sep 24);10(5)

44. McCarty PL, McKinney RE. Volatile acid toxicity in anaerobic digestion. J Water Pollut Control Fed. 1961;223–32.

45. Wijekoon KC, Visvanathan C, Abeynayaka A. Effect of organic loading rate on VFA production, organic matter removal and microbial activity of a two-stage thermophilic anaerobic membrane bioreactor. Bioresour Technol. 2011 May;102(9):5353–60.

46. Williams J, Williams H, Dinsdale R, Guwy A, Esteves S. Monitoring methanogenic population dynamics in a full-scale anaerobic digester to facilitate operational management. Bioresour Technol. 2013 Jul;140:234–42.

47. Griffin ME, McMahon KD, Mackie RI, Raskin L. Methanogenic population dynamics during start-up of anaerobic digesters treating municipal solid waste and biosolids. Biotechnol Bioeng. 1998;57(3):342–55.

48. Pullammanappallil PC, Chynoweth DP, Lyberatos G, Svoronos SA. Stable performance of anaerobic digestion in the presence of a high concentration of propionic acid. Bioresour Technol. 2001;78(2):165–9.

49. Seppälä M, Pyykkönen V, Väisänen A, Rintala J. Biomethane production from maize and liquid cow manure – Effect of share of maize, post-methanation potential and digestate characteristics. Fuel. 2013 May;107(0):209–16.

50. Sprott GD, Shaw KM, Jarrell KF. Ammonia/potassium exchange in methanogenic bacteria. J Biol Chem. 1984;259(20):12602–8.

51. Fotidis IA, Karakashev D, Kotsopoulos TA, Martzopoulos GG, Angelidaki I. Effect of ammonium and acetate on methanogenic pathway and methanogenic community composition. FEMS Microbiol Ecol. 2013 Jan;83(1):38–48.

52. Calli B, Mertoglu B, Inanc B, Yenigun O. Methanogenic diversity in anaerobic bioreactors under extremely high ammonia levels. Enzyme Microb Technol. 2005 Sep;37(4):448–55.

53. Sprott GD. Ammonia toxicity in pure cultures of methanogenic bacteria. Syst Appl Microbiol. 1986 May;Volume 7(Issues 2–3):Pages 358–63.

54. Chen Y, Cheng JJ, Creamer KS. Inhibition of anaerobic digestion process: A review. Bioresour Technol. 2008 Jul;99(10):4044–64.

55. Yenigün O, Demirel B. Ammonia inhibition in anaerobic digestion: A review. Process Biochem. 2013 May;48(5-6):901–11.

56. McCarty PL, McKinney RE. Salt toxicity in anaerobic digestion. J Water Pollut Control Fed. 1961;399–415.

57. Gottschalk G, Thauer RK. The Na+-translocating methyltransferase complex from methanogenic archaea. Biochim Biophys Acta BBA - Bioenerg. 2001 May 1;1505(1):28–36.

58. Feijoo G, Soto M, Méndez R, Lema JM. Sodium inhibition in the anaerobic digestion process: Antagonism and adaptation phenomena. Enzyme Microb Technol. 1995 Feb;(17):180–8.

59. Rinzema A, Boone M, van Knippenberg K, Lettinga G. Bactericidal Effect of Long Chain Fatty Acids in Anaerobic Digestion. Water Environ Res. 1994 Jan 1;66(1):40–9.

60. Conklin , Stensel HD, Ferguson J. Growth Kinetics and Competition between Methanosarcina and Methanosaeta in Mesophilic Anaerobic Digestion. Water Environ Res. 2006 May 1;78(5):486–96.

61. Hori T, Haruta S, Ueno Y, Ishii M, Igarashi Y. Dynamic Transition of a Methanogenic Population in Response to the Concentration of Volatile Fatty Acids in a Thermophilic Anaerobic Digester. Appl Environ Microbiol. 2006 Feb 1;72(2):1623–30.

62. De Vrieze J, Hennebel T, Boon N, Verstraete W. Methanosarcina: The rediscovered methanogen for heavy duty biomethanation. Bioresour Technol. 2012 May;112:1–9.

63. Huser BA, Wuhrmann K, Zehnder AJB. Methanothrix soehngenii gen. nov. sp. nov., a New Acetotrophic Non-hydrogen-oxidizing Methane Bacterium. Arch Microbiol. 1982 Jul;132(1):1–9.

64. Oren A. The Family Methanosarcinaceae. In: The Prokaryotes - Other Major Lineages of Bacteria and the Archaea. 4th ed. Springer-Verlag Berlin Heidelberg; 2014. p. 1028.

65. Romesser JA, Wolfe RS, Mayer F, Spiess E, Walther-Mauruschat A. Methanogenium, a new genus of marine methanogenic bacteria, and characterization ofMethanogenium cariaci sp. nov. andMethanogenium marisnigri sp. nov. Arch Microbiol. 1979 May;121(2):147–53.

66. Dridi B, Fardeau M-L, Ollivier B, Raoult D, Drancourt M. Methanomassiliicoccus luminyensis gen. nov., sp. nov., a methanogenic archaeon isolated from human faeces. Int J Syst Evol Microbiol. 2012 Aug 1;62(Pt 8):1902–7.

67. Whitford MF, Teather RM, Forster RJ. Phylogenetic analysis of methanogens from the bovine rumen. BMC Microbiol. 2001;1(1):5.

68. Ohkuma M, Noda S, Kudo T. Phylogenetic relationships of symbiotic methanogens in diverse termites. FEMS Microbiol Lett. 1999;171(2):147–53.

69. Schlüter A, Bekel T, Diaz NN, Dondrup M, Eichenlaub R, Gartemann K-H, et al. The metagenome of a biogas-producing microbial community of a production-scale biogas plant fermenter analysed by the 454-pyrosequencing technology. J Biotechnol. 2008 Aug;136(1-2):77–90.

70. Kröber M, Bekel T, Diaz NN, Goesmann A, Jaenicke S, Krause L, et al. Phylogenetic characterization of a biogas plant microbial community integrating clone library 16S-rDNA sequences and metagenome sequence data obtained by 454-pyrosequencing. J Biotechnol. 2009 Jun;142(1):38–49.

71. Claesson MJ, O'Sullivan O, Wang Q, Nikkilä J, Marchesi JR, Smidt H, et al. Comparative Analysis of Pyrosequencing and a Phylogenetic Microarray for Exploring Microbial Community Structures in the Human Distal Intestine. Ahmed N, editor. PLoS ONE. 2009 Aug 20;4(8):e6669.

72. Nyonyo T, Shinkai T, Mitsumori M. Improved culturability of cellulolytic rumen bacteria and phylogenetic diversity of culturable cellulolytic and xylanolytic bacteria newly isolated from the bovine rumen. FEMS Microbiol Ecol. 2014 Jun;88(3):528–37.

73. Grabowski A. Petrimonas sulfuriphila gen. nov., sp. nov., a mesophilic fermentative bacterium isolated from a biodegraded oil reservoir. Int J Syst Evol Microbiol. 2005 May 1;55(3):1113–21.

74. Chen S, Dong X. Proteiniphilum acetatigenes gen. nov., sp. nov., from a UASB reactor treating brewery wastewater. Int J Syst Evol Microbiol. 2005 Nov 1;55(6):2257–61.

75. Li A, Chu Y, Wang X, Ren L, Yu J, Liu X, et al. A pyrosequencing-based metagenomic study of methane-producing microbial community in solid-state biogas reactor. Biotechnol Biofuels (Internet). 2013 (cited 2015 May 29);6(3)

76. Delbes C, Moletta R, Godon J-J. Monitoring of activity dynamics of an anaerobic digester bacterial community using 16S rRNA polymerase chain reaction–single-strand conformation polymorphism analysis. Environ Microbiol. 2000;2(5):506–15.

77. Fernández A, Huang S, Seston S, Xing J, Hickey R, Criddle C, et al. How Stable Is Stable? Function versus Community Composition. Appl Environ Microbiol. 1999 Aug 1;65(8):3697–704.

78. Lee S-H, Park J-H, Kang H-J, Lee YH, Lee TJ, Park H-D. Distribution and abundance of Spirochaetes in full-scale anaerobic digesters. Bioresour Technol. 2013 Oct;145:25–32.

79. Jumas-Bilak E, Marchandin H. The Phylum Synergistetes. In: The Prokarytoes - Other Major Lineages of Bacterialand the Archaea. 4th ed. Springer-Verlag Berlin Heidelberg; 2014.

80. Baena S, Fardeau ML, Labat M, Ollivier B, Thomas P, Garcia JL, et al. Aminobacterium colombiensegen. nov. sp. nov., an amino acid-degrading anaerobe isolated from anaerobic sludge. Anaerobe. 1998 Oct;4(5):241–50.

81. Baena S, Fardeau M-L, Labat M, Ollivier B, Garcia J-L, Patel B. Aminobacterium mobile sp. nov., a new anaerobic amino-acid-degrading bacterium. Int J Syst Evol Microbiol. 2000;50(1):259–64.

82. Yamada T. Anaerolinea thermolimosa sp. nov., Levilinea saccharolytica gen. nov., sp. nov. and Leptolinea tardivitalis gen. nov., sp. nov., novel filamentous anaerobes, and description of the new classes Anaerolineae classis nov. and Caldilineae classis nov. in the bacterial phylum Chloroflexi. Int J Syst Evol Microbiol. 2006 Jun 1;56(6):1331–40.

83. Martini M, Marcone C, Lee I-M, Firrao G. The Family Acholeplasmataceae (including Phytoplasmas). In: The Prokarytoes - Firmicutes and Tenericutes. 4th ed. Springer-Verlag Berlin Heidelberg; 2014.

84. Tauch A, Sandbote J. The Family Corynebacteriaceae. In: The Prokaryotes - Actinobacteria. 4th ed. Springer-Verlag Berlin Heidelberg; 2014.

85. Lee KCY, Dunfield PF, Stott MB. The Phylum Armatimonadetes. In: The Prokaryotes - Other Major Lineages of Bacteria and the Archaea. 4th ed. Springer-Verlag Berlin Heidelberg; 2014.

86. Teixiera LM, Merquior VLC. The Family Moraxellaceae. In: The Prokarytoes - Gammaproteobacteria. 4th ed. Springer-Verlag Berlin Heidelberg; 2014.

87. Chumpitazi BP, Cope JL, Hollister EB, Tsai CM, McMeans AR, Luna RA, et al. Randomised clinical trial: gut microbiome biomarkers are associated with clinical response to a low FODMAP diet in children with the irritable bowel syndrome. Aliment Pharmacol Ther. 2015 Aug 1;42(4):418–27.

88. Loudon AH, Woodhams DC, Parfrey LW, Archer H, Knight R, McKenzie V, et al. Microbial community dynamics and effect of environmental microbial reservoirs on red-backed salamanders (Plethodon cinereus). ISME J. 2014 Apr;8(4):830–40.

89. Jiménez DJ, Dini-Andreote F, van Elsas JD. Metataxonomic profiling and prediction of functional behaviour of wheat straw degrading microbial consortia. Biotechnol Biofuels. 2014 Jun 12;7:92.

90. Karatan E, Michael AJ. A wider role for polyamines in biofilm formation. Biotechnol Lett. 2013 Nov;35(11):1715–7.

91. Pelmenschikov V, Blomberg MRA, Siegbahn PEM, Crabtree RH. A Mechanism from Quantum Chemical Studies for Methane Formation in Methanogenesis. J Am Chem Soc. 2002 Apr;124(15):4039–49.

92. Thauer RK, Kaster A-K, Goenrich M, Schick M, Hiromoto T, Shima S. Hydrogenases from Methanogenic Archaea, Nickel, a Novel Cofactor, and H $_2$ Storage. Annu Rev Biochem. 2010 Jun 7;79(1):507–36.

93. Murray WD, van den Berg L. Effects of Nickel, Cobalt, and Molybdenum on Performance of Methanogenic Fixed-Film Reactor. Appl Environ Microbiol. 1981 Sep;42(3):502–5.

94. Gonzalez-Gil G, Kleerebezem R, Lettinga G. Effects of nickel and cobalt on kinetics of methanol conversion by methanogenic sludge as assessed by on-line CH4 monitoring. Appl Environ Microbiol. 1999;65(4):1789–93.

95. Zandvoort MH, van Hullebusch ED, Fermoso FG, Lens PNL. Trace Metals in Anaerobic Granular Sludge Reactors: Bioavailability and Dosing Strategies. Eng Life Sci. 2006 Jun;6(3):293–301.

96. Mori, K., Iino, T., Suzuki, K.-I., Yamaguchi, K., and Kamagata, Y. (2012) Aceticlastic and NaCl-Requiring Methanogen “Methanosaeta pelagica” sp. nov., Isolated from Marine Tidal Flat Sediment. *Applied and Environmental Microbiology* **78**: 3416–3423.

Chapter 3

Trace elements supplement fermenting bacteria rather than methanogens in biogas mono-digestion of grass silage.

Jamie A. FitzGerald,[1,2,] David M. Wall [2,3], Stephen A. Jackson,[1] Jerry D. Murphy[2,3] and Alan D.W. Dobson[1,2,] *

[1] School of Microbiology, University College Cork, Ireland.

[2] The MaREI Centre, Environmental Research Institute, University College Cork, Ireland

[3] School of Engineering, University College Cork, Ireland

This chapter has been submitted for consideration to the journal *Renewable Energy* under the same title and is currently awaiting review.

Abstract

Trace elements (TE) are known to play a crucial role in microbial metabolism, and to improve biogas output in anaerobic digestion (AD), although the mechanisms are not well characterised.

We have characterised the microbial communities associated with anaerobic mono-digestion of grass silage through initiation, stable operation, inhibition at high organic loading rates, and rescue through addition of trace elements (iron, nickel and cobalt). Comparison of these communities with communities from unsupplemented anaerobic co-digestion of a grass silage:slurry mix shows TE supplementation to be significantly associated with increases in genera known to be involved in the metabolism of volatile fatty acids (*Gelria*, *Anaerovorax*, *Dethiobacter*), hydrolysis (*Clostridia*), and in particular the uncharacterised clostridial order MBA03. However, a decrease was seen in the abundance of methanogenic Archaea, indicating TE supplementation improves mono-digestion of grass silage through augmented fermentation rather than improved methanogenesis.

1. Introduction

1.1 Use of Grass for Biogas Production

Anaerobic digestion (AD) of various organic materials (including municipal, agricultural, and industrial wastes, and energy crops) is an important element in both sustainable waste management and renewable energy strategies at a global level. Grasses are popular substrates for biogas production due to their ease of cultivation, high energy content, favourable carbon:nitrogen ratio (>20:1), and relatively low ligno-cellulosic fraction when harvested early (Nizami et al., 2009; Prochnow et al., 2009; van der Weijde et al., 2013). Grasses are regularly preserved for later use through ensiling, where crops are stored in an air-tight state which quickly becomes anaerobic and partially ferments to a stable acidic end-point. Grass silage is an improved biogas feedstock when compared to raw grass, due to this 'pre-digestive' hydrolysis of polysaccharides by lactic acid bacteria and the resultant fermentative acids (Elgersma et al., 2003). With approximately one quarter of the Earth's land mass covered by grass or arable land, the use of grasses and grass silage as a resource for biogas production is encouraged both within the European Union and internationally (Prochnow et al., 2009).

1.2 Use of Trace Elements in Anaerobic Digestion

The diverse range of microorganisms which contribute to AD require balanced macronutrients (nitrogen, phosphorous, potassium) and micronutrients (including various trace elements, TE) for efficient biogas production (Demirel and Scherer, 2011). High organic loading rates (OLR) of mono-digested feedstocks (such as sugar beet, maize, seaweed, grains) are known to destabilise microbial communities, primarily due to an 'unbalanced diet'; TE scarcity in AD is often cited for accumulation of organic acids, or gradual decline and failure to thrive (Lebuhn et al., 2008; Demirel and Scherer,

2009; De Vries et al., 2012; Allen et al., 2014; Wintsche et al., 2016).

In industrialised biogas production, TE supplementation is often a *de-facto* safeguard to ensure reliable operation, with AD guidelines describing TE dosing regimes (Drosg, 2013). The high efficacy of supplementation has encouraged studies into its effects on the microbial community, with an emphasis on improving methanogenesis, with a summary of the literature presented in Table 1. Gustavsson and colleagues described changes in mesophilic grain digesters when Co and Ni became limiting, resulting in methanogen populations shifting from acetoclastic *Methanosarcinales* towards hydrogenotrophic *Methanoculleus*, as well as increases in volatile fatty acids (VFAs) (Gustavsson et al., 2013). Minor shifts in bacterial taxa were observed, with an overall *Bacteroidetes*/*Firmicutes* majority. Similarly, Wintshe and colleagues reported that removal of TE (Ni, Co, Mo, Mn, W) supplementation increased VFA content together with an increased abundance in *Methanoculleus* relative to *Methanosarcina*, suggesting hydrogenotrophic methanogens may have a reduced requirement for Ni due to the biochemical pathways they employ in methane formation (Wintsche et al., 2016). Other studies have reported that the addition of Fe, Co and Ni increased the rate of methanogenesis via syntrophic acetate oxidation (SAO) and hydrogenotrophy, despite hydrogenotrophic *Methanomicrobiales* being displaced by *Methanosarcinales* as VFA levels rose in semi-continuous anaerobic digesters treating household and food wastes (Karlsson et al., 2012).

The effectiveness of supplementation is attributed to the many TE-containing enzyme complexes involved in AD, such as the end-step in archaeal methanogenesis which is catalysed by methyl-coenzyme M reductase (MCR), shown by (Ermler et al., 1997) to contain Ni^{2+} as the functional electrophilic core in methyl-translocation; while cobalt in cobalamine (vitamin B12) is used by methanogens to capture methyl groups from acetate, CO_2 (via THMPT) or methylated compounds (Roth et al., 1996). Similarly, bacteria use Co in cobalamine to improve reduction potential in small

Study	Feed	Loading Rate kgVS/m^3 * = kg/m^3	HRT	Supplemented (mg/L) Co	Fe	Ni	supplemented performance	note	Other TE added (mg/L)
Gustavsson et al., 2011	GrnS	4	20	0.5	0.5	0.2	Yield CH4: 0.4 m^3/kgVSL	Supplementation necessary for rate trialled	n/a
Zhang & Jahng, 2012	FW	6.64	20	2	100	10	Yield CH4: 2.4 L /L	Incr. yield, VFA degradation. Supplemented every 5 days	Mo: 5
Qiang et al., 2012	FW	6.3*	30	1	10	1	Yield CH4: 0.42 m^3/kgTS	Incr. yield, VFA degradation. Irregularly supplemented, Co+Ni most effective	n/a
Karlsson et al., 2012	SW, FW, MSW	2.5	30	0.5	500	0.25	Yield CH4: 1270 L/kgVS	Yield unaffected, improved stability, VFA degradation. Supplement added to substrate.	n/a
Qiang et al., 2013	FW (55°C)	6.3 *	30	1	10	1	Improved CH_4: 30L/kgVS	Incr. yield, VFA degradation. Supplement every 45 days	n/a
Wall et al., 2014	GS	4	19	0.13 ^	74.4	2.48	Improved CH_4: 44 L/kgVS	Incr. yield, VFA degradation Source samples from this study	n/a
Wintsche et al., 2016	DS	5	25	0.92	987	3.15	no significant change in yield	TE deprivation leads to accumulation of VFA, TAN, H2S	Mo: 0.8; Mn: 39; W: 1.23; Zn: 10.5
Bougrier et al., 2018	BSG	2.23	40	15	200	15	Yield CH4: 348 L/kgVS	Incr. stability, yield, VFA degradation. Final TE values in soluble fraction (mg/L):	Cu, Mn
				118	1000	59	Yield CH4: 374 L/kgVS	Co: 0.02 & 0.1; Fe: 3 ; Ni: 0.01 & 0.05	

Review	Ranges in Literature Co	Fe	Ni	units
Schattauer et al., 2013	0.001 - 20	1 - 200	0.005 - 30	mg/L
Choong et al., 2016	0.1 - 1	1 - 100	0.1 - 5	mg/L
Zhang et al., 2018	2.5 - 5	1200 - 7000	2.5 - 20	mg/kg
Ye et al., 2018	0.05 - 0.66	7.17-230.7	0.42 - 9.12	mg/kgTS

Table 1: Recommended trace element values of cobalt (Co), iron (Fe) and nickel (Ni) from literature. In all studies, HRT and loading (OLR, COD) were calulated at a daily basis.

Legend: BSG: Brewers Spent Grains; COD: Chemical Oxygen Demand; DG: Distiller's Grains; FW: Food Waste; GS: Grass Silage; GrnS: Grain Stillage; HRT: Hyrdaulic Retention Time; MSW: Municipal Solid Waste; OLR: Organic Loading Rate; SW: Slaughterhouse Waste; VS: Volatile Solids. **Trace elements**: Co: cobalt; Cu: copper; Fe:

molecules (propanediol, glycerol, ethanol-amine) through moiety rearrangements, enabling fermentation at thermodynamic limits of reduction (Roth et al., 1996). Hydrogenases, classed based on the Ni-Fe, Fe-Fe or Fe functional groups at their core, split H_2 or reduce protons to facilitate bidirectional oxidation/reduction reactions. In methanogenesis, Ni-Fe and Fe hydrogenases gradually reduce CO_2 to CH_4, while hydrolysis and fermentation utilise hydrogenases for redox reactions and energy conservation (Vignais and Billoud, 2007). Thus, trace elements such as Fe, Co, and Ni are crucial in all stages of biogas production. For a summary of these reactions, and the relative importance of trace elements, see Chapter 1 Figure 1.

However, these routes of supplementation have not been characterised, nor are the overall effects on microbial communities understood. As such, the actual mechanisms through which TE might supplement AD remain obscure.

1.3 Understanding the role of Trace Element supplementation

In a previous study by our group, it was demonstrated that supplementation of grass silage mono-digestion with Fe, Ni and Co increased biogas output and reduced VFA burden. Wall et al., (2014) showed mono-digestion of a ryegrass-silage to have a biomethane potential (BMP) of 398L CH_4 per kilogram of volatile solids (LCH_4/kgVS). Continuous anaerobic mono-digestion of this grass-silage at 37°C (Reactor: Grass, 'R-G') reached specific methane yields (SMY) above this BMP value (i.e. biomethane efficiency, SMY/BMP=B_{eff}, ≈1.0) for OLR2-2.5kgVS/d, but faltered at OLR above 2.5kgVS$m^{-3}d^{-1}$ and deteriorated above 3.5kgVS/m^3.d (Figure 1A).

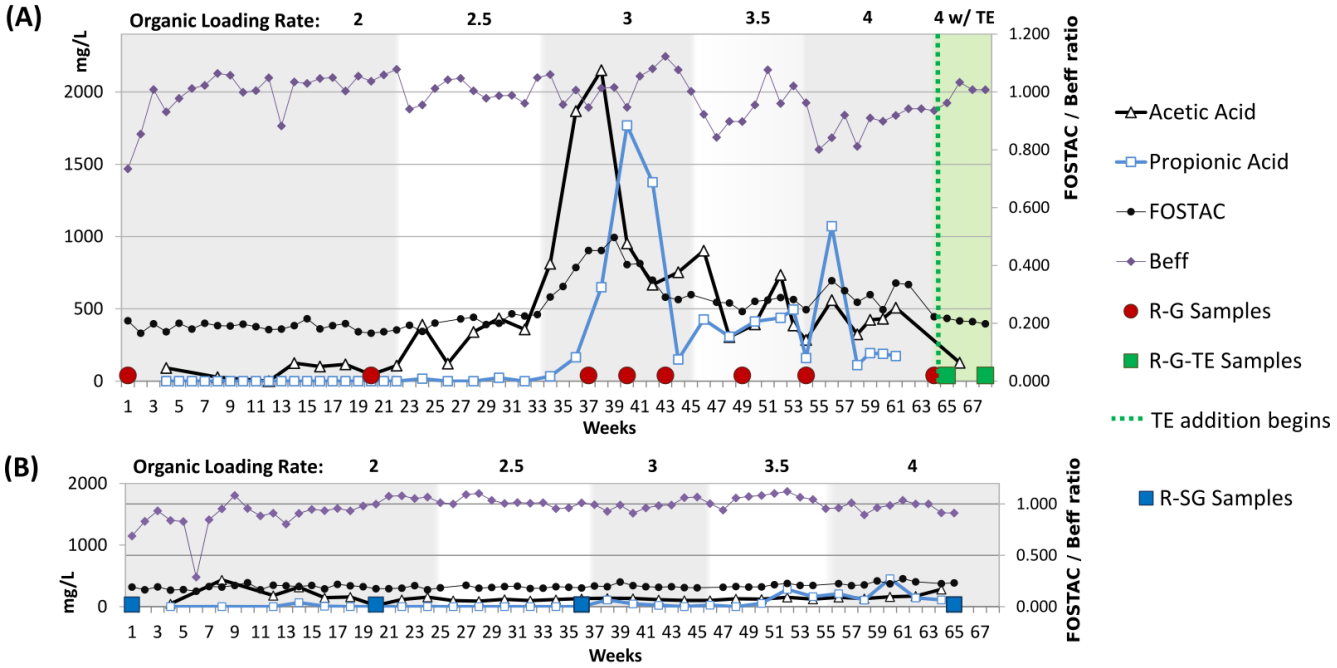

***Figure 1**: Biogas Performance for Reactor R-G: grass silage (A); reactor R-SG: silage-slurry (B). Samples were taken at weeks as indicated on the X axes, with both graphs drawn to the same scales. Values on secondary X axes are unit-free measurements (FOSTAC, B_{eff}). Abbreviations: R-G: Reactor: Grass; R-G-TE: Reactor: Grass with TE; R-SG: Reactor: Grass-Silage; FOSTAC: a ratio of acidic carbon:inorganic carbon, reflecting process stability; B_{eff}: biomethane efficiency, see section 1.3.*

In response to falling B_{eff} in R-G, TE levels were compared against those of a mesophilic reactor digesting an 80% ryegrass silage:20% dairy-slurry mix (Reactor: Slurry-Grass, R-SG, operated in parallel with R-G, see Figure 1B) which displayed no interruption in performance with respect to biogas production. Despite a lower overall BMP (346 L CH_4/kgVS), R-SG was able to sustain a B_{eff} ≈1.0 at the elevated OLR of 4kgVS/m^3.d. This superior performance was attributed to the TE content provided by the 20% slurry inclusion in R-SG (Wall et al., 2014). When investigated via mass spectrometry, TE concentrations for both reactors were within suggested and non-toxic ranges (see Table 1 and Section 2.3). However, reactor TE contents can vary widely depending on the feedstock and inoculum used (Schattauer et al., 2011) and R-G appeared depleted in Co, Fe and Ni with respect to the

corresponding TE levels in R-SG. A supplement of Ni, Fe, and Co was added to R-G which restored biological stability and increased B_{eff} back to approximately 1.0, associated with an improved SMY of 404 $LCH_4kg^{-1}VS$.

To better understand how TE supplementation improved lignocellulosic monodigestion, 16S microbial communities at different TE levels were characterised through pyrosequencing to identify functional microbial populations (e.g. hydrolysers, acetogens, methanogens) associated with the improvement of biogas production through supplementation.

As such, this study aims to:

1. Characterise development of the microbial communities in grass silage mono-digestion, and grass silage-slurry mono-digestion
2. Identify microbial populations unique to reactors R-G and R-SG, as well as key populations common to either setup
3. Identify significant differences in population structure between mono-digestion (i.e. R-G: low TE availability) and mono-digestion supplemented with Fe, Ni, and Co (i.e. R-G: high TE availability)
4. Relate TE availability, changes in functional microbial populations, and changes in biogas production
5. Identify likely routes for TE supplementation to improve the anaerobic mono-digestion of lignocellulosics.

2. Materials and Methods

Detailed descriptions of R-G and R-SG operation, feedstock, and TE supplementation have previously been reported (Wall et al., 2014), but are summarised below.

2.1 Reactor Operation

Briefly, two 5L continuously stirred tank reactors (4L operating volume) were inoculated with 4L of a 1:1 mix of digestate from food waste and poultry-/cattle-effluent digesters. The reactors were maintained at 37°C and fed on a daily basis, initially at an organic loading rate (OLR) of 2 kgVS/m^3/day. Over a duration of 65 (R-SG) and 68 weeks (R-G), OLR was increased to 4 kgVS/m^3/day in increments of 0.5 kgVS/m^3/day. To reduce viscosity in either reactor, its effluent was used to dilute incoming feed to 100gDS/kg. Hydraulic retention time (HRT) was recalibrated to account for this change, as previously reported (Wall et al. 2014).

2.2 Feedstock

Silage feedstock was a ryegrass (*Lolium perenne*) first-cut at inflorescence, wilted for 24 hours and ensiled for 5 weeks in polyethylene film at 18-20°C. Silage was then frozen until use at -20°C and shredded to ≤ 1cm prior to addition to the reactor. Dry Solids (DS) were 293g/kg and Volatile Solids (VS) were 920g/kgDS, with a C:N ratio of 26:1. A quantity of slurry was obtained from dairy cattle and stored at -20°C until use, with an average dry solids of 76g/kg and volatile solids of 750g/kgDS.

2.3 TE Measurement & Supplementation

Trace element (TE) concentrations in feedstock and reactors were measured through mass-

spectrometry, with R-G and R-SG measured at each HRT. On the basis of high biomethane efficiencies in R-SG at OLR 3.5 kgVS/m^3/day, TE levels at this loading rate were used as a benchmark for supplementation of cobalt (Co), nickel (Ni) and iron (Fe) in R-G. From R-G week 65, a TE supplement solution of $CoCl_2.6H_20$, $FeCl_3.6H_20$ and $NiCl_2.6H_20$ in deionised water was added daily, equating to the addition of 0.13 mg Co/l, 74.40 mg Fe/l and 2.48 mg Ni/l to R-G. These values were within ranges from the literature, which vary depending on reactor operation and feedstock (see Table 1). Other trace elements (e.g. molybdenum, selenium) were comparable between reactor setups and were not supplemented.

2.4 Sampling

10 samples were selected from R-G spanning time points of interest, with 4 samples taken from R-SG to enable comparison with a stable analogous reactor. Samples covered the following stages: reactor startup (R-G & R-SG weeks 01); established reactor, as judged from VFA and FOS:TAC profiles (R-G & R-SG weeks 20); VFA disturbance in R-G at OLR increase from 2.5 to 3 (R-G weeks 37, 40, 43, 49; R-SG week 37), pre-TE addition (R-G weeks 54, 64), and post-TE addition (R-G weeks 65, 68, hereafter 'R-G-TE'; R-SG week 65). For each timepoint sampled, approximately 50ml of digestate was removed to a sterile 50ml tube and frozen at -20°C before processing.

2.5 DNA Extraction & Molecular Methods

Total nucleic acids were extracted using a Tris-EDTA-NaCL-polyvinylpyrolidone buffer with proteinase K and CTAB followed by a phenol-chloroform extraction and precipitation with sodium acetate/isopropanol (see Appendix B). Each sample had its total nucleic acids extracted in three

technical replicates, before combining equilibrated volumes for polymerase chain reaction. PCR was applied to each sample using pyrosequencing primers containing adapter, key, Roche MID (1-14) sequences, and primer sequences S-D-Univ-0905-a-S-18 (TGA AAC TYA AAG GAA TTG) (Gao et al., 2015) and S-D-Univ-1492-a-A-19 (GGT TAC CTT GTT ACG ACT T) (Leser et al., 2002). Each sample was amplified in three technical replicates, and combined for purification. Products were cleaned using a gel extraction (QIAquick Gel Extraction Kit, QIAGEN) and purification kit (MinElute PCR Purification Kit, QIAGEN), before being combined in 50ul, at 5ng/µl per sample. Pyrosequencing was carried out on a Roche-454 FLX+ by Macrogen (Seoul, Republic of Korea).

2.6 Bioinformatics

Sequences obtained were de-multiplexed using QIIME's split_libraries.py script (Caporaso et al., 2010), and uploaded to the ARB-SILVA NGS version 1.63/1.3.9 (Quast et al., 2013) portal for filtering, clustering at 98%, and taxonomy assignment at 95%. Tables of operational taxonomic units (OTUs) and taxonomy were explored in R using ggplot2, phyloseq, and RStudio (Wickham, 2009; McMurdie and Holmes, 2013; R Core Team, 2013). Abundances were transformed using the *variancestabilisingtransformation* function from the DESeq2 package (Love et al., 2014), before being tested in LEfSe (Segata et al., 2011) for differential abundances (sequentially applying Kruskal-Wallis rank sum test, Wilcoxon pair test, and linear discriminant analysis (LDA)) between R-G, R-G-TE, and R-SG. Week 01 samples (R-G Week 01, R-SG Week 01) were not included in the LEfSe analysis as they were not considered representative of established communities during biogas operation (Figure 2). Default significance cut-offs of alpha=0.05 were used, with an elevated LDA threshold of 3. The sequence data from this study were submitted as a single SFF file to the ENA databases under accession PRJEB22994, accessible at the URL http://www.ebi.ac.uk/ena/data/view/PRJEB22994

3. Results and Discussion

3.1 Community Composition

Community relative abundances are outlined in Figure 2. Despite clear differences in performance between R-G and R-SG, the common setup, inoculum, and overlap in feedstock supported the development of two closely-related communities. In both reactors the major community components were *Firmicutes* (84% of all reads) and *Bacteroidetes* (13% of all reads), underscoring the importance of these metabolically diverse phyla (hydrolysers, fermenters, acido/acetogens) in grass-based AD.

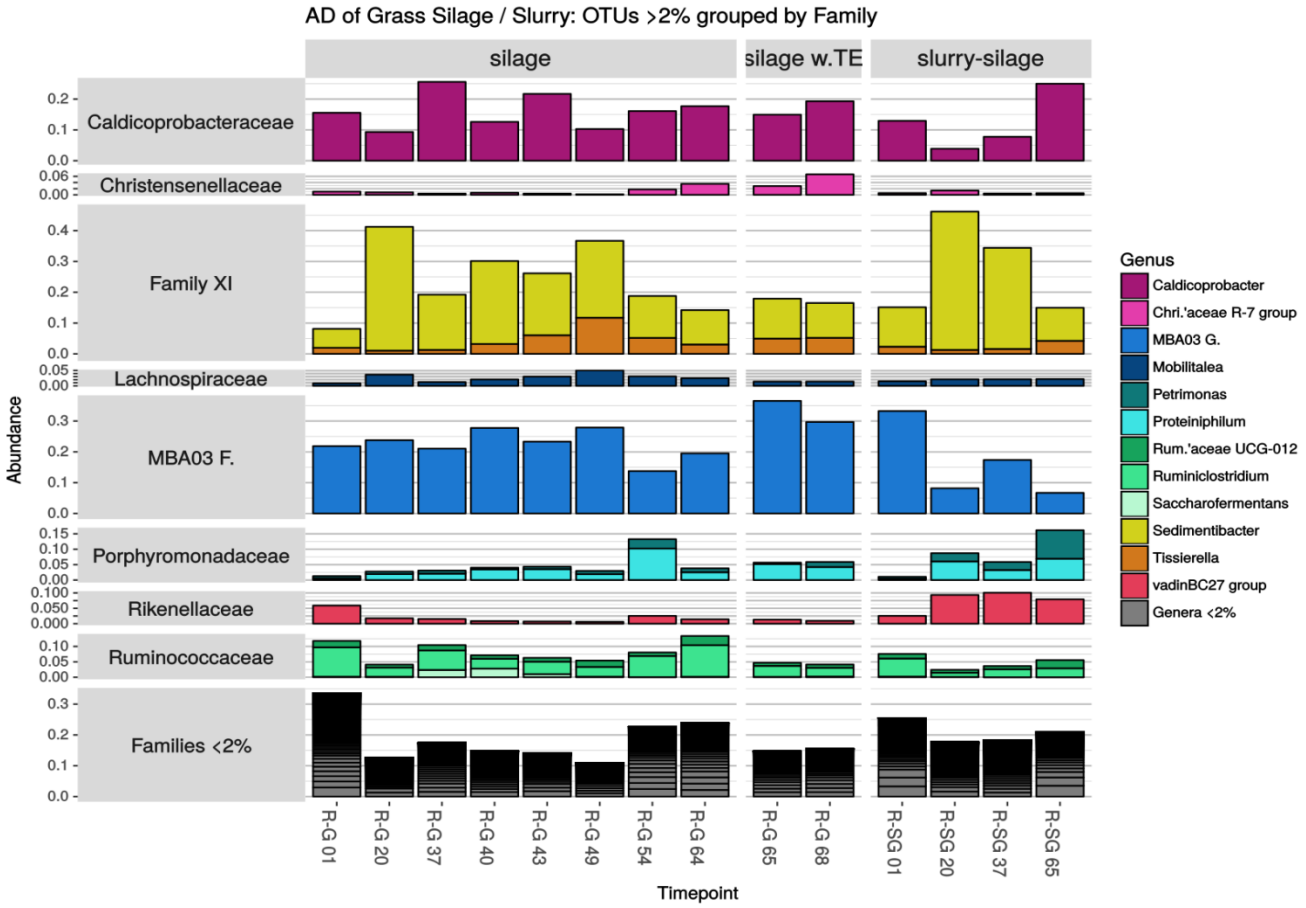

***Figure 2**: Relative Community Composition for R-G, R-G-TE, and R-SG. OTUs below 2% total relative abundance are grouped at bottom.*

21% of total reads were contributed by the uncharacterised *Firmicute* order MBA03, originally isolated from municipal thermophilic AD (Tang et al., 2004), and often detected in thermophilic

and/or cellulolytic biogas reactors (Lebuhn et al., 2008; Smith et al., 2014; Wei et al., 2015). 63% of total reads was allocated to the *Firmicute* order *Clostridiales* (23% *Sedimentibacter*; 15% *Caldicoprobacter*; <5% *Ruminoclostridium*, *Tissierella*, *Mobilitalea*, *Ruminococcaceae*, *Christensenellaceae*, *Gelria*; <1% others), representing genera known to hydrolyse polymers (celluloses and other polysaccharides, peptides,) and ferment monomers (amino acids, carbohydrate), acting as acidogens/acetogens (producing acetate, butyrate, lactate, CO_2, H_2) in the process (Matthies et al., 2000; Breitenstein, 2002; Plugge et al., 2002; Yutin and Galperin, 2013).

13% of total reads were assigned to closely-related families in order *Bacteroidales* (6% *Porphyromonadaceae*, 4% *Rikenellaceae*, <1% *Marinilabiaceae*, several uncultured taxa), again representing fermenters of saccharides or protein, and acidogens and acetogens known for production of short VFAs (acetate, propionate, iso-valerate, butyrate) and CO_2/H_2.

A final 3% of total reads contributed a diverse range of bacterial phyla (*Tenericutes*, *Proteobacteria*, *Fibrobacteres*, *Actinobacteria*), as well as the methanogenic Archaea crucial for biogas reactor function (*Euryarchaeota*). Notably, only hydrogenotrophic *Methanobacterium* (0.3% total reads) was well represented throughout this study; other Archaea were visible only at Week 1 (*Methanothrix*, *Methanoculleus*) or intermittently at very low abundances (<0.02% total reads: *Methanosarcina, Methanothermobacter*, *Methanobrevibacter*, *Methanosphaera*) (Figure 3).

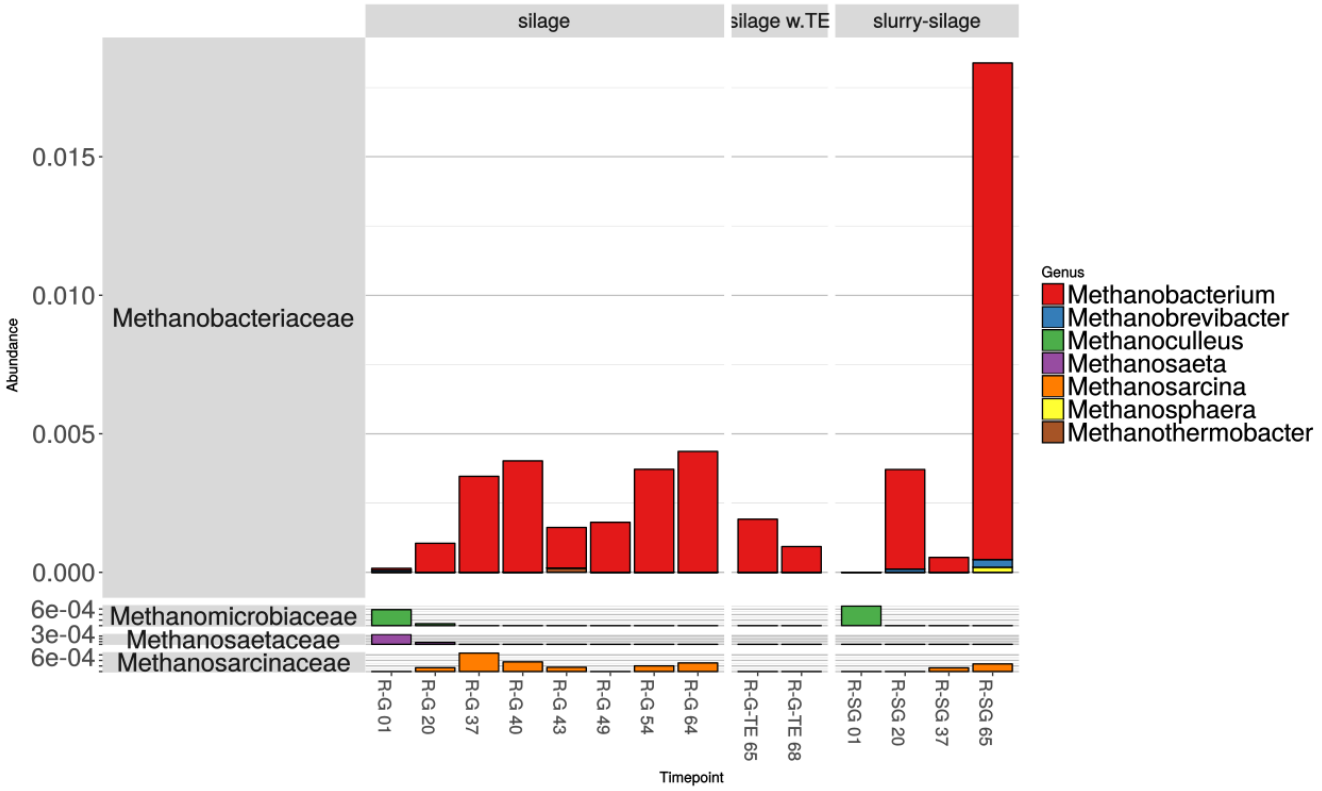

***Figure 3*: Relative abundances for archaeal (methanogen) taxa**: *R-G, R-G-TE, and R-SG. Note variable scale (Y axis).*

3.2 Differential Abundance Testing

To investigate how differences in feedstock and TE availability shaped reactor community structure and biogas function, 16S communities were sampled (see Figure 1) and compared between low TE levels (R-G Weeks 01 - 64), supplemented TE levels (R-G-TE Weeks 65 – 68), and TE-rich feedstock (R-SG Weeks 01 - 65) using LEfSe (Segata et al., 2011). Significant associations and likely metabolic roles in AD are given in Table 2 and summarised in Figure 4. Full statistical outputs are provided via Appendix D, or the data hosted at https://zenodo.org/record/1249599.

Treatment	Clade	Taxon	Likely Roles in AD					Association (LDA score)	Signif.
			H	F	Ac	At	M		
R-SG - Grass Silage	class	*Methanomicrobia*					•	3.02	0.04
	family	*Comamonadaceae*						3.13	0.04
	genus	*Ruminiclostridium*	•	•	•	•		3.23	0.04
		Pelotomaculum		•	•	•		3.19	0.03
		Sporobacter		•		•		3.15	0.03
R-G-TE - Grass Silage w. TE Suppl.	class	*Clostridia*	•	•	•	•		4.42	0.01
	order	MBA03	-	-	-	-	-	3.56	0.02
	genus	M2PB4-65 Termite group	-	-	-	-	-	3.47	0.02
		Gelria		•	•	•		3.43	0.04
		Anaerovorax (Family XIII)		•	•	•		3.33	0.04
		Dethiobacter						3.15	0.04
		P palm C A 51 (*Clostridiales*)	-	-	-	-	-	3.02	0.02
R-SG - Grass Silage -Slurry	class	*Mollicutes*						3.48	0.02
	genus	NK3A20 group (*Lachnospiraceae*)	•					3.41	0.04
		Erysipelothrix		•	•	•		3.33	0.04
		vadin BC27 group (*Rikenellaceae*)	-	-	-	-	-	3.25	0.04
		Mogibacterium (Family XIII)						3.21	0.04
		AD3011 (Family XIII)	-	-	-	-	-	3.19	0.02
		Trichococcus		•	•	•		3.12	0.04
		Acetitomaculum		•		•		3.08	0.02

Table 2: Significant associations between taxa and the three characterised conditions: *Grass Silage AD with declining TE (R-G), TE-Supplemented Grass Silage AD (R-G-TE), and Grass Silage-Slurry AD (R-SG). Roles in AD for significant taxa are presented where possible as identified in the literature (point = activity, gap = no activity, dash = unknown). Association (LDA score) indicates how reliable the association is between taxon and a given treatment (e.g. R-G-TE) on a log10 scale (conservative cut-off of 3); Significance refers to strength of association between taxon and treatment. Abbreviations: AD: Anaerobic Digestion;* ***Ac****: Acidogen;* ***At****: Acetogen;* ***F****: Fermentation;* ***H****: Hydrolysis;* ***LDA****: Linear Discriminant Analysis;* ***Signif****: Significance.*

3.2.1 Community Differences Between Reactor Feedstocks

Statistical analysis indicated that R-G was enriched with polysaccharide (i.e. plant biomass) degrading and fermenting taxa, while R-SG was enriched for taxa associated with the animal gut (i.e. included in R-SG through daily addition of 20% slurry feedstock).

Briefly, 9 genera and 8 higher taxa were significantly associated with R-G, while 8 genera and 4 higher taxa were significantly associated with R-SG. Although both reactors were composed largely of *Clostridia* taxa, abundance was significantly higher in R-G (LDA: 3.5), with *Ruminococcaceae* (LDA: 3.9), Order MBA03 (LDA: 3.3), *Gelria* (LDA: 3.3), and *Caldicoprobacter* (LDA: 3.3) showing the strongest R-G association. In contrast, R-SG displayed stronger associations with gut-associated, non-clostridial *Firmicutes*: *Lachnospiraceae* (LDA: 3.8), *Erysipelotrichaceae* (LDA: 3.6), *Peptostreptococcaceae* (LDA: 3.3), Family XIII members (LDA: 3.1-3.2), and *Trichococcus* (LDA: 3.1), as well as *Mollicutes* (LDA: 3.5) and *Rikenellaceae* (LDA: 3.2). A complete list of significant associations is given in Table 2.

3.2.2 Community Differences after Addition of Trace Elements

Having identified taxa associated with underlying differences in reactor feedstock, the microbial community was then tested for increases in abundance following TE supplementation in R-G to levels seen in R-SG (Figure 4 and Table 2).

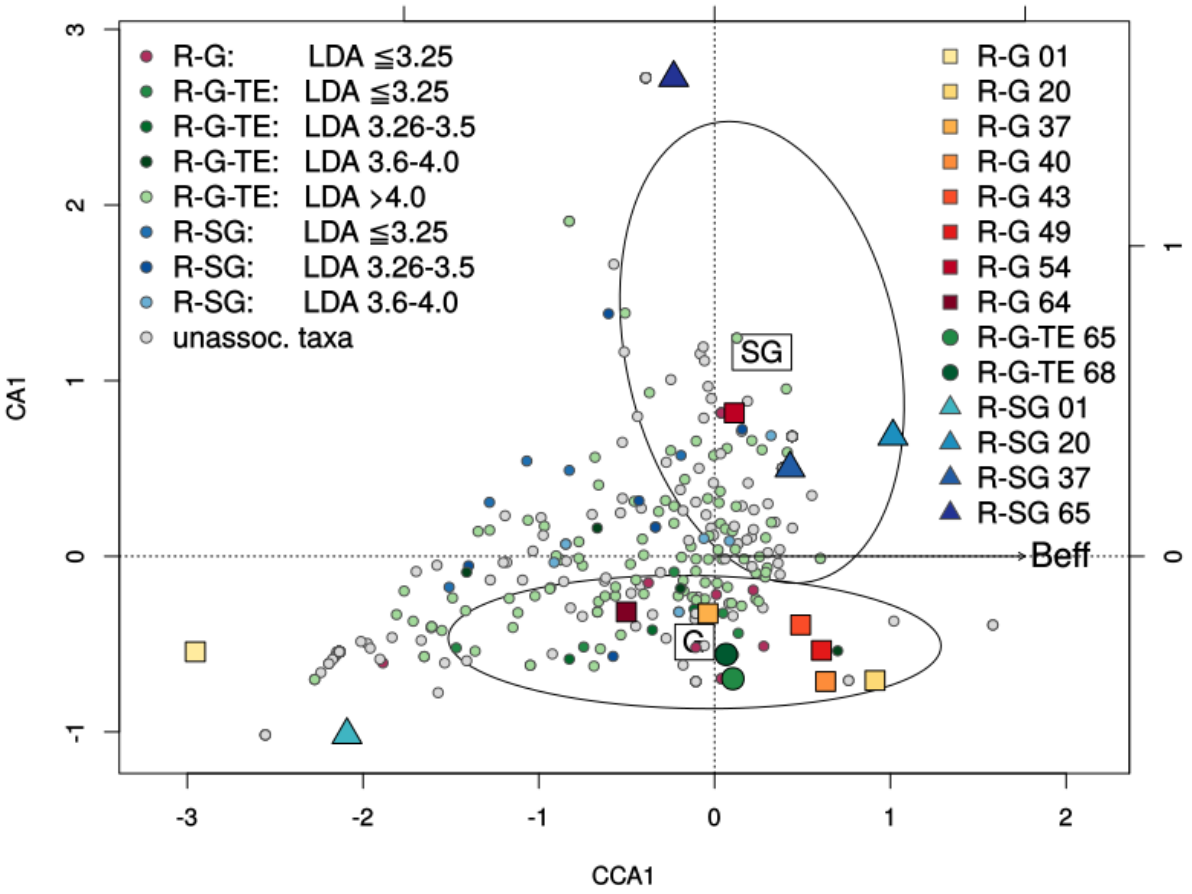
R-G: LDA ≦3.25
R-G-TE: LDA ≦3.25
R-G-TE: LDA 3.26-3.5
R-G-TE: LDA 3.6-4.0
R-G-TE: LDA >4.0
R-SG: LDA ≦3.25
R-SG: LDA 3.26-3.5
R-SG: LDA 3.6-4.0
unassoc. taxa
R-G 01
R-G 20
R-G 37
R-G 40
R-G 43
R-G 49
R-G 54
R-G 64
R-G-TE 65
R-G-TE 68
R-SG 01
R-SG 20
R-SG 37
R-SG 65
SG
C
Beff
CA1
CCA1

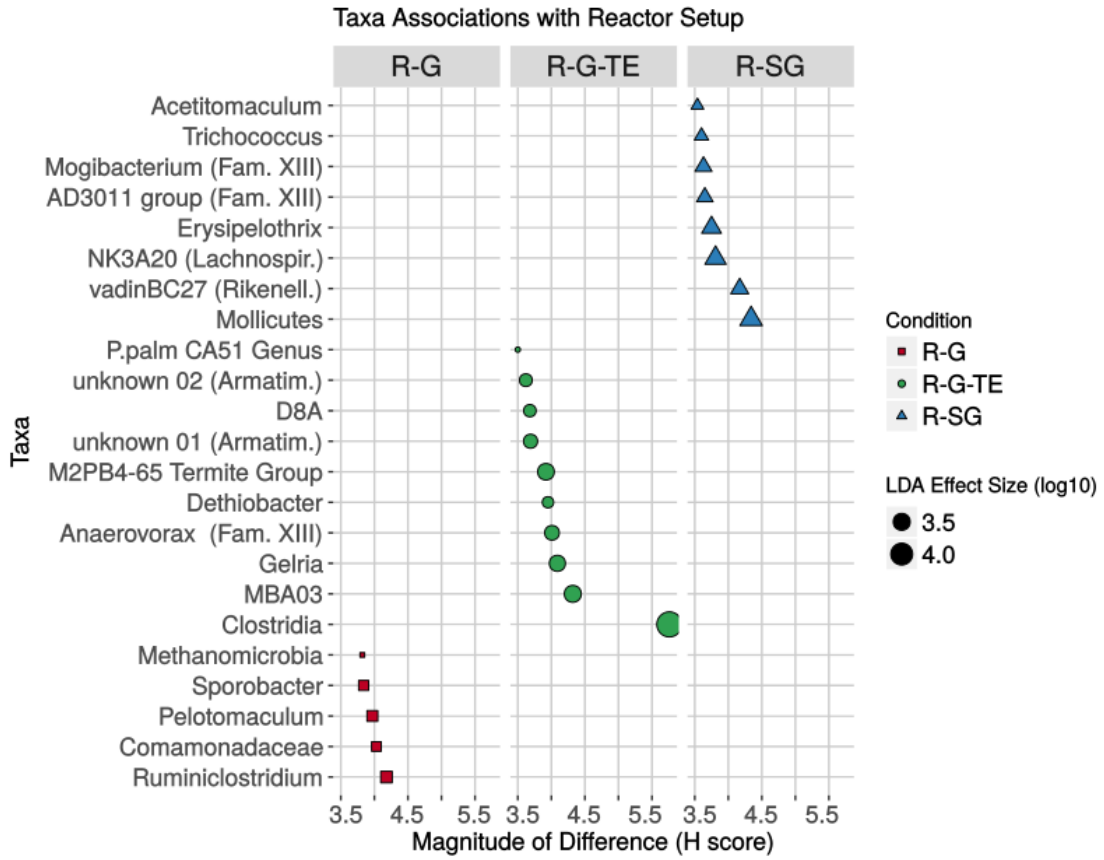
Taxa Associations with Reactor Setup
R-G
R-G-TE
R-SG
Acetitomaculum
Trichococcus
Mogibacterium (Fam. XIII)
AD3011 group (Fam. XIII)
Erysipelothrix
NK3A20 (Lachnospir.)
vadinBC27 (Rikenell.)
Mollicutes
P.palm CA51 Genus
unknown 02 (Armatim.)
D8A
unknown 01 (Armatim.)
M2PB4-65 Termite Group
Dethiobacter
Anaerovorax (Fam. XIII)
Gelria
MBA03
Clostridia
Methanomicrobia
Sporobacter
Pelotomaculum
Comamonadaceae
Ruminiclostridium
Taxa
3.5 4.5 5.5 3.5 4.5 5.5 3.5 4.5 5.5
Magnitude of Difference (H score)
Condition
R-G
R-G-TE
R-SG
LDA Effect Size (log10)
3.5
4.0

Figure 4 A: Constrained Correlation Analysis (CCA) of samples with respect to Biomethane Efficiency (B_{eff}). *Clustering of timepoints is apparent after week 20 (established biogas community), and also between R-G and R-SG. Although TE supplementation allowed restoration of Beff, clustering of R-G-TE (timepoints in green) away from R-SG (timepoints in blue) suggests the improvement is due to community composition specific to R-G setup (i.e. grass silage mono-digestion, timepoints in red). Significantly associated taxa are highlighted based on their Linear Discriminant Analysis (LDA) score, which estimates how reliably taxa associate with a given condition (e.g. R-G-TE). LDA scores are given in Table 2.*

Figure 4 B: Significant associations between taxa and TE regime, ordered by increasing association (H score). *Size of point indicates reliability of association (linear discriminant analysis (LDA) score, log10 scale). Abbreviations: Armatim.: Armatimonadetes; Fam. XIII: Family XIII; Lachnospir.: Lachnospiraceae; Rikenell.: Rikenellaceae.*

The OTU most strongly associated with TE-supplementation in R-G was assigned to order MBA03 (R-G-TE assoc.: LDA: 3.5), frequently observed in cellulose-based biogas reactors (Wirth et al., 2010; Heeg et al., 2014; Goux et al., 2016). Although the role of order MBA03 is as-yet unknown, clustering of all MBA03 reads to one OTU at 98% indicates a single large population (21% average relative abundance across samples), with a generally higher abundance in R-G suggesting a role in hydrolysis and/or fermentation of grass silage (Figure 2). Joint declines in B_{eff} (Figure 1) and MBA03 abundance (Weeks 54-64), followed by increases in B_{eff} and MBA03 abundance after TE addition (Weeks 65-68) are of interest and make MBA03 an attractive target for further characterisation.

Other genera associated with R-G-TE (R-G-Te assoc.: 3.5 – 3.1) are known acetogens/acetoclasts and end-stage fermenters: *Gelria*, *Anaerovorax*, *Dethiobacter*, as well as unknown genera from phylum *Armatimonadetes*, and termite group M2PB-4-65. Although *Anaerovorax* was associated with R-G-TE, two closely-related genera were associated with R-SG instead (AD3011 group, *Mogibacterium*: LDA

3.2), suggesting an overlap in community composition between R-G and R-SG mediated by TE availability.

However, the strongest trend associated with TE-supplementation in R-G-TE was seen above the genus-level: TE supplementation in Weeks 65 and 68 associated strongly with a broad increase in abundance of taxa in class *Clostridia* (R-G-TE assoc.: LDA: 4.4), with an average increase in reads of 87% to 90% (Figure 2).

In contrast, cellulolytic and hydrolytic *Ruminococcaceae* genera were abundant in R-G but declined markedly after supplementation: in particular *Ruminoclostridium* was strongly associated with R-G (LDA 4.2), reaching peak abundance at week 64 before decreasing from Week 65. Similarly, *Methanomicrobia*, *Comamonadaceae* and the clostridial genera *Pelotomaculum* and *Sporobacter* also associated with R-G (LDA: 3.1-.3.2) declined after TE supplementation. Notably, co-association of methanogenic *Methanomicrobia* with *Pelotomaculum*, an obligate syntrophic propionate oxidiser (de Bok et al., 2005), suggests a route for propionate reduction when TE levels are lacking, as in R-G before TE addition.

3.3 Significance of Trace Elements in VFA metabolism

The original rationale for TE addition to R-G was a decline in biogas production (as shown by decrease in B_{eff} with increasing OLR over time), and an accumulation of acetate and propionate (Weeks 49-64). After TE supplementation, B_{eff} improved from Week 65 onwards and VFA concentrations decreased. Rather than directly supplementing archaeal methanogenesis, we suggest that the primary response to TE addition was in specific bacterial populations mentioned above (i.e. acetogens, acetoclasts, end-stage fermenters) catabolising acetate and propionate to CO_2, H_2, and cellular material, with

secondary increases in the abundance of *Clostridia*, representing broader responses by hydrolysing and fermenting bacteria to the improved metabolism of VFAs.

Conversion of acetate and propionate to CO_2 + H_2 represents a metabolic bottleneck, where unfavourable thermodynamics make further fermentation energetically costly. As a result, many hydrolysing and fermenting bacteria "side-step" the investment required and instead excrete short-chain VFAs into their surroundings (i.e. acetogenesis). Accumulation of these VFAs (as in R-G Weeks 54-64, Figure 1) can exacerbate unfavourable conditions for AD, inhibiting fermentation while also making the reactor less hospitable (accumulation of acidic by-products, lower pH, decreased CO_2 availability, decreased buffering capacity). Acetoclasts (e.g. *Syntrophomonas*, *Methanosarcinales*) and propionoclasts (e.g. *Syntrophobacter*, *Smithella*) occupy specialist niches which reduce this VFA backlog, contributing to process stability and biogas production directly (acetoclastic methanogenesis) or through co-operative (syntrophic) coupling between bacteria and methanogens (syntrophic acetate oxidation, (SAO)).

Many acetoclasts and acetogens use the bidirectional Wood-Ljungdahl (Reductive Acetyl-Coenzyme A) pathway to reversibly convert acetate to $2H_2$ + CO_2 dependent on availability (Ragsdale, 2008), and for many anaerobic acetoclasts it is the main route of carbon fixation (Ragsdale and Pierce, 2008). This requires the enzymes carbon monoxide dehydrogenase-acetyl-coenzyme A synthase (CODH-ACS) and methyl-transferase-Ac Co-A, dependent on a generalised ratio of 1Co : 3Ni : 16Fe enzyme-bound atoms (Dobbek et al., 2001; Bender et al., 2011). Similarly, β-reduction of propionate requires TE-dependent conversion to a cellular intermediate before it can be metabolised, e.g. cobalt-mediated enzymatic conversion of propionate to succinyl-CoA (Takahashi-Iñiguez et al., 2012).

These reactions yield very little energy (e.g. acetate to bicarbonate: +25kJ ΔG°; propionate to acetate: +18kJ ΔG° (Thauer et al., 1977)); therefore syntrophy, rapid turnover and relatively large amounts of

associated TE are expected to be required for growth in acetoclastic/propionoclastic populations. Elevated OLR, and dependence on syntrophic partners (e.g. methanogens) with their own TE requirements may further increase the need for TE in VFA degradation.

3.4 Possible mechanism for TE supplementation

There are several reports of TE restoring or altering methanogen populations, enabling increased biogas output or stability (Banks et al., 2011; Karlsson et al., 2012; Gustavsson et al., 2013; Wintsche et al., 2016).

Despite this trend, we observed no increases in methanogen abundance in response to TE addition. Instead, methanogens proliferated during VFA accumulation and falling B_{eff}, but visibly declined when TE were added (Table 2, Supporting Figure 4). Rather than an inhibitory effect of surplus TE, this may reflect methanogens capitalising on acetate accumulation in weeks when it was available, with populations receding when supplementation reduced VFA levels.

In contrast, specific bacterial genera involved in hydrolysis, fermentation and VFA metabolism increased significantly after supplementation (Table 2), alongside improvements in VFA removal, reactor stability (FOS:TAC), and biomethane output as shown by increased biomethane efficiency (B_{eff}) as reported by (Wall et al. 2014).

As such, low availability of TE in AD may form a rate-limiting condition for bacterial catabolism of acetate and propionate, separate from any restriction imposed on subsequent methanogenesis. Conversely, TE supplementation may relax this constraint and improve energetic yields of hydrolysis and fermentation, thereby allowing increased output of biomethane.

4. Conclusions

Fermenters, highly abundant in any biogas reactor, require Fe, Ni, and Co to oxidise acetate and propionate. We provide evidence that fermenting populations are the likely candidates for supplementation with these trace elements in grass silage mono-digestion, with improved end-fermentation encouraging hydrolysing taxa and increasing rates of biogas production. Methanogens showed affinity for VFA accumulation (Weeks 37-43), but declined after supplementation despite improved biogas output. Many taxa significantly associated with addition of TE are uncharacterised; in particular the clostridial order MBA03, which is an attractive target for future work on grass-based AD and the role of TE supplementation in biogas production.

5. References

1. Allen, E., Wall, D.M., Herrmann, C., and Murphy, J.D. (2014) Investigation of the optimal percentage of green seaweed that may be co-digested with dairy slurry to produce gaseous biofuel. *Bioresour. Technol.* **170**: 436–444.

2. Banks, C.J., Chesshire, M., Heaven, S., and Arnold, R. (2011) Anaerobic digestion of source-segregated domestic food waste: Performance assessment by mass and energy balance. *Bioresour. Technol.* **102**: 612–620.

3. Bender, G., Pierce, E., Hill, J.A., Darty, J.E., and Ragsdale, S.W. (2011) Metal centers in the anaerobic microbial metabolism of CO and CO2. *Metallomics* **3**: 797–815.

4. Bougrier, C., Dognin, D., Laroche, C., and Cacho Rivero, J.A. (2018) Use of trace elements addition for anaerobic digestion of brewer's spent grains. *Journal of Environmental Management* **223**: 101–107.

5. Breitenstein, A. (2002) Reclassification of *Clostridium hydroxybenzoicum* as *Sedimentibacter hydroxybenzoicus* gen. nov., comb. nov., and description of *Sedimentibacter saalensis* sp. nov. *Int. J. Syst. Evol. Microbiol.* **52**: 801–807.

6. Caporaso, J.G., Kuczynski, J., Stombaugh, J., Bittinger, K., Bushman, F.D., Costello, E.K., et al. (2010) QIIME allows analysis of high-throughput community sequencing data. *Nat. Methods* **7**: 335–336.

7. Choong, Y.Y., Norli, I., Abdullah, A.Z., and Yhaya, M.F. (2016) Impacts of trace element supplementation on the performance of anaerobic digestion process: A critical review. *Bioresour. Technol.* **209**: 369–379.

8. de Bok F., Harmsen H., Plugge C., de Vries M., Akkermans A., de Vos W., Stams A. (2005) The first true obligately syntrophic propionate-oxidizing bacterium, *Pelotomaculum schinkii* sp. nov., co-cultured with *Methanospirillum hungatei*, and emended description of the genus *Pelotomaculum*. *Int. J. Syst. Evol. Microbiol.* **55(4)**:1697-1703

9. De Vries, J.W., Vinken, T.M.W.J., Hamelin, L., and De Boer, I.J.M. (2012) Comparing environmental consequences of anaerobic mono- and co-digestion of pig manure to produce bio-energy – A life cycle perspective. *Bioresour. Technol.* **125**: 239–248.

10. Demirel, B. and Scherer, P. (2009) Bio-methanization of energy crops through mono-digestion for continuous production of renewable biogas. *Renew. Energy* **34**: 2940–2945.

11. Demirel, B. and Scherer, P. (2011) Trace element requirements of agricultural biogas digesters during biological conversion of renewable biomass to methane. *Biomass Bioenergy* **35**: 992–998.

12. Dobbek, H., Svetlitchnyi, V., Gremer, L., Huber, R., and Meyer, O. (2001) Crystal Structure of a Carbon Monoxide Dehydrogenase Reveals a [Ni-4Fe-5S] Cluster. *Science* **293**: 1281–1285.

13. Drosg, B. (2013) Process monitoring in biogas plants.

14. Elgersma, A., Ellen, G., van der Horst, H., Muuse, B.G., Boer, H., and Tamminga, S. (2003) Comparison of the fatty acid composition of fresh and ensiled perennial ryegrass (Lolium perenne L.), affected by cultivar and regrowth interval. *Anim. Feed Sci. Technol.* **108**: 191–205.

15. Ermler, U., Grabarse, W., Shima, S., Goubeaud, M., and Thauer, R.K. (1997) Crystal Structure of Methyl-Coenzyme M Reductase: The Key Enzyme of Biological Methane Formation. *Science* **278**: 1457–1462.

16. Gao, Z.-M., Wang, Y., Tian, R.-M., Lee, O.O., Wong, Y.H., Batang, Z.B., et al. (2015) Pyrosequencing revealed shifts of prokaryotic communities between healthy and disease-like tissues of the Red Sea sponge *Crella cyathophora*. *PeerJ* **3**: e890.

17. Goux, X., Calusinska, M., Lemaigre, S., Marynowska, M., Klocke, M., Udelhoven, T., et al. (2015) Microbial community dynamics in replicate anaerobic digesters exposed sequentially to increasing organic loading rate, acidosis, and process recovery. *Biotechnol. Biofuels* **8**: 122.

18. Goux, X., Calusinska, M., Fossépré, M., Benizri, E., and Delfosse, P. (2016) Start-up phase of an anaerobic full-scale farm reactor - Appearance of mesophilic anaerobic conditions and establishment of the methanogenic microbial community. *Bioresour. Technol.* **212**: 217–226.

19. Gustavsson, J., Shakeri Yekta, S., Sundberg, C., Karlsson, A., Ejlertsson, J., Skyllberg, U., and Svensson, B.H. (2013) Bioavailability of cobalt and nickel during anaerobic digestion of sulfur-rich stillage for biogas formation. *Appl. Energy* **112**: 473–477.

20. Heeg, K., Pohl, M., Sontag, M., Mumme, J., Klocke, M., and Nettmann, E. (2014) Microbial communities involved in biogas production from wheat straw as the sole substrate within a two-phase solid-state anaerobic digestion. *Syst. Appl. Microbiol.* **37**: 590–600.

21. Karlsson, A., Einarsson, P., Schnürer, A., Sundberg, C., Ejlertsson, J., and Svensson, B.H. (2012) Impact of trace element addition on degradation efficiency of volatile fatty acids, oleic acid and phenyl acetate and on microbial populations in a biogas digester. *J. Biosci. Bioeng.* **114**: 446–452.

22. Lebuhn, M., Liu, F., Heuwinkel, H., and Gronauer, A. (2008) Biogas production from mono-digestion of maize silage–long-term process stability and requirements. *Water Sci. Technol.* **58**: 1645–1651.

23. Lee, K.C.Y., Dunfield, P.F., and Stott, M.B. (2014) The Phylum Armatimonadetes. In, *The Prokaryotes - Other Major Lineages of Bacteria and the Archaea*. Springer-Verlag Berlin Heidelberg.

24. Leser, T.D., Amenuvor, J.Z., Jensen, T.K., Lindecrona, R.H., Boye, M., and Møller, K. (2002) Culture-Independent Analysis of Gut Bacteria: the Pig Gastrointestinal Tract Microbiota Revisited. *Appl. Environ. Microbiol.* **68**: 673–690.

25. Love, M.I., Huber, W., and Anders, S. (2014) Moderated estimation of fold change and dispersion for RNA-seq data with DESeq2. *Genome Biol.* **15**:550.

26. Matthies, C., Evers, S., Ludwig, W., and Schink, B. (2000) *Anaerovorax odorimutans* gen. nov., sp. nov., a putrescine-fermenting, strictly anaerobic bacterium. *Int. J. Syst. Evol. Microbiol.* **50 Pt 4**: 1591–1594.

27. McMurdie, P.J. and Holmes, S. (2013) phyloseq: An R Package for Reproducible Interactive Analysis and Graphics of Microbiome Census Data. *PLoS ONE* **8**: e61217.

28. Mori, K., Iino, T., Suzuki, K.-I., Yamaguchi, K., and Kamagata, Y. (2012) Aceticlastic and NaCl-Requiring Methanogen “Methanosaeta pelagica” sp. nov., Isolated from Marine Tidal Flat Sediment. *Applied and Environmental Microbiology* **78**: 3416–3423.

29. Nizami, A.-S., Korres, N.E., and Murphy, J.D. (2009) Review of the Integrated Process for the Production of Grass Biomethane. *Environ. Sci. Technol.* **43**: 8496–8508.

30. Plugge, C.M., Balk, M., Zoetendal, E.G., and Stams, A.J. (2002) Gelria glutamica gen. nov., sp. nov., a thermophilic, obligately syntrophic, glutamate-degrading anaerobe. *Int. J. Syst. Evol. Microbiol.* **52**: 401–407.

31. Prochnow, A., Heiermann, M., Plöchl, M., Linke, B., Idler, C., Amon, T., and Hobbs, P.J. (2009) Bioenergy from permanent grassland – A review: 1. Biogas. *Bioresour. Technol.* **100**: 4931–4944.

32. Qiang, H., Lang, D.-L., and Li, Y.-Y. (2012) High-solid mesophilic methane fermentation of food waste with an emphasis on Iron, Cobalt, and Nickel requirements. *Bioresource Technology* **103**: 21–27.

33. Qiang, H., Niu, Q., Chi, Y., and Li, Y. (2013) Trace metals requirements for continuous thermophilic methane fermentation of high-solid food waste. *Chemical Engineering Journal* **222**: 330–336.

34. Quast, C., Pruesse, E., Yilmaz, P., Gerken, J., Schweer, T., Yarza, P., et al. (2013) The SILVA ribosomal RNA gene database project: improved data processing and web-based tools. *Nucleic Acids Res.* **41**: D590–D596.

35. R Core Team (2013) R: A Language and Environment for Statistical Computing R Foundation for Statistical Computing, Vienna, Austria.

36. Ragsdale, S.W. (2008) Enzymology of the Wood-Ljungdahl Pathway of Acetogenesis. *Ann. N. Y. Acad. Sci.* **1125**: 129–136.

37. Ragsdale, S.W. and Pierce, E. (2008) Acetogenesis and the Wood–Ljungdahl pathway of CO2 fixation. *Biochim. Biophys. Acta BBA - Proteins Proteomics* **1784**: 1873–1898.

38. Roth, J.R., Lawrence, J.G., and Bobik, T.A. (1996) Cobalamin (coenzyme B12): synthesis and biological significance. *Annu. Rev. Microbiol.* **50**: 137–181.

39. Schattauer, A., Abdoun, E., Weiland, P., Plöchl, M., and Heiermann, M. (2011) Abundance of trace elements in demonstration biogas plants. *Biosystems Engineering* **108**: 57–65.

40. Segata, N., Izard, J., Waldron, L., Gevers, D., Miropolsky, L., Garrett, W.S., and Huttenhower, C. (2011) Metagenomic biomarker discovery and explanation. *Genome Biol* **12**: R60.

41. Smith, A.M., Sharma, D., Lappin-Scott, H., Burton, S., and Huber, D.H. (2014) Microbial community structure of a pilot-scale thermophilic anaerobic digester treating poultry litter. *Appl. Microbiol. Biotechnol.* **98**: 2321–2334.

42. Sorokin, D.Y., Tourova, T.P., Mussmann, M., and Muyzer, G. (2008) *Dethiobacter alkaliphilus* gen. nov. sp. nov., and *Desulfurivibrio alkaliphilus* gen. nov. sp. nov.: two novel representatives of reductive sulfur cycle from soda lakes. *Extrem. Life Extreme Cond.* **12**: 431–439.

43. Takahashi-Iñiguez, T., García-Hernandez, E., Arreguín-Espinosa, R., and Flores, M.E. (2012) Role of vitamin B12 on methylmalonyl-CoA mutase activity. *J. Zhejiang Univ. Sci. B* **13**: 423–437.

44. Tang, Y., Shigematsu, T., Ikbal, Morimura, S., and Kida, K. (2004) The effects of micro-aeration on the phylogenetic diversity of microorganisms in a thermophilic anaerobic municipal solid-waste digester. *Water Res.* **38**: 2537–2550.

45. Thauer, R.K., Jungermann, K., and Decker, K. (1977) Energy conservation in chemotrophic anaerobic bacteria. *Bacteriol. Rev.* **41**: 100–180.

46. Vignais, P.M. and Billoud, B. (2007) Occurrence, Classification, and Biological Function of Hydrogenases: An Overview. *Chem. Rev.* **107**: 4206–4272.

47. Wall, D.M., Allen, E., Straccialini, B., O'Kiely, P., and Murphy, J.D. (2014) The effect of trace element addition to mono-digestion of grass silage at high organic loading rates. *Bioresour. Technol.* **172**: 349–355.

48. Wei, Y., Zhou, H., Zhang, J., Zhang, L., Geng, A., Liu, F., et al. (2015) Insight into Dominant Cellulolytic Bacteria from Two Biogas Digesters and Their Glycoside Hydrolase Genes. *PloS One* **10**: e0129921.

49. van der Weijde, T., Alvim Kamei, C.L., Torres, A.F., Vermerris, W., Dolstra, O., Visser, R.G.F., and Trindade, L.M. (2013) The potential of C4 grasses for cellulosic biofuel production. *Front. Plant Sci.* **4**:107.

50. Wickham, H. (2009) ggplot2 - Elegant Graphics for Data Analysis 1st ed. Springer-Verlag New York.

51. Wintsche, B., Glaser, K., Sträuber, H., Centler, F., Liebetrau, J., Harms, H., and Kleinsteuber, S. (2016) Trace Elements Induce Predominance among Methanogenic Activity in Anaerobic Digestion. *Front. Microbiol.* **7**:2034.

52. Wirth, R., Lakatos, G., Böjti, T., Maróti, G., Bagi, Z., Kis, M., et al. (2010) Metagenome changes in the mesophilic biogas-producing community during fermentation of the green alga Scenedesmus obliquus. *J. Biotechnol.* **215**: 52–61.

53. Ye, M., Liu, J., Ma, C., Li, Y.-Y., Zou, L., Qian, G., and Xu, Z.P. (2018) Improving the stability and efficiency of anaerobic digestion of food waste using additives: A critical review. *Journal of Cleaner Production* **192**: 316–326.

54. Yutin, N. and Galperin, M.Y. (2013) A genomic update on clostridial phylogeny: Gram-negative spore formers and other misplaced clostridia: Genomics update. *Environ. Microbiol.* **10**: 2631-41.

55. Zhang, L. and Jahng, D. (2012) Long-term anaerobic digestion of food waste stabilized by trace elements. *Waste Management* **32**: 1509–1515.

56. Zhang, L., Loh, K.-C., and Zhang, J. (2018) Enhanced biogas production from anaerobic digestion of solid organic wastes: Current status and prospects. *Bioresource Technology Reports*.

Chapter 4

Methanothermobacter is the key *ex situ* methanogen in a thermophilic upgrading study, but shows no association with changes in biogas output.

Jamie A. FitzGerald [a,b], Amita J. Guneratnam [c], Stephen Jackson [a], Jerry Murphy [b,c] and Alan Dobson [a,c]

a Department of Microbiology, University College Cork

b The MaREI Centre, Environmental Research Institute, University College Cork, Ireland

c School of Engineering, University College Cork, Ireland

Material from this chapter contributed to the original reseach article "Study of the performance of a thermophilic biological methanation system.", Guneratnam et al., 2017, *Bioresource Technology* **225**: 308–315. The article is available online at http://www.sciencedirect.com/science/article/pii/S0960852416315875.

ABSTRACT

Ex situ biomethanation is a cost-effective modification of anaerobic digestion, in which hydrogenotrophic methanogens are provided excess hydrogen (H_2) and carbon dioxide (CO_2) in the absence of a solid biogas feedstock, placing both the process and metabolic emphasis on near-total conversion of CO_2 and H_2 to biomethane. The concept can be applied *ex situ* as 'biological upgrading' to biogas from anaerobic digestion, and is usually carried out at thermophilic temperatures (>50°C) in order to accelerate methanogenesis. The *ex situ* methanogenic community responsible for this upgrading is currently poorly characterised but is expected to feature abundant methanogens specialising in fixation of CO_2 and H_2 to CH_4. Given the lack of a digestion feedstock, the importance of bacteria in an upgrading community is less clear. In this study, the methanogenic and microbial communities involved in thermophilic *ex situ* upgrading of a 1 CO_2 : 4 H_2 mix were characterised during disruption and restoration of biogas production due to a process shift to higher temperatures (55°C to 65°C). Although DGGE, 16S clone library and 16S pyrosequencing approaches showed *Methanothermobacter* to be the dominant methanogen throughout operation, no relationship was evident between decreased upgrading function and *Methanothermobacter* abundance. Instead, it is possible that biogas production was restored through addition of organic and/or inorganic substrate in a re-inoculation event. This implies a role for the *ex situ* bacterial community, the majority of which (>50% reads) belong to uncharacterised *Firmicutes* taxa, in particular the MBA03 group.

1. Introduction

1.1 Motivation

The potential of anaerobic digestion as a biofuel technology is considerably restricted by the composition of the biogas produced (Patterson *et al.*, 2011). Along with CH_4, biogas contains CO_2, CO, H_2O, can contain trace amounts of H_2, H_2S, and NH_3, as well as volatile organic compounds, all of which detract from the gas's use as a biofuel. These components are naturally produced within the reactor, and coalesce to bubble up through the digestate, or simply diffuse into the gas phase at the digestate-air interface.

Removing impurities or non-calorific components (CO_2, H_2O, H_2S etc.) from the biomethane increases the costs of transferring biogas to gas networks, restricting the ability of biogas to compete with traditional or fossil fuels (Patterson *et al.*, 2011). This provides an incentive to maximise the methane proportion of the biogas, both to increase value as a fuel and reduce the relative amount of purification required. The largest undesirable portion of biogas is CO_2, with quantities of at least 30-40% being reported in anaerobic digestion (AD) (Sun *et al.*, 2015; Ullah Khan *et al.*, 2017). Although CO_2 is a major by-product of hydrolysis and fermentation, it is also a product of, and substrate for, methanogenesis ($CH_3COOH \rightarrow CH_4 + CO_2$; $CO_2 + H_2 \rightarrow CH_4$). This allows repurposing of 'waste' CO_2 in the improvement of biomethane content.

1.2 Industrial Upgrading

Several industrial methods exist to improve the calorific value of biogas, all of which appeal to the differing physical characteristics of the constituent gasses (solubility, molecular size, condensation point etc., see Patterson *et al.*, 2011 and Sun *et al.*, 2015 for review). Many of these technologies are

in active development, with efficiencies varying from 82%-98% methane output. However these technologies have associated costs, including capital for construction and operation, energy demands (2.5-8% of energy generated), and methane losses (up to 18%) which may make them unsuitable for certain situations or scales (Patterson *et al.*, 2011).

1.3 Biological Upgrading

In light of costs facing industrial methanation, the biogas process should be reconsidered. If the biogas reactor is the source of these impurities, how can microbial biogas communities be managed to improve biomethane output and reduce other components?

One method is *in situ* upgrading: raising the reagent concentration (CO_2, H_2) within the reactor, thereby shifting the thermodynamic equilibrium towards the product (CH_4), and increasing the rate of reaction. Exogenous H_2 can be supplied to the reactor setup, stimulating hydrogenotrophic methanogenesis (hydrogen upgrading). As CH_4 is poorly soluble, increasing the concentration of CO_2 can be achieved by simply routing output biogas back through the digestate to re-dissolve excess CO_2. When recirculated in a stochiometric ratio of at least 4:1 H_2:CO_2, it should be possible to achieve total biomethanation of biogas during AD. However, there are problems associated with these approaches: several processes, in particular short-chain VFA metabolism, are highly sensitive to increases in concentration of H_2, which can destabilise the biogas process through inhibitive acid accumulation and decreasing pH (Fukuzaki *et al.*, 1990; Luo *et al.*, 2012; Dolfing, 2013). *In situ* upgrading may be particularly suited to batch AD setup due to the longer latency of gas in the reactor, and might not be ideal for high-throughput operations, e.g. Continuously-Stirred Tank Reactors (CSTRs), due to limited solubility of H_2 (Kougias *et al.*, 2017). Difficulties maximising the solution of H_2 in digestate may also

require redesign of reactors to extend gas transit. This is most often addressed by use of baffles, packing material or hollow fibre membranes to maximise the contact area for hydrogen dissolution.

An alternative upgrading method is full separation of biomethane upgrading from the main biogas reactor: *ex situ* upgrading. The setup creates a secondary reactor focusing on the conversion of CO_2 + $H_2 \rightarrow CH_4$, which avoids acetoclastic methanogenesis, and inhibition in the biogas process (i.e. at hydrolysis, fermentation, acidogenesis etc.). *Ex situ* digestion avoids competition between AD and upgrading biomethanation for substrates and space, as well as decoupling process disruptions in either stage. *Ex situ* reactors can also to be smaller than primary AD reactors, therefore making them easier to deploy, operate and heat. Most importantly, *ex situ* upgrading subsets methanogenesis into a new environment that can be optimised in isolation. The desired driving force behind this setup are large hydrogenotrophic populations of methanogens, encouraged by high concentrations of H_2 and CO_2, supplemented by a minimal medium. Although the reactor is expected to emphasise archaeal abundance, conditions are likely to encourage non-target autotrophic (e.g. acetogenic) or heterotrophic (e.g. fermenting) microbes. This is especially true if the reactor is inoculated from reactor sludge or some other digestate, as the biomass used will include diverse founder populations and nutrifying, carbon-rich material. Endogeneous microbial biomass will also represent a carbon source once the reactor is established. To avoid fostering bacteria unconnected to methanogenesis, the liquid media supplied should be as limiting as possible while still allowing methanogen growth, with supplied biogas (CO_2, CO, CH_4) as the major carbon source (Angelidaki and Sanders, 2004).

It should be noted that *ex situ* biogas upgrading is specifically a technology for the conversion of CO_2 to CH_4. Although some fixation of nitrogenous (amines, nitrates, nitrites) and sulphurous (H_2S) compounds into the community is expected (Oren, 2014) *ex situ* upgrading reactors are not intended to sequester these products. Instead, consideration should be given to process design (e.g. optimising

feedstock composition, use of serial reactors) in order to minimalise production of these detrimental by-products. Where such emissions are unavoidable, these contaminants will need to be removed through alternative upgrading technologies (e.g. membrane filtration, water scrubbing; Sun et al, 2015)

1.4 Increasing the Rate of Biological Upgrading

How can methanogenesis be maximised? As the terminal step of methanogenesis is now separated from hydrolysis, acidification, etc., this question differs from the above question (section 1.3) regarding improving biogas, and specifically addresses the factors governing the rate of methane formation and the proportion of methane in the biogas. The first obstacle to be addressed in the *ex situ* upgrading environment is the large amounts of CO_2 generated during fermentation. Although this may be stochiometrically mixed with H_2, preventing further endogenous production of CO_2 *ex situ* is important. CO_2 plays a number of roles in the AD process: foremost CO_2 is a product of hydrolytic and fermentative metabolism, and is the main output in unhindered fermentation (Thauer et al., 2008). Some of the CO_2 produced escapes into the gaseous phase. However, much of the CO_2 dissolves in the digestate and adds to the buffering capacity of the reactor as bicarbonate (H_2CO_3-). The ratio of this dissolved inorganic carbon to organic volatile fatty acids (VFA) is commonly used to measure reactor buffering capacity (FOSTAC; Nordmann, 1977) and guide feeding regimes (Drosg, 2013). Exclusion of hydrolysis and fermentation in *ex situ* AD greatly restricts endogenous carbon cycling and CO_2 production, constraining microbes to rely upon supplied carbon (biogas, minimal media) and emphasises methane formation, thereby increasing the quality of associated biogas.

However, fermentation and hydrolysis are not the only sources of CO_2, as dissolved bicarbonate is also cycled by autotrophs for energy and carbon fixation. Autotrophic acetogens and acetoclasts can alternatively convert $2\ CO_2 + 2H_2 <-> CH_3COOH$ (Ragsdale and Pierce, 2008; Thauer *et al.*, 2008), dependent on the most energetically favourable direction. This can lead to production of CO_2 when acetate concentrations rise, at elevated pH, or at lower temperatures. Equally, conversion of plentiful H_2 and CO_2 to acetate may encourage acetoclastic methanogenesis, where disproportionation of CH_3COOH produces equal amounts of CH_4 and CO_2, again devaluing output biogas.

The feasibility of methanogenesis can be improved by appealing to Le Chatelier's principle, whereby increasing the activity (available concentration) of reactants (i.e. CO_2 and H_2) shifts equilibrium towards the product (i.e. CH_4). This is in part the motivation behind adding hydrogen to the *ex situ* reactor. To achieve total upgrading of biogas, H_2 must be dissolved to an activity of at least four times the dissolved CO_2. Hydrogen is poorly soluble, and notoriously liable to loss due to its low atomic size. As such, addition of volumes in excess of 4x might be required; however, as noted above this can have adverse effects on the microbial ecology of the reactor.

A third way of increasing the rate of methanogenesis is through increasing temperature. Although methanogenesis follows the trend of metabolic processes proceeding at higher rates with increased temperature, it also becomes less thermodynamically favourable as temperatures increase, leading to a reduced cell yield per mol ATP and a decreased rate of growth, despite the increased production of methane (Amend and Shock, 2001; Thauer *et al.*, 2008). The observed increase in the rate of methanogenesis may be a combination of an overall reduction in metabolic activation energies, as well as a requirement for increased methane turnover due to the lower energetic yields.

As temperatures increase (>60°C), the energy yield of acetoclastic methanogenesis becomes untenable, and methanogenesis from acetate is carried out by syntrophic pairings of acetoclastic

bacteria and hydrogenotrophic methanogens (Thauer *et al.*, 2008). The greater specificity of methanogens for hydrogen (x10) outcompetes homoacetogenic acetogens, reducing acetate production. As such, acetoclastic genera such as *Methanosarcina* and *Methanothrix* are generally not involved in methanogenesis above 50°C, which precludes the production of additional CO_2 in methanogenesis.

Instead, heating has been shown to encourage hydrogenotrophic methanogenesis, of which several taxa are known from thermophilic (50-70°C: *Methanobacteriales, Methanococcales, Methanomicrobiales*) or even hyperthermophilic environments (<110°C: *Methanopyrales*). Although the energetic yield of hydrogenotrophic methanogenesis decreases with increasing temperature, hydrogenotrophic methanogens possess the cellular machinery required to persist at reduced energy yields, largely due to their ability to manufacture ATP at much lower concentrations of hydrogen (Thauer *et al.*, 2008). Several studies bare out this feature, with shifts from mesophilic to thermophilic operation excluding acetoclastic in favour of hydrogenotrophic methanogens.(Zinder *et al.*, 1984; Luo and Angelidaki, 2012; Bassani *et al.*, 2015).

1.5 Relating Temperature to Community

Increased temperature expedites the biomethanation process significantly, but also affects the microbial community structure due to differences in optimal growth temperatures. Similarly, addition of hydrogen can shift process equilibrium towards the methane product (Luo *et al.*, 2012; Bassani *et al.*, 2015, 2017) but can also adversely affect reactor performance (Luo *et al.*, 2012; Mulat *et al.*, 2017). Inhibition of hydrolysing and fermenting populations has serious implications for reactor stability, where acid accumulation can cause reactor stalling or failure if not managed. However, in an

ex situ reactor where the methanogenic step has been propagated to a new environment, the importance of additional bacterial populations for stable biogas production is not clear, nor is the overall *ex situ* community structure well characterised. To determine the effects of different upgrading strategies on the microbial community, several studies have included microbial characterisations of *ex situ* and *in situ* upgrading reactors.

In a two-stage *in situ* setup, Bassani *et al.* (2015) documented a higher AD process under thermophilic (55°C versus 35°C) conditions (20% increase in substrate degradation), but a slightly lower proportion of methane (85% versus 89% by volume), as well as an increase in pH, increased consumption of CO_2, and increased total VFA levels when hydrogen/biogas upgrading was applied. They also documented a rise in hydrogenotrophic *Methanoculleus* and a decrease in *Methanosarcina*.

Kougias *et al.* (2017) studied a number of thermophilic (52°C) digestate-fed *ex situ* reactor setups designed to increase solution of biogas/hydrogen in the medium. Setups trialled H_2 solubility at two H_2 flow rates (4L/h, 12L/h), achieving conversion efficiencies up to 73% CH_4 by volume. Reactor setups supported a mix of homoacetogenic and syntrophic acetate oxidising (SAO) bacteria and exclusively hydrogenotrophic methanogens, but also encouraged sulphate reducing bacteria (SRB) which are known to destabilise the biogas process through production of H_2S. Although no analysis was presented of the effect of H_2 flow rate on populations, abundant SRB in the CSTR setup were attributed to the use of digestate as the feedstock.

Luo and Angelidaki (2012) introduced the concept of "fully" *ex situ* upgrading (supplying CO_2, H_2, N_2 and minimal media only), and demonstrated thermophilic conversion efficiencies between 90-95% at different rates of gas loading, dependent on mixing rate. They also demonstrated increases in hydrogenotrophic methanogens from inoculum to established reactors, and from mesophilic to thermophilic reactors. However, no further characterisation was carried out.

Guneratnam *et al.* (2017) reproduced the findings of Luo & Angelidaki, demonstrating a high level of biomethanation using triplicate ex-situ reactors fed minimal media, CO_2, and H_2. Given the positive relationship between temperature and rate of methanogenesis, the reactor operating temperature was then increased from 55°C (Stage B) to 65°C (stage C). This increased the rate of methanogenesis, with CH_4 composition after 12 hours at 55% by volume, compared to 22% in Stage B. However, total CH_4 volume was reduced under thermophily from 88% to 85% at 24 hours. In an effort to restore efficiency, reactors at 65°C were re-inoculated with seed sludge. This improved biomethanation to 92% CH_4 by volume after 24 hours.

To determine how operating temperatures and re-inoculation influenced this biomethanation setup, the methanoarchaea in the *ex situ* reactors were investigated at three stages: steady-state operation at 55°C (stage B); operation at 65°C (stage C); and operation at 65°C with re-inoculation (stage D). 16S sequences were used to investigate (a) the archaeal community structure at 55°C, (b) how did the increase in temperature to 65°C affect the community structure and was there an obvious loss of methanogenic activity when temperature was increased, and (c) how did re-inoculation influence methanogenesis, allowing increased function? A preliminary study was performed using denaturing gradient gel electrophoresis (DGGE), followed by more in-depth characterisations using a clone and pyrosequencing library approaches. To our knowledge, this is the most thorough characterisation to date of an autonomous *ex situ* microbial community, reliant on biogas for carbon and hydrogen (i.e. not fed/influenced by digestate).

2. Materials and Methods

2.1 Reactor Operation

Reactor setup is described in greater detail in (Guneratnam *et al.*, 2017). Inoculum was sourced from a thermophilic (55°C) maize, grass and farmyard manure anaerobic digester, and fed cellulose for one week (OLR =1 kgVS/M/d). Each of three replicate reactors consisted of a 1L Duran bottle with dual tubes affixed by rubber seal with three-way stopcock, placed in a shaking incubator at the desired temperature (55°C or 65°C). This allowed for daily sampling (removal of 50ml headspace gas), replenishment of synthetic biogas (760ml H_2, 190ml CO_2), and of minimal media (25ml, Angelidaki and Sanders, 2004).

2.2 Reactor Sampling, DNA extraction and Molecular Cloning

The stages of the process were broken into (A) acclimatisation at 55^{o}C; (B) steady state at 55^{o}C; (C) initial trial at 65^{o}C and (D) reseeded reactor trial at 65^{o}C. Approximately 30ml of suspended solids from each Reactor (1, 2, and 3) for stages B, C and D were centrifuged at 10,000g to pellet biomass (9 samples total). Nucleic acids were extracted in triplicate from these pellets using a CTAB-based lysis buffer (see Appendix B) and two rounds of phenol-chloroform-isoamyl alcohol extraction.

2.3 Denaturing Gradient Gel Electrophoresis

Archaeal primers for DGGE were taken from Casamayor *et al.* (2001): S-D-Arch-0344-a-S-20 (ACG GGG YGC AGC AGG CGC GA) and S-D-Arch-0915-a-A-20 (GTG CTC CCC CGC CAA TTC CT). Bacterial primers were selected from Klindworth *et al.* (2012): S-D-Bact-0517-a-S-17 (GCC AGC AGC CGC GGT AA) and S-D-Bact-1061-a-A-17 (CRR CAC GAG CTG ACG AC). Both forward primers also included a 5’ GC-clamp to

prevent total melting, thereby retaining the amplicons in the poly-acrylamide gel (Muyzer *et al.*, 1993). For each sample, an optimised *Taq* polymerase (DreamTaq, ThermoFisher) was used to amplify 50µl of product directly from the extracted nucleic acids in polymerase chain reaction, with the following 'touchdown' thermocycler programs for archaea and bacteria respectively:

- 4 minutes at 94°C; twenty cycles of 1 minute at 94°C, 1 minute at 70°C decreasing by 0.5°C each step, 3 minutes at 72°C; fifteen cycles of 1 minute at 94°C, 1 minute at 60°C, 3 minutes at 72°C; 10 minutes final extension at 72°C.
- 4 minutes at 94°C; twenty cycles of 1 minute at 94°C, 1 minute at 68°C decreasing by 0.5°C each step, 3 minutes at 72°C; fifteen cycles of 1 minute at 94°C, 1 minute at 58°C, 3 minutes at 72°C; 10 minutes final extension at 72°C.

Polyacrylamide gels with a denaturing gradient from 15% to 85% of urea/formamide were prepared in a DCode electrophoresis rig (Bio-Rad Laboratories), and run at 40V for 17 hours to separate the amplicons. Gels were then stained in 1x SYBR Gold (ThermoFisher) for 30 minutes at 28°C with gentle shaking, and viewed on a transilluminator.

2.4 Construction of Archaeal Clone Library

To produce amplicons for cloning, improved archaeal primers S-D-Arch-0349-a-S-17 (GYG CAS CAG KCG MGA AW) and S-D-Arch-1041-a-A-18 (GGC CAT GCA CCW CCT CTC) (Klindworth *et al.*, 2012) spanning 16S V3-V6 were selected and appraised using the SILVA testprime database (Klindworth *et al.*, 2012) with parameters of 0 base-pair mismatches, and of 1 base-pair mismatch outside the last 3 3'-base-pairs. Under these constraints, coverage was 70% and 85% for Archaea, 77% and 89% for *Euryarchaeota*, and at least 82%, 75%, 86%, and 100% of the major methanogenic clades

(*Methanobacteria*, *Methanomicrobia*, *Methanococci* and *Methanopyri*) respectively. Coverage provided by this primer pair was likely to capture a majority of archaeal sequences. A 692bp product was generated via an optimised *Taq* polymerase (DreamTaq, ThermoFisher) using a PCR program of initial denaturing for 4min at 94°C; x30 cycles of 1min at 94°C, 54°C, and 72°C each; and a final extension of 4 min at 72°C. Amplicons were purified via gel extraction (QIAGEN) and ligated in EZ-Competent cells (QIAGEN) before being plated on ampicillin; twelve successfully transformed colonies per Reactor per Stage (108 clones total) were used for M13 PCR before commercial sequencing by GATC (Konstanz, Germany).

2.5 Clone Library Sequence Analysis

Chromatograms were manually curated in FinchTV 1.3.1 (Geospiza Inc.) for read length and accurate base-pair calling (>200bp, PHRED scores ≥20). Chimera-checking and OTU (operational taxonomic unit) clustering (<97% identity) were carried out using USEARCH v9.0 (Edgar, 2010). All sequences were submitted to NCBI BLASTn (Altschul *et al.*, 1990) to retrieve 16S reference sequences with closest identities. 16S reference sequences were also retrieved for major methanogenic groups and a bacterial outgroup (*Psychrobacter spcs.*, NR_118027.1). Gapless alignments and Neighbour-Joining phylogenetic trees were generated using MUSCLE v3.8.31 (Edgar, 2004) and formatted in MEGA7 (Kumar *et al.*, 2016). Sequences were uploaded to Genbank under accessions KY077158 - KY077249.

2.6 Preparation for Pyrosequencing

Using the same 9 samples, PCR was carried out with pyrosequencing primers including adapter, key, Roche MID (1-14), and primer sequences S-D-Univ-0905-a-S-18 (TGA AAC TYA AAG GAA TTG; Gao *et*

al., 2015) and S-D-Univ-1492-a-A-19 (GGT TAC CTT GTT ACG ACT T; Leser *et al.*, 2002). To provide technical replicates, each sample was amplified three times and combined for purification. Products were then cleaned (QIAquick Gel Extraction Kit, QIAGEN) and purified (MinElute PCR Purification Kit, QIAGEN), before being combined to a single 50µl pool, at 5ng/µl per timepoint. Macrogen (Seoul, Republic of Korea) carried out pyrosequencing externally, using the Roche-454 FLX+ platform.

2.7 Pyrosequencing Analysis

QIIME's `split_libraries.py` script (Caporaso *et al.*, 2010) was used to de-multiplex the returned sequences, which were then uploaded to the ARB-SILVA NGS suite, version 1.63/1.3.9 (Quast *et al.*, 2013) for filtering, clustering at 100% sequence identity, and assigning taxonomies at the default identity of 93%. The programming language R was used to compile operational taxonomic units (OTUs) and taxonomy using the libraries ggplot2, phyloseq, and the RStudio interface (Wickham, 2009; McMurdie and Holmes, 2013; R Core Team, 2013). The sequence data from this study were submitted as a single SFF file to the ENA databases under accession number PRJEB26841 and are accessible at the URL https://www.ebi.ac.uk/ena/data/view/PRJEB26841.

3. Results and Discussion

3.1 DGGE Community Profile

A preliminary characterisation of community structure was carried out for archaeal and bacterial populations across the nine samples (Figure 1).

The archaeal populations visualised through DGGE are highly consistent, with little or no variation between either reactor conditions (55°C, 65°C, 65°C with re-inoculation) or replicates. The persistent strong band at A4 indicates a dominant archaeal population common to all stages of reactor operation, implying that once established the archaeal community saw little disruption over the three stages characterised. Additionally, a number of faint bands (A5, 6, 8, 9) show little variety between the different stages, and are likely to represent smaller, stable methanogen populations. One exception to this is band A7 in stage B (55°C), which does not persist at 65°C, nor reappear once re-inoculated at 65°C. Nevertheless, the overall archaeal population appears remarkably stable, despite changes in operational conditions.

Bacterial banding patterns show higher diversity, particularly towards the lower-resolution, high-denaturant zone at the gel's base (B17 - B23). Similar to the archaeal bands, at least two strongly persistent populations are visible across all stages of reactor operation (B4, B8), alongside faint but persistent bands (B9-11), and a number of intermittent or undefined bands towards the gel base (B15 - 23). Clustering of bands at the base of the gel reflects co-migration of sequences with similar GC content, requiring higher concentrations of denaturant in order to be separated thoroughly. In general, bacterial banding patterns reiterate a relatively consistent community structure between the three stages.

A number of artefacts were present, to a greater or lesser degree, in all gels. Some were linked to issues in PCR amplification: product was often diffuse or caused large ‘smears’, most evident at the base of the gel. Also, amplification of samples from Stage B was difficult and gave low amounts of product. Neither issue was fully resolved despite purification of reagents, template, and product, as well as cleaning of materials. Although additional troubleshooting may have improved visualisation, the clear persistence of a dominant archaeon throughout all reactor stages warranted characterisation at a greater resolution.

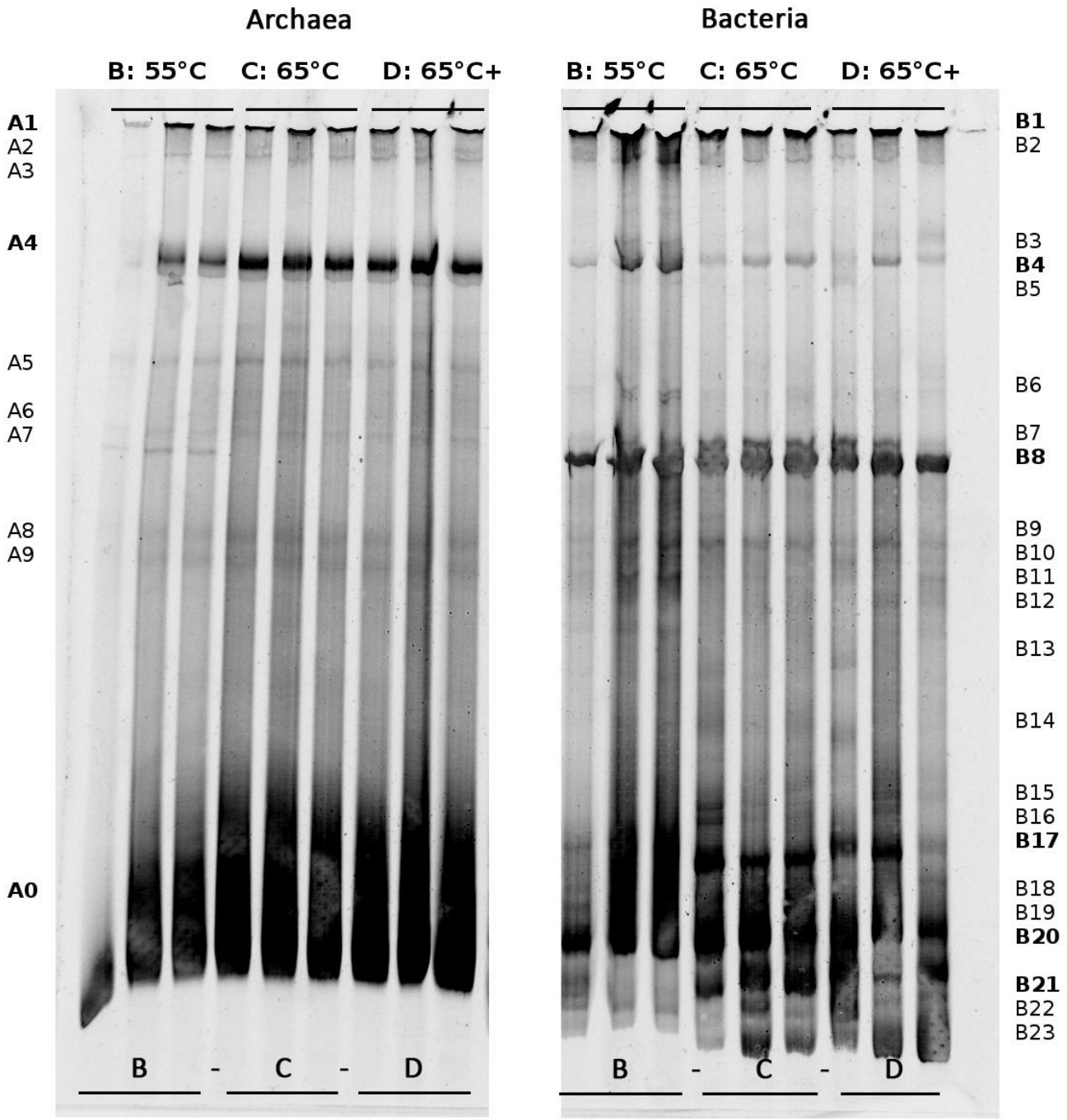

Figure 1: Denaturing Gradient Gel Eelctrophoresis of replicate ex situ samples, across three stages for Archaea and Bacteria. *Although bacterial banding patterns show a greater variety than archaeal bands, there is strong consistency between the three operation stages (B, C, D). One particularly robust population is visible in the archaeal bands (A4), while two such bands are visible for Bacteria (B4, B8). A denaturing gradient of 15% (top) to 85% (base) was used. Bands have been notated A (Archaeal) and B (Bacterial) for reference. Stage B: thermophilic operation at 55°C; Stage C: thermophilic operation at 65°C; Stage D: thermophilic operation at 65°C with re-inoculation.*

3.2 Clone Library Community Analysis

Stages B, C and D were sampled through PCR and transformation, producing 9 clone libraries of archaea 16S sequences. Of the 108 clones sequenced, 92 passed quality filters (average length = 626bp), and were clustered @ 97% similarity identifying 5 closely-related archaeal OTUs. Four OTUs aligned at sequences identities >99% with both *Methanothermobacter wolfeii* (OTUs 13B, F01, B12; reference accession KT368944.1) and *Methanothermobacter thermautotrophicus* (OTU D04; reference accession HJQ346751.1). *M. wolfeii* grows optimally at 55-65°C, pH 7.0-7.7, requiring relatively high concentrations of tungsten (8µM) as a growth factor (Wasserfallen *et al.*, 2000). A fifth OTU (E04) associated with *Methanobacterium formicicum* Mb9 (accession JN205060.1) at identities >99%. *M. formicicum* can metabolise a slightly wider range of carbon sources (CO_2 and formate; 2-propanol and 2-butanol without methanogenesis) but is associated with a much lower temperature range of 37-45°C (Jarvis *et al.*, 2000).

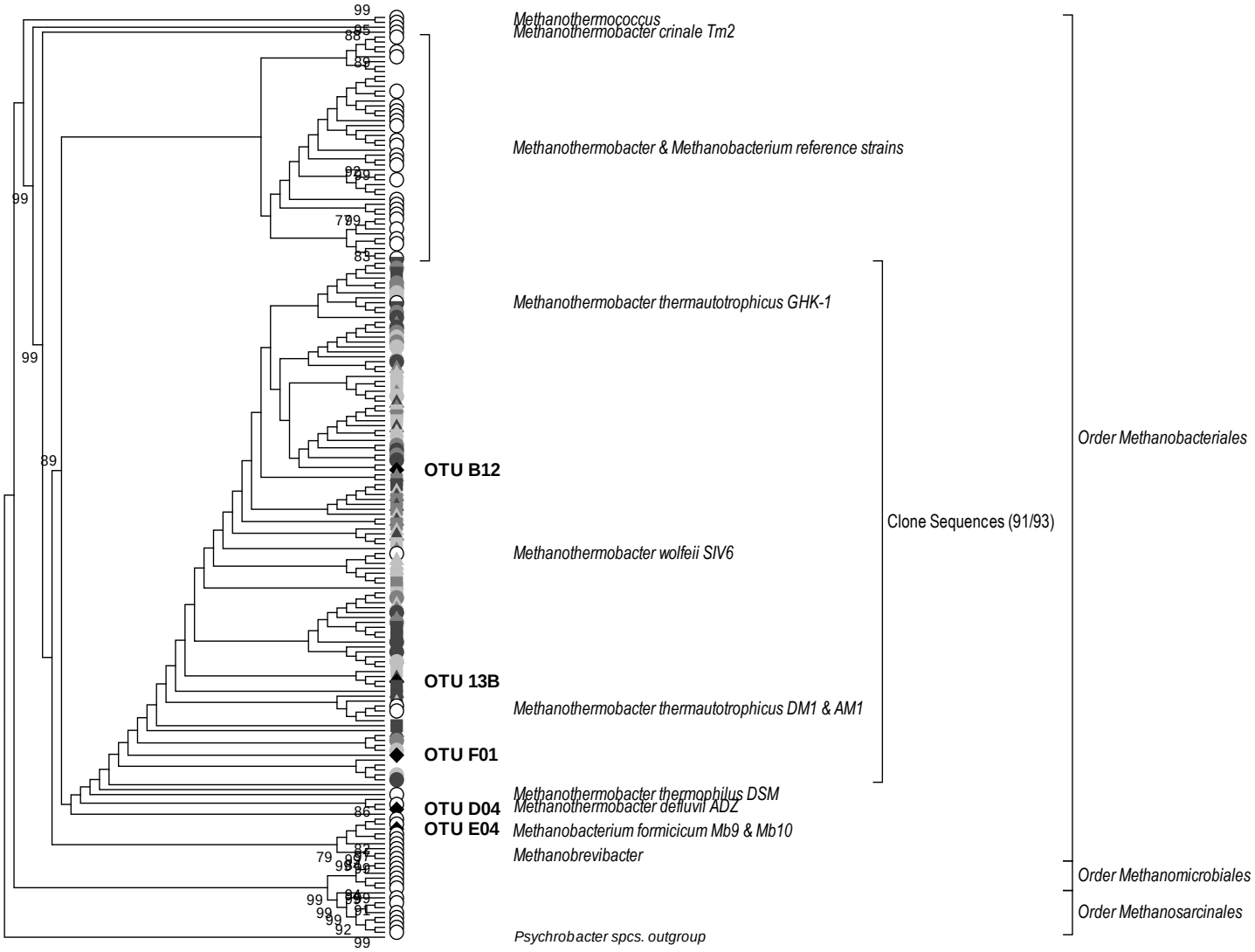

Figure 2: Consensus tree (Neighbour-Joining method with Tamura-Nei distances through 1000 iterations, showing evolutionary distances between cloned and reference sequences in this study.

Note segregation of Orders Methanosarcinales and Methanomicrobiales with respect to Order Methanobacteriales and clone sequences. The majority of cloned sequences are located among Methanothermobacter sequences. Tight clustering with short branch-length reflects the high sequence-similarity of the dataset. No clustering of clones by Reactor or Stage is readily apparent. Only bootstrap values above 75% are presented.

Legend:

Reference sequences: ○; clustered reference OTUs: ◆; Reactor 1:●; Reactor 2: ▲ ; Reactor 3: ■.

Stage B: ; Stage C: ; Stage D: .

A cladogram of clone library sequences, as well as related reference sequences, is provided in Figure 2 and an OTU table is presented in Table 1**.**

Methanothermobacter-associated OTUs dominate the archaeal community in this thermophilic *ex situ* setup. OTU 13B comprises 85% of all sequences and is evenly distributed across the study, despite a slightly lower abundance in reactors at Stage D. Figure 2 shows clone sequences clearly clustering with *Methanothermobacter* references*,* indicating a highly homogenous archaeal community throughout the trial. Association of OTU E04 with *M. formicicum* suggests closely related taxa at lower abundances. Notably, no sequences align with other methanogenic clades or non-methanogenic Archaea, despite predicted coverage of these groups. In particular, the absence of acetoclastic methanogens (Order *Methanosarcinales*) reaffirms that carbon-limited thermophilic conditions are unsuitable for acetoclasts. The significance of OTUs D04 and E04 is less clear given that they occur only once in this study.

	Stage B			Stage C			Stage D			
Reactor	R. 1	R. 2	R. 3	R. 1	R. 2	R. 3	R. 1	R. 2	R. 3	Closest Identity
OTU 13B	8	11	10	10	8	6	5	10	10	*Methanothermobacter wolfeii*
OTU F01	2	1	1	1	0	1	3	1	1	*Methanothermobacter wolfeii*
OTU B12	0	0	0	0	0	1	1	0	0	*Methanothermobacter wolfeii*
OTU D04	0	0	0	0	0	0	1	0	0	*Methanothermobacter thermautotrophicum*
OTU E04	0	0	0	0	0	0	1	0	0	*Methanobacterium formicicum*

Table 1: *Reference OTUs for sequences clustered at 97% as well as the closest identities found (BLASTn)*

3.3 Community Pyrosequencing

3.3.1 Pyrosequencing Output

Sequencing of the 16S V6-V9 regions produced 65,779 reads, which provided 55,913 reads after quality filtering, with an average of 6208 ± 3012 reads per sample. Clustering and taxonomic assignment using the SILVA-NGS platform produced 103 taxa across the 9 samples. Rarefaction curves for the sequenced time points were not yet level but had passed into the late linear phase, illustrating that although this sequencing depth does not capture all diversity present in these communities, the major components are sufficiently sequenced to allow an overview of community topology.

3.3.2 Pyrosequencing Community Composition

Archaea (*Methanothermobacter*) comprised 8.3% of total reads, and although this validates the identities obtained through sequencing of the 16S clone library in section 3.2, the extreme variations in methanogen abundance observed across the trial contradict the consistent DGGE banding patterns obtained (Figure 1). *Methanothermobacter* relative abundances varied from 0-3% in stage B replicates, exceeded 40% in stage C, and returned to lower values of 4-8% in stage D. High abundance at Stage C is counter-intuitive to expectations, as this stage saw a decline in biogas output (Guneratnam *et al.*, 2017). It was originally thought that this decline in biogas function was due to loss of methanogens through rapid hydraulic retention times, or a lack of trace elements (TE): however it now seems likely that a decline in the abundance of methanogenic archaea was not to blame for the decreased biomethane output seen in Stage C

Phylum *Firmicutes* comprised the majority of reads at all stages (82% total reads), while the phyla *Tenericutes* (*Haloplasma*, 5.8%), *Halanaerobiaeota* (*Halocella*, 1.8%), *Chloroflexi* (uncharacterised,

1.5%), and ten minor phyla (pooled abundance: 3.9%) comprised the remainder of the observed populations. Of the *Firmicute* majority, most sequences were assigned to the uncharacterised order MBA03, comprising between 10% (reactor3, stage C) and 70% (reactor 2, stage B) of sample abundance (34% total reads). Reads assigned to uncultured *Firmicutes* contributed a further 19% of total reads, suggesting that the majority (53%) of the *ex situ* community is phylogenetically novel, with unknown metabolic activity. This is likely to be due to the constrained niche provided in this study, selecting for as-yet uncharacterised diversity. However, it should also be noted that reads for these two major OTUs are agglomerated at the order- and phylum-levels respectively, and as such each represents multiple related populations of varying size. In addition, a slight decline in MBA03 abundance is noted during stage C (decreased biogas output at 65°C), indicating a potentially positive role for this population in biogas production.

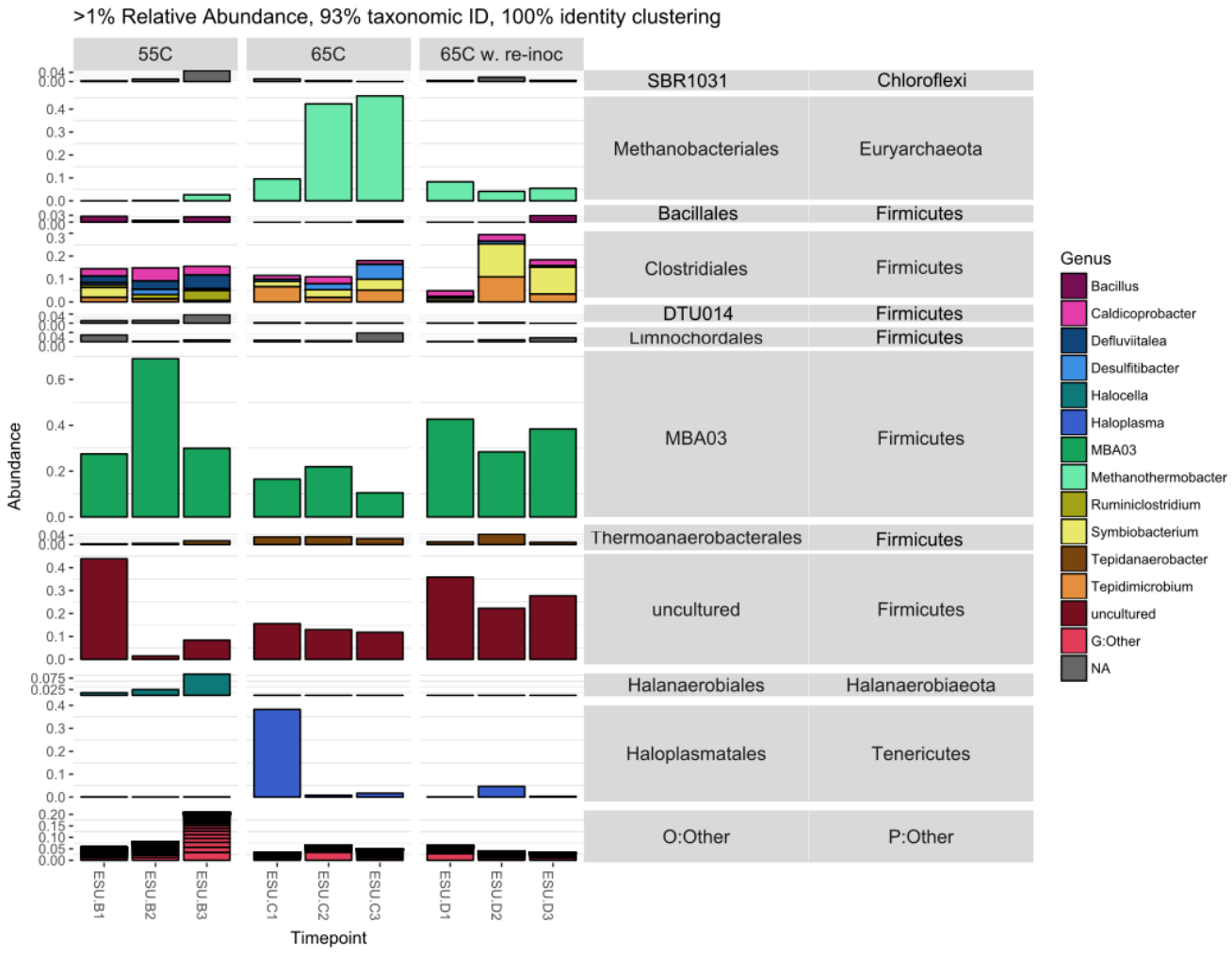

Figure 3: Microbial community abundances generated through 16S pyrosequencing. *Replicate community relative abundances, grouped by the three stages in this study, with taxonomic assignments provided for populations with abundance >1% in 3 or more samples. Populations are arranged by phyla and order, and coloured by identified genus. Populations with abundances below 1% have been grouped to other at base. Note that the scale of the Y axis (Abundance) varies between clades to better present changes between populations of different size.*

16S community profiles show *ex situ* bacterial communities possess both dynamic and stable populations. Although the largest bacterial components (uncultured *Firmicutes* and MBA03 OTUs) cannot be closely scrutinised, several other populations remain relatively abundant throughout operation (*Caldicoprobacter, Symbiobacterium Tepidimicrobium*), and are known to be thermophilic

hydrolysers (xylans, peptone) and general fermenters of saccharides and amino acids, with variable respiratory activities depending on available electron acceptors (nitrate, nitrite, Fe, thiosulphite, sulphur)(Niu *et al.*, 2009; Yokoyama *et al.*, 2010; Shiratori-Takano *et al.*, 2014). These metabolic activities are consistent with thermophilic digestion inoculated with thermophilic agricultural/cellulose digestate, while the presence of end-fermenters (*Tepidanaerobacter, Desulfitibacter***)** possibly reflects the *ex situ*, nutrient-limited nature of these reactors. There is an obvious spike in abundance of *Haloplasma* (<1% to 30%) in replicate 1 of stage C, corresponding to a lower abundance of *Methanothermobacter* in replicate 1 in comparison with other replicates for the same time point (9.6% versus 42-46%). An explanation for this difference in community structure at stage C is provided through the use of sodium hydroxide (NaOH) as a buffering agent used to maintain a neutral pH in all replicates throughout the trial, and in particular during replicate 1 (Guneratnam *et al.*, personal communication) during this stage. This would result in a higher concentration of sodium in the reactor, encouraging halophiles such as *Haloplasma* (Figure 3) and could have inhibited *Methanothermobacter* which have a lower optimal sodium tolerance (Whitman *et al.*, 2014).

Many taxa of minor abundance (<1%) show relatively large changes in abundance between stages, dropping from 1-8% in stage B to 1% or lower in stages C and D (*Bacillus, Defluvitalea, Halocella, Hydrogenispora, Ruminococcaceae, Peptococcaceae; see* Appendix A, Supplementary Figure 4.1). These taxa follow the general emphasis on thermophilic saccharide fermentation seen above, but declines in abundance indicate that they do not transition to higher thermophilic temperatures (55 to 65°C).

3.4 Microbial community development

Characterisation of triplicate reactors at 55°C, 65°C, and 65°C with re-inoculation was performed using DGGE and indicated a homogenous archaeal population and relatively stable bacterial populations throughout *ex situ* operation. Construction of an archaeal 16S clone library verified the dominance of a single hydrogenotrophic methanogen population. A more thorough community profile through 16S pyrosequencing showed large, persistent populations of uncharacterised Firmicutes, while confirming *Methanothermobacter* as the functional methanogen. Pyrosequencing also revealed a greater variability in community structure both between stages, and between replicates. Nevertheless, given the large changes in reactor conditions (10° C increase in temperature, re-inoculation), the consistency of these communities indicates a robust acclimatisation that is stable once established, with *Methanothermobacter* species representing likely and resilient candidates for thermophilic biogas upgrading.

The genus *Methanothermobacter* was formed to accommodate a number of methanogen isolates from the sister genus *Methanobacterium* which were observably distinct in both physiology and phylogeny (Wasserfallen *et al.*, 2003). In addition to nesting within the methanogenic, hydrogenotrophic class *Methanobacteria*, archaea from this genus are characteristically thermophiles, with growth optima circa 65°C and upper growth limits in some isolates around 80°C. Cells are usually rod-shaped, and possess fimbriae. *Methanothermobacter* grow well under CO_2/H_2 with minimal supplementation (Whitman *et al.*, 2014), and can have doubling times in the region of 12-16 hours (Nakamura *et al.*, 2012; Oren 2014). As thermophilic autotrophic methanogens, they ideally combine the CO_2-sequestering function of biogas upgrading with the temperature-associated increase in rate of methane formation desired for industrial applications. When originally defined, *Methanothermobacter* contained three consistent clusters of 16S phylogeny, which were codified as

M. marburgensis, *M. thermautotrophicum*, and *M. wolfeii* . These represented isolates or uncultured sequences from thermophilic sludges, digesters, manure and sediments. Since the genus' publication, a fourth cluster of 16S phylogeny has been observed, representing two species (*M. crinale*, *M. tenebrarum*) associated with decomposition of crude oil to methane via thermophilic syntrophic acetate oxidation (SAO) (Cheng *et al.*, 2011; Nakamura *et al.* 2013). *Methanothermobacter*'s prominent niche as a thermophilic methanogen has made it a popular research topic, with several genomes produced from isolates and metagenomic libraries: *M. thermautotrophicum* in particular is represented by more than 40 genomes.

The majority of clone library sequences in this study (90 of 92) identified with *M. wolfeii,* noted in section 3.2 as having an elevated requirement for tungsten (Winter *et al.*, 1984). Sequence analysis of *M. wolfeii* (Luo *et al*., 2001) has shown that it also contains a prophage-encoded endoisopeptidase which leads to lysis when autotrophy is interrupted e.g. through starvation of hydrogen (König *et al.*,1985). To produce energy, autotrophs also rely on uptake of CO_2 which in thermophilic methanogens is done through use of a tungsten-bound active site. In this context, reliance on *M. wolfeii* in biogas upgrading could represent a point of fragility, where decreased tungsten availability could lower energy metabolism and destabilise methanogen abundance. Adequate trace element supplementation of tungsten might allow further optimisation of this upgrading setup. Additionally, although methanogenesis proceeds more rapidly with increasing temperature (Amend and Shock, 2001; Thauer *et al.*, 2008), the genus observed throughout this study presents a biological hurdle to further increases in *ex situ* temperature. All species within *Methanothermobacter* show growth optima circa 65°C-70°C, and although *M. crinale* and *M. tenebrarum* show limited growth up to 80°C, studies of these species (Cheng *et al.*, 2011; Mayumi *et al.*, 2011) suggest a niche of syntrophic (co-operative acetate catabolism) rather than autotrophic (CO_2 fixation) methanogenesis, as well as

relatively lower growth rates. As such, the biogas upgrading functionality of *Methanothermobacter* taxa at temperatures above 65°C is as-yet unproven.

Re-inoculation of the reactors at Stage D was associated with some improvement in function (from 80-90% to 90-92% CH_4 composition after 24hr) but no significant change in Archaea was observed in the clone library or following DGGE, while pyrosequencing showed a significant decrease in the abundance of *Methanothermobacter* (from 9-45% in stage C to 4-8% in stage D). Given the observed decrease in abundance, and the consistent archaeal taxonomy employing three consecutive primer pairs it is unlikely that restructuring of methanogenic populations or inoculation of an alternative methanogen had a role in the increased (stage C) or decreased (stage D) levels of biomethane produced. Similarly, although re-inoculation improved process performance, pyrosequencing of the bacterial community shows that it did not correspond with obvious functional shifts in community structure, nor did novel populations appear which could explain recovery of biogas yield. Instead, the inoculum may have allowed rescue through the introduction of depleted organic or inorganic materials. The inoculum would provide a relatively rich substrate for the carbon-limited *ex situ* community, and is likely to account for an increase in abundance of fermenting and hydrolysing *Firmicutes* in stage D: a positive effect on biogas output through this route would suggest that hydrogenotrophic biogas upgrading was supplemented by 'traditional AD', through substrate degradation to acetate, CO_2 and H_2 for use in methanogenesis. The response to re-inoculation seen in Stage D could also indicate the need for additional growth factors in thermophilic setups - in particular, an elevated requirement for tungsten by *Methanothermobacter wolfeii* may be relevant (Winter *et al.*, 1984), particularly as this was the dominnat methanogen encountered (98% of clone libraries in this study). Previous studies have identified the importance of trace elements in biogas-orientated *in-situ* anaerobic digesters (Demirel and Scherer, 2011; Wall *et al.*, 2014). As such, if the

'recovery' observed is simply due to addition of alternative substrates, it indicates that *ex situ* upgrading can be further refined to emphasise independent methanogenesis.

Although the microbial resolution in this study may be constrained to some extent by primer coverage and depth of sequencing, it does however outline the major methanogenic and bacterial components of this system through a consistent clustering of sequences in the case of methanogens, and persistent abundances in the case of bacteria. While some of the central bacterial components remain uncharacterised, thermophilic (55°C-65°C) *ex situ* biogas upgrading is nevertheless likely to rely upon select, stable hydrogenotrophic populations of *Methanobacteriaceae*, with a central role for novel *Firmicutes* clades.

4. Conclusions

Ex situ biogas upgrading presents both a cost-effective solution to increasing biogas yields in the energy sector, and an extremophilic microbial niche that is not as-yet fully understood. Although biogas output may be seen to vary over time and between temperatures, this does not necessarily reflect disruptions or decline in methanogen abundance, which instead appears to be stimulated during periods of decreased biogas output, and at higher temperatures (65°C rather than 55°C). As such, observed improvements in reactor function or stability may rely on the non-target bacterial populations who nevertheless co-habit in the *ex situ* reactor, possibly through supplementary hydrolysis and fermentation of available materials (e.g. inoculum). Additionally, the minimal media used should be re-evaluated to include trace nutrients and elements known to facilitate methane formation by the observed methanogens, including tungsten, nickel, iron, and cobalt amongst others. Finally, a lack of observed acetoclastic archaea supports the understanding that thermophilic conditions are unsuitable for direct methane generation from acetate. Further exploration of this topic will require more in-depth analysis of community dynamics and a wider range of samples.

5. References

1. Altschul, S.F., Gish, W., Miller, W., Myers, E.W., and Lipman, D.J. (1990) Basic local alignment search tool. *J. Mol. Biol.* **215**: 403–410.

2. Amend, J.P. and Shock, E.L. (2001) Energetics of overall metabolic reactions of thermophilic and hyperthermophilic Archaea and Bacteria. *FEMS Microbiol. Rev.* **25**: 175–243.

3. Angelidaki, I. and Sanders, W. (2004) Assessment of the anaerobic biodegradability of macropollutants. *Rev. Environ. Sci. Biotechnol.* **3**: 117–129.

4. Bassani, I., Kougias, P.G., Treu, L., and Angelidaki, I. (2015) Biogas Upgrading via Hydrogenotrophic Methanogenesis in Two-Stage Continuous Stirred Tank Reactors at Mesophilic and Thermophilic Conditions. *Environ. Sci. Technol.* **49**: 12585–12593.

5. Bassani, I., Kougias, P.G., Treu, L., Porté, H., Campanaro, S., and Angelidaki, I. (2017) Optimization of hydrogen dispersion in thermophilic up-flow reactors for ex situ biogas upgrading. *Bioresour. Technol.* **234**: 310–319.

6. Caporaso, J.G., Kuczynski, J., Stombaugh, J., Bittinger, K., Bushman, F.D., Costello, E.K., et al. (2010) QIIME allows analysis of high-throughput community sequencing data. *Nat. Methods* **7**: 335–336.

7. Casamayor, E.O., Muyzer, G., Pedrós-Alió, C., and others (2001) Composition and temporal dynamics of planktonic archaeal assemblages from anaerobic sulfurous environments studied by 16S rDNA denaturing gradient gel electrophoresis and sequencing. *Aquat. Microb. Ecol.* **25**: 237–246.

8. Cheng, L., Dai, L., Li, X., Zhang, H., and Lu, Y. (2011) Isolation and Characterization of Methanothermobacter crinale sp. nov., a Novel Hydrogenotrophic Methanogen from the Shengli Oil Field. *Appl Environ Microbiol* **77**: 5212–5219.

9. Demirel, B. and Scherer, P. (2011) Trace element requirements of agricultural biogas digesters during biological conversion of renewable biomass to methane. *Biomass Bioenergy* **35**: 992–998.

10. Dolfing, J. (2013) Syntrophic Propionate Oxidation via Butyrate: a Novel Window of Opportunity under Methanogenic Conditions. *Appl. Environ. Microbiol.* **79**: 4515–4516.

11. Drosg, B. (2013) Process monitoring in biogas plants.

12. Edgar, R.C. (2004) MUSCLE: multiple sequence alignment with high accuracy and high throughput. *Nucleic Acids Res.* **32**: 1792–1797.

13. Edgar, R.C. (2010) Search and clustering orders of magnitude faster than BLAST. *Bioinformatics* **26**: 2460–2461.

14. Fukuzaki, S., Nishio, N., Shobayashi, M., and Nagai, S. (1990) Inhibition of the Fermentation of Propionate to Methane by Hydrogen, Acetate, and Propionate. *Appl. Environ. Microbiol.* **56**: 719–723.

15. Gao, Z.-M., Wang, Y., Tian, R.-M., Lee, O.O., Wong, Y.H., Batang, Z.B., et al. (2015) Pyrosequencing revealed shifts of prokaryotic communities between healthy and disease-like tissues of the Red Sea sponge *Crella cyathophora*. *PeerJ* **3**: e890.

16. Guneratnam, A.J., Ahern, E., FitzGerald, J.A., Jackson, S.A., Xia, A., Dobson, A.D.W., and Murphy, J.D. (2017) Study of the performance of a thermophilic biological methanation system. *Bioresour. Technol.* **225**: 308–315.

17. Jarvis, G.N., Strömpl, C., Burgess, D.M., Skillman, L.C., Moore, E.R.B., and Joblin, K.N. (2000) Isolation and Identification of Ruminal Methanogens from Grazing Cattle. *Curr. Microbiol.* **40**: 327–332.

18. Klindworth, A., Pruesse, E., Schweer, T., Peplies, J., Quast, C., Horn, M., and Glöckner, F.O. (2012) Evaluation of general 16S ribosomal RNA gene PCR primers for classical and next-generation sequencing-based diversity studies. *Nucleic Acids Res.* gks808.

19. König, H., Semmler, R., Lerp, C., and Winter, J. (1985) Evidence for the occurrence of autolytic enzymes in *Methanobacterium wolfei*. *Arch. Microbiol.* **141**: 177–180.

20. Kougias, P.G., Treu, L., Benavente, D.P., Boe, K., Campanaro, S., and Angelidaki, I. (2017) Ex-situ biogas upgrading and enhancement in different reactor systems. *Bioresour. Technol.* **225**: 429–437.

21. Kumar, S., Stecher, G., and Tamura, K. (2016) MEGA7: Molecular Evolutionary Genetics Analysis version 7.0 for bigger datasets. *Mol. Biol. Evol.* msw054.

22. Leser, T.D., Amenuvor, J.Z., Jensen, T.K., Lindecrona, R.H., Boye, M., and Møller, K. (2002) Culture-Independent Analysis of Gut Bacteria: the Pig Gastrointestinal Tract Microbiota Revisited. *Appl. Environ. Microbiol.* **68**: 673–690.

23. Luo, Y., Pfister, P., Leisinger, T., and Wasserfallen, A. (2001) The Genome of Archaeal Prophage ΨM100 Encodes the Lytic Enzyme Responsible for Autolysis of Methanothermobacter wolfeii. *J Bacteriol* **183**: 5788–5792.

24. Luo, G. and Angelidaki, I. (2012) Integrated biogas upgrading and hydrogen utilization in an anaerobic reactor containing enriched hydrogenotrophic methanogenic culture. *Biotechnol. Bioeng.* **109**: 2729–2736.

25. Luo, G., Johansson, S., Boe, K., Xie, L., Zhou, Q., and Angelidaki, I. (2012) Simultaneous hydrogen utilization and in situ biogas upgrading in an anaerobic reactor. *Biotechnol. Bioeng.* **109**: 1088–1094.

26. Mayumi, D., Mochimaru, H., Yoshioka, H., Sakata, S., Maeda, H., Miyagawa, Y., et al. (2011) Evidence for syntrophic acetate oxidation coupled to hydrogenotrophic methanogenesis in the high-temperature petroleum reservoir of Yabase oil field (Japan): Methanogenesis in a high-temperature oil reservoir. *Environmental Microbiology* **13**: 1995–2006.

27. McMurdie, P.J. and Holmes, S. (2013) phyloseq: An R Package for Reproducible Interactive Analysis and Graphics of Microbiome Census Data. *PLoS ONE* **8**: e61217.

28. Mulat, D.G., Mosbæk, F., Ward, A.J., Polag, D., Greule, M., Keppler, F., et al. (2017) Exogenous addition of H 2 for an in situ biogas upgrading through biological reduction of carbon dioxide into methane. *Waste Manag.* **68**: 146–156.

29. Muyzer, G., De Waal, E.C., and Uitterlinden, A.G. (1993) Profiling of complex microbial populations by denaturing gradient gel electrophoresis analysis of polymerase chain reaction-amplified genes coding for 16S rRNA. *Appl. Environ. Microbiol.* **59**: 695–700.

30. Nakamura, K., Takahashi, A., Mori, C., Tamaki, H., Mochimaru, H., Nakamura, K., et al. (2012) Methanothermobacter tenebrarum sp. nov., a hydrogenotrophic, thermophilic methanogen isolated from gas-associated formation water of a natural gas field. *Int. J. Syst. Evol. Microbiol.* **63**: 715–722.

31. Niu, L., Song, L., Liu, X., and Dong, X. (2009) Tepidimicrobium xylanilyticum sp. nov., an anaerobic xylanolytic bacterium, and emended description of the genus Tepidimicrobium. *Int. J. Syst. Evol. Microbiol.* **59**: 2698–2701.

32. Nordmann, W. (1977) Die Überwachung der Schlammfaulung. KA-Informationen für das Betriebspersonal, Beilage zur Korrespondenz Abwasser.

33. Oren, A. (2014) The Family *Methanobacteriaceae*. In, *The Prokaryotes*. Springer, Berlin, Heidelberg, pp. 165–193.

34. Patterson, T., Esteves, S., Dinsdale, R., and Guwy, A. (2011) An evaluation of the policy and techno-economic factors affecting the potential for biogas upgrading for transport fuel use in the UK. *Energy Policy* **39**: 1806–1816.

35. Quast, C., Pruesse, E., Yilmaz, P., Gerken, J., Schweer, T., Yarza, P., et al. (2013) The SILVA ribosomal RNA gene database project: improved data processing and web-based tools. *Nucleic Acids Res.* **41**: D590–D596.

36. R Core Team (2013) R: A Language and Environment for Statistical Computing R Foundation for Statistical Computing, Vienna, Austria.

37. Ragsdale, S.W. and Pierce, E. (2008) Acetogenesis and the Wood–Ljungdahl pathway of CO2 fixation. *Biochim. Biophys. Acta BBA - Proteins Proteomics* **1784**: 1873–1898.

38. Shiratori-Takano, H., Akita, K., Yamada, K., Itoh, T., Sugihara, T., Beppu, T., and Ueda, K. (2014) Description of Symbiobacterium ostreiconchae sp. nov., Symbiobacterium turbinis sp. nov. and Symbiobacterium terraclitae sp. nov., isolated from shellfish, emended description of the genus Symbiobacterium and proposal of Symbiobacteriaceae fam. nov. *Int. J. Syst. Evol. Microbiol.* **64**: 3375–3383.

39. Sun, Q., Li, H., Yan, J., Liu, L., Yu, Z., and Yu, X. (2015) Selection of appropriate biogas upgrading technology-a review of biogas cleaning, upgrading and utilisation. *Renew. Sustain. Energy Rev.* **51**: 521–532.

40. Thauer, R.K., Kaster, A.-K., Seedorf, H., Buckel, W., and Hedderich, R. (2008) Methanogenic archaea: ecologically relevant differences in energy conservation. *Nat. Rev. Microbiol.* **6**: 579–591.

41. Ullah Khan, I., Hafiz Dzarfan Othman, M., Hashim, H., Matsuura, T., Ismail, A.F., Rezaei-DashtArzhandi, M., and Wan Azelee, I. (2017) Biogas as a renewable energy fuel – A review of biogas upgrading, utilisation and storage. *Energy Convers. Manag.* **150**: 277–294.

42. Wall, D.M., Allen, E., Straccialini, B., O'Kiely, P., and Murphy, J.D. (2014) The effect of trace element addition to mono-digestion of grass silage at high organic loading rates. *Bioresour. Technol.* **172**: 349–355.

43. Wasserfallen, A., Nölling, J., Pfister, P., Reeve, J., and Conway de Macario, E. (2000) Phylogenetic analysis of 18 thermophilic Methanobacterium isolates supports the proposals to create a new genus, *Methanothermobacter* gen. nov., and to reclassify several isolates in three species, *Methanothermobacter thermautotrophicus* comb. nov., *Methanothermobacter* wolfeii comb. nov., and *Methanothermobacter marburgensis* sp. nov. *International Journal of Systematic and Evolutionary Microbiology* **50**: 43–53.

44. Whitman, W.B., Bowen, T.L., and Boone, D.R. (2014) The Methanogenic Bacteria. In, Rosenberg,E., DeLong,E.F., Lory,S., Stackebrandt,E., and Thompson,F. (eds), *The Prokaryotes*. Springer, Berlin, Heidelberg, pp. 123–163.

45. Wickham, H. (2009) ggplot2 - Elegant Graphics for Data Analysis 1st ed. Springer-Verlag New York.

46. Winter, J., Lerp, C., Zabel, H.-P., Wildenauer, F.X., König, H., and Schindler, F. (1984) Methanobacterium wolfei, sp. nov., a New Tungsten-Requiring, Thermophilic, Autotrophic Methanogen. *Syst. Appl. Microbiol.* **5**: 457–466.

47. Yokoyama, H., Wagner, I.D., and Wiegel, J. (2010) Caldicoprobacter oshimai gen. nov., sp. nov., an anaerobic, xylanolytic, extremely thermophilic bacterium isolated from sheep faeces, and proposal of Caldicoprobacteraceae fam. nov. *Int. J. Syst. Evol. Microbiol.* **60**: 67–71.

48. Zinder, S.H., Anguish, T., and Cardwell, S.C. (1984) Effects of temperature on methanogenesis in a thermophilic (58 C) anaerobic digestor. *Appl. Environ. Microbiol.* **47**: 808–813.

Chapter 5

High-Resolution 16S Microbial Upgrading Communities: Contrasting In Situ and Ex Situ Setups

J. A. FitzGerald [a,b], M. Voelklein [b,c], Jerry D. Murphy [b,c], and A. D. W. Dobson [a,b]

a Department of Microbiology, University College Cork

b The MaREI Centre, Environmental Research Institute, University College Cork, Ireland

c School of Engineering, University College Cork, Ireland

ABSTRACT

As biogas from anaerobic digestion becomes an increasingly attractive biofuel, the need to improve the quality of biogas has come to the fore. Biological upgrading focuses on adding enough hydrogen to a thermophilic biogas reactor to allow methanation of the remaining carbon dioxide by methanogenic Archaea. This can be achieved in the primary digester (*in situ*) by supplying additional hydrogen to anaerobic digestion, or biogas and hydrogen can be mixed in a secondary vessel independent of feedstock and operated exclusively to facilitate methanogenesis (*ex situ*). This novel technology is however known to encounter inhibition at high loading rates of hydrogen, but in contrast to anaerobic digestion, the dynamics of this thermophilic microbial community are poorly characterised. 16S rDNA community profiles from four anaerobic biogas upgrading reactors were characterised through deep sequencing, to determine how input of feedstock, hydrogen, and carbon dioxide shape the microbial community. Large differences were seen between *in situ* and *ex situ* communities, largely attributed to the lack of feedstock in *ex situ* upgrading. The difference in feedstock conditions determined the main archaeal populations, as well as influencing populations of hydrolysing and fermenting *Firmicutes*. High hydrogen flow rates (~37L/day) led to a collapse in methanogenic *Methanothermobacter* populations *in situ*, as well as a proliferation of likely homoacetogens. However, *ex situ* hydrogen rates could greatly exceed these levels (~400L/day) without collapse of *Methanobacterium*, although some instability was observed. Subsequent reduction of hydrogen rates *ex situ* (259L/day) led to an apparent deficit of hydrogen, indicated by increased abundance of a variety of syntrophic fermenters known to supply biogenic hydrogen. In either case, instability coincided with a disruption of fermenting and hydrolysing populations attributed to high rates of hydrogen input.

1. Introduction

1.1 *In situ* and *ex situ* approaches

Biogas produced by anaerobic digestion (AD) can contain between 50 and 70% methane, and is thus not sufficiently pure to be used immediately as a biofuel. Contaminants (carbon dioxide, hydrogen sulfide, ammonia) can be removed though biological or physical-chemical upgrading. Biological upgrading is a relatively simple technique, and uses mature technologies developed for biofuel AD. It relies on a subset of the anaerobic community active in AD to convert undesirable carbon dioxide into methane, and can also remove hydrogen sulphide (Oren, 2014). *In situ* biomethanation supplies additional H_2 to the AD reactor, on the basis that improved availability of the H_2 reagent to hydrogenotrophic methanogens will shift thermodynamic equilibrium towards the product, making methanogenesis more favourable, thereby increasing biomethane production. However, AD relies heavily on substrate fermentation, and can be inhibited if hydrogen concentrations are too high. In comparison, *ex situ* upgrading avoids these complications by separating biomethanation from AD, relying on conversion of exogenous H_2 and CO_2 to methane in a separate vessel enriched for hydrogenotrophic methanogens. In an integrated energy network, *ex situ* biomethanation provides a route for converting excess CO_2 and electrical power (via electrolytic formation of H_2) into methane for use or storage. Previous studies have successfully demonstrated biological upgrading in laboratory scale operations (Bassani *et al.*, 2015; Guneratnam *et al.*, 2017; Kougias *et al.*, 2017). While it has already been shown that thermophilic *ex situ* hydrogen upgrading can depend on durable populations of *Methanobacteriales* (chapter 3), the overall community structure remains to be determined.

The microbial ecology of AD is well characterised, with a broad understanding of how archaeal and bacterial community members interact in a stepwise manner to convert biomass into biogas. As a

novel technology, the microbial dynamics of biomethane upgrading are much less clear, although they must include many (perhaps most) of the same microbial components. In particular, each upgrading method poses significant questions - how does *in situ* hydrogen addition influence the microbial communities in its parent process, anaerobic digestion; and in *ex situ* upgrading how does physical separation of methanogenesis from anaerobic digestion change the community structure? Are similar inhibitory effects seen under hydrogen addition between *in situ* and *ex situ*, and can changes in community structure reveal what components are being disrupted? Although these questions have previously been considered (Luo and Angelidaki, 2012; Guneratnam *et al.*, 2017), thorough characterisation of the community was hampered by low sequencing depth, or a constrained taxonomic range for nucleic primers.

1.2 Leveraging Next-Generation Sequence Data for Improved Resolution

Four reactor setups were trialled in series to characterise both *in situ* and *ex situ* high-rate biogas upgrading under thermophilic conditions, using a continuous community propagated from one setup to the next. In this study, deep 16S rDNA amplicon sequencing was used to thoroughly characterise microbial community development in each setup, and contrast the compositions of *in situ* and *ex situ* upgrading communities, as well as batch and continuous *ex situ* processes.

To improve community profiling, the massive sequencing volumes allowed by 'next-generation' sequencing were used to display the 'true' variety of 16S amplicon sequences present in the reactor environments. The software library DADA2 for R (Callahan *et al.*, 2016) leverages the enormous coverage afforded by platforms such as MiSeq (Illumina) to create highly accurate models of base

substitution in the sequencing process. This can then be used to resolve small sequence differences as artefacts or actual community diversity, creating a 16S community profile of Amplicon Sequence Variants (ASVs) with single base-pair resolution. ASVs are functionally similar to Operational Taxonomic Units (OTUs) produced by pipelines like MOTHUR and QIIME, but differ in key points. To create an OTU population, sequences are clustered at an arbitrary 'species identity' threshold (usually 97%). Each OTU sequence then represents an 'averaged' consensus, which is then assigned taxonomy. Through modelling actual sequence composition, ASVs represent the actual molecular 16S diversity of a sample at 100% identity, allowing fine changes in community composition to be tracked.

Interpreting shifts in community abundance becomes increasingly difficult as sequence volumes and taxonomic resolution increase. To reduce the number of interactions that must be considered, differential abundance (DA) testing is often used to highlight segments of the microbial community whose abundance correlates with changes in reactor conditions, meriting further examination. A popular method for detecting DA is DESeq2's test for differences in log2 fold-change (i.e., magnitude of difference in log2 abundance), which was originally developed for detecting changes in gene expression while controlling for differences in sample size (Love *et al.*, 2014). DESeq2 uses an approach similar to that of DADA2, where massive sequence volumes are used to model the unknown 'original' populations being sampled, thereby ameliorating differences and improving comparability between samples. DESeq2 also performs independent filtering which removes low-abundance features whose significance cannot be estimated (due to insufficient data) but would still have to be corrected for, thereby improving overall DA sensitivity. This method is particularly appropriate for Next-Generation Sequencing 16S community datasets, which are likely to have a large number of extremely rare members. A second method to highlight how setups influence community structure is

to compute correlations between microbial populations. However, another problem inherent to sampling is 'compositional data', i.e. data that has a defined cap (i.e. 100% in relative abundances, 1.0 in a proportion, or a defined capacity to sample a population). For example, two populations (e.g. A_n=20, B_n=20) that are equally abundant (A_{ab}=50%, B_{ab}=50%), cannot be introduced to a third population (A_n=20, B_n=20, C_n=15) without implying a negative correlation of C with A and B (A_{ab}=36%, B_{ab}=36%, C_{ab}=27%), despite a lack of interaction. This effect can grossly over-estimate correlations (both positive and negative) in microbial communities (Friedman and Alm, 2012). The software package SparCC avoids this by correlating log-ratio abundances and providing significance estimates through iterative resampling of the community abundance table (Friedman and Alm, 2012). This approach provides a much improved false discovery rate, reducing spurious correlations.

Using these techniques, this study aims to improve characterisation of microbial upgrading populations, with a particular emphasis on continuous *ex situ* digestion. Characterisation of the upgrading populations over time, and across different reactor setups, should provide a deeper understanding of how biomethanating communities and the upgrading process interact.

2. Materials and Methods

2.1 Reactor setup

A 9L continuously-stirred stainless-steel reactor, with a working volume of 6.9L (ISA, ISB) or 5.5L (BES, CES), was commissioned by Voelklein et al. (unpublished results) and run in four trials over a period of 520 days. The reactor had three-way luer-stopcock outlet and inlet valves to allow addition of upgrading gasses and removal of biogas during the experiment. Upgrading gasses were pure hydrogen (ISA, ISB, BES, CES) and CO_2 (BES, CES), stored in self-sealing bags and administered through a fishstone (ISA) or ceramic (ISB, BES, CES) diffuser connected to a peristaltic pump. The fishstone diffuser had poorer rates of hydrogen solution (lower H_2 solution efficiency). Reactor health was monitored through effluent biogas composition and the FOSTAC ratio of inorganic (bicarbonate) to organic (volatile fatty acid, etc) carbon in the reactors. Established optimal FOSTAC values range from 0.2-0.4, although different setups can exceed these values without suffering (Nordmann, 1977). The seed inoculum for these trials came from a thermophilic maize-fed biogas digester. Trial temperature was maintained at 55^{o}C and setups were run sequentially, i.e. digestate from the end of ISA was used as inoculum for ISB; digestate from ISB was used as inoculum for BES; and digestate from BES was used as inoculum for CES. For an overview of the differences between AD, in situ, and *ex situ* reactors, see Figure 3, Chapter 1.

2.2 Reactor operation:

In situ reactor A (ISA) was the first reactor commissioned in this study, and operated from day 0 to day 138. ISA timepoint 1 represents the seed inoculum for these trials, sampled prior to addition

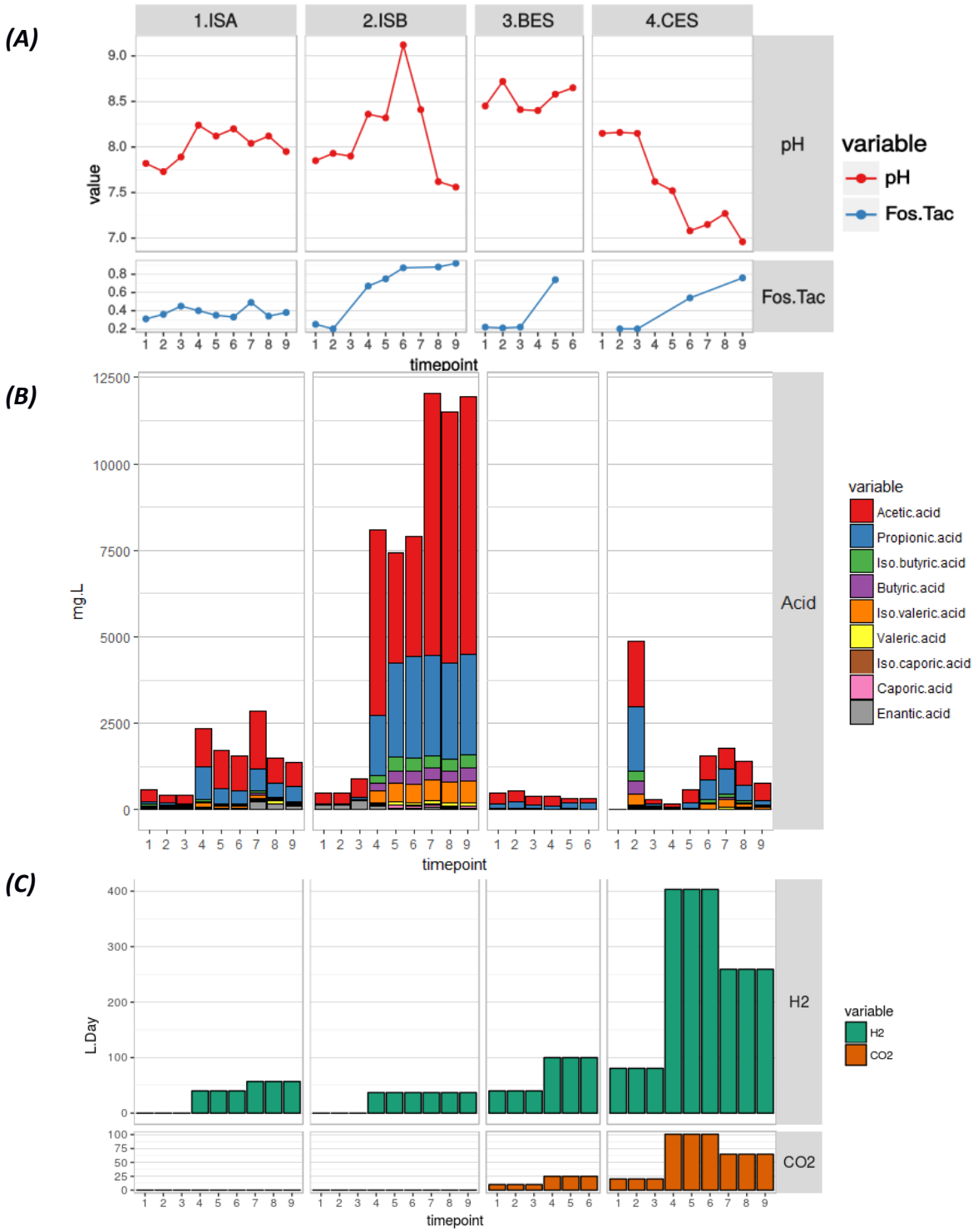

Figure 1: *A: Process variables as measured during reactor operation (Voelklein et al., unpublished data); B: Volumes of volatile fatty acids detected (ml/L); and C: upgrading gas added (L/day) during reactor operations. Note some data points (pH, FOS:TAC) were not recorded: the line has been continued to the next point to indicate the overall trend.*

to the reactor. From days 0 to 47, starting inoculum for the trials was fed grass silage only until the reactor had acclimatised, as determined by biogas output maintaining a pre-calculated optimal yield. From days 49 to 93, the reactor received 40L/day of hydrogen. From days 96 to 138, the reactor received 57L day of hydrogen. The trial was completed on day 138. At the end of the trial, digestate was retained in the reactor at 55°C with occasional feeding of grass until use as seed inolculum in the next commissioned reactor. *In situ* reactor B (ISB) was the second commissioned reactor, and operated from day 262 to 317. The reactor was acclimatised from days 262 to 292, being fed grass only. From day 293 until day 317 (reactor failure), the reactor received 37L/ day of hydrogen at the established OLR: with hydrogen upgrading, FOSTAC became elevated (0.67 – 0.87) as VFAs increased from below 1000µl/L to ~8000µl/L, eventually rising to FOSTAC values of 0.88-0.9 with total VFA levels in the reactor rising to ~12000µl/L (primarily acetic and propionic acid) towards the end of the trial. This lead to reactor failure at day 317 (FOSTAC=0.92, pH=7.56). At the end of the trial, digestate was retained in the reactor at 55°C with occasional feeding of grass until use as seed inolculum in the next reactor.

Batch *Ex Situ* reactor (BES) was the third reactor trialled (days 383 to 431) and from days 383 to 400 the reactor was fed 40L/day of hydrogen and 10L/day of CO_2. From days 424 to 460, the reactor received an increased input of 100L/day of hydrogen and 25L/day of CO_2. At the end of the trial, digestate was retained in the reactor at 55°C with intermittent feeding of hydrogen gas until use as seed inolculum in the next commissioned reactor.

A Continuous *Ex Situ* reactor (CES) was the fourth and final reactor commissioned in this study, and operated from day 460 to 522. From days 460 to 474 the reactor was supplied with a continuous feed of 56ml/min of hydrogen and 14ml/min of CO_2 (i.e. 81 and 20 L/day respectively). From day 481 to

496, the gas flow rate was increased to 280ml/min hydrogen and 70ml/min of CO_2 (i.e. 403 and 100L/day respectively). To increase reactor stability, as determined by FOSTAC, the gas flow rate was decreased to 180ml/min hydrogen and 25ml/min CO_2 (i.e. 259 and 65L/day respectively) from day 508 to completion of the trial at day 522.

In Figure 1, changes in reactor pH are clearly visible as H_2 supply rates increase in the reactors (in particular, reactors ISB and CES). Given that pH represents the activity of H^+ ions in solution, some interaction between pH and increased concentrations of H_2 is expected. However, the sudden drop in pH at ISB 7-9 (~8.5 to ~7.6) and CES 4-9 (~8.2 to 7) indicates changes in pH are related to the inhibition of upgrading function and the resulting increase in VFA concentrations, as the rate of H_2 supply did not change during this period (see section 3.4.2 for further discussion of pH and homoacetogenesis).

The effects of pH changes in this range on biogas upgrading are unknown. Although substrate acidification and alkalinification are used as pre-treatments to enhance breakdown of lingo-cellulsoic substrates in anaerobic fermentation (Singh et al., 2015), a change in reactor pH from mildly alkaline to neutral (i.e. pH 8.5 to pH 7) is not expected to observably accelerate feedstock hydrolysis. Additionally, it is likely that any change directly related to pH would be obscured by the inhibitory effect of hydrogen on fermentation and the associated build-up of VFAs. Taking into account the diversity of hydrolysing and fermenting bacteria observed in anaerobic digestion, changes in pH level could select for microbes better acclimated to the lower pH levels seen in late ISB and late CES, and may have contributed to population shifts seen during these timepoints (see discussion of microbial population shifts in ISB, section 3.4.2). Methanogen pH optima range from slightly acidic (pH 6.5) to alkaline (pH 8) (Whitman et al., 2014), with similar pH optima of 6.8-8 for the thermophilic methanogens expected in this study. As such, values observed are unlikely to affect methanogenesis.

2.3 Reactor sampling

Reactors were sampled using a sterile container to scoop digestate from the reactor, before being sealed, and frozen at -20^{o}C until extraction. Sample time points were chosen to provide even coverage of microbial communities throughout each reactor's lifespan, covering starting inoculum, operation, and completion or failure of reactors. This provided 9 samples from ISA, ISB, and CES respectively, and 6 samples from BES (33 samples total). For each sample, three 1.8g digestate replicates were removed to 2ml eppendorf tubes. The tubes were spun at maximum centrifugal speed for one minute to partition liquid and solid contents. The liquid portion was decanted, and the solid portion was used for extraction of nucleic acids.

2.4 DNA extraction and Sequencing

DNA extraction was performed using a 60^{o}C CTAB/PVPP extraction buffer with proteinase K, followed by Phenol:Chloroform:IsoAmyl Alcohol phase separation, isopropanol precipitation, and ethanol washing, as detailed in Appendix B. Digestate replicates (as described above) were processed, and the replicate extracts were recombined in equimolar quantities to give a final aliquot of 2ng/µl for each of the 33 samples. The quality of extracts was assessed using agarose gel electrophoresis, Nanodrop spectrophotometer D-1000 (ThermoFisher, USA), and Qubit 3 fluorometer (ThermoFisher, USA). Once standardised and demonstrated to work in standard 16S PCR reactions, the samples were submitted for sequencing.

Sample preparation and sequencing was carried out by MACROGEN (Seoul, South Korea) on a MiSeq platform using paired-end reads. As the composition of thermophilic *ex situ* upgrading communities is

unknown, efforts were made to obtain the widest taxonomic representation possible from sequencing. Sequencing primers were selected from the Earth Microbiome Project, (16S Illumina Amplicon Protocol : Earth Microbiome Project), which would provide comprehensive coverage. Primers S-D-Univ-0515-b-S-19 (GTG YCA GCM GCC GCG GTA A) (Caporaso *et al.*, 2012) and S-D-Univ-0926-b-A-20 (CCG YCA ATT YMT TTR AGT TT) (Walters *et al.*, 2016) were chosen and evaluated in TestPrime (Klindworth *et al.*, 2012), giving coverage of 84, 88 and 86% of Archaea, Bacteria and Eukarya respectively, and an amplicon length of around 410bp.

2.5 Sequence analysis and Bioinformatics

Sample data was processed using DADA2 (Callahan *et al.*, 2016) in RStudio (R Core Team, 2013) to carry out primer-sequence trimming, error model estimation, dereplication, paired-end merging, chimera removal and taxonomy assignment, as well as providing sequence provenance (see Appendix C); finally producing unique amplicon sequence variants (ASV) rather than operational taxonomic units (OTUs, see section 1.2). Based on a sequence length histogram, sequences were also post-filtered for length, removing any reads shorter than 350bp. Exploration and management of sequence, abundance and taxonomic data was carried out in R using the venerable packages phyloseq (McMurdie and Holmes, 2013), ggplot2 (Wickham, 2009), heatmaply (Galili *et al.*), vegan (Oksanen *et al.*, 2014), and R Studio (R Core Team, 2013).

Differential abundance testing of ASVs between reactor setups was carried out using the DESeq2 package (Love *et al.*, 2014) and visualised in ggplot2. As the DESeq2 method explicitly requires untransformed data, no transformation of the data was carried out.

For ordination (DCA, CCA), species abundances were transformed using the Hellinger method (i.e.: for a species abundance **i** at site **j**, Hellinger transformation equals the square root of the quotient given by species **i** abundance at site **j** divided by total abundance for site **j**). The Hellinger transformation reduces differences in order between very rare and very abundant species which can 'unfairly' weight community composition (Ramette, 2007). Hellinger transformation was carried out using vegan's decorana package, and managed using phyloseq. Ordination was carried out using phyloseq and vegan.

Sequence data for this study was submitted to the ENA database under accession number PRJEB26863 and are accessible at the URL http://www.ebi.ac.uk/ena/data/view/PRJEB26863.

3. Results and Discussion

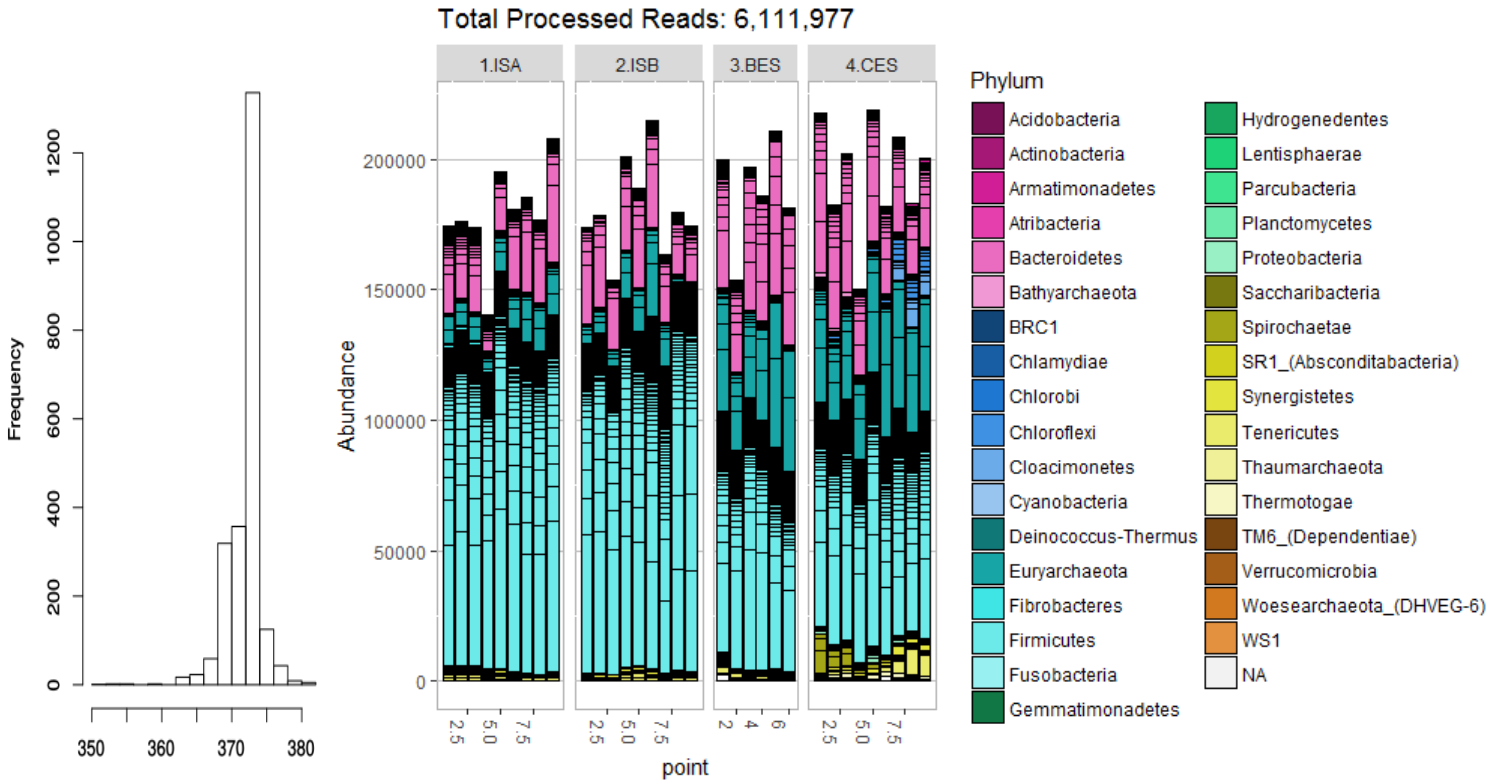

***Figure 2**: (A) histogram of ASV sequence lengths, illustrating the majority of ASVs were above the threshold of 350bp. (B) Stacked bar chart of processed reads per sample, coloured by phylum.*

3.1 Sequencing output and processing

From the 33 samples, 10.6 million reads were produced, giving 321,000 ±78,000 reads per sample. Once processed in DADA2, this contracted to 6,114,729 sequences in total, assigned to 2,444 unique amplicon sequence variants (ASVs). Although 2,444 unique ASVs were detected, 144 of these were below a threshold amplicon length of 350bp (Figure 2) and were assigned as 'unknown' or eukaryotic taxa of no identity. These ambiguous reads were removed, leaving 2,300 ASVs. Thus the final dataset

consisted of 2,300 ASVs, totalling 6,111,977 reads with an average of 185,295 (±19,764) reads per sample.

For convenience, community profiles are often subject to minimal arbitrary abundance cut-offs, removing ASVs (or OTUs) whose occurrence is too intermittent to be informative. For the purposes of displaying and discussing gross community composition (e.g. Figures 5, 8), ASVs were combined to 'Other' if their abundances were below 1% overall. This greatly reduced the number of ASVs being considered to 37 (4,815,987 reads), while 'Other' comprised between 15-25% of a sample (total 2263 ASVs, 1,295,990 reads).

3.2 Microbial Community Overview

A graphical overview of community diversity is provided in Figure 3, and an overview of relative abundances is provided in Figure 5. The major community components across all samples belonged to phyla *Firmicutes* (73-44%), *Bacteroidetes* (26-17%), and *Euryarchaeota* (22-7%). *Firmicutes* and *Bacteroidetes* presented a huge diversity of taxa (1425 and 195 ASVs respectively), in keeping with observations that these clades are typical, if not central to biogas setups (St-Pierre and Wright, 2013; Sundberg *et al.*, 2013). A further 2-12% represent 31 smaller phyla contributing 638 ASVs. Although variable, diversity in the *in situ* samples was expected to be relatively high due to the high nutrient and microbial load of the rich grass-based feedstock; while *ex situ* digestion is tailored to thermophilic, with minimal nutrient conditions to encourage autotrophic methanogenesis, and might be expected to support a community of reduced complexity. However, as can be seen here and as has been previously reported (chapter 3; Kougias *et al.*, 2017) it is clear that *ex situ* conditions can in fact

support as much, if not more diversity than *in situ* conditions. In this study, CES showed the highest diversity (observed ASV >500/sample; Shannon Index H': >3.4; Inverse Simpson Index D1: >11, Figure 3), indicating complex communities are encouraged even in these niche environments. ISA, ISB and BES cover lower ranges of ASV observation: 450-320/sample, with ISB showing the lowest sequence diversity, possibly due to a decreased evenness of abundance related to VFA accumulation and reactor stress.

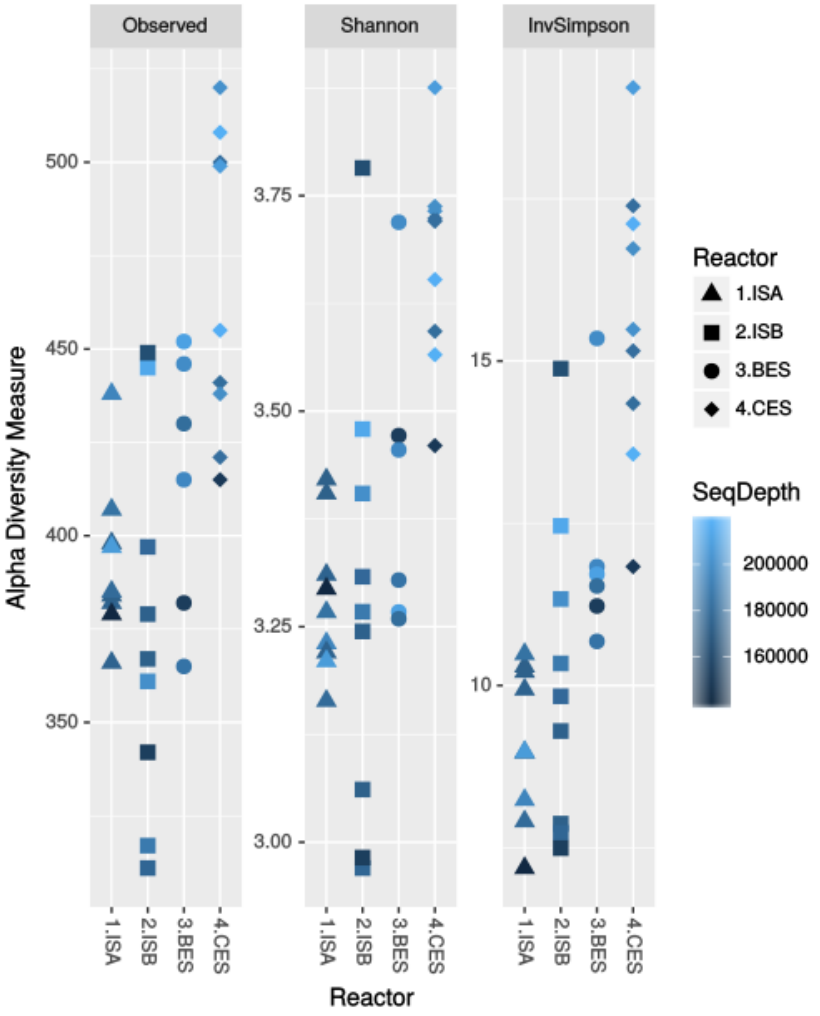

Figure 3: *Community diversity indices: Observed: number of unique ASVs per sample; Shannon Index: measure of ability to predict a random observation (i.e. richness); Inverse Simpson's Index: inverse of probability that two observations are of different species (sensitive to abundant species and evenness). In all cases, higher values indicate greater diversity.*

3.3 Detrended Correlation Analysis

Community composition from *in situ* and *ex situ* setups was explored through Detrended Correlation Analysis (DCA). DCA allows relationships between samples and relationships between species to be simultaneously visualised, and can reveal factors underlying community composition (i.e. indirect gradient analysis).

There was a positive relationship between the number of observed ASVs and number of reads per sample (Figure 3). DCA was used to rule out undue influence of sequencing depth on 16S community profiles, by overlaying community similarity with 16S sequencing depth (i.e. reads, Figure 4). Timepoints show no clustering by sequence depth, indicating community composition is more strongly informed by experimental factors than by sampling effects.

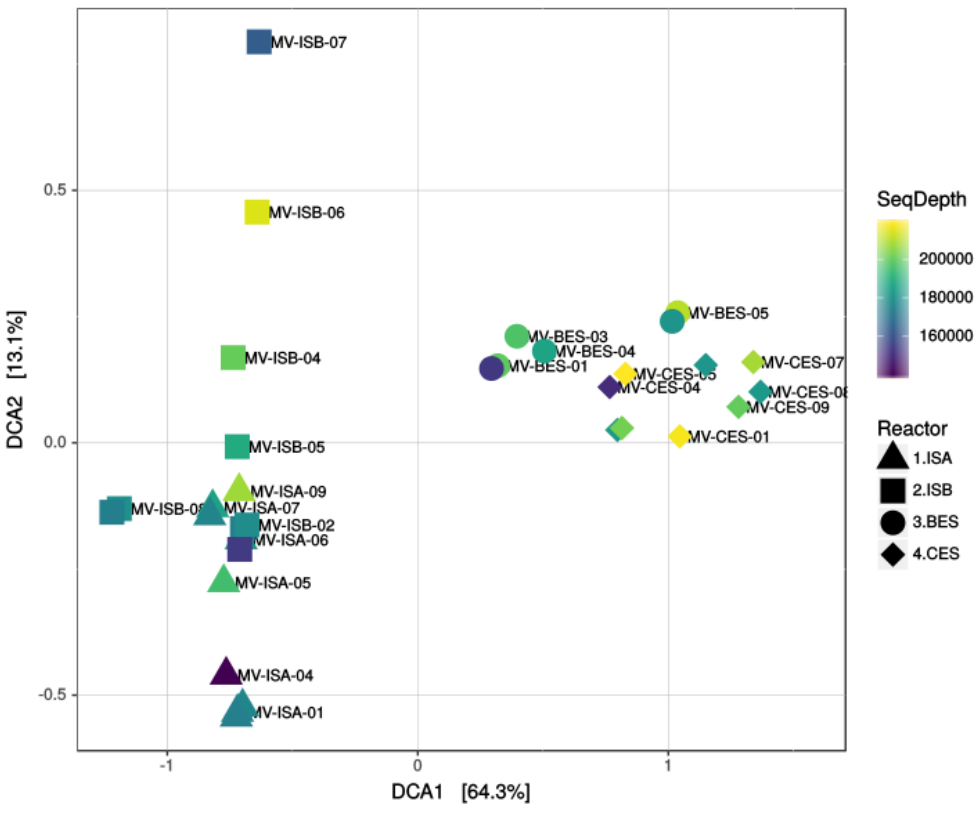

Figure 4: Detrended Correlation Analysis of community structure (under Hellinger transformation). *Reactor operation strongly influenced community composition, with clustering of related setups (X axis). Note also progression of samples on Y axis from ISA commissioning to failure of ISB, as well as a lack of separation in ex situ setup indicative of relative stability. Colouration reflects total number of reads per sample, illustrating a lack of interaction between coverage and structure.*

Samples in this study were well differentiated by reactor conditions, as shown by strong within-reactor clustering of samples (Figure 4). *In situ* samples differentiate along the Y axis (13% of variance in community composition), while batch and continuous *ex situ* samples align along the X axis (63% of community variation). This separation of samples accurately reflects both differences in reactor setup and variability during the study. ISA timepoints 1-3 segregate during commissioning of the reactor seed sludge, followed by clustering of 'established' *in situ* samples, culminating in a gradual decline of late ISB (timepoints 8 and 9) when reactor failure occurred, during high concentrations of VFAs. In contrast, *ex situ* timepoints diverge from the community patterns established *in situ*, leading to further clusters of *ex situ* timepoints, possibly reflecting increasing levels of H_2 flow. Notably, differentiation between *in situ* and *ex situ* represents the major source of community variation between timepoints (63%), indicating that reactor configuration is the strongest force shaping community composition.

Notably, ISB 6 and 7 diverge further from the main *in situ* cluster than timepoints from late reactor failure (ISB 8 and 9). Based on the emphasis provided in Figure 4, this is not due to differences in depth of sequencing. Rather, this is likely a period of transition in community structure highlighted by the Hellinger transformation which emphasises composition of minor populations. Although no according change in population abundances is visible in Figure 5, Supplementary Figure 5.1 (Appendix A) shows a large grouping of other/minor abundance ASV which increase between timepoints ISB 4-7. This turnover in community structure may be a symptom of reactor inhibition, where various low abundance taxa are able to capitalise on changes in substrate availability or composition. The influence of this compositional shift on reactor performance is not known, but is followed by the large

shift in community structure and reactor failure seen in ISB 8 & 09 where methanogen abundance is displaced by fermenters.

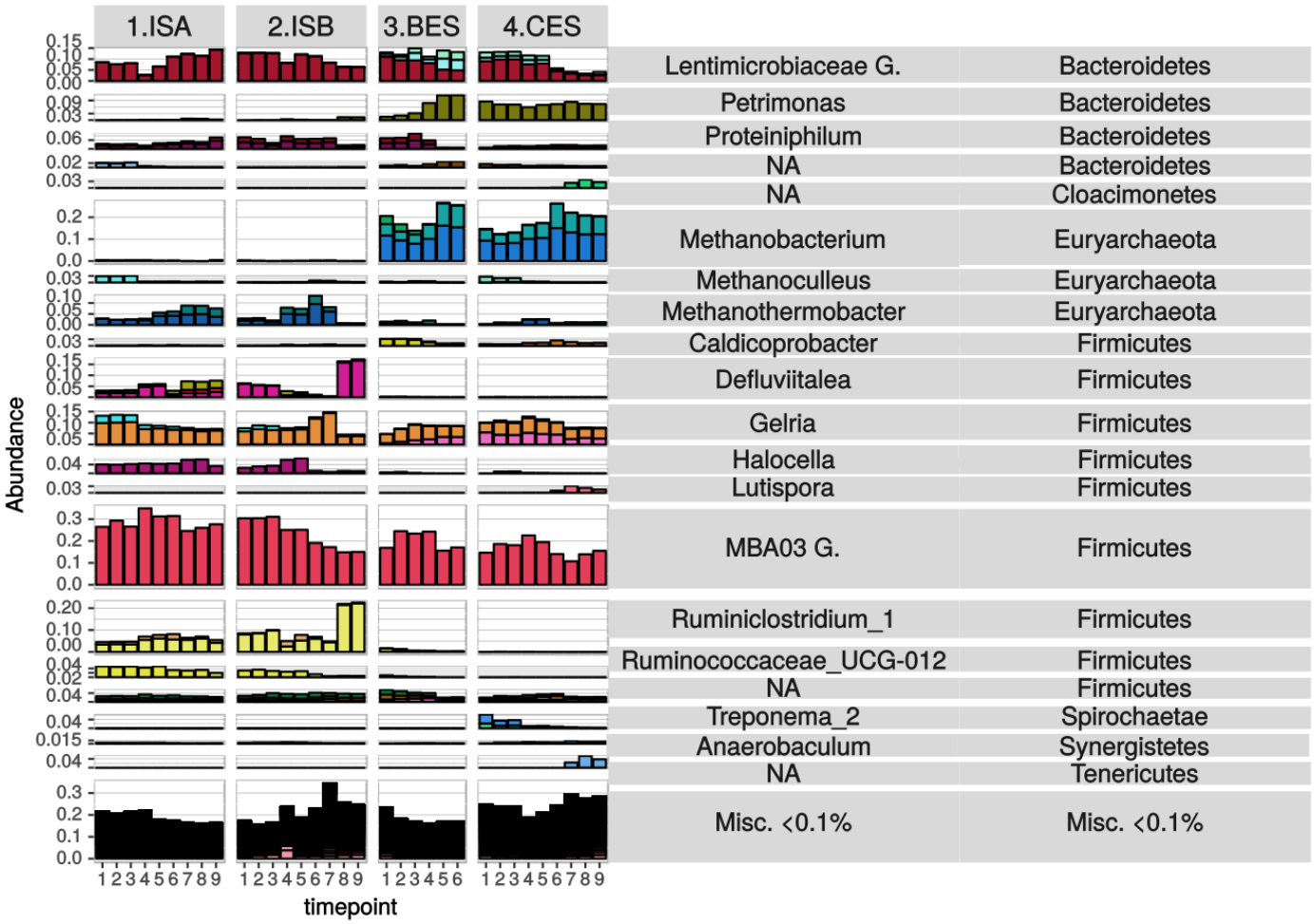

Figure 5: *Relative abundances of major ASVs (>1% sample abundance in 3 or more samples). Each coloured cell represents a single ASV population (e.g. MBA03 = 1 ASV population; Gelria = 3 ASV populations). Note variability of scale in the Y axis (% relative abundance) to improve visibility. ASVs <1% relative abundance (15-34% of sample abundances) have been omitted for clarity but are presented in Appendix A.*

3.4 Differential Abundance

The strong differentiation of timepoints with respect to reactor setup (Figure 4) indicates significant differences between *in situ* and *ex situ* populations caused by major differences in feedstock input (i.e. grass, grass & gas, gas only). To better understand how specific microbial populations facilitate biogas upgrading, Differential Abundance (DA) testing was used to compare differences in reactor setup with changes in ASV abundance, highlighting significant interactions between process and microbiology. Unless noted, all differences discussed below were found to be statistically significant between the *in situ* and *ex situ* timepoints (p-value=0.01, adjusted p-value=0.01).

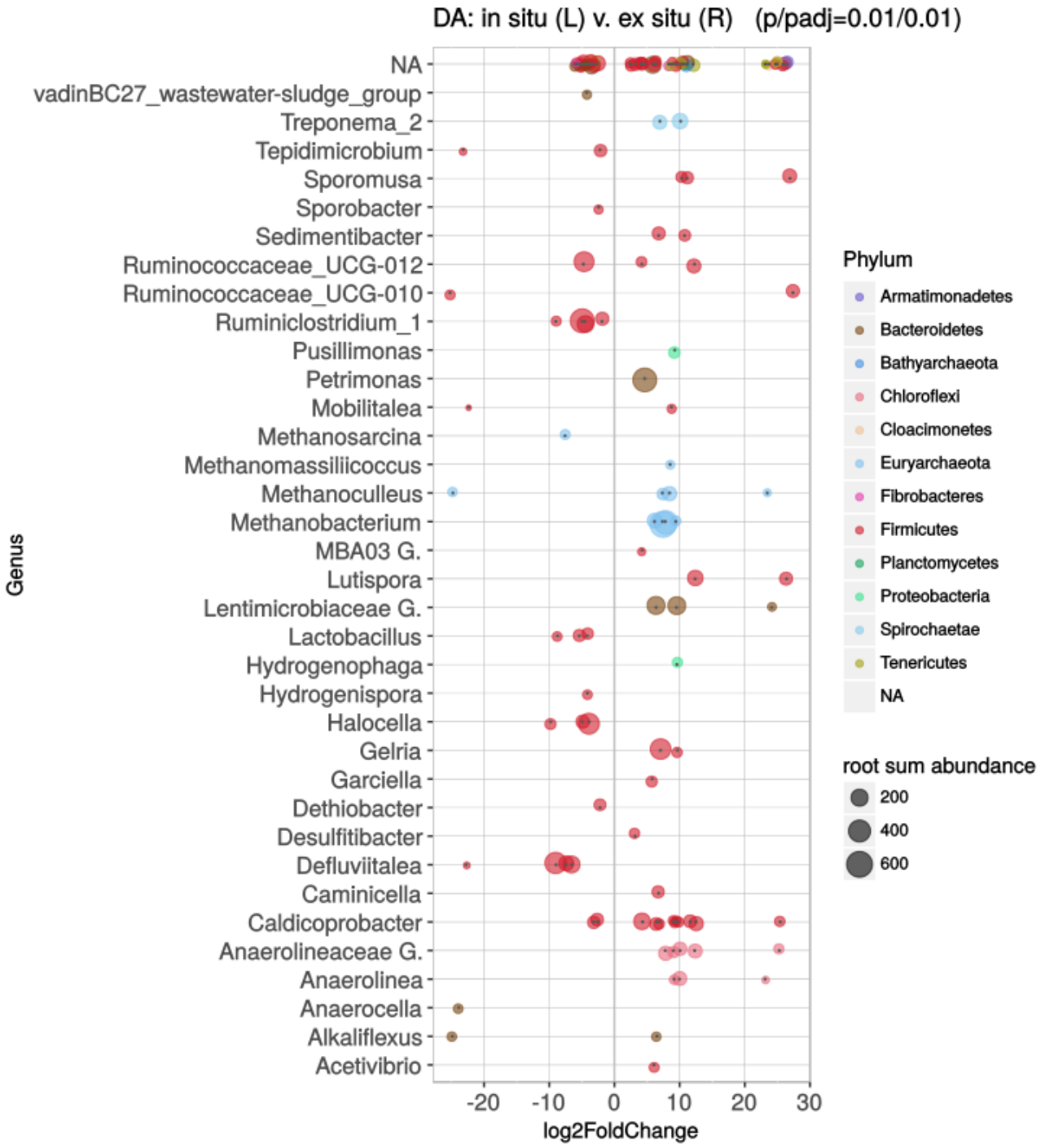

Figure 6: *ASVs detected as significantly differentially abundant between in situ and ex situ conditions, with the average change in abundance between either setup represented as log_2 fold-change (i.e. increase from 2 to 8 = log_2 fold change of 3). Taxa uncharacterised at genus-level ("NA") are presented in Appendix A, Figure 5.*

3.4.1 Differential Abundance: Archaea

Perhaps the strongest distinction between *in situ* and *ex situ* timepoints was the differing abundances of methanogenic Archaea (Figure 7). *In situ* reactors saw rising abundances of *Methanothermobacter* (mvsv0008, mvsv0017, mvsv0043, mvsv0401; Appendix D) during operation, while upgrading hydrogen flow rates increased from 0L/day to 57L/day at lower H_2 solution efficiencies (ISA), and 0L/day to 37L/day at improved H_2 solution efficiencies (ISB). *Methanothermobacter* is a filamentous hydrogenotrophic methanogen which grows rapidly on CO_2 and H_2 with mineral media (Wasserfallen *et al.*, 2000; Oren, 2014). *Methanothermobacter* abundances peaked in ISB7 (15%), before dropping to ~1% during reactor failure in ISB 8 & 9, and maintained ~1% abundance in *ex situ* conditions. It is not clear whether this population "crash" at ISB 8 & 9 represents inhibition due to competition, hydrogen concentrations, or high VFA levels. The latter seems unlikely as VFA levels were highest on ISB 7 (peak *Methanothermobacter* abundance), and populations did not recover in BES and CES despite reduced VFA levels and the taxon's persistence in the reactor. In support of a competition-based explanation, populations of *Defluviitalea* and *Ruminiclostridium* (acetogenic saccharide and polysaccharide hydrolysers, discussed later) rose markedly over the same two timepoints as abundance of *Methanothermobacter* collapsed. Although changes in *Methanothermobacter* abundance were not found to be statistically significant between setups, visible abundance *in situ* and absence elsewhere strongly suggests an association with anaerobic digestion of feedstock. However, disappearance of *Methanothermobacter* in ISB 8 & 9 does not appear to affect VFA accumulation, which suggests *Methanothermobacter* metabolism focused on autotrophic methanogenesis (i.e. biogas upgrading) rather than methanogenesis via syntrophic acetate oxidation (SAO). In this light, its co-occurrence with feedstock (i.e. *in situ*) is interesting and suggests a reliance on additional factors.

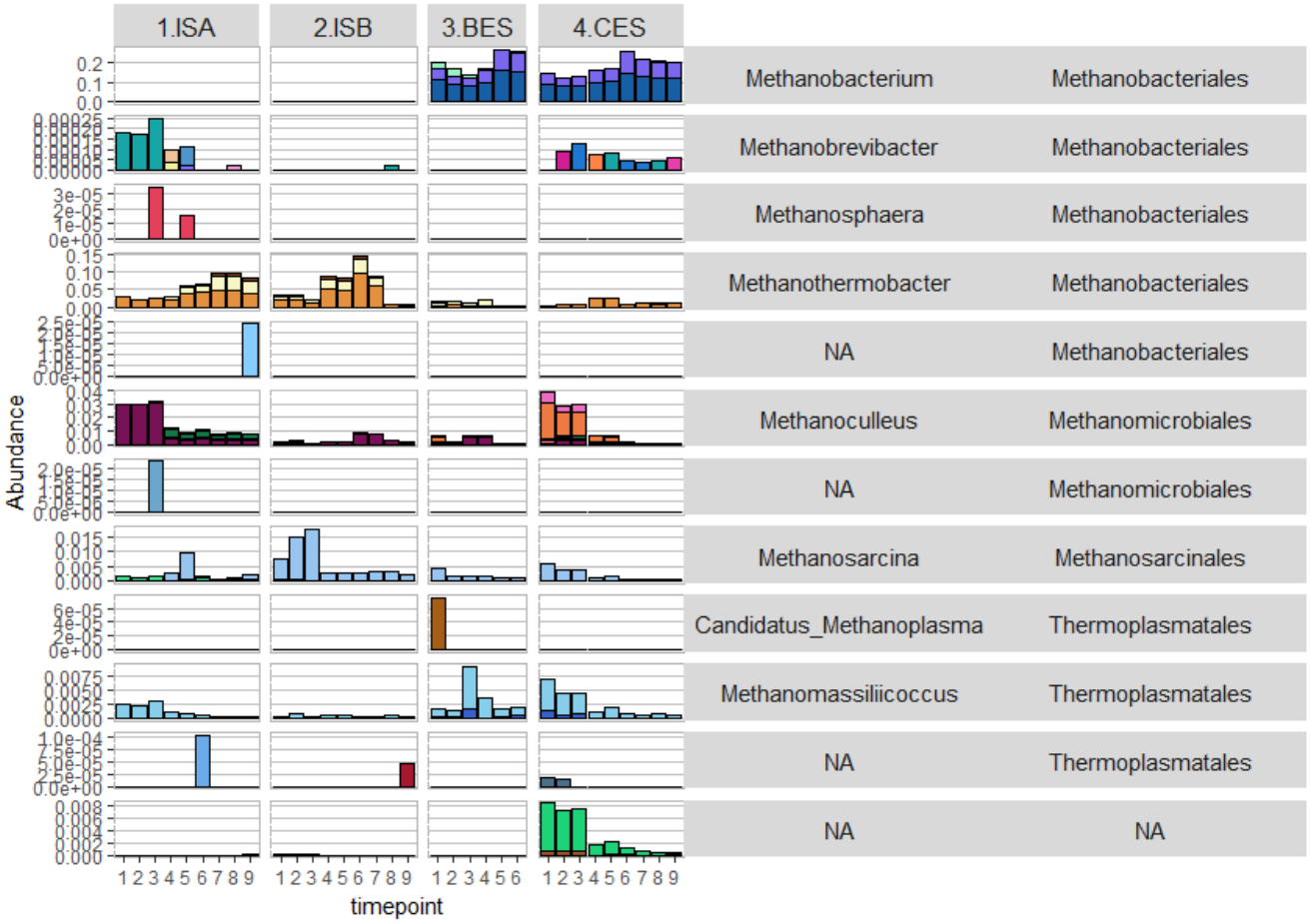

Figure 7: *Relative abundance of all archaeal ASVs. Each coloured cell represents a single ASV population over the trial duration (e.g. Methanomassiliicoccus = 2 ASV populations; Methanoplasma= 1 ASV population). Note variability of scale in the Y axis (% relative abundance) to allow visualisation.*

Ex situ reactors saw strong, stable populations of Euryarchaeota throughout operation: 21-22% in ES versus 7-8% in IS. In particular, two consistently abundant *Methanobacterium* populations (mvsv0004, mvsv0007; Appendix D) increased over the course of BES & CES operation (10-25%) and were significantly associated with *ex situ* operation. *Methanobacterium* is another filamentous hydrogenotrophic methanogen, with a similar rapid growth under CO_2+ H_2 and mineral media to that of *Methanothermobacter. Methanobacterium* also responds positively to supplementation of the

growth culture (yeast extract, cysteine, cobalamine) (Oren, 2014). A decrease in abundance in later CES samples may reflect the decrease in gas flow carried out to reduce VFA accumulation, suggesting this is the target *ex situ* upgrading population, relying on metabolism of exogenous H_2/CO_2. However, as greater relative abundances were seen in BES under lower gas flow rates (40L/day versus ~259L/day), it is likely that additional factors are involved.

Other methanogenic taxa (hydrogenotrophic *Methanoculleus*, *Methanomassiliicoccus*, *Methanobrevibacter*; acetoclastic *Methanosarcina*) remained at low or intermittent abundances (<4%) (Figure 7)**.** A minor note is the appearance of *Methanoculleus* at two disparate points in reactor operation: initiation of ISA, and of CES. The reason for the recurring appearance and disappearance is puzzling, but as *Methanoculleus* is a frequent meso/thermophilic bioreactor isolate with a well-documented requirement or response to additional factors, this may reflect syntrophic association with mass feedstock breakdown at reactor inceptions.

3.4.2 Differential Abundance: Bacteria

The second major trend in community composition is the lower proportion of Firmicutes *ex situ*, decreasing from 72-73% *in situ* to 44-47% *ex situ*. This can be seen in Figure 5 (*Ruminoclostridium*, MBA03, *Defluviitalea*, *Halocella* etc.), and in Figure 6, where the greater proportion of *Firmicutes* taxa associate with *in situ* conditions. Given the role of *Firmicutes* as hydrolysers and degraders of polymers and the lack of digestable feedstock *ex situ*, this is perhaps unsurprising: nonetheless, the decline in abundance of several specific *Firmicutes* ASVs are worth noting.

The most abundant taxon overall belongs to a single large ASV population assigned to the uncharacterised MBA03 order (10-35% of relative abundances). MBA03 is one of a number of unknown *Firmicute* clones previously obtained from thermophilic sludge in anaerobic digestion (Tang *et al.*, 2004), which matches well with its presence in these samples and the current lack of characterisation. However, the sequence derived from the MBA03 population in this study (mvsv0001; Appendix D) shows only 90% identity with reference MBA03 sequences (www.arb-silva.de, Pruesse *et al.*, 2012), which at the time of writing is a grouping of +2000 uncharacterised representative sequences. As a result, the MBA03 ASV encountered in this study is impossible to assign beyond Order level. Sequences assigned to MBA03 have represented a major community member in related AD setups involving thermophily and upgrading (chapters 2 and 3; Bassani *et al.*, 2017; Kougias *et al.*, 2017; Rago *et al.*, 2018). Maintenance of a single large population with 100% sequence identity suggests highly successful niche exploitation, and it is assumed to have a central role in reactor metabolism in both upgrading setups. The assignment of MBA03 to *Clostridiales*, prevalence in AD, and persistence both *ex situ* and *in situ* suggests a role in end-stage fermentation rather than direct hydrolysis. Although MBA03 was not significantly associated with either setup, abundance *in situ* appeared elevated until the latter half of ISB, (possibly a response to increased hydrogen flow or accumulating VFA).

Many (75) other *Firmicutes* ASVs are differentially abundant between *in situ* and *ex situ*, with many of these populations also fluctuating between different hydrogen flow rates. *Defluviitalea* and *Ruminiclostridium* show matching trends of abundance in *in situ* reactors, both spiking in ISB 8 & 9 (from 3-5% to 15-20%), during a period of hydrogen upgrading, pH decline, VFA accumulation, and reactor failure. Both genera are saccharide-fermenting acetogens (Ben Hania *et al.*, 2012; Yutin and

Galperin, 2013), while *Ruminoclostridium* is also a notable degrader of polysaccharides (cellulose, starch), suggesting a role in feedstock degradation. *Methanothermobacter* declines sharply at the same time-points wherein *Defluviitalea* and *Ruminiclostridium* peak in abundance, while Figure 5 shows the decline of several other taxa such as *Gelria* and *Proteiniphilum* at the same timepoints, with co-segregation of timepoints ISB 8&9 in Figure 4 illustrating a large shift in community structure, including changes in lower abundance populations. This change in community structure during ISB may reflect a shift in hydrogen use from methanogenesis to acetogenesis. Autotrophic homoacetogenesis ($H_2 + CO_2 \rightarrow CH_3COOH$ ΔG^o=-104; Conrad and Wetter, 1990) is distinct from heterotrophic acetogenesis as seen in the fermentation of celluloses etc. by a consortium, and can be carried out by a single population through reversal of the Acetyl-CoA pathway (Ferry, 1992; Ragsdale and Pierce, 2008). In general, the hydrogen concentration thresholds required for acetogenesis are much higher (i.e., hydrogen must be more abundant) than those required by methanogens, allowing methanogens to outcompete homoacetogens in AD, thereby keeping hydrogen partial-pressure (pH_2) low enough to facilitate biomass degradation (<100Pa H_2; Conrad, 1999; Thauer *et al.*, 2008). Although homoacetogens have higher H_2 thresholds than methanogens, at sufficient H_2 concentrations (>200Pa) a higher maximal kinetic rate (Vmax) allows slower-growing methanogens to be outcompeted (Kotsyurbenko *et al.*, 2001). There are also indications that acidic conditions allow homoacetogens to outcompete methanogens (Drake *et al.*, 2013). In timepoints ISB 8 and 9, H_2 was being supplied exogenously at a rate of 37L/day: this likely exceeded acetogenic threshold values (≥100Pa H_2), providing an opportunity for homoacetogens to proliferate. Additionally, pH decreased notably from 9.1 in ISB6, to 8.4 in ISB7, to 7.6 in ISB 8 & 9 (see Figure 1A). Autotrophic fixation of carbon (hydrogenotrophic methanogenesis, homoacetogenesis) could reduce the reactor buffering

capacity by removing dissolved CO_2 (i.e. bicarbonate) leading to a decrease in pH. A rapid decline in pH and increase in acetogenic bacteria could indicate excess homoacetogenesis at these timepoints, with the resultant pH change influencing community composition. However, there is no increase in acetate levels specific to ISB 8 & 9 (Figure 1B), suggesting instead that homoacetogenesis was contributing to VFA accumulation for a longer time period (e.g. ISB 4-9). In this case, a sudden drop in pH (ISB 8 & 9) could instead reflect saturation of the reactor buffering capacity followed shortly by a lack of methanogenesis and reactor failure.

Between timepoints ISB 5 and ISB 9, *Halocella* and UCG-012 (*Ruminococcaceae*) also show simultaneous declines in abundance from 7 and 3% to 1 and 0.6% respectively, suggesting similar responses to the same conditions. Although UCG-012 is uncharacterised, placement in the *Ruminococcaceae* implies a role in cellulose degradation and acetate production (Yutin and Galperin, 2013), while *Halocella* is a known acetogenic cellulose degrader (Simankova *et al.*, 1993). Reasons for inhibition are unclear, but again may correspond to increases in VFA, decreases in pH and reduced buffering capacity.

A third difference between *in situ* and *ex situ* is the slightly greater proportion of *Bacteroidetes* in ES: 21-27% versus 17% *in situ*. *Proteiniphilum* is a protein degrading acetogen common across *in situ* reactor samples (1-2%), but which declines in BES to lower levels (0.5-1%). Several taxa obscured *in situ* develop into larger populations *ex situ*; in particular the abundance of *Petrimonas* (a saccharide degrading acetogen) seems to replace *Proteiniphilum*, to which it is closely related (Chen and Dong, 2005; Grabowski, 2005). *Lentimicrobiaceae* (saccharide fermenting acetogens) showed variable abundance across all reactors, with abundance decreasing in CES.

3.5 *Ex situ* comparison: BES v CES

Comparison of *in situ* and *ex situ* communities illustrates the importance of large methanogenic populations, as well as the decreased emphasis on hydrolysing and fermenting bacteria when biomethanation is isolated from AD. Inhibition of VFA catabolism can arise from high hydrogen concentrations (Fukuzaki *et al.*, 1990; Siriwongrungson *et al.*, 2007), but the community dynamics involved are as yet unknown. In an industrial context, *ex situ* upgrading is likely to be used in continuous process, with high gas flow rates. Contrasting batch and continuous operation offers insight into taxa encouraged (or discouraged) by such intensive conditions, exploring the requirements for long term continuous *ex situ* upgrading. To highlight the difference between batch and continuous *ex situ* upgrading communities (i.e. BES and CES; Figure 8), further DA was carried out using BES as a 'basic' case of *ex situ* upgrading (i.e. batch operation).

181 taxa show DA between BES and CES: however, the mean abundances of all such taxa are within 0-4%, therefore the change from batch to continuous upgrading does not appear to greatly alter the microbial community despite the increase in gas flow rate from 40-100L/day to 80-400L/day. For instance, although some methanogen ASV populations (*Methanobacterium*; ASV ID: mvsv0017, *Methanothermobacter;* ASV ID: mvsv0035; Appendix D) are differentially abundant between CES and BES (0.2-3% abundance), they are overshadowed by the two *Methanobacterium* ASVs which are highly abundant in both cases (15-25%, discussed in section 3.4.1), characteristic of *ex situ* conditions in this study.

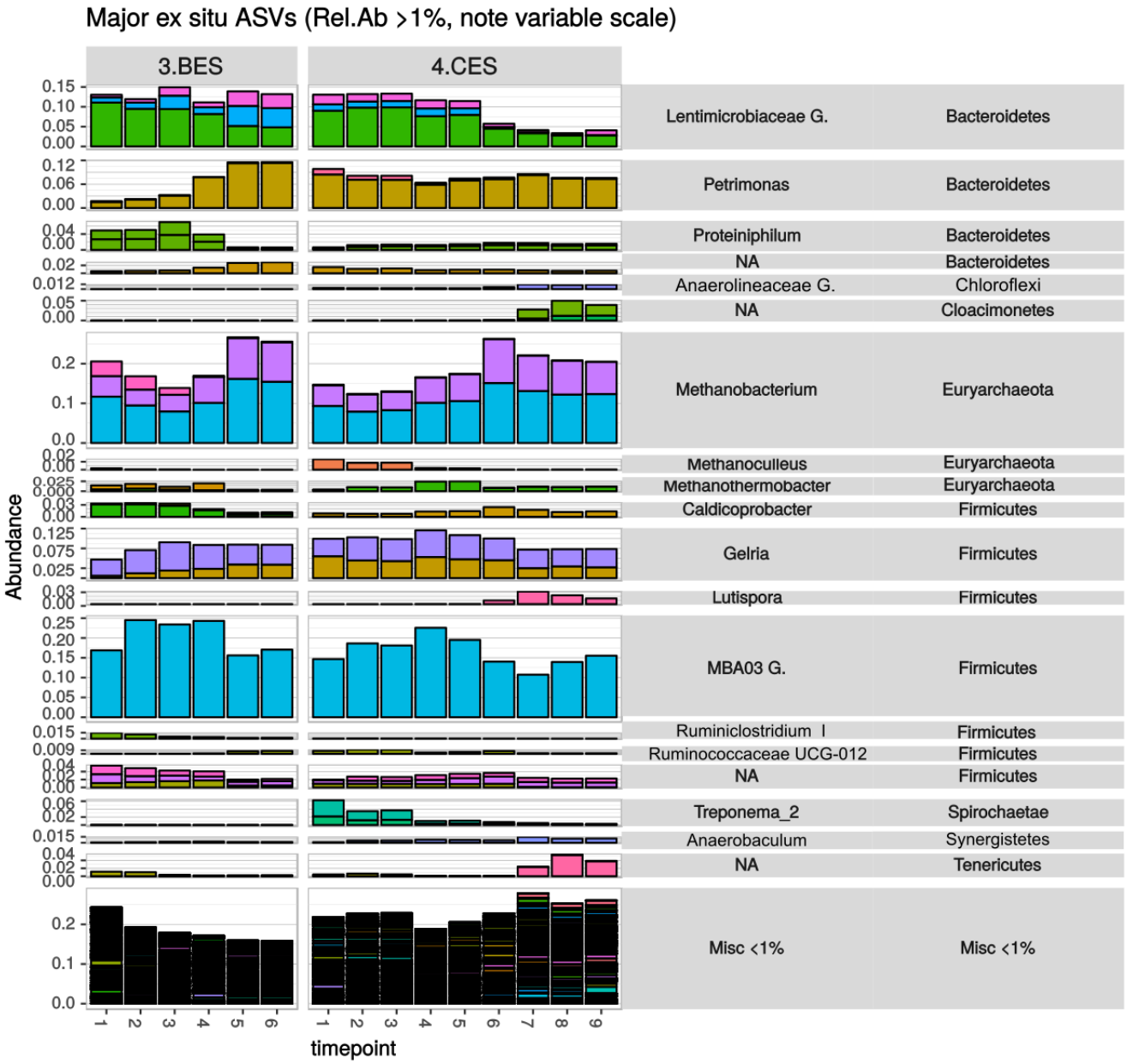

Figure 8: *Relative abundances of major ASVs ex situ (>1% sample abundance in 3 or more samples). Each coloured cell represents a single ASV population (e.g. Gelria = 2 ASV populations; Lentimicrobiaceae genus= 3 ASV populations). ASVs <1% relative abundance (15-34%) have been grouped to 'Misc.' at base. Note variability of scale in the Y axis (% relative abundance) to improve legibility.*

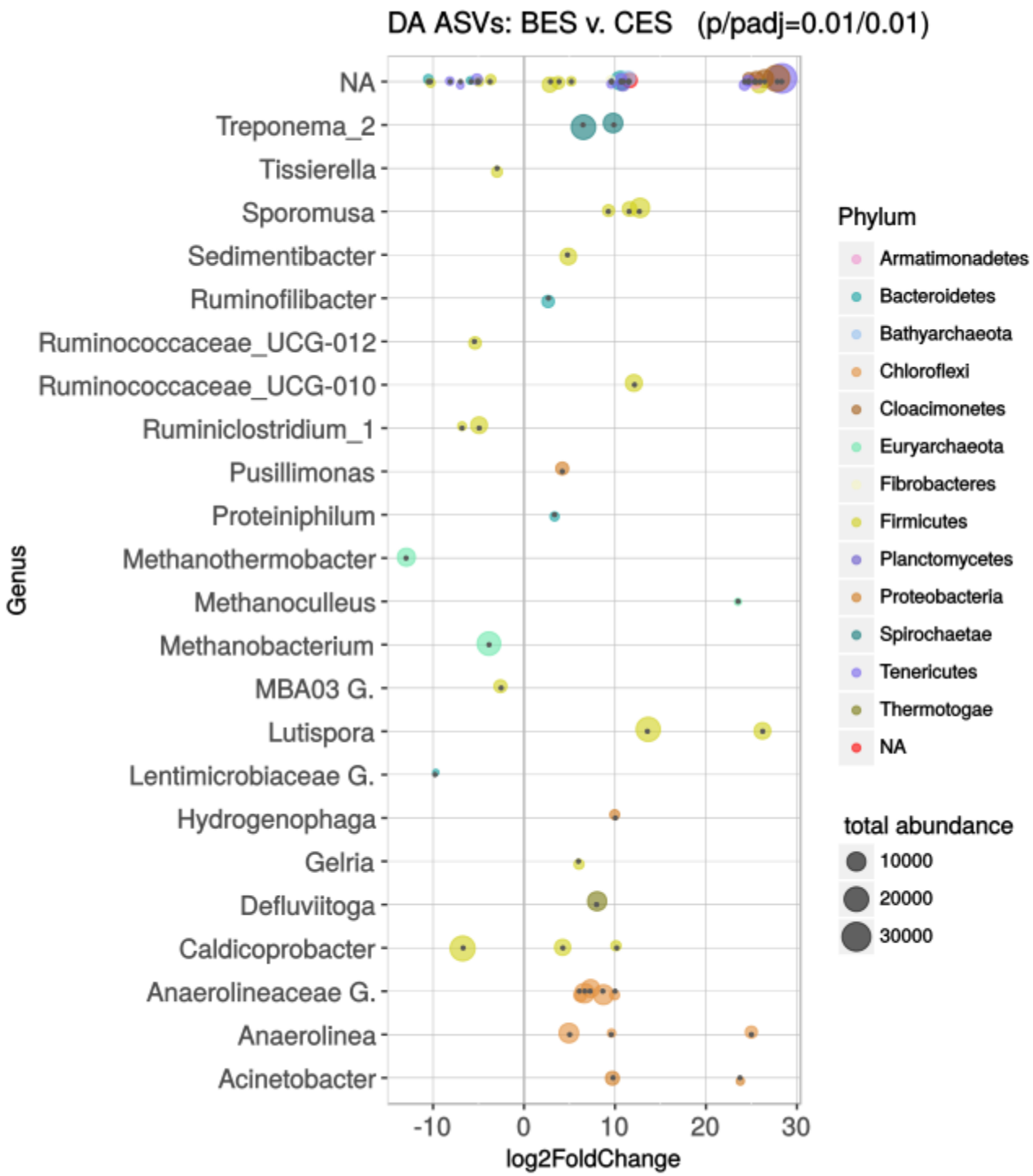

Figure 9: *ASVs detected as significantly differentially abundant between BES and CES conditions, with the average change in abundance between either setup represented as log_2 fold-change (i.e. increase from 2 to 8 = log_2 fold change of 3). Taxa uncharacterised at genus-level ("NA") are presented in Appendix A.*

Similarly, many taxa present in CES had an abundance of zero in BES, artificially inflating the log2 fold-change (Figure 9), despite small changes in read (actual) abundance. Several of these CES-specific taxa belong to *Firmicutes* (*Gracilibacteraceae*, *Caldicoprobacteraceae*, *Veillonellaceae*, *Thermoanaerobacteraceae*), representing known broad-spectrum fermenters, with abundances up to 4%. Although abundances are low in individual ASVs, there is an overall trend in CES for proliferation of homoacetogenic and hydrogen-producing populations: *Sporomusa* (homoacetogen and trimethylamine producer: Möller *et al.*, 1984), *Treponema* (homoacetogens best characterised in hydrogenotrophic syntrophy with intestinal termite fungi: (Dröge *et al.*, 2008; Drake *et al.*, 2013), *Hydrogenophaga* (hydrogenotrophic facultative anaerobe and homoacetogen; Willems *et al.*, 1989) and several members of *Anaerolineaceae* (hydrogen-producing obligate syntrophs: Sekiguchi, 2003). A number of uncharacterised bacteria also show higher abundance in CES, in particular clusters of uncharacterised *Cloacimonetes* (W5) and *Mollicutes* (group NB1-n) (Appendix A; Supplementary Figure 5:3). The candidate phylum *Cloacimonetes* is poorly characterised, but metagenome assembly suggests production of hydrogen in acetogenic amino acid degradation (Pelletier *et al.*, 2008). The uncharacterised NB1-n *Tenericutes* clade is known from methane seeps, and based on metagenome assembly is a fermenter of simple sugars, acids, and amino acids, and can oxidise reducing equivalents to produce hydrogen (Skennerton *et al.*, 2016). It is surprising that a hydrogen-saturated reactor encourages hydrogen-producing microbial populations, as thermodynamics suggests this environment would be inhibitive. However, enrichment for hydrogen producing taxa (*Anaerolineaeceae*, *Sporomusa*, *Mollicutes:* NB1-n, *Cloacimonetes:*W5) is greatest in CES 7-9, where such taxa increased to 13-19% of total reactor abundance. At these timepoints, hydrogen flow rates

were reduced from 403L/day to 259L/day, and these increased abundances may reflect fermenting populations expanding to fulfil the hydrogen requirements of *Methanobacteriales*. Development of large methanogen populations may also have encouraged 'satellite' syntrophic populations reliant on autotrophs to maintain thermodynamic potential for fermentation and acetogenesis. This arrangement would benefit methanogens when exogenous H_2 is limiting, allowing continued methane production, much as in standard AD.

3.6 Correlation Heatmap

To better characterise taxa interactions over the course of the study, a correlation matrix was formed of a subset of taxa abundances (i.e., taxa with abundance >2% in more than three samples (i.e. Figure 5) and taxa that were differentially abundant between *in situ* and ex situ (i.e. Figure 6). This identified two opposing clusters representing the strongest ASV-ASV correlations *in situ* and *ex situ* (Figure 10).

Clustering of abundant *ex situ* taxa grouped *Methanobacterium*, *Lentimicrobiaceae*, *Petrimonas*, *Gelria*, NB1-n, and W5 together based on shared strong correlations (R=0.75-1.0) with methanogens (*Methanobacterium*, *Methanoculleus*), acetogens and hydrogen-formers(*Caldicoprobacter*, *Anaerloineaceae*, *Pusilimonas*, *Acetevibrio*, and *Gelria)*.

Clustering of taxa abundant *in situ* grouped *Methanothermobacter* and *Methanoculleus* with a Clostridia cohort (MBA03, *Ruminococcaceae*, *Gelria*, *Defluviitalea*, *Halocella*). While *Methanothermobacter* abundance was correlated with NB1-n (uncharacterised hydrogen producer), *Claldicoprobacter*, *Halocella*, and *Ruminoclostridium* (R=0.73-0.80), the larger *Clostridia* cohort formed a cluster of stronger correlations (as high as R=0.94) with numerous other *Clostridia (Ruminoccaceae*,

Dethiobacter, *Tepidimicrobium*, *Caldicoprobacter*, *Defluviitalea*, *Halocella*, *Lactobacillus*, *Hydrogenispora*,) and other bacteria (*Anaerocella, Fibrobacteraceae, Porphyromonadaceae)*.

The unsupervised clustering of taxa into *in situ* and *ex situ* groups re-iterates how strongly the microbial communities were differentiated as a result of differences in operation. It is particularly interesting to note the relatively sparse association of *Methanothermobacter* with fermenting taxa, possibly suggesting a greater independence through autotrophy. In contrast, *Methanobacterium* clusters more deeply within the *ex situ* cohort due to stronger associations with other taxa, while the cohort also shows stronger correlations with other methanogens (*Methanoculleus, Methanomassiliicoccus*) and bacteria (*Acetivibrio*, *Lentimicrobiaceae*, *Gelria*, *Caldicoprobacter, Anaerolinea*), as well as several uncharacterised taxa (R=0.73-94). This may reflect common niches in reactor function, and/or larger community shifts in response to decreased H_2 flow as detailed above.

Fi

Figure 10: *Correlation heatmap of major taxa (>1% abundance) and differentially abundant taxa. Note segregation into two opposing clusters, as highlighted by respective positive (yellow) and negative (blue) associations.*

:u Setups

In addition, two smaller cohorts were observed in the correlation heatmap: *Cloacimonetes*: W5 and *Mollicutes*: NB1-n (R=0.7-0.80), and *Gelria* and *Treponema* (R=0.66-0.82) which form adjacent clusters with a range of correlated taxa (*Clostridia, Mollicutes:* W5*, Cloacimonetes:* NB1-n*, Caldicoprobacter, Anaerolineaceae* and *Lutispora; Anaerolineaceae, Sporomusa, Gelria, Hydrogenophaga, and Treponema respectively*) discussed above as producers and consumers of hydrogen. This may represent a cluster of taxa involved in non-target hydrogen metabolism, producing acetate (*Sporomusa, Treponema*) from exogenous and endogenous hydrogen (*Caldicoprobacter, Anaerolineaceae, Gelria* etc.).

Finally, the differentiation between *in situ* and *ex situ* microbial communities is further supported by corresponding negative correlations between *in situ* and *ex situ* cohorts (coloured in blue), showing that taxa positively correlated with one setup tended to correlate negatively with taxa abundances from the alternative setup (Figure 6). This indicates that although there are a large number of uncorrelated or unassociated taxa, the different setups lead to distinct communities which comprise the abundant majority in either case.

4. Conclusions

Methanobacteriales are the strongest candidates for biomethane upgrading in this study. More specifically, in the setups profiled, *Methanothermobacter* was the dominant methanogen *in situ*, while *ex situ* biomethanation selected strongly for *Methanobacterium*. The most obvious cause for this dichotomy is digestate decomposition in ISA/ISB, which either provided required factors for *Methanothermobacter,* or in concert with VFA accumulation produced an environment where *Methanobacterium* was unable to compete. Although they are non-acetoclastic methanogens, some *Methanothermobacter* can incorporate acetate and formate as cellular sources of carbon (Wasserfallen *et al.*, 2000). Additionally, some *Methanothermobacter* taxa require or are stimulated by extra organic and inorganic factors for growth (Wasserfallen *et al.*, 2000; Oren, 2014), which could be supplied by feedstock. Availability of growth factors and abundant carbon sources could provide a competitive edge *in situ*. In particular, it is noted that *Methanothermobacter* showed an overall positive relation with VFA levels across ISA/ISB, notwithstanding a collapse in abundance during ISB 8&9 when the overall community profile shifted dramatically (Figure 4). This positive relation may reflect a tolerance or even affinity for elevated levels of organic acids, under certain conditions. *Methanobacterium*'s abundance in *ex situ* conditions indicates that it has a lower reliance on supplementation, as documented for some species of *Methanobacterium* (Wasserfallen *et al.*, 2000; Oren, 2014). However, response of *Methanobacterium* abundances to changes in hydrogen flow rate appear slow, which may reflect the aforementioned lack of stimulating factors, longer microbial cell doubling times, or hydrogen's limited solubility, a known issue for biogas upgrading. Increased abundance of hydrogen-producing fermenters (<1% to 13-19%) after gas flow rates were reduced (CES 7-9) indicates an increased demand for biological hydrogen. These diverse fermenting 'satellite'

populations may contribute to biogas output and serve to buffer methanogenic populations during disruptions in supply of H_2. If so, this represents a positive role for species diversity in upgrading setups.

Degradation of feedstock (i.e. *in situ* upgrading) is also attributed with causing instability at increased hydrogen flow rates, eventually leading to collapse of the methanogen populations and likely replacement by homoacetogenic metabolism. Supporting this conclusion, significant accumulation of VFAs was not seen in *ex situ* digestion despite the far greater volume of hydrogen supplied. As such, the relative stability of *ex situ* upgrading is attributed to a lack of feedstock hydrolysis. This highlights the unsuitability of *in situ* upgrading for high rate, industrial biogas upgrading, as the quantities of hydrogen required would represent an indirect but serious disruption to biomethane production *in situ*.

5. REFERENCES

1. 16S Illumina Amplicon Protocol : Earth Microbiome Project.

2. Bassani, I., Kougias, P.G., Treu, L., and Angelidaki, I. (2015) Biogas Upgrading via Hydrogenotrophic Methanogenesis in Two-Stage Continuous Stirred Tank Reactors at Mesophilic and Thermophilic Conditions. *Environ. Sci. Technol.* **49**: 12585–12593.

3. Ben Hania, W., Godbane, R., Postec, A., Hamdi, M., Ollivier, B., and Fardeau, M.-L. (2012) Defluviitoga tunisiensis gen. nov., sp. nov., a thermophilic bacterium isolated from a mesothermic and anaerobic whey digester. *Int. J. Syst. Evol. Microbiol.* **62**: 1377–1382.

4. Callahan, B.J., McMurdie, P.J., Rosen, M.J., Han, A.W., Johnson, A.J.A., and Holmes, S.P. (2016) DADA2: High-resolution sample inference from Illumina amplicon data. *Nat. Methods* **13**: 581–583.

5. Caporaso, J.G., Lauber, C.L., Walters, W.A., Berg-Lyons, D., Huntley, J., Fierer, N., et al. (2012) Ultra-high-throughput microbial community analysis on the Illumina HiSeq and MiSeq platforms. *ISME J.* **6**: 1621–1624.

6. Chen, S. and Dong, X. (2005) Proteiniphilum acetatigenes gen. nov., sp. nov., from a UASB reactor treating brewery wastewater. *Int. J. Syst. Evol. Microbiol.* **55**: 2257–2261.

7. Conrad, R. (1999) Contribution of hydrogen to methane production and control of hydrogen concentrations in methanogenic soils and sediments. *FEMS Microbiol. Ecol.* **28**: 193–202.

8. Conrad, R. and Wetter, B. (1990) Influence of temperature on energetics of hydrogen metabolism in homoacetogenic, methanogenic, and other anaerobic bacteria. *Arch. Microbiol.* **155**: 94–98.

9. Drake, H.L., Küsel, K., and Matthies, C. (2013) Acetogenic Prokaryotes. In, Rosenberg,E., DeLong,E.F., Lory,S., Stackebrandt,E., and Thompson,F. (eds), *The Prokaryotes*. Springer Berlin Heidelberg, Berlin, Heidelberg, pp. 3–60.

10. Dröge, S., Rachel, R., Radek, R., and König, H. (2008) Treponema isoptericolens sp. nov., a novel spirochaete from the hindgut of the termite Incisitermes tabogae. *Int. J. Syst. Evol. Microbiol.* **58**: 1079–1083.

11. Ferry, J.G. (1992) Biochemistry of Methanogenesis. *Crit. Rev. Biochem. Mol. Biol.* **27**: 473–503.

12. Friedman, J. and Alm, E.J. (2012) Inferring Correlation Networks from Genomic Survey Data. *PLOS Comput. Biol.* **8**: e1002687.

13. Fukuzaki, S., Nishio, N., Shobayashi, M., and Nagai, S. (1990) Inhibition of the Fermentation of Propionate to Methane by Hydrogen, Acetate, and Propionate. *Appl. Environ. Microbiol.* **56**: 719–723.

14. Galili, T., O'Callaghan, A., Sidi, J., and Sievert, C. heatmaply: an R package for creating interactive cluster heatmaps for online publishing. *Bioinformatics*.

15. Grabowski, A. (2005) Petrimonas sulfuriphila gen. nov., sp. nov., a mesophilic fermentative bacterium isolated from a biodegraded oil reservoir. *Int. J. Syst. Evol. Microbiol.* **55**: 1113–1121.

16. Guneratnam, A.J., Ahern, E., FitzGerald, J.A., Jackson, S.A., Xia, A., Dobson, A.D.W., and Murphy, J.D. (2017) Study of the performance of a thermophilic biological methanation system. *Bioresour. Technol.* **225**: 308–315.

17. Klindworth, A., Pruesse, E., Schweer, T., Peplies, J., Quast, C., Horn, M., and Glöckner, F.O. (2012) Evaluation of general 16S ribosomal RNA gene PCR primers for classical and next-generation sequencing-based diversity studies. *Nucleic Acids Res.* gks808.

18. Kotsyurbenko, O.R., Glagolev, M.V., Nozhevnikova, A.N., and Conrad, R. (2001) Competition between homoacetogenic bacteria and methanogenic archaea for hydrogen at low temperature. *FEMS Microbiol. Ecol.* **38**: 153–159.

19. Kougias, P.G., Treu, L., Benavente, D.P., Boe, K., Campanaro, S., and Angelidaki, I. (2017) Ex-situ biogas upgrading and enhancement in different reactor systems. *Bioresour. Technol.* **225**: 429–437.

20. Love, M.I., Huber, W., and Anders, S. (2014) Moderated estimation of fold change and dispersion for RNA-seq data with DESeq2. *Genome Biol.* **15**:.

21. Luo, G. and Angelidaki, I. (2012) Integrated biogas upgrading and hydrogen utilization in an anaerobic reactor containing enriched hydrogenotrophic methanogenic culture. *Biotechnol. Bioeng.* **109**: 2729–2736.

22. McMurdie, P.J. and Holmes, S. (2013) phyloseq: An R Package for Reproducible Interactive Analysis and Graphics of Microbiome Census Data. *PLoS ONE* **8**: e61217.

23. Möller, B., Oßmer, R., Howard, B.H., Gottschalk, G., and Hippe, H. (1984) Sporomusa, a new genus of gram-negative anaerobic bacteria including Sporomusa sphaeroides spec. nov. and Sporomusa ovata spec. nov. *Arch. Microbiol.* **139**: 388–396.

24. Nordmann, W. (1977) Die Überwachung der Schlammfaulung. KA-Informationen für das Betriebspersonal, Beilage zur Korrespondenz Abwasser.

25. Oksanen, J., Blanchet, F.G., Kindt, R., Legendre, P., Minchin, P.R., O'Hara, R.B., et al. (2014) vegan: Community Ecology Package.

26. Oren, A. (2014) The Family *Methanobacteriaceae*. In, *The Prokaryotes*. Springer, Berlin, Heidelberg, pp. 165–193.

27. Pelletier, E., Kreimeyer, A., Bocs, S., Rouy, Z., Gyapay, G., Chouari, R., et al. (2008) "Candidatus Cloacamonas acidaminovorans": genome sequence reconstruction provides a first glimpse of a new bacterial division. *J. Bacteriol.* **190**: 2572–2579.

28. Pruesse, E., Peplies, J., and Glöckner, F.O. (2012) SINA: Accurate high-throughput multiple sequence alignment of ribosomal RNA genes. *Bioinformatics* **28**: 1823–1829.

29. R Core Team (2013) R: A Language and Environment for Statistical Computing R Foundation for Statistical Computing, Vienna, Austria.

30. Ragsdale, S.W. and Pierce, E. (2008) Acetogenesis and the Wood–Ljungdahl pathway of CO2 fixation. *Biochim. Biophys. Acta BBA - Proteins Proteomics* **1784**: 1873–1898.

31. Ramette, A. (2007) Multivariate analyses in microbial ecology: Multivariate analyses in microbial ecology. *FEMS Microbiology Ecology* **62**: 142–160.

32. Sekiguchi, Y. (2003) Anaerolinea thermophila gen. nov., sp. nov. and Caldilinea aerophila gen. nov., sp. nov., novel filamentous thermophiles that represent a previously uncultured lineage of the domain Bacteria at the subphylum level. *Int. J. Syst. Evol. Microbiol.* **53**: 1843–1851.

33. Simankova, M.V., Chernych, N.A., Osipov, G.A., and Zavarzin, G.A. (1993) Halocella cellulolytica gen. nov., sp. nov., a New Obligately Anaerobic, Halophilic, Cellulolytic bacterium. *Syst. Appl. Microbiol.* **16**: 385–389.

34. Singh, J., Suhag, M., and Dhaka, A. (2015) Augmented digestion of lignocellulose by steam explosion, acid and alkaline pretreatment methods: A review. *Carbohydrate Polymers* **117**: 624–631.

35. Siriwongrungson, V., Zeng, R.J., and Angelidaki, I. (2007) Homoacetogenesis as the alternative pathway for H_2 sink during thermophilic anaerobic degradation of butyrate under suppressed methanogenesis. *Water Res.* **41**: 4204–4210.

36. Skennerton, C.T., Haroon, M.F., Briegel, A., Shi, J., Jensen, G.J., Tyson, G.W., and Orphan, V.J. (2016) Phylogenomic analysis of Candidatus 'Izimaplasma' species: free-living representatives from a Tenericutes clade found in methane seeps. *ISME J.* **10**: 2679–2692.

37. St-Pierre, B. and Wright, A.-D.G. (2013) Metagenomic analysis of methanogen populations in three full-scale mesophilic anaerobic manure digesters operated on dairy farms in Vermont, USA. *Bioresour. Technol.* **138**: 277–284.

38. Sundberg, C., Al-Soud, W.A., Larsson, M., Alm, E., Yekta, S.S., Svensson, B.H., et al. (2013) 454 pyrosequencing analyses of bacterial and archaeal richness in 21 full-scale biogas digesters. *FEMS Microbiol. Ecol.* **85**: 612–626.

39. Tang, Y., Shigematsu, T., Ikbal, Morimura, S., and Kida, K. (2004) The effects of micro-aeration on the phylogenetic diversity of microorganisms in a thermophilic anaerobic municipal solid-waste digester. *Water Res.* **38**: 2537–2550.

40. Thauer, R.K., Kaster, A.-K., Seedorf, H., Buckel, W., and Hedderich, R. (2008) Methanogenic archaea: ecologically relevant differences in energy conservation. *Nat. Rev. Microbiol.* **6**: 579–591.

41. Walters, W., Hyde, E.R., Berg-Lyons, D., Ackermann, G., Humphrey, G., Parada, A., et al. (2016) Improved Bacterial 16S rRNA Gene (V4 and V4-5) and Fungal Internal Transcribed Spacer Marker Gene Primers for Microbial Community Surveys. *mSystems* **1**: e00009-15.

42. Wasserfallen, A., Nölling, J., Pfister, P., Reeve, J., and Conway de Macario, E. (2000) Phylogenetic analysis of 18 thermophilic Methanobacterium isolates supports the proposals to create a new

genus, Methanothermobacter gen. nov., and to reclassify several isolates in three species, Methanothermobacter thermautotrophicus comb. nov., Methanothermobacter wolfeii comb. nov., and Methanothermobacter marburgensis sp. nov. *Int. J. Syst. Evol. Microbiol.* **50**: 43–53.

43. Whitman, W.B., Bowen, T.L., and Boone, D.R. (2014) The Methanogenic Bacteria. In, Rosenberg,E., DeLong,E.F., Lory,S., Stackebrandt,E., and Thompson,F. (eds), *The Prokaryotes*. Springer, Berlin, Heidelberg, pp. 123–163.

44. Wickham, H. (2009) ggplot2 - Elegant Graphics for Data Analysis 1st ed. Springer-Verlag New York.

45. Willems, A., Busse, J., Goor, M., Pot, B., Falsen, E., Jantzen, E., et al. (1989) Hydrogenophaga, a New Genus of Hydrogen-Oxidizing Bacteria That Includes Hydrogenophaga flava comb. nov. (Formerly Pseudomonas flava), Hydrogenophaga palleronii (Formerly Pseudomonas palleronii), Hydrogenophaga pseudoflava (Formerly Pseudomonas pseudoflava and “Pseudomonas carboxydoflava”), and Hydrogenophaga taeniospiralis (Formerly Pseudomonas taeniospiralis). *Int. J. Syst. Evol. Microbiol.* **39**: 319–333.

46. Yutin, N. and Galperin, M.Y. (2013) A genomic update on clostridial phylogeny: Gram-negative spore formers and other misplaced clostridia: Genomics update. *Environ. Microbiol.* **10**: 2631-41.

Chapter 6

General Discussion & Conclusions

The preceding chapters have given some insight into the microbial communities at play across several reactor configurations, involved in the digestion of a range of modern biogas substrates. In particular, these studies have identified microbial taxa associated with reactor function (or malfunction), and suggested underlying mechanisms through which these taxa interact with each other and the reactor environment.

1.1 OVERVIEW OF CHAPTERS

Chapter 2 dealt with the loss of reactor function due to the loss of acetoclastic *Methanosarcina*, which can be attributed to accumulation of ammonia from digestion of the highly proteinaceous substrate *Ulva lactuca*. Although *Methanosarcina* abundance collapsed, hydrogenotrophic methanogens persisted at low levels and were likely the main methane source for the duration of high-*Ulva* content digestion (R1). Although ammonia accumulation is universally toxic, culture studies have shown that hydrogenotrophic methanogens have higher thresholds for ammonia toxicity (Sprott *et al.*, 1984; Westerholm *et al.*, 2011). Ammonia toxicity in methanogens is caused by diffusion of free ammonia (NH_3) into the cell, where it causes rapid loss of cellular potassium (Sprott, 1986) and inhibits methanogenesis. Animal models show ammonia affects the regulation of a Na-K-Cl-transport protein (NKCC1), causing a loss in the ability to transport ions out of the cell and membrane depolarisation (Rangroo Thrane *et al.*, 2013). In prokaryotes, an analogous mechanism for membrane depolarisation by ammonia has not yet been established; however methanogens do show a wide variation in cellular potassium concentrations, with acetoclasts (e.g. *Methanosarcina*) showing concentrations at least 5 times lower than members of the *Methanobacteriaceae* (Jarrell *et al.*, 1984; Sprott *et al.*, 1984). This may in part explain the sensitivity of *Methanosarcina* to ammonia concentrations, but given the

importance of membrane potential there are likely other factors at play, with cell membrane composition (Whitman *et al.*, 2014) and energy conservation (including membrane-bound proteins) in methanogens differentiating along phylogenetic grounds (Thauer *et al.*, 2008). Despite the visible loss of Methanosarcina in R1, the remaining hydrogenotrophic methanogen population was sufficient to produce 177L CH_4/kgVS, albeit at a much less intensive rate of operation. Declining biogas output late in R6 operation may indicate ammonia-based inhibition of acetogenesis during long-term operation, as acetate became limiting despite accumulation of higher levels of volatile fatty acids (VFAs: iso-caproate, valerate). Ultimately, ammonia from *U. lactuca* provided the strongest influence on reactor community structure (chapter 2, Figure 3), leading to a loss of acetoclastic methanogens which accounts for VFA accumulation. Successful anaerobic digestion of lower quantities of *U. lactuca* relied on the presence of this same population of acetoclastic methanogens, reflecting the importance of matching feedstock composition with efficient acetate catabolism in AD.

In chapter 3, the microbial community underlying grass silage mono-digestion was evaluated, identifying microbial components that responded to supplementation of the trace elements (TE) cobalt, nickel and iron. Despite an observed decline in biomethane output at higher OLR, grass silage mono-digestion was associated with cellulolytic and fermenting bacteria, as well as the hydrogenotrophic methanogen *Methanomicrobia* (likely due to VFA accumulation midway through operation, c. week 40). Methanogens however showed no response to TE supplementation, which was instead associated with a number of known secondary- or end-fermenters, along with a broader increase in the abundance of bacteria from Class *Clostridia*. Although the emphasis in biogas technology is on the supplementation of methanogens due to their documented requirement for

trace elements (Fe, Ni, Co, W, Mo, Se, etc.), this study shows that the TE requirements for fermenting bacteria pose a more immediate bottleneck for biogas in the mono-digestion of grass silage. It was noted that although the reactors were operated at increasing OLR, the stress placed on the reactor was not excessive, i.e. no obvious loss of functional microbial populations or toxic accumulation occurred. As such, TE supplementation bolstered the function of the existing microbial community, rather than allowing recruitment or recovery of lost populations. It is however possible that reactor communities under greater (or different) stresses would respond in an alternate manner.

The methods used in this study do not allow for direct accounting of TE usage; however, a number of crucial steps in end fermentation require the TE supplemented in this study (Fe, Ni, Co): in particular the catabolism of propionate to acetate which involves the use of a cobalt-containing cobalamine/methylmalonyl-CoA mutase complex. While many of the taxa significantly associated with TE supplementation are acidogens or acetogens, one genus (P:*Firmicutes:* O:*Thermoanaerobacteriales*: *Gelria*) is also known to utilise a novel glutamate → propionate pathway in the presence of syntrophs (Plugge *et al.*, 2002), with statistically significant increases in *Gleria* abundance (chapter 3, Figure 4B) potentially reflecting an improved metabolism of propionate. Additionally, unidentified OTUs assigned to *Clostridia* order MBA03 have been previously documented but none have been described (Kougias *et al.*, 2017; Rago *et al.*, 2018). Given its high abundance and positive relationship with biomethane efficiency (B_{eff}), it is an attractive candidate for future culturing and characterisation. In summary, the response of end-fermenting bacteria to TE supplementation underlines the importance of end-fermentation as a conduit connecting methanogenesis to the AD community; this connection should be considered from a practical perspective when supplementing or engaging in biogas production.

While both chapters 2 and 3 described apparent inhibition of microbial communities through surfeits (chapter 2) or deficits (chapter 3) of end fermentation products, chapter 4 considered a different approach to biogas production, which attempts to decouple the final methanogenic step from preceding AD stages through establishing biomethanation in an *ex situ* reactor. The appeal of *ex situ* biogas is partly a simplification of the biogas process to avoid complications in feedstock degradation (e.g. ammonia toxicity, VFA accumulation) affecting methanogenesis, which would enable the use of more diverse or potentially difficult feedstocks (assuming process setup allowed for adequate separation of secondary and end fermentation products). However, the main appeal of *ex situ* biomethanation is direct conversion of CO_2 to biomethane. In this context, *ex situ* reactors can biologically 'scrub' biogas of contaminants such as H_2S and CO_2 (Oren, 2014; Whitman *et al.*, 2014; Sun *et al.*, 2015) and produce high-purity methane for use as fuel. Just as the previously mentioned partitioning of the biogas process might preserve methanogenesis, segregation of biogas upgrading to *ex situ* reactors also avoids the inhibition of fermentation due to high concentrations of hydrogen required to achieve total CO_2 conversion. *Ex situ* biomethanation is under active research, and as a result there is significant overlap between AD and *ex situ* biomethanation. For example, in work conducted by some groups (Bassani *et al.*, 2015; Bassani, 2017; Kougias *et al.*, 2017), *ex situ* operation is carried out using filtered AD leachate as a complex, undefined feedstock. Although this has merits in terms of practicality, it effectively forms a 'secondary AD' rather than AD *ex situ*, as the substrate will contain a wide variety of undigested materials, including dissolved primary feedstock, fermenting bacteria and fermentation products. In comparison, process setup used by other groups (Luo and Angelidaki, 2012; Guneratnam *et al.*, 2017; see chapter 4) involve a defined and minimal medium

(Angelidaki and Sanders, 2004) which should provide all the requirements to allow hydrogenotrophic methanogenesis when combined with CO_2 and H_2. These approaches reflect the different benefits of *ex situ* digestion mentioned above (i.e. segregation versus upgrading), but are likely to rely on microbial communities of significantly different composition due to the influences of feedstock. Chapter 4 assesses the microbial community in an example of 'minimal' *ex situ* upgrading, supplied a minimal defined medium, stoichiometrically determined quantities of CO_2 and H_2, and incubated at two different thermophilic temperatures (55^{o}C, 65^{o}C).

Before this work was conducted, it was unclear how the microbial community (founded by thermophilic AD inoculum from digestion of a plant-based feedstock) would be shaped by both the restricted inputs of the *ex situ* setup and the thermophilic conditions. It was assumed that the resultant community would focus on methanogenesis via fixation of CO_2, with limited fermentation of the minimal media supplied, and that methanogens would form the major community member.

However, community profiling through DGGE and pyrosequencing makes it clear that conditions for *ex situ* methanogenesis support a relatively diverse bacterial majority in addition to the methanogen population of interest (*Methanothermobacter*), presenting a community that is consistent across variations in operation, thermophilic temperatures, and between replicates. Guneratnam *et al.* (2017) speculated that a gradual decline in biogas function (i.e. stage C) resulted from attenuation of the medium, and saw improvement when reactors were re-inoculated with the source biomass (stage D). Given the positive response to re-inoculation while methanogen populations declined, improved process performance could reflect a functional shift in bacterial populations, or simply a gain of additional resources (carbohydrates, trace elements). Despite 16S community pyrosequencing, the significance of the bacterial community remains unclear due to the uncharacterised nature and

undocumented metabolic characteristics of the two largest OTUs (MBA03, uncultured *Firmicutes*). However, the metabolism of acetate and other SCFA (which remained stable and below inhibitory concentrations) is likely mediated by bacterial syntrophs (i.e. via SAO) given the lack of acetoclastic methanogens under thermophilic conditions, and may be a core function of the uncharacterised *ex situ* bacterial populations.

Nevertheless, one thing which is clear from this study is the importance of *Methanothermobacter*, and in particular *Mtb. wolfei* as the functional methanogen in this setup, as seen in the consistency of the 16S clone library and pyrosequencing results (see table 1 and figure 3, Chapter 4). *Mtb. wolfei* is a well-characterised thermophilic hydrogenotroph, with an usually high dependence on tungsten for growth (Winter *et al.*, 1984). This requirement provides a mechanism for re-supplementation (stage D) to improve reactor performance as documented by Guneratnam *et al.* (2017), and provides a basis for re-evaluating the composition of the minimal media used. However, given the restricted nature of the *ex situ* reactor, re-inoculation is likely to have also relaxed constraints elsewhere on the structure of the *ex situ* (bacterial) communities (as seen in chapter 3), and the effect of this on reactor function cannot be discounted.

The previous chapter (4) provided insights into a surprisingly complex *ex situ* upgrading community, in particular showing the prevalence of *Methanothermobacter* as the dominant methanogen. To allow a better understanding of the upgrading community and its dynamics, chapter 5 provides deep community sequencing of *in situ* and *ex situ* biogas upgrading communities under different conditions of hydrogen flow and feedstock composition. Operated and seeded in series, characterisation of these reactor setups makes it clear that the strongest determinant of community structure was the

presence of feedstock *in situ* versus absence in *ex situ* operation, irrespective of hydrogen enrichment or feeding conditions (e.g. batch v. continuous) (Chapter 5, Figures 4, 5, and 10). Additionally, deep sequencing data supported the community characterisation of chapter 4, clearly showing these setups involve *Methanobacteriaceae* as the dominant upgrading methanogens, and encourage diverse bacterial communities much as in 'standard' AD.

Although prevalence of *Methanobacteriaceae* across reactor setups (chapter 3: continuous *ex situ;* chapter 4: *in situ* continuous, batch *ex situ*, continuous *ex situ*) highlights this clade's relevance as an agent for biomethanation, the dominant *Methanobacteriaceae* genus clearly differed between setups in chapter 5: *Methanothermobacter* for *in situ*, versus *Methanobacterium* for *ex situ* (both 55°C). This contrasts with chapter 4, where *Methanothermobacter wolfei* was the consistent methanogen in an *ex situ* setup (55-65°C). The genera *Methanobacterium* and *Methanothermobacter* are extremely close phylogenetically (Wasserfallen *et al.*, 2000; Oren, 2014; Whitman *et al.*, 2014) with recent taxonomic separation published but not recognised under the International Code of Nomenclature of Bacteria. Phylogenetic delineation of the two genera reflects niche separation based on meso-thermophily in Methanobacterium (optima: 35-40°C), and thermophily in the aptly-named *Methanothermobacter* (optima: 55-65°C: Wasserfallen *et al.*, 2000; Oren, 2014). Taxonomic assignment in chapter 5 placed *Methanothermobacter* populations outside of a species taxon, so it is unclear whether these *in situ* populations share the heightened requirements of *Mtb. wolfei* for tungsten – if so, this might explain its association with complex feedstock, which is known to supplement digestion through inclusion of micronutrients (Drosg, 2013; Seppälä *et al.*, 2013). Tungsten is used by thermophilic methanogens in the capture of CO_2 by the metallo-isoenzyme formylmethanofuran-dehydrogenase (Fwd), and although *Mtb. wolfei* shows an unusually high

requirement for tungsten (Winter *et al.*, 1984) it is a requirement for known thermophilic methanogens (e.g. *Methanothermobacter*) with a greater reliance in hyperthermophiles (i.e. *Methanopyrus*) due to co-expression of two tungsten-containing isoenzymes of Fwd (Vorholt *et al.*, 1997). In contrast, mesophilic methanogens substitute molybdenum in the metallo-isoenzyme to produce Fmd (e.g. *Methanosarcina barkeri,* Karrasch *et al.*, 1990), while meso-thermophilic methanogens can use both elements but may have higher tungsten requirements than mesophiles due to constitutive expression of the tungsten isoenzyme Fwd (Hochheimer *et al.*, 1998). As such, there is a relationship between increasingly thermophilic temperatures, micronutrient availability (especially with respect to feedstock), and the major hydrogenotrophic methanogen encouraged. With consideration of chapters 3, 4, and 5, adequate supply of TE in biogas upgrading could allow for methanogens that are better adapted to optimal process temperatures. Further exploration of the potential role of tungsten in thermophilic biomethane upgrading might therefore be of interest for industrial upgrading applications.

Given the differences in reactor setup between *in situ* and *ex situ*, the relationship between exogenous hydrogen, microbial community composition, and biogas function was of great interest as a model for hydrogen inhibition of fermentation. Gas flow rates appear to cripple ISB at a hydrogen flow rate of 37L/day, while hydrogen flow in CES was far in excess of this (81-403L/day) and caused little deterioration, despite FOS:TAC climbing to levels similar to those seen in ISB (0.9 from ISB 6 onwards; 0.5 at CES 6; 0.8 at CES 9). Major indications of hydrogen inhibition in ISB are seen in later time points (ISB 6-9) with FOS:TAC and total VFA increases (chapter 5, Figure 1), corresponding to a decline of known and putative hydrolysers and fermenters (MBA03 population, *Halocella*, *Ruminicoccaceae* UCG-012, *Ruminiclostridium*, *Defluvitalea, Lentimicrobiaceae*).

Populations of the syntrophic short-chain fatty acid (SCFA) oxidisers *Syntrophomonas* (Müller *et al.*, 2010; Schink and Muñoz, 2014) also declined as hydrogen flow rates increased over both ISB 4-9 and CES 4-9 (Figure 1).

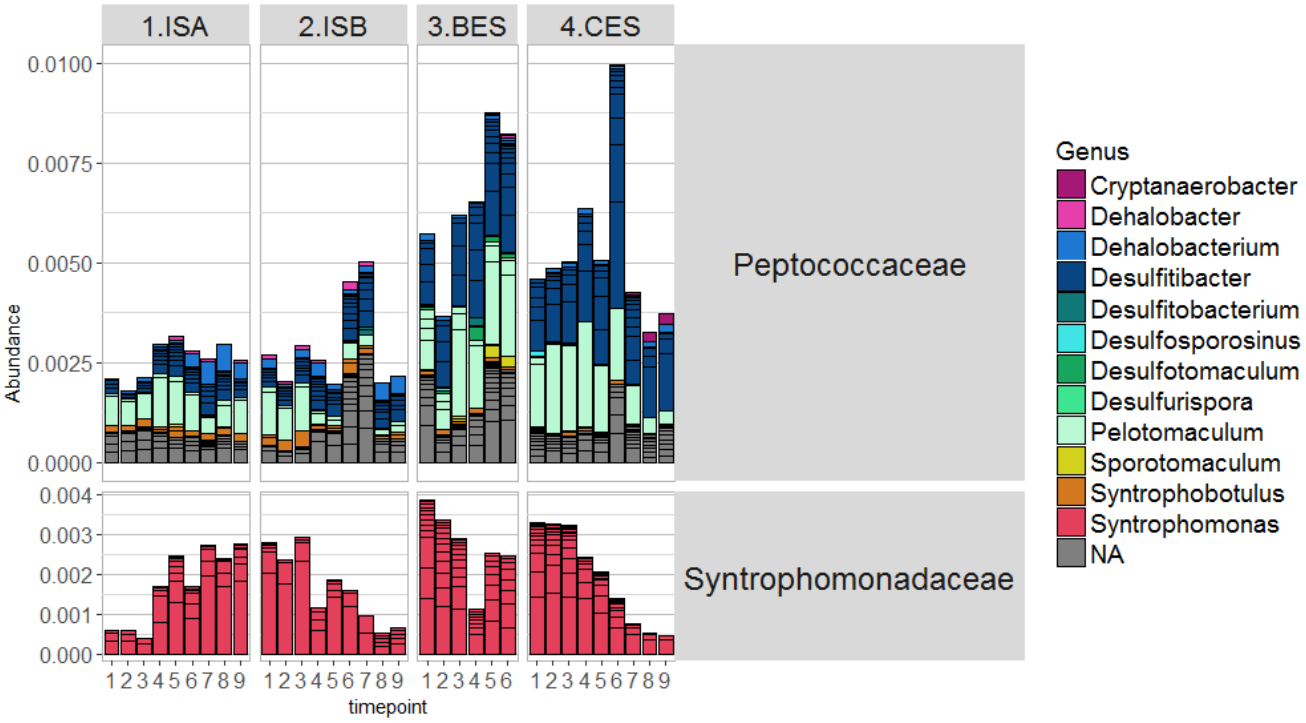

Figure 1: *Examples of relative abundances of known syntrophs (Peptococcaceae, Syntrophomonadaceae) during in situ and ex situ reactor operation. Decline in Syntrophomonadaceae during periods of peak gas flow strongly suggests inhibition due to increasing concentrations of upgrading hydrogen. Peptococcaceae however show no such inhibition, and instead increase in abundance during a shift in microbial community structure (ISB 6, 7) similar to Gelria and a number of minor populations. Note variable scale on y-axis.*

Although the average abundance of these populations was low (<0.5%), attenuation with increasing gas flow rates indicates the inhibition of a secondary fermenting population by rising levels of hydrogen, with consequences for reactor stability. Oxidation of SCFA (e.g. propionate, butyrate) is a

key metabolic bottleneck in AD, with inhibition leading to VFA accumulation (Nielsen *et al.*, 2007; Gallert and Winter, 2008; Müller *et al.*, 2010). Syntrophs (e.g. *Syntrophomonas*) rely on extremely low hydrogen partial pressures (10^{-8} – 10^{-15} bar; Müller *et al.*, 2010) in order to oxidise SCFA; with excess hydrogen inhibiting these activities by making them thermodynamically unfeasible (Amend and Shock, 2001). The volume of SCFA & VFA that must be catabolised via AD of many feed stocks can make this extremely challenging if hydrogen is not kept at low levels.

In situ reactor failure also coincided with the collapse of the dominant methanogen population and a large shift in bacterial community composition. Disappearance of hydrogenotrophic *Methanothermobacter* and increases in the acetogens *Defluviitalea* and *Ruminoclostridium* (ISB 8 & 9) suggests threshold hydrogen concentrations for homoacetogenesis were exceeded and eventually allowed methanogens to be displaced by the faster-growing bacteria. Large shifts were also seen in diverse, minor populations, culminating in the sudden differentiation of the community at ISB 8 and 9 (see segregation of time points 7 – 9 (chapter 5, Figures 4 & 5). Crucially, ISB displayed critical FOS:TAC levels from time point ISB 4 onwards (>0.4), approaching 0.9 by ISB 6. The reactor was therefore in difficulty before disappearance of the methanogens, with hydrogen concentration the most likely parameter involved. The collapse of the methanogens appears to exacerbate reactor failure, with FOS:TAC exceeding 0.9 at time point ISB 9. As such, hydrogen enrichment *in situ* raises two clear issues: decline of hydrolysing/fermentating populations, and sudden displacement of methanogens by apparent homoacetogens.

Differences in the composition of bacterial populations were observed when comparing the *in situ* and *ex situ* setups, with major differences in the abundance of cellulose degraders reflecting feedstock availability (i.e. *ex situ* dearth of cellulolytic *Ruminococcaceae*), and increases in abundance

of hydrogen producers *ex situ* when exogenous H_2 flow was reduced (CES 7 – 9). In contrast, a number of bacterial populations were relatively consistent between setups, reflecting perhaps the common origin of the communities or gross similarity in reactor microbial ecology. *Gelria* (P:*Firmicutes*; C:*Thermoanaerobacteriales*) is a fermenting acetogen with a unique pathway for degrading glutamate to propionic acid that is energetically favourable only in the presence of syntrophs (Plugge *et al.*, 2002). *Gelria* abundances remain between 5 and 15% over all four stages, possibly reflecting constitutive turnover of reactor biomass (e.g. glutamate) through the assistance of available syntrophic partners. Interestingly, at inhibited ISB timepoints 6 and 7, abundances of *Gelria* swell during the large shift in community structure (chapter 5, Figure 4), but drop to their lowest values (5%) during reactor failure at ISB 8 and 9. Other populations of known syntrophic SCFA degraders (e.g.*Peptococcaceae*) also follow this abundance trend ISB 6-9, suggesting inhibition through increasing hydrogen levels was not applied equally across all niches.

A single population from the uncharacterised Order MBA03 comprised the majority of sequence abundances in this study but only differed slightly between setups, with a non-significant decrease *ex situ*. This population shows no obvious correlation with hydrogenotrophic methanogens (chapter 5, Figure 10), but correlates strongly with several *Ruminococcaceae* taxa as well as *Dethiobacter*, *Halocella* and *Caldicoprobacter* (R=0.7-0.79). A population placed in Order MBA03 also associated with grass silage digestion in chapters 2 (responding positively to TE supplementation) and 3 (showing a slight decline during periods of decreased biogas output). Commonalities in feedstock composition suggest MBA03 is involved in the metabolism of hydrolysis products, i.e. secondary fermentation. A slight decline in abundance during periods of elevated hydrogen concentration supports this role, as low hydrogen concentrations are crucial for hydrolysis and fermentation. The re-occurrence of this

group as a major community component suggests an important role in the AD of ligno-cellulosics, and earmarks Order MBA03 for extensive further characterisation.

1.2 Concluding Remarks

Although reactors in these works were characterised based on the differences between setups, there are a number of common features between setups which allow recommendations for future microbial management. The route taken by carbon to the final methanogenic stage is a crucial factor in biogas production and management. Although methanogens are extremely sensitive to oxygen and have micronutrient requirements which can become limiting, their ubiquity, continued output of biogas during reactor inhibition and presence in multiple parallel populations suggests they are perhaps a “hardier” clade than is generally recognised. Shifts in community structure presented in these studies indicate that reactor inhibition can instead often be traced back to issues with bacterial populations involved in secondary fermentation (declining acetate production in late R6, chapter 2; TE-linked decline of *Clostridia* in chapter 3; likely decreases in secondary fermenters in chapter 4**;** homoacetogens and acid accumulation in chapter 5). AD operation could therefore be improved by supporting populations involved in the transfer of end-fermented carbon to methanogenesis, encompassing secondary fermenters, syntrophs and methanogens themselves. Trace element supplementation is one widely practiced method of doing this; however, consideration should be given to the trace elements required for a specific setup e.g.: Fe, Ni, Co etc. to supplement fermentation and catabolism of fermentation products; W for thermophilic biogas upgrading and Mo for mesophilic biogas upgrading.

A second approach to improve biogas production (chapters 4, 5) is the segregation of methanogenesis from primary AD of feedstock (*ex situ* methanogenesis), which can reduce inhibition and allow functional populations to be managed independently. This approach has particular merit when considering AD setups with problematic substrates (e.g. *U. lactuca*, chapter 2) where feedstock digestion can inhibit methanogenic populations, or recalcitrant substrates (e.g. *Lolium perenne*) although inhibiting factors must be ameliorated or addressed prior to *ex situ* biomethanation.

In the work presented, differences in feedstock composition repeatedly provided the greatest patterning effects on the microbial community between comparable reactors. Similarly, the removal (or reduction) of feedstock will cause huge changes in community composition, effectively creating a new subset of anaerobic *ex situ* communities, each iteration of which is informed by practicalities in reactor design and substrate composition (i.e. minimal, defined, complex, leachate). Although *Methanobacteriaceae* are predicted to continue to be the dominant methanogen of relevance in thermophilic upgrading, as development of *ex situ* methanation continues and allows for greater separation from AD, techniques may favour transition to hyperthermophilic methanogens (e.g. *Methanopyrus*) or less energy-intensive mesophilic conditions (e.g. *Methanomicrobiaceae*, *Methanococcaceae,* etc.), depending on conditions required. Although specifics will vary, micro-nutrient requirements and transfer/uptake of carbon to methanogens are likely to be major considerations in future work.

2 REFERENCES

1. Amend, J.P. and Shock, E.L. (2001) Energetics of overall metabolic reactions of thermophilic and hyperthermophilic Archaea and Bacteria. *FEMS Microbiol. Rev.* **25**: 175–243.
2. Angelidaki, I. and Sanders, W. (2004) Assessment of the anaerobic biodegradability of macropollutants. *Rev. Environ. Sci. Biotechnol.* **3**: 117–129.
3. Bassani, I. (2017) Hydrogen assisted biological biogas upgrading.
4. Bassani, I., Kougias, P.G., Treu, L., and Angelidaki, I. (2015) Biogas Upgrading via Hydrogenotrophic Methanogenesis in Two-Stage Continuous Stirred Tank Reactors at Mesophilic and Thermophilic Conditions. *Environ. Sci. Technol.* **49**: 12585–12593.
5. Drosg, B. (2013) Process monitoring in biogas plants.
6. Gallert, C. and Winter, J. (2008) Propionic acid accumulation and degradation during restart of a full-scale anaerobic biowaste digester. *Bioresour. Technol.* **99**: 170–178.
7. Guneratnam, A.J., Ahern, E., FitzGerald, J.A., Jackson, S.A., Xia, A., Dobson, A.D.W., and Murphy, J.D. (2017) Study of the performance of a thermophilic biological methanation system. *Bioresour. Technol.* **225**: 308–315.
8. Hochheimer, A., Hedderich, R., and Thauer, R.K. (1998) The formylmethanofuran dehydrogenase isoenzymes in Methanobacterium wolfei and Methanobacterium thermoautotrophicum: induction of the molybdenum isoenzyme by molybdate and constitutive synthesis of the tungsten isoenzyme. 5.
9. Jarrell, K.F., Sprott, G.D., and Matheson, A.T. (1984) Intracellular potassium concentration and relative acidity of the ribosomal proteins of methanogenic bacteria. *Can. J. Microbiol.* **30**: 663–668.

10. Karrasch, M., Börner, G., and Thauer, R.K. (1990) The molybdenum cofactor of formylmethanofuran dehydrogenase from Methanosarcina barkeri is a molybdopterin guanine dinucleotide. *FEBS Lett.* **274**: 48–52.

11. Kougias, P.G., Treu, L., Benavente, D.P., Boe, K., Campanaro, S., and Angelidaki, I. (2017) Ex-situ biogas upgrading and enhancement in different reactor systems. *Bioresour. Technol.* **225**: 429–437.

12. Luo, G. and Angelidaki, I. (2012) Integrated biogas upgrading and hydrogen utilization in an anaerobic reactor containing enriched hydrogenotrophic methanogenic culture. *Biotechnol. Bioeng.* **109**: 2729–2736.

13. Müller, N., Worm, P., Schink, B., Stams, A.J.M., and Plugge, C.M. (2010) Syntrophic butyrate and propionate oxidation processes: from genomes to reaction mechanisms. *Environ. Microbiol. Rep.* **2**: 489–499.

14. Nielsen, H.B., Uellendahl, H., and Ahring, B.K. (2007) Regulation and optimization of the biogas process: Propionate as a key parameter. *Biomass Bioenergy* **31**: 820–830.

15. Oren, A. (2014) The Family *Methanobacteriaceae*. In, *The Prokaryotes*. Springer, Berlin, Heidelberg, pp. 165–193.

16. Plugge, C.M., Balk, M., Zoetendal, E.G., and Stams, A.J. (2002) Gelria glutamica gen. nov., sp. nov., a thermophilic, obligately syntrophic, glutamate-degrading anaerobe. *Int. J. Syst. Evol. Microbiol.* **52**: 401–407.

17. Rago, L., Zecchin, S., Marzorati, S., Goglio, A., Cavalca, L., Cristiani, P., and Schievano, A. (2018) A study of microbial communities on terracotta separator and on biocathode of air breathing microbial fuel cells. *Bioelectrochemistry Amst. Neth.* **120**: 18–26.

18. Rangroo Thrane, V., Thrane, A.S., Wang, F., Cotrina, M.L., Smith, N.A., Chen, M., et al. (2013) Ammonia triggers neuronal disinhibition and seizures by impairing astrocyte potassium buffering. *Nat. Med.* **19**: 1643–1648.

19. Schink, B. and Muñoz, R. (2014) The Family <Emphasis Type="Italic">Syntrophomonadaceae</Emphasis>. In, *The Prokaryotes*. Springer, Berlin, Heidelberg, pp. 371–379.

20. Seppälä, M., Pyykkönen, V., Väisänen, A., and Rintala, J. (2013) Biomethane production from maize and liquid cow manure – Effect of share of maize, post-methanation potential and digestate characteristics. *Fuel* **107**: 209–216.

21. Sprott, G.D. (1986) Ammonia toxicity in pure cultures of methanogenic bacteria. *Syst. Appl. Microbiol.* **Volume 7**: Pages 358–363.

22. Sprott, G.D., Shaw, K.M., and Jarrell, K.F. (1984) Ammonia/potassium exchange in methanogenic bacteria. *J. Biol. Chem.* **259**: 12602–12608.

23. Sun, Q., Li, H., Yan, J., Liu, L., Yu, Z., and Yu, X. (2015) Selection of appropriate biogas upgrading technology-a review of biogas cleaning, upgrading and utilisation. *Renew. Sustain. Energy Rev.* **51**: 521–532.

24. Thauer, R.K., Kaster, A.-K., Seedorf, H., Buckel, W., and Hedderich, R. (2008) Methanogenic archaea: ecologically relevant differences in energy conservation. *Nat. Rev. Microbiol.* **6**: 579–591.

25. Vorholt, J.A., Vaupel, M., and Thauer, R.K. (1997) A selenium-dependent and a selenium-independent formylmethanofuran dehydrogenase and their transcriptional regulation in the hyperthermophilic Methanopyrus kandleri. *Mol. Microbiol.* **23**: 1033–1042.

26. Wasserfallen, A., Nölling, J., Pfister, P., Reeve, J., and Conway de Macario, E. (2000) Phylogenetic analysis of 18 thermophilic Methanobacterium isolates supports the proposals to create a new genus, Methanothermobacter gen. nov., and to reclassify several isolates in three species, Methanothermobacter thermautotrophicus comb. nov., Methanothermobacter wolfeii comb. nov., and Methanothermobacter marburgensis sp. nov. *Int. J. Syst. Evol. Microbiol.* **50**: 43–53.

27. Westerholm, M., Dolfing, J., Sherry, A., Gray, N.D., Head, I.M., and Schnürer, A. (2011) Quantification of syntrophic acetate-oxidizing microbial communities in biogas processes. *Environ. Microbiol. Rep.* **3**: 500–505.

28. Whitman, W.B., Bowen, T.L., and Boone, D.R. (2014) The Methanogenic Bacteria. In, Rosenberg,E., DeLong,E.F., Lory,S., Stackebrandt,E., and Thompson,F. (eds), *The Prokaryotes*. Springer Berlin Heidelberg, Berlin, Heidelberg, pp. 123–163.

29. Winter, J., Lerp, C., Zabel, H.-P., Wildenauer, F.X., König, H., and Schindler, F. (1984) Methanobacterium wolfei, sp. nov., a New Tungsten-Requiring, Thermophilic, Autotrophic Methanogen. *Syst. Appl. Microbiol.* **5**: 457–466.

Appendices

Appendix A – Supplementary Figures

Figures in Appendix A have been referenced in the main text (see locations noted below), and are presented in the same order.

Chapter 2:

Supplementary Figure 2.1: Section 2:3.4.1

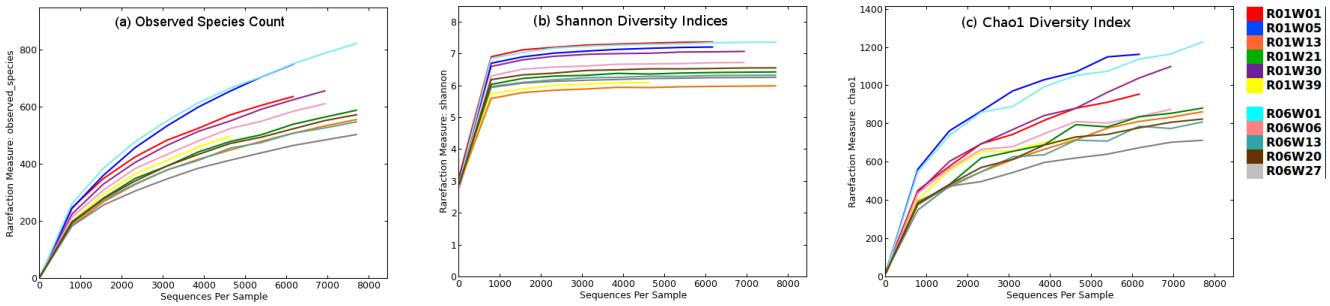

Rarefied ecological diversity curves across all samples characterised in chapter 2, illustrating that the major community components are well characterised under the depth of sequencing obtained, as shown by the plateau in Shannon index and approaching plateaus in Chao1 and observed species counts.

Chapter 4:

Supplementary Figure 4.1: Section 3:3.4

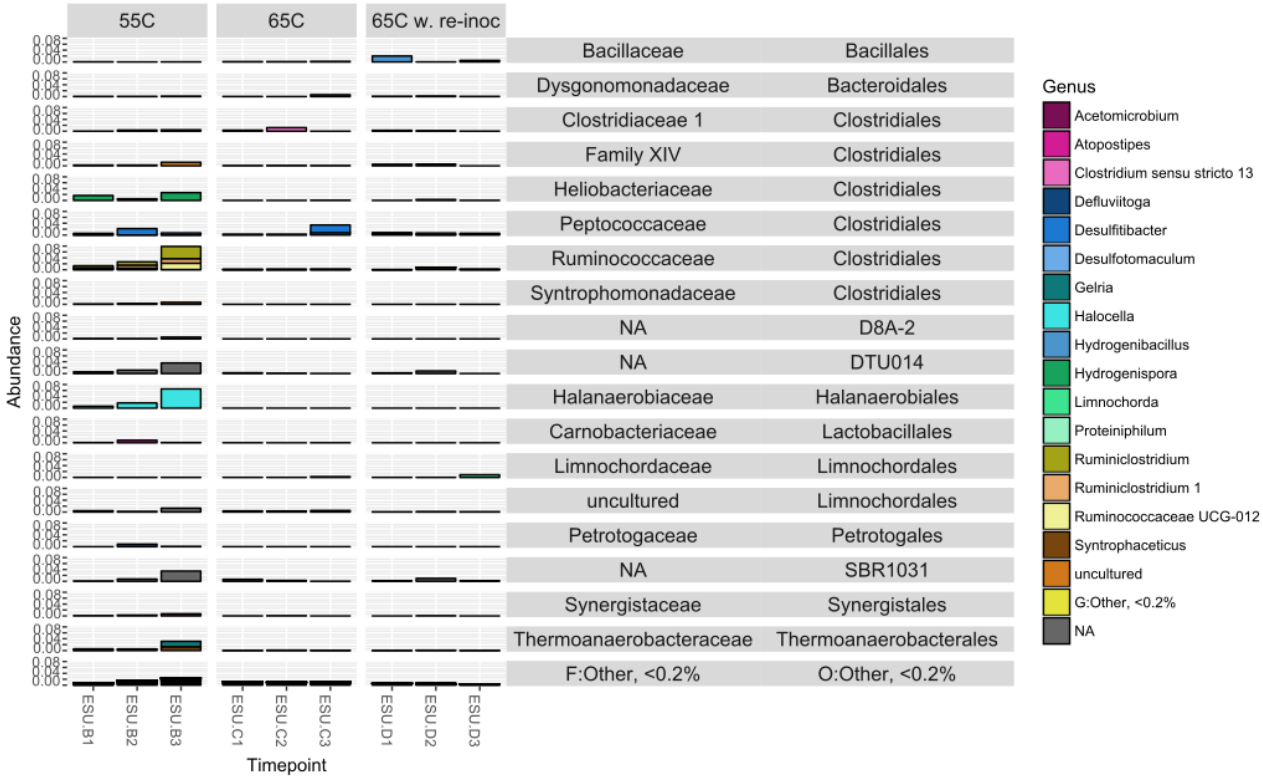

Minor OTU populations, with relative abundances not above 1% in at least two timepoints (i.e. agglomerated to 'Other' in Chapter 4 Figure 3)

Chapter 5:

Supplementary Figure 5.1: Section 5:3.3

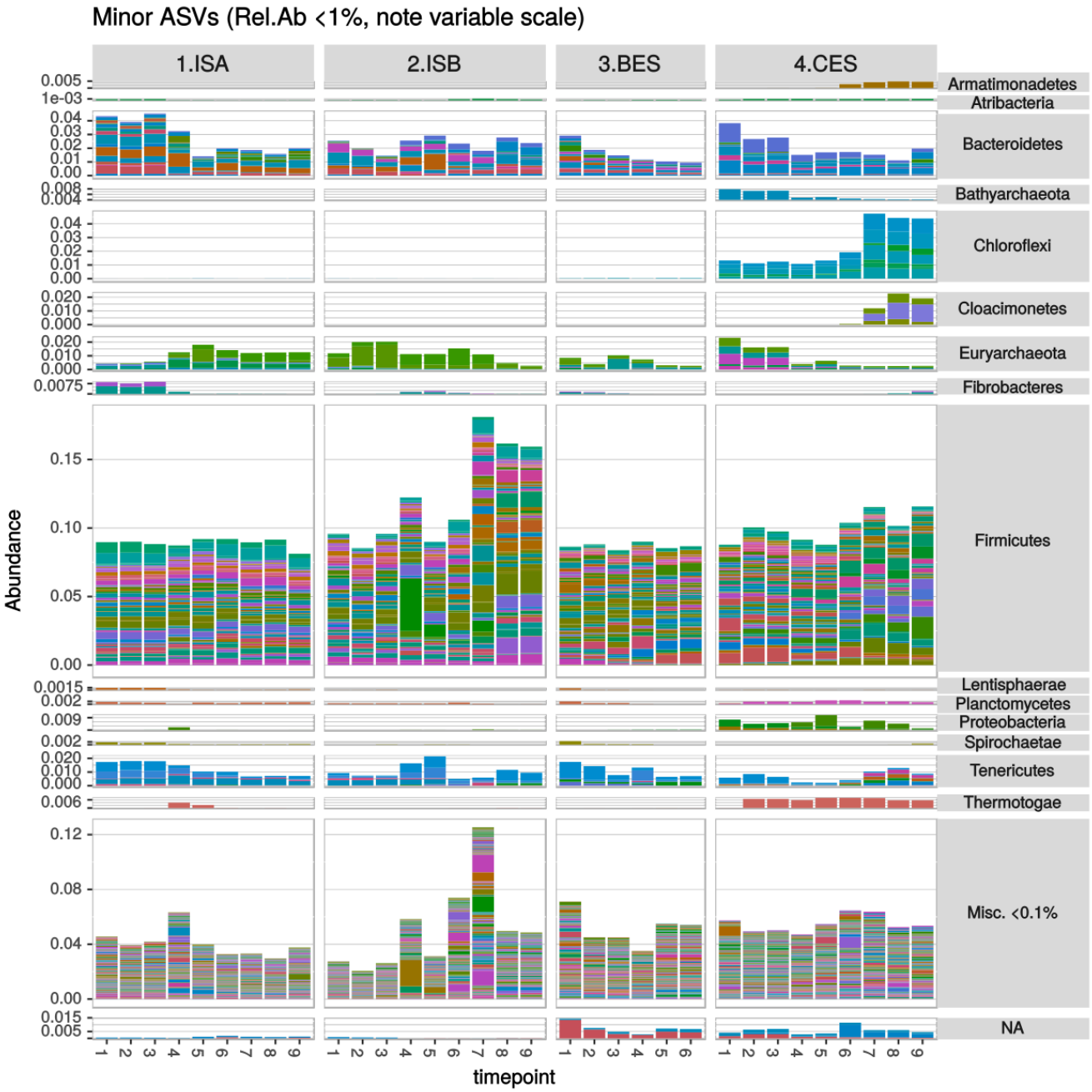

Relative abundance of minor ASV populations, relative abundances not above 1% in at least three timepoints(i.e. agglomerated as 'Other' in chapter 5, Figure 5)

Supplementary Figure 5.2: Section 5:3.4 **IS-ES NA DA:**

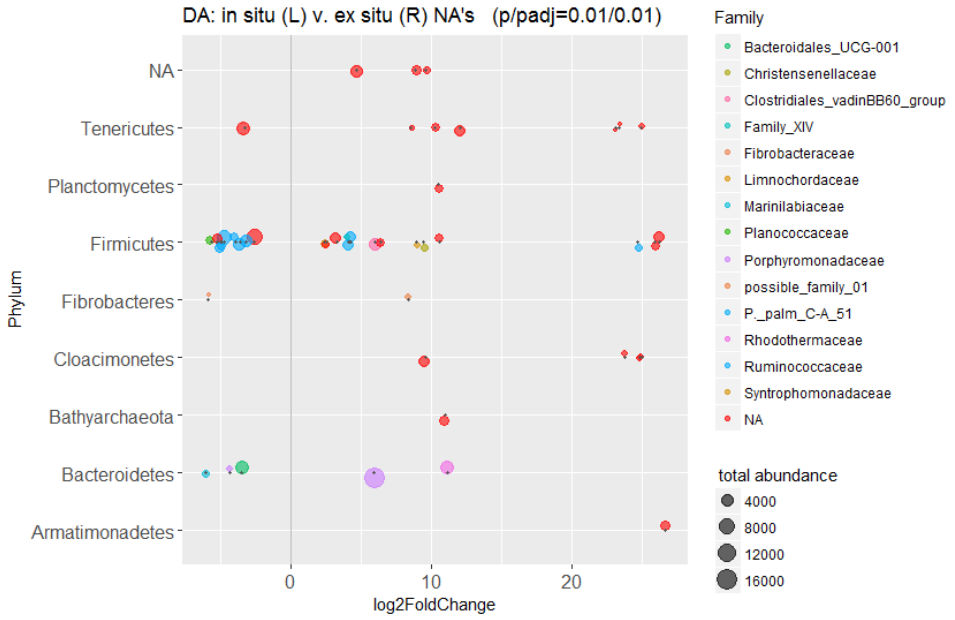

ASVs uncharacterised at genus-level ("NA" in Ch5: Figure IS-ES-RA) but differentially abundant between *in situ* and *ex situ* conditions, with the average change in abundance between either setup represented as $\log_2$ fold-change (i.e. increase from 2 to 8 = $\log_2$ fold change of 3).

Supplementary Figure 5.2: Section 5:3.4 **ES only NA DA:**

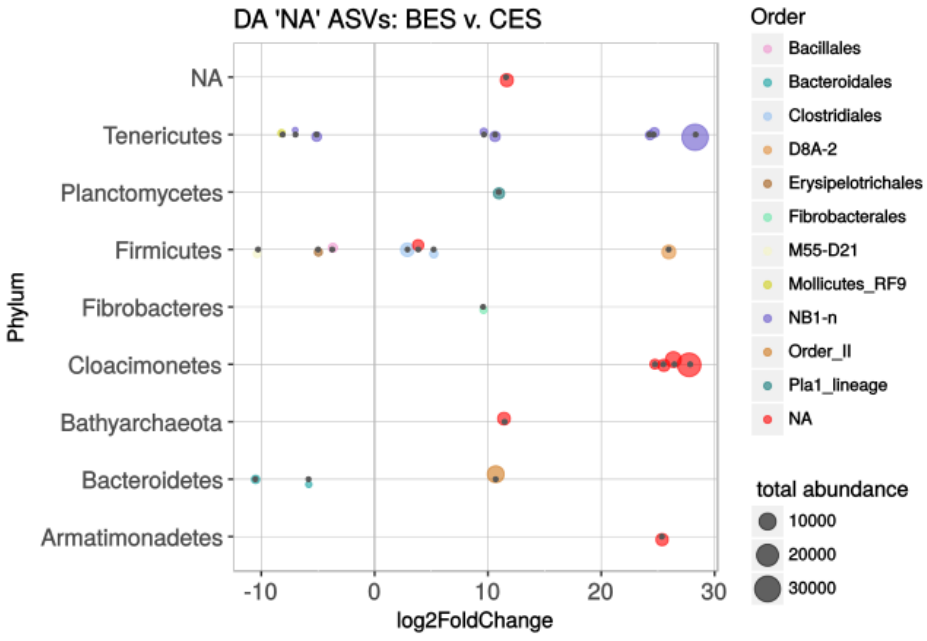

ASVs uncharacterised at genus-level ("NA" in Ch5: Figure BES-CES-RA) but differentially abundant between BES and CES conditions, with the average change in abundance between either setup represented as $\log_2$ fold-change (i.e. increase from 2 to 8 = $\log_2$ fold change of 3).

Appendix B – TENP-P DNA Extraction Protocol

Appendix B details the DNA extraction protocol developed during the course of this thesis and used for chapters 3, 4, and 5.

The TENP-P DNA extraction buffer was extremely useful in reliably extracting nucleic acids from digestate, due to its high salt content (lysis and isolating DNA from CTAB-related degradation) and PVPP polymer (humic acid removal). The second 'P' in 'TENP-P' refers to habitual use of proteinase K in an additional step (i.e. not included in buffer), although efficacy seemed to vary based on sample composition.

Note also that this extraction buffer lacks the popular detergent SDS, which was seen to seriously inhibit DNA recovery when used with this recipe.

The extraction buffer is adapted from a combination of Wilson, 2000 and Shan et al., 2007.

B.i Reagents

TENP-P extraction buffer

1.25ml TRIS @ 1M

1ml EDTA @ 0.5M

12.5ml NaCl @ 5M

2.5ml PVPP @ 10% w/v

bring to 25ml w. TE buffer

autoclave before use, add

10% CTAB buffer

0.7M NaCl

10% weight/volume CTAB

autoclave before use

Proteinase K solution

As provided by supplier

B.ii Preparation:

- Anaerobic reactor sludges frozen at -80°C were rapidly defrosted through immersion of the containers in a water bath at 50°C. Once sufficiently defrosted, sludges were coarsely homogenised with a sterilised rod to ensure sedimentation did not affect sampling.
- For each of timepoints described in the main text, 3 technical replicates of approx. 1g wet-weight sludge biomass were removed to a 2ml ependorf tube (e.g. 10 timepoints gives 30 eppendorf tubes total, containing 1g biomass each). All tubes were processed identically in successive batches (6 tubes per batch), using the same methodology and batch of stock reagents (see recipe).
- Note that volume constraints will produce four 1.5ml ependorf tubes for every one 2ml tube started with.
- TENP solution was made up immediately prior to use, from stock solutions. Hot plate set to 60°C.

B.iii Extraction:

1. Each sample was spun at 1000G for 1 minute to separate sample into supernatant and supernatant-and-pellet for ease of processing: equal volumes (approx. 500µl) were partitioned to 2ml ependorf tubes, and treated as separate samples.
2. To each sample (i.e. each 2ml tube), 800µl of TENP extraction buffer was added. The pipette head was used to disrupt the biomass pellet as necessary.
3. 12µl of proteinase K was added to each sample, mixed by inversion, and incubated at 60°C for two hours.
4. 150µl of 10% w/v CTAB buffer was added, and each sample was incubated for a further 15 minutes at 60°C.
5. Samples were spun at 1000G for two minutes, and then separated to separate 2ml tubes in equal volumes (supernatants only; supernatant and biomass) of approx 750µl each.
6. 800µl of 25:24:1 Phenol:Chloroform:Iso-amyl alcohol (PCI) was added to each tube (i.e. slightly more than equal volume of lysed sample).
7. Samples were spun at max available centrifuge speed at 0°C for ten minutes.

8. Sample supernatant (i.e. aqueous portion) was carefully removed to clean 2ml ependorf tubes with all due deference paid to the interface layer. Sample tube with the remaining interface and organic fraction was disposed of appropriately.
9. A further 750µl of PCI were added to the supernatant in the fresh 2ml tube, mixed by inversion, and spun at maximum available centrifuge speed at 0°C for 30 minutes.
10. Aqueous supernatant was carefully removed from the centrifuged tube, and pipetted to a sterile 1.5ml ependorf tube. The organic fraction was disposed of appropriately.
11. To the aqueous sample, 0.2 volumes (~140µl) of Na-Acetate was added, and mixed by inversion. Then, 0.8 volumes (~450µl) of iso-propanol was added, mixed by inversion, and spun at highest possible centrifuge speed for 100 minutes at 0°C.
12. Supernatant was discarded, and pelleted material was cleaned by adding cold 70% volume/volume ethanol to the tube, centrifuging for 10 minutes, followed by careful decanting of the ethanol. This was repeated three times.
13. The nucleic acid pellet was air-died under the draft of an open bunsen burner for 3o minutes, after which 100µl of TE was added and the pellet left re-dissolve. Extracts were stored at 8°C.

B.iv Recombining Technical Replicates:

Each timepoint was extracted in three technical replicates. Each replicate processed was subdivided at steps 1 and 5 above, giving 4x 100µl extracts per replicate. For each timepoint, this produced twelve 100µl nucleic acid extracts. Each timpeoint was pooled at 25µl per 100µl fraction (i.e. to 300µl total per timepoint), concentration was standardised using a spectrophotometer, and then stored at 8°C until use. Raw extracts were frozen for eternity at -20°C.

Appendic C – Bioinformatics Materials

C.i Primers

The following primers were used to generate amplicons during this thesis (PCR, DGGE, clone libraries, pyrosequencing, Illumina sequencing), and are formatted after Alm et al., 2000.

Chapter	Name	Sequence (5' - 3')	Reference
2	S-*-Univ-0789-a-S-18 S-*-Univ-1053-a-A-16	TAG ATA CCC SSG TAG TCC CTG ACG RCR GCC ATG C	Baker *et al.*, 2003
3, 4	S-*-Univ-0905-m-S-18 S-*-Univ-1492-m-A-19	TGA AAC TYA AAG GAA TTG GGT TAC CTT GTT ACG ACT T	Gao *et al.*, 2015 Leser *et al.*, 2002
4	S-D-Arch-0349-a-S-17 S-D-Arch-1041-a-A-18	GYG CAS CAG KCG MGA AW GGC CAT GCA CCW CCT CTC	Casamayor *et al.,* 2002
4	S-D-Bact-0517-a-S-17 S-D-Bact-1061-a-A-17	GCC AGC AGC CGC GGT AA CRR CAC GAG CTG ACG AC	Klindworth *et al*., 2012
5	S-D-Univ-0515-b-S-19 S-D-Univ-0926-b-A-20	GTG YCA GCM GCC GCG GTA A CCG YCA ATT YMT TTR AGT TT	Caporaso *et al.,*, 2012 Walters *et al.*, 2016

C.ii Bioinformatics

Scripts for data processing, including raw sequence preparation, filtering and demultiplexing, clustering, chimera detection, dereplication, taxonomy assignment, differential abundance testing, metabolic capability prediction and general data manipulation have been separated out and hosted externally for reference, at https://github.com/handibles/jfg_thesis_appendix_C.ii.

The version accessions provided below correspond to the version of each file submitted for this thesis. These accessions uniquely identify both the script and the the script version provided for this thesis, allowing the corresponding files to be provided for posterity alongside updates and/or revisions where applicable.

chapter	file	version accession ('commit')	language	program/library
2, 3	chapter2-3_lefse_local.v4.sh	b157aab	Python	LEfSe
2	chapter2_get_QIIME_on_data_v.23.txt	b157aab	Python	QIIME
2	chapter2_import_seqs_and_graph.R	b157aab	R	phyloseq, ggplot2
3, 4	chapter3-4_get_seq_libraries_for_silva.txt	b157aab	Python	QIIME
3	chapter3_import_OTUs_and_graph.R	b157aab	R	phyloseq, ggplot2
4	chapter4_import_OTUs_and_graph.R	b157aab	R	phyloseq, ggplot2
5	chapter5_DADA2_on_seq_data.r	b157aab	R	DADA2
5	chapter5_Sparcc_v.2.sh	b157aab	Python	SparCC
5	chapter5_import_ASV_and_graph.r	b157aab	R	phyloseq, ggplot2
5	chapter5_import_correlation_matrix.R	b157aab	Python	heatmaply, ggplot2
5	chapter5_demo-recreate_images.R	b157aab	R	phyloseq, ggplot2
5	chapter5_test_ASVs.R	b157aab	R	DESeq2, phyloseq, ggplot2

Appendix D – Abundance Tables and Statistical Outputs

Absolute community abundances, process data, predicted metabolic capabilities and statistical outputs have been hosted externally for reference (in a single entry), as detailed below. The data is provided in tab-separated **.txt** format.

The version accessions and DOI provided for data below uniquely identify both the data and its history, allowing the corresponding files to be provided for reference, while also allowing updates or notes to these files to be recorded and identified with clarity.

Appendix Digital Object Identifier (DOI) and Location:

- DOI: 10.5281/zenodo.1249599
- Location: https://doi.org/10.5281/zenodo.1249599
- Version: thesis_1.0.0

Appendix Contents:

- D.i: Community Abundances
- D.ii: Process data
- D.iii: Predicted Metabolic Capability
- D.iv: Statistical Outputs

Appendix E – Data statements & submissions

E.i: Chapter 2

Pyrosequencing data for chapter 2 were deposited in the MG-RAST database under project number 14106, which is publicly available at the URL http://metagenomics.anl.gov/linkin.cgi?project=14106.

E.ii: Chapter 3

The pyrosequencing data from chapter 3 were submitted as a single SFF file to the public ENA databases under accession number PRJEB22994 (secondary accession: ERP104726), accessible at the URL http://www.ebi.ac.uk/ena/data/view/PRJEB22994.

E.iii: Chapter 4

Clone library sequences for chapter 4 were uploaded to Genbank under accessions KY077158 – KY077249.

Pyrosequencing data from this study were submitted in SFF format to the public ENA databases, accession number PRJEB26841 (secondary accession: ERP108868) and are accessible at the URL https://www.ebi.ac.uk/ena/data/view/PRJEB26841

E.iv: Chapter 5

Sequence data for this study were submitted to the public ENA database in fastq.gz format under accession number PRJEB26863 (secondary accession: ERP108887) and are accessible at the URL http://www.ebi.ac.uk/ena/data/view/PRJEB26863.

References

1. Alm, E.W., Oerther, D.B., Larsen, N., Stahl, D.A., and Raskin, L. (1996) The oligonucleotide probe database. *Appl Environ Microbiol* **62**: 3557–3559.
2. Baker, G.C., Smith, J.J., and Cowan, D.A. (2003) Review and re-analysis of domain-specific 16S primers. *Journal of Microbiological Methods* **55**: 541–555.
3. Caporaso, J.G., Lauber, C.L., Walters, W.A., Berg-Lyons, D., Huntley, J., Fierer, N., et al. (2012) Ultra-high-throughput microbial community analysis on the Illumina HiSeq and MiSeq platforms. *ISME J* **6**: 1621–1624.
4. Casamayor, E.O., Muyzer, G., Pedrós-Alió, C., and others (2001) Composition and temporal dynamics of planktonic archaeal assemblages from anaerobic sulfurous environments studied by 16S rDNA denaturing gradient gel electrophoresis and sequencing. *Aquatic Microbial Ecology* **25**: 237–246.
5. Gao, Z.-M., Wang, Y., Tian, R.-M., Lee, O.O., Wong, Y.H., Batang, Z.B., et al. (2015) Pyrosequencing revealed shifts of prokaryotic communities between healthy and disease-like tissues of the Red Sea sponge *Crella cyathophora*. *PeerJ* **3**: e890.
6. Klindworth, A., Pruesse, E., Schweer, T., Peplies, J., Quast, C., Horn, M., and Glöckner, F.O. (2012) Evaluation of general 16S ribosomal RNA gene PCR primers for classical and next-generation sequencing-based diversity studies. *Nucl. Acids Res.* gks808.
7. Leser, T.D., Amenuvor, J.Z., Jensen, T.K., Lindecrona, R.H., Boye, M., and Møller, K. (2002) Culture-Independent Analysis of Gut Bacteria: the Pig Gastrointestinal Tract Microbiota Revisited. *Appl. Environ. Microbiol.* **68**: 673–690.
8. SHAN, G., JIN, W., LAM, E.K., and XING, X. (2008) Purification of total DNA extracted from activated sludge. *Journal of Environmental Sciences* **20**: 80–87.
9. Walters, W., Hyde, E.R., Berg-Lyons, D., Ackermann, G., Humphrey, G., Parada, A., et al. (2016) Improved Bacterial 16S rRNA Gene (V4 and V4-5) and Fungal Internal Transcribed Spacer Marker Gene Primers for Microbial Community Surveys. *mSystems* **1**: e00009-15.
10. Wilson, K. (2001) Preparation of Genomic DNA from Bacteria. In, *Current Protocols in Molecular Biology*. John Wiley & Sons, Inc.

Thesis Bibliography

1. FitzGerald, J.A., Allen, E., Wall, D.M., Jackson, S.A., Murphy, J.D., and Dobson, A.D.W. (2015) Methanosarcina Play an Important Role in Anaerobic Co-Digestion of the Seaweed Ulva lactuca: Taxonomy and Predicted Metabolism of Functional Microbial Communities. *PLoS ONE* **10**: e0142603.
2. Guneratnam, A.J., Ahern, E., FitzGerald, J.A., Jackson, S.A., Xia, A., Dobson, A.D.W., and Murphy, J.D. (2017) Study of the performance of a thermophilic biological methanation system. *Bioresource Technology* **225**: 308–315.
3. Herrmann, C., FitzGerald, J., O'Shea, R., Xia, A., O'Kiely, P., and Murphy, J.D. (2015) Ensiling of seaweed for a seaweed biofuel industry. *Bioresource Technology* **196**: 301–313.